

Characterization of Lipid- and Protein Co-oxidation Mechanisms in Oleogels using Kinetic Modelling and Multivariate Statistics

Dissertation

zur Erlangung des Doktorgrades

der Mathematisch-Naturwissenschaftlichen Fakultät

der Christian-Albrechts-Universität zu Kiel

vorgelegt vom

staatl. gepr. Dipl.-Lebensmittelchemiker

Philipp Meissner

Kiel, 2021

Erste Gutachterin:

Prof. Dr. Karin Schwarz

Zweite Gutachterin:

Prof. Dr. Regina Scherließ

Tag der mündlichen Prüfung:

30.11.2020

Philipp Meissner

Characterization of Lipid- and Protein Co-oxidation Mechanisms in Oleogels using Kinetic

Modelling and Multivariate Statistics

Cover design – Lisa Pannek

dedicated to A, M

Acknowledgement

Many people contributed in one way or another to the completion of this thesis. At first, special thanks to Prof. Dr. Karin Schwarz for supervising me and helping with all the manuscripts. It was also a pleasure to have so many constructive and exciting discussions with you, in which I often forgot the time.

I am sincerely grateful to my supervisor, Dr. Julia Keppler, for her guidance, support and generous help throughout the practical work and during the preparation of this thesis.

At this place I also like to thank Dr. Heiko Stöckmann, who inspired me especially at the beginning of this thesis and was always one of the most critical internal reviewers.

I would like to thank Dr. Tobias Demetrowitsch for sharing his expertise in response to numerous questions about ICR-MS measurements.

My special thanks are extended to the staff of the department of food technology.

I would like to thank Prof. Dr. Kroh and the (former) members of his working group, for their guidance during my studying, discussions and helpful advises in my PhD time: Dr. Martin Kaufmann, Dr. Stefan Schibilsky, Sandra Grebenteuch. There are a lot more of members in this group here, which are in grateful memory.

There are also lasting memories of the encounter of former tutors and helpful advisors, which I would like to appreciate: Prof. Dr. Hasler in relation to statistics, Prof. Tholey in relation to amino acid sequencing, Prof. Zeev Wiesman in relation to some interactions, Prof. Dr. Schaur in relation of protein carbonyls, Dr. Dirksen in relation to R and Mrs. Dr. Göttlöber, Mrs. Richter, Mr. Dr. Leuer, Mrs. Noak and Mrs. Lange for their interesting lessons in relation to my interest in science.

A special thank you to my colleagues Matthias, Jonas, Jule, Nesskea, Jaqueline, Timon, Eva, Rasha, Monique, Sarah and fellow graduate students: Carolin, Eilina, Vanessa, Lisa and Lina.

I dearly thank my parents Andrea and Matthias, and my family and friends who encouraged me during the last years: Daniel, Christian, Robert, Stefan, Lisa, Patrick, Eva, Simon, Andi, Meinart, Bene, Georg, Tim, Markus, Lena, Stefan und Matthias.

Many thanks to all of you, who have also proofread my thesis.

Finally, I want to thank Laura not only for proofreading my thesis, but for everything she has done for me and enabled for our future. It was and will be a great and exciting journey.

Kiel, 2021

Philipp Meissner

Publications related to this thesis

Articles:

Meissner, P. M., Keppler, J. K., Stöckmann, H. , Schrader, K. and Schwarz, K. (2019) Influence of Water Addition on Lipid Oxidation in Protein Oleogels, *Eur. J. Lipid Sci. Technol.*, 121: 1800479 (special issue), DOI:10.1002/ejlt.201800479

Meissner, P. M., Keppler, J. K., Stöckmann, H. and Schwarz, K. (2019) Oleogel – das Fett neu erfinden, Schriftenreihe der öffentlichen Hochschultagung der Agrar- und Ernährungswissenschaftlichen Fakultät der Christian-Albrechts-Universität zu Kiel. (Volume 126, not yet published)

Meissner, P. M., Keppler, J. K., Stöckmann, H. and Schwarz, K. (2020) Cooxidation of Proteins and Lipids in Whey Protein Oleogels with Different Water Amounts, *Food Chem.*, 328, <https://doi.org/10.1016/j.foodchem.2020.127123>

Meissner, P. M., Keppler, J. K., Stöckmann, H. and Schwarz, K. (2020) Changes in Protein Fluorescence in a Lipid-Protein Co-oxidizing Oleogel, *J. Agric. Food Chem.*, 68 (39), 10865-10874, DOI: 10.1021/acs.jafc.0c02911

Meissner, P. M., Keppler, J. K., and Schwarz, K. (2020) Lipid oxidation induced Protein Scission (not yet published, manuscript form)

Contributions:

Keppler, J. K., Heyn, T. R., Meissner, P. M., Schrader, K. and Schwarz, K. (2019) Protein oxidation during temperature-induced amyloid aggregation of beta-lactoglobulin, *Food Chem.*, 289, 223-231 (Accepted 2019, DOI:10.1016/j.foodchem.2019.02.114)

Abramovič, H., Alberdi Cedeño, J., Amft, J., Bernal, C., Bravo-Días, C., Derewiaka, D., Forte, E., Genot, C., Guillén, M. D., Hennebelle, M., Jacobsen, C., Martins, F. P., Meissner, P. M., Merx, D., Meynier, A., Perez-Portabella, I., Pignetter, M., Porcellana, T., Prió, B., Ruiz Aracama, A., Schwarz, K., Sels, H., Steffen-Heins, A., Stöckmann, H., Valesco, J., van Duynhoven, J., Yesiltas, B. (alphabetical order), representing a consortium of interested participants of the 2nd International Symposium on Lipid Oxidation and Antioxidants 2018 in Graz, eds. **Amft, J., Meissner, P. M. and Schwarz, K.**, “ring study for the evaluation

and harmonization of lipid oxidation related measurement methods” (title approximately, not yet published)

Book chapters:

Meissner, P. M., Amft, J. and Schwarz, K. (2018) Fettsäureprofile und Sterine (not yet published, manuscript form).

Amft, J., Meissner, P. M. and Schwarz, K. (2019) Reduktion von Fett (not yet published, manuscript form).

Conference lectures and posters:

Meissner, P. M., Keppler, J. K., Stöckmann, H. and Schwarz, K. Kinetik der Lipidoxidationsmarker in wasserarmen Feststoffsuspensionen (2017). Abstract available (2018, Regionalverband Nord – Tagung am 27./28. Februar 2017 in Hamburg. Lebensmittelchemie, 72: 12-16. DOI:10.1002/lemi.201870104) – Lecture

Meissner, P. M., Keppler, J. K., Hasler, M., Stöckmann, H. and Schwarz, K. Kinetic of Oxidation Compounds in Low and Medium Moisture Suspensions (Euro Fed Lipid Congress 2017 in Uppsala) – Poster

Meissner, P. M., Krebs, C., Keppler, J. K., Stöckmann, H. and Schwarz, K. Lipidoxidation und Proteinoxidation in einem Modell Molkenprotein – Oleogel (Deutscher Lebensmittelchemikertag 2017 in Würzburg). Abstract available (2018, Poster ”Lebensmittelsicherheit”. Lebensmittelchemie, 72: 126-134. doi:10.1002/lemi.201870507) – Poster

Meissner, P. M., E., Keppler, J. K. and Schwarz, K. Qualitative und Oxidative Schädigung lipid- und proteinreicher Systeme – Studie zu einem Proteinoleogel als Modellsystem (Kiel Life Science Tagung 2017) – Poster

Meissner, P. M., Jalas, E., Keppler, J. K., Stöckmann, H. and Schwarz, K. Lipid and Protein Oxidation in Oleogels with Low Water Content (2nd International Symposium on Lipid Oxidation and Antioxidants, 2018 in Graz) – Lecture

Meissner, P. M., J alas, E., Keppler, J. K., Stöckmann, H. and Schwarz, K. Interaktion von Aldehyden der Lipidoxidation mit Proteinen in Oleogelen (Deutscher Lebensmittelchemikertag 2018 in Berlin). Abstract available (2019, Poster „Food Fraud/Food Safety”. Lebensmittelchemie, 73: 81-96. doi:10.1002/lemi.201970404) – Poster

Meissner, P. M. and Schwarz, K. Oleogel – das Fett neu erfinden. 69. Hochschultagung der Agrar- und Ernährungswissenschaftlichen Fakultät der Christian-Albrechts-Universität zu Kiel (2019) – Lecture

Meissner, P. M., E., Keppler, J. K. and Schwarz, K. Veränderung intrinsischer Tryptophan-Fluoreszenz und Fluoreszenzbildung in einem co-oxidierenden Protein-Lipid-Gel aufgelöst durch partial least squares regression (Deutscher Lebensmittelchemikertag 2019 in Dresden). Abstract will be available in the journal Lebensmittelchemie soon. – Poster

Meissner, P. M., E., Keppler, J. K. and Schwarz, K. Lipidoxidation induced Scission of Proteins (Kiel Mass Spectrometry Forum 2019 in Kiel) – Poster

Summary

Lipid oxidation is one of the main causes of food spoilage. In addition, co-oxidation can lead to toxic products, which are even classified as carcinogenic. However, despite the lability of unsaturated fatty acids, they are important health promoting compounds according to the mediterranean diet and prevent for example cardiovascular diseases. Furthermore, ω 3-fatty acids are essential compounds of our nutrition as they are precursors of hormones. In this context, the aim of this thesis was to investigate the interaction of proteins and lipids in oxidizing systems that lack typical lipid oxidation indicators of food monitoring. For this purpose, lipid-rich suspensions with low moisture were incubated with the addition of amino acids at moderately elevated temperatures related to room temperature to simulate the storage condition of a food, but not to change basic mechanisms by increased thermal energy. The suspensions provide insights into the relevance of interfaces for the interaction of primary lipid oxidation products, their formation and degradation (**Chapter 2**). Whey protein oleogels were introduced as model systems to subsequently maximize the protein-lipid interface and to focus on protein-lipid co-oxidation. This is a relative new class of lipids, which is a high unsaturated fat alternative to saturated and conventional hardened fat, which are associated with disease promoting trans-fatty acids. The lipid oxidation in such protein-based oleogels, as far as the author knows, was characterized for the first time and it could be shown that especially characteristic volatile aldehydes are degraded in such systems (**Chapter 3**). Furthermore, the degradation reactions of the lipid oxidation products are accompanied by modifications of the protein, which were characterized in relation to lipid oxidation in oleogels (**Chapter 4**). These protein modifications were then further investigated by multivariate statistical methods to identify the underlying potential major mechanisms and to evaluate their overall contribution (**Chapters 5 and 6**).

Lipid-protein co-oxidation is an interdependent relationship in which the protein can act as an oxidation initiator. On the other hand, lipids are known for their autocatalyzed formation of lipid hydroperoxides, which fragment into hydroxyl radicals and other radicals as well as other oxygen-containing products such as aldehydes. By regression of a differential reaction equation, a model was utilized in which the formation rate of lipid hydroperoxides (as conjugated dienes) in this system correlates with the addition of water. The formation of water droplets and thus the formation of additional interfaces plays an important role in the formation of dienes. In contrast, it has been shown that the degradation rate decreases slightly with the addition of water. During this degradation a large number of different secondary lipid oxidation products are formed, whereby aldehydes, such as hexanal, the most common lipid oxidation product, react with amino groups of the protein to form Schiff's bases and addition products corresponding to those of

Michael reaction products. These compounds, some of which are brown polymers, could then be detected by fluorescence spectroscopy and protein carbonyl content. For the latter, it was concluded that these carbonyls, as well as those formed in the lipid phase, are subject to degradation reactions, which prevent the accumulation of carbonyls. In addition to the secondary lipid oxidation products, hydroxyl radicals among other radicals are also formed by the decomposition of lipid hydroperoxides. These highly reactive radicals are able to abstract hydrogen atoms from the amino acid residues as well as from the protein peptide backbone. The former is involved in the formation of dityrosine and *N*-formylkynurenine, which are typical oxidation products of tyrosine and tryptophan and can be detected by fluorescence spectroscopy. In contrast, when the peptide bond is cleaved, which is promoted by a lipophilic amino acid residue, additional protein carbonyls and primary amines are formed, which in turn counteracts the accumulation of secondary lipid aldehydes.

Zusammenfassung

Lipidoxidation ist einer der Hauptgründe für den Verderb von Lebensmitteln. Zusätzlich kann die Oxidation zu toxischen Produkten führen, die sogar als kanzerogen eingestuft werden. Trotz der Anfälligkeit von ungesättigten Fettsäuren, sind sie als gesundheitsfördernde Inhaltsstoffe als Bestandteil der sogenannten Mittelmeerdiet bekannt und verhindern zum Beispiel Herz-Kreislaufkrankungen. Weiterhin sind insbesondere ω 3-Fettsäuren essentieller Bestandteil unserer Ernährung, da sie als Vorstufen von Hormonen dienen. In diesem Rahmen, war das Ziel dieser Arbeit die Interaktion von Proteinen und Lipiden in oxidierenden Systemen zu untersuchen, in welchem typische Lipidoxidationsindikatoren der Lebensmittelüberwachung fehlen. Dafür wurden lipidreiche Suspensionen mit geringer Feuchtigkeit mit dem Zusatz von Aminosäuren bei moderat in Vergleich zur Raumtemperatur gehobenen Temperaturen inkubiert, um Lagerzeit eines Lebensmittels zu simulieren, jedoch nicht grundlegende Mechanismen durch erhöhte thermische Energie zu ändern. Dabei liefern die Suspensionen Einblicke für die Relevanz von Phasengrenzen für die Interaktion von primären Lipidoxidationsprodukten, deren Bildung und auch deren Abbau (**Kapitel 2**). Um im Anschluss die Protein-Lipid-Phasengrenze zu maximieren und um sich auf die Protein-Lipid-Kooxidation zu fokussieren, wurden Molkenprotein Oleogele als Modellsysteme eingeführt. Dabei wurde die Lipidoxidation in solchen Protein-basierten Oleogelen, soweit dem Autor bekannt, zum ersten Mal überhaupt charakterisiert und es konnte gezeigt werden, dass insbesondere charakteristische flüchtige Aldehyde in solchen Systemen abgebaut werden (**Kapitel 3**). Weiterhin werden die Abbaureaktionen der Lipidoxidationsprodukte durch Modifikationen des Proteins begleitet, welche im Bezug zur Lipidoxidation im Oleogel charakterisiert wurde (**Kapitel 4**). Diese Proteinmodifikationen wurden dann durch multivariate statistische Methoden weiter erforscht um die zu Grunde liegenden Hauptmechanismen zu identifizieren sowie deren Gesamtbeitrag zu bewerten (**Kapitel 5 und 6**).

Die Lipid-Protein-Kooxidation ist eine zweiseitige Beziehung, in welcher das Protein durchaus als Oxidationsinitialisierer fungieren kann. In der anderen Richtung sind Lipide für ihre autokatalysierte Bildung von Lipidhydroperoxiden bekannt, welche sich in Hydroxylradikale und anderen Radikalen sowie andere sauerstoffhaltige Produkte wie Aldehyde fragmentiert. Es wurde mittels der Regression einer differentiellen Reaktionsgleichung gezeigt, dass Lipidhydroperoxidverwandte konjugierte Diene in diesem System mit der Wasserzugabe korrelieren, wobei die Bildung von Wassertropfen und damit die Ausbildung zusätzlicher Grenzflächen eine wichtige Rolle bei der Bildung der Diene spielt. Im Gegensatz dazu wurde gezeigt, dass die Abbauraten mit der Wasserzugabe leicht abnimmt. Bei diesem Abbau wird eine große Anzahl an

unterschiedlichen sekundären Lipidoxidationsprodukten gebildet, wobei Aldehyde, wie z.B. Hexanal, das häufigste Lipidoxidationsprodukt, mit Aminogruppen des Proteins unter Ausbildung von Schiff'schen Basen und Michael-Additionsprodukten verwandten Stoffe reagieren. Diese Stoffe, von denen einige braune Polymere sind, konnten dann fluorimetrisch und durch den Proteincarbonylgehalt detektiert werden. Für letztere wurde geschlossen, dass diese, ebenso wie die Lipid erhaltenen Aldehyde, Abbaureaktionen unterliegen, welche dazu führen, dass Carbonyle nicht akkumulieren. Neben den sekundären Lipidoxidationsprodukten, werden auch Hydroxylradikale und andere Radikale durch den Zerfall von Lipidhydroperoxiden gebildet. Diese hochreaktiven Radikale sind in der Lage Wasserstoffatome der Aminosäurereste als auch vom Proteinpeptidrückgrat zu abstrahieren. Erstgenanntes ist dabei bei der Bildung von Dityrosin und *N*-Formylkynurenin beteiligt, die typische Oxidationsprodukte von Tyrosin und Tryptophan sind und über Fluoreszenzmessungen detektiert werden können. Bei der Trennung der Peptidbindung hingegen, welche durch einen lipophilen Aminosäurerest gefördert wird, werden zusätzliche Proteincarbonyle und primäre Amine gebildet, welche der Bildung von sekundären Lipidaldehyden zudem entgegenwirken.

Contents

Acknowledgment

List of original Publications VIII

Summary XII

1 General Introduction1

1.1	Motivation and Objectives	2
1.2	Theoretical Background	6
1.2.1	Lipids and Fatty Acids	6
1.2.2	Lipid Oxidation	7
1.2.3	Proteins	11
1.2.4	Protein Oxidation	11
1.2.5	Oleogels	16
1.3	Experimental Approach	18
1.3.1	Pretreatment of Oils	18
1.3.2	Preparation of Oleogels	19
1.3.3	Extraction of Protein and Lipids References	21
1.3.4	Measurement of Lipid Properties and Lipid Oxidation	22
1.3.5	Measurement of Protein Properties and Protein Oxidation	26
1.3.6	Chromatography and Mass spectrometry	30
1.3.7	Measurement of Oleogel Properties	35
1.3.8	Statistical Calculations	36

2 Protein Amino Acid Lipid Co Oxidation – Preliminary Investigations ...47

2.1	Introduction	48
2.2	Material & Methods	49
2.3	Results & Discussion	52
2.3.1	Lipid induced Oxidation of Leucine in Low Moisture Suspensions	52
2.3.2	Lipid and Amino Acid Oxidation Varied by Water Activity	59
2.3.3	Lipid Protein Co Oxidation in Oleogels	67
2.4	Conclusion	72
2.5	References	72

3 Influence of Water Addition on Lipid Oxidation in Protein Oleogels77

3.1	Introduction	79
3.2	Materials & Methods	79
3.2.1	Purification of safflower oil	80
3.2.2	Sample preparation	80
3.2.3	Color formatin of conjugated dienes	81
3.2.4	Determination of conjugated dienes	81
3.2.5	Volatiles	81
3.2.6	Rheology	81
3.2.7	Determination of water content & water activity	82
3.2.8	Statistical analysis and calculations	82
3.3	Results & Discussion	82
3.3.1	Formation of primary lipid oxidation products	82
3.3.2	Formation of volatile secondary lipid oxidation products	85
3.3.3	Differences in gels appearances and color formation	87
3.3.4	Water content and gelling efficiency	89
3.3.5	Rheological properties	91
3.4	Conclusion	92
3.5	References	93

4 Cooxidation of Proteins and Lipids in Whey Protein Oleogels with Different Water Amounts99

4.1	Introduction	101
4.2	Materials & Methods	103
4.2.1	Materials	103
4.2.2	Purification of safflower oil	103
4.2.3	Sample preparation	103
4.2.4	Determination of lipid hydroperoxides	104
4.2.5	Determination of carbonyl content	104
4.2.6	Measurement of free amines	105
4.2.7	Estimation of dityrosine formation	105
4.2.8	Degradation of volatiles	106
4.2.9	Statistical Analysis	106
4.3	Results & Discussion	106
4.3.1	Formation of the primary lipid oxidation products	106

4.3.2	Dityrosine formation estimation using fluorescence analysis	107
4.3.3	Formation of protein carbonyls	108
4.3.4	Formation of primary amines	111
4.3.5	Degradation of aldehydes	113
4.4	Conclusion	116
4.5	References	117
5	Changes in Protein Fluorescence in a Lipid-Protein Co-oxidizing Oleogels	123
5.1	Introduction	125
5.2	Materials & Methods	126
5.2.1	Material	126
5.2.2	Purification of oil	126
5.2.3	Sample preparation	126
5.2.4	Extraction of proteins and determination of primary lipid oxidation products	127
5.2.5	Spectroscopic measurements	127
5.2.6	Size-exclusion chromatography (SEC)	128
5.2.7	Statistical analysis	128
5.3	Results & Discussion	130
5.3.1	Intrinsic fluorescence of tryptophan	130
5.3.2	Size-exclusion chromatography (SEC)	132
5.3.3	Fluorescence signals and PLS	135
5.3.4	Curve-fitted compounds	139
5.4	References	142
6	Lipid oxidation induced Protein Scission measured by high resolution mass spectrometry and evaluated by partial least squares regression ...	147
6.1	Introduction	149
6.2	Materials & Methods	150
6.2.1	Materials	150
6.2.2	Purification of Safflower Oil	150
6.2.3	Sample Preparation	150
6.2.4	Measurement of Protein Conformation with Fourier Transformation Attenuated Total Reflection Infrared Spectroscopy	151

6.2.5	Determination of Lipid Hydroperoxides	151
6.2.6	Measurement of Peptides with Fourier Transformation Ion Cyclotron Resonance Mass Spectroscopy	152
6.2.7	Preparation of the Annotation List	152
6.2.8	Data Evaluation	152
6.2.9	Statistical Analysis	153
6.3	Results & Discussion	153
6.3.1	Identification of oxidized peptides	153
6.3.2	Correlation of peptides with lipid oxidation	155
6.3.3	Amino Acid Scission Sites	160
6.3.4	Radical Scission Pathways	161
6.3.5	Comparison of oxidants	163
6.4	Conclusion	164
6.5	References	166
7	General Discussion	173
7.1	Reaction of Radicals with Proteins	174
7.2	Reaction of Secondary Lipid Oxidation Products with Protein	176
7.3	Influence of Water on Lipid Protein Cooxidation	178
7.4	Influence of Texture and Lipid Protein Ratio	180
7.5	Closing remarks and outlook	182
7.6	References	185
8	Appendix	191
8.1	Supporting information for chapter 3	192
8.2	Supporting information for chapter 5	193
8.3	Scripts used with R	195
8.3.1	R-scripts related to chapter 2	195
8.3.2	R-scripts related to chapter 3	197
8.3.3	R-scripts related to chapter 5	201
8.3.4	R-scripts related to chapter 6	204
	List of figures	211
	List of tables	215

Chapter 1

General Introduction

1.1 Motivation and Objectives

Fats and essential fatty acids are a fundamental part of our daily nutrition and serve in general as energy source. Further, they contain vitamins and are in many essential for the preparation of food [1]. In addition, unsaturated fat acids are an essential precursors of body own hormones for cell communication and thus, they influence inflammatory diseases, fever, pain and blood coagulation [2]. Unsaturated lipids are therefore an element of a healthy nutrition. Especially the polyunsaturated fatty acids eicosapentaenoic acid and docosahexaenoic acid are known for their health benefits [3].

This healthy prospect of unsaturated lipids leads to an enrichment strategy of them in food and cosmetic articles. These desired healthier products are accompanied by the highest vulnerability to autoxidation and deterioration [4, 5]. Deterioration of fats is a reason for off-flavors, rancidity and finally inedibility, which is the reason why naturally oils contain antioxidants like vitamin E (tocopherols), or fat-containing foods have to be enriched with antioxidants to guarantee acceptable shelf-life [1].

The toxicological aspect of the combination of oxidized lipids and proteins in foods is less known. Reactive lipid species from the oxidation can be highly lipophilic, which allows them to pass inner cell membranes, modify and damage protein and genes [6–10]. Variation of genes is per definition genotoxic and indicates the high relevance. In our body, oxidized lipids associated with oxidized low density lipoprotein are also known to form plaque in blood vessels leading to atherosclerosis related diseases like myocardial infarction (heart attack) and stroke [11]. However, investigation of lipid induced protein deterioration outside of our body has been absent for decades, despite there are no active repair, antioxidative enzymes or other mechanics in difference to “in vivo” systems. In the meanwhile, many oxidation related modifications of proteins and their amino acids have been proven [6, 7, 12]. Therefore, protein oxidation causes a lower nutritional value, a reduced digestibility and products with carcinogenic potential [13, 14].

In order to control oxidation in foods and cosmetics, a deep knowledge of lipid protein co-oxidation is needed. So far, the determination of oxidation status of products is based on lipid oxidation characteristics, which can lead to false results, as typical oxidation products and intermediates are sometimes lacking in complex systems [12]. Despite of the presence of proteins, the analysis of protein oxidation marker in is not common in such systems. However, as foods usually contain many compounds besides of lipids and proteins, food models are complex systems, in which oxidation is influenced from many sites. For the investigation of lipid protein

co-oxidation, emulsion and suspensions have been proposed, but those models are limited to their physical stability and greatly influenced by their physical attributes [15]. To focus on protein oxidation, radical attacks were often induced in aqueous Fenton-reaction metal based systems [16, 17], but in those systems typical fragmentation products of lipid oxidation are lacking. Furthermore, the hydroxyl radicals formed by the Fenton-reaction systems are oxygen centered, whereas lipid radicals are often carbon centered, which can leads to other radical mechanisms and reactions [18]. Moreover, a model for lipid protein cooxidation does not exist so far.

As the deterioration of protein rich lipid matrices, where typical lipid oxidation markers are lacking, is of interest, the main objective of the present thesis is to characterize the protein lipid co oxidation. The autoxidation of lipids could not be separated from the Maillard reaction in high protein and high fat foods. Both reaction types are of cascade like nature, which gear together and influence each other, whereas the formation of oxidized lipids and secondary fragmentations products can be inhibited, enhanced or masked [19, 20]. In addition, secondary products are often volatile. The analysis the oxidative status of such high fat high protein products by typical lipid oxidation markers can therefore be misleading. Therefore, this thesis should provide a basis for the determination of the oxidative status and offer insights into protein lipid cooxidation, which might be useful for evaluation of the shelf life of the referred products.

This doctoral thesis with the topic of lipid protein co-oxidation attempt to push limits by introducing protein structured oil gels, so called oleogels. This pseudo homogenous system is physical more stable as comparable emulsions or suspensions, whereas no stabilizers (e.g. emulsifier) are needed, which will omit the influence of other components. In addition, as lipid oxidation has a broad product spectrum and proteins are exhibit in addition to the primary structure up to a quaternary structure, the evaluation of the oxidative status could not base on the measurement of single aspects. Multivariate statistics, which can consider more compounds, should help the investigation of lipid protein cooxidation and is implemented in this thesis. In order to guide the protein lipid cooxidation experiments, several working hypotheses have been developed:

Hypotheses 1:

The water content of complex systems (oleogels and suspensions) influence the colloidal and structural properties of the system and thereby the reaction of lipid protein cooxidation.

Background

Lipid oxidation is known to be highly influenced by water [21, 22]. As water is a polar protic reaction medium, interactions of proteins and lipid oxidation derived compounds should play a significant role. Further, as proteins are partly lipid insoluble, the protein lipid interface will be altered by the availability of water. It is known that lipid oxidation compounds have an amphiphilic character [23, 24], which leads them to accumulate on interfaces. Thereby, the intrinsic properties of lipid oxidation compounds to migrate and accumulate on this interface should play a role in their reaction with protein.

Experimental Approach

Temperature has a great influence on reaction rates and diffusion processes [25]. Therefore experiments will be conducted at a moderate increased temperature of 40 °C, which is accepted as a temperature for room temperature conditions, which provides decreased experimental times and does not enable artificial reactions, which activation energy is commonly too high in storage conditions (general discussion on the 2nd international symposium of lipidoxidation and antioxidants, Graz, 2018). Oxidation is followed in low moisture models and oleogels. Oleogels will especially be useful for the investigation of lipid protein interfaces, as the protein is used as stabilizer in the system, which provides a model with colloidal stability for the interaction of amphiphilic proteins and lipid oxidation compounds without adding compounds that leads to interactions, e.g. emulsifiers on interfaces. In low moisture suspensions and oleogel systems, water can be added over the equimolar water protein ratio. Thereby, the water holding capacity of base materials in suspension or the protein in oleogels determines the availability of water as a reaction medium.

Hypothesis 2:

Lipid oxidation derived aldehydes and other oxygen containing products react with proteins and amino acids to aldol-, addition- and other condensation products, which are followed by the formation of protein modifications and causes rather the absence of lipid oxidation compounds than the inhibition of lipid oxidation.

Background

The oxidation status of lipid rich food is often proven by the measurement of volatile compounds, such as the most abundant lipid oxidation product hexanal. As hexanal is a carbonyl compound, which is known to react with amines by the named reactions [12], the lack of oxidation derived carbonyls may be caused by protein aldehyde adduct formation.

Experimental Approach

Secondary lipid oxidation aldehydes are volatile and can therefore be measured using gas chromatography approaches including the coupling with mass spectrometry for identification. The reaction with the protein can be followed by the coloration of protein carbonyls with dinitrophenylhydrazine (carbonyl remaining adducts) [26, 27], the measurement of involved amino groups by their reaction with *ortho*-phtalaldehyde [28, 29], the formation of known fluorescent compounds like dityrosine by fluorescence spectroscopy [30, 31] and the variation of functional groups in the system by infrared spectroscopy.

Hypotheses 3:

Lipid and protein oxidation are complex processes, which partly gear into each other. These complex processes are rather be characterized and classified using non-target analysis and multivariate statistics than by single compound evaluation. Thereby the correlation to known, leading oxidation compounds will reveal unnoticed compounds and hidden aspects of interest.

Background

Amino acids and especially their amino function are involved in formation of higher molecular compounds in the developing process of oxidation. There are pathways in which the protein is modified by secondary lipid oxidation products like aldehydes [12, 32, 33] and pathways in which the protein is altered by radical attack of hydroxyl radicals which are generated by the decomposition of lipid hydroperoxides or lipid oxidation derived protein hydroperoxides [30, 31]. In both pathways, some of these compounds are typically colored and fluorescent, which should provide insights in these pathways. Further, the nature of part of these modifications can cross link or introduce peptide cleavages [12, 30, 34], which both alter the macroscopic attributes of such systems.

Experimental Approach

A detailed profile of fluorescent modifications of products can be achieved using excitation emission matrix fluorescence spectroscopy. This profile may then be analyzed using multivariate statistics to provide detailed information of correlating fluorescent compounds, which can then be used to assign intrinsic variables to model compounds with known formation mechanism, which in turn give insights in the overall oxidation of the used system. Further, an enzymatic digest combined with size exclusion chromatography, will provide insights in modification as enzymes targeting specific amino acids will cause miscleavages. Protein peptide cleavages or cross-linking will both alternate the protein structure [12], which can be measured by infrared spectroscopy. Further, protein backbone cleavages will lead to small peptide like fragments [34], which can be identified and qualified using high resolution mass spectrometry. An in silico generated filter of relevant masses will support the identification. In both areas, spectroscopic and spectrometric measurements, the multivariate statistics will be principal component regression and partial linear least squares regression, which are able to dissolve networks of correlation in high complex situations.

1.2 Theoretical Background

1.2.1 Lipids and Fatty Acids

Lipids are a collection of lipophilic compounds, to which free fatty acids isoprenoids (steroids, carotenoids, monoterpenes), tocopherols and their derivatives with alcohols (e.g. mono-, di-, triacylglycerides, waxes), phosphates (phospholipids) and carbohydrates (glycolipids) belong. The inner attribute of lipids to consist as combination of single components makes this class very manifold. The most abandoned compounds in oils and fats are triacylglycerides, which is a triester of three fatty acids with glycerol (see Figure 1.1) [1].

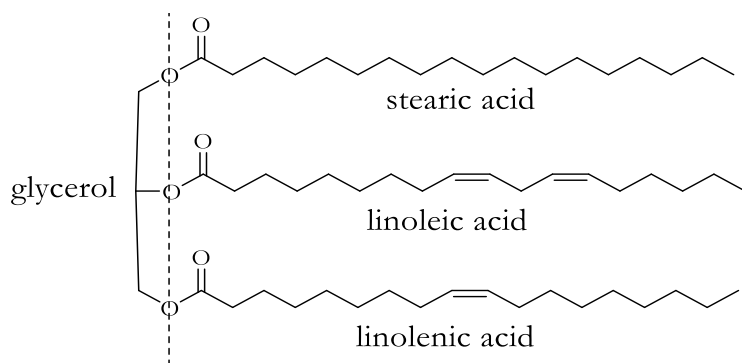


Figure 1.1: A typical triacylglyceride – an ester of glyceryl with stearic acid (no double bonds), linolenic acid (two double bonds) and linoleic acid (one double bond).

Fatty acids are hydrocarbons with one carboxylic group at the C1 position and are typically 18 carbon atoms long, whereas the length varying from butyric acid (4 C) to over 24 carbons. The most common fatty acids also have an equal number of unbranched carbon atoms and have up to three double bonds in *cis* configuration. The number of double also defines if one fatty belong the class of saturated fatty acids (no double bonds) or (poly-)unsaturated fatty acids (>1 double bonds) [1].

1.2.2 Lipid Oxidation

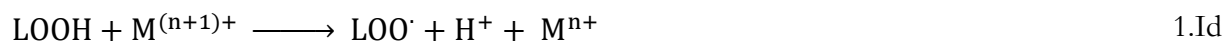
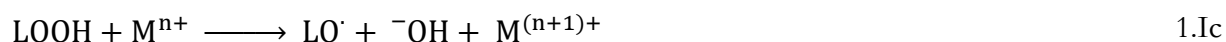
1.2.2.1 Primary Lipid Oxidation Products

The term lipid oxidation describes in general the deterioration of fats and oils and is most cases synonym to the term autoxidation, which describes a radical chain reaction with oxygen. Unsaturated fatty acids and especially polyunsaturated fatty acids are vulnerable to oxidation in form of radical hydrogen abstraction, due their ability to form mesomeric stabilized radicals, which lowers the initial dissociation energy of the C-H bonds by double bond conjugation and electron delocalization. This reaction is called *Initiation* and is the first part of three in of lipid oxidation, besides *Propagation* and *Termination*. This step initiates a radical chain reaction of lipids (LH) with initiators (I), whereas free alkyl radicals (L \cdot) are formed (see equation 1.1a) [35].

Initiation:



There are three kinds of possible initiators, which all form radicals. The simplest kind will be the thermal dissociation of weak bonds like lipid hydroperoxides (LOOH), which could be present as impurities (see equation 1.1b). Also the decomposition of ketones by light induces radical formation. Lipid hydroperoxides are decomposed by ubiquitous redox metals (M), too (see equation 1.1c, 1.1d) [35]. Other initiator could be proteins, e. g. myoglobin induces the lipid peroxidation by either a ferryl species in the porphyrin ring or a tyrosine peroxy radical [36]. In addition hydroxyl side chain can mediate strong hydrogen bonding, thus they may induce lipid hydroperoxide decomposition (molecule-assisted homolysis) [12].



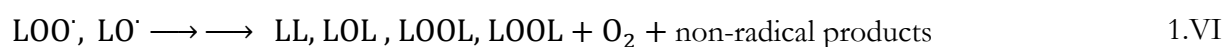
The second step of the lipid peroxidation is called *Propagation* and describes how the radical chain continues. At this point, lipid can react with atmospheric oxygen as lipid alkyl radicals to peroxy radicals (LOO^\cdot , see equation 1.II). A direct oxidation of lipids with normal triplet oxygen ($^3\text{O}_2$) is spin forbidden. The further reaction of peroxy radicals occurs much slower and forms hydroperoxides (equation 1.III), which are together with the peroxy radicals called primary lipid oxidation products [35].

Propagation:



The third step of lipid oxidation is called *Termination* and describes the end of the autocatalytic radical chain by recombination of peroxy, alkoxy and alkyl radicals to non-radical products (see equation 1.IV, 1.V) [35].

Termination:



1.2.2.2 Kinetic of Lipid Oxidation

Based on classical laws the oxidation rate of fatty acids would be correspond only to the concentration of oxygen and fatty acids (equation 1.VII), however this is actually not true, since the oxidation of fatty acids is a complex autocatalyzed reaction [21].

$$\frac{d(\text{LOOH})}{d(t)} = -\frac{d(\text{O}_2)}{d(t)} = k[\text{L}][\text{O}_2] \quad 1.\text{VII}$$

Several criteria for the radical addition of oxygen exist, which attributes the mechanism [21]:

- the number of double bonds drastically increase the reaction rate, which is known by the different dissociation energies of hydrogen atom in oleate to linolenate [1],
- the yield of radicals in calculation is greater than one,
- the reaction is accelerated or inhibited in drastic way by various compounds,
- there is a very long induction period, also known as lag time, when pure material is applied,
- the activation energy is moderately high.

Based on the bimolecular initiation reaction of two LOOH with the reaction constant k_1 and the reactions 1.II-1.VI with the reaction constants k_2 - k_6 and making the assumption that $k_5^2 = k_4k_6$, the reaction can be described by the complex equation 1.VIII [21, 37], whereas $\frac{d(\text{LOOH})}{d(t)}$ is the formation rate of lipid hydroperoxides:

$$\frac{d(\text{LOOH})}{d(t)} = k_3 \sqrt{\frac{k_1}{k_6}} [\text{LOOH}][\text{L}] \frac{k_2 \sqrt{k_6} [\text{O}_2]}{k_2 \sqrt{k_6} [\text{O}_2] + k_3 \sqrt{k_4} [\text{L}] + \sqrt{k_1 k_4 k_6} [\text{LOOH}]} \quad 1.VIII$$

The term $\sqrt{k_1 k_4 k_6} [\text{LOOH}]$ could be easily shown to be negligible, as the oxidative chain length be about 100 [38]. Further when the reaction starts with only one initiator (equation 1.I, monomolecular, M), the equation 1.VIII facilitates to equation 1.IX

$$\frac{d(\text{LOOH})}{d(t)} = k \sqrt{[\text{LOOH}]} [\text{L}] \frac{[\text{O}_2]}{[\text{O}_2] + k' \sqrt{[\text{L}]}} \quad 1.IX$$

To solve equation 1.IX several important assumptions can be made. The concentration alkyl and peroxy radicals should be constant as these compounds would be in a steady state, therefore their change over time is zero. Furthermore, the amount of oxygen is not limiting, and the amount of oxygen produced by decomposition of peroxides is negligible. As metals (M) can act as true catalyst, it was shown with these assumption that equation 1.IX can further facilitated to 1.X with the rate constants of reactions: initiation (i), propagation (p) and termination (t) [39, 40], in which several constant factors can melted to a single constant K_m .

$$\frac{d(\text{LOOH})}{d(t)} = \frac{k_p \sqrt{k_i}}{\sqrt{2k_t}} \sqrt{[M]} [\text{L}] \cdot \sqrt{[\text{LOOH}]} = K_M \cdot \sqrt{[\text{LOOH}]} \quad 1.X$$

This equation can easily be integrated to equation XI [39], which can be used to calculate oxidation constants in a ring study of oxidation of oils, where monomolecular decomposition predominates. As K_m contains rate constants this can also be used in Arrhenius plots to determine the overall activation energy in oils. In pure lipids K_m is in the order of 10^{-2} to 10^{-3} (moles/mole) $^{1/2}$ h $^{-1}$ (30-40 °C)[21]. For a bimolecular initiation (B), as stated above, the resulting equation is 1.XII, whereas K_B is at 37 °C about 10^{-2} h $^{-1}$ [21].

$$\sqrt{[\text{LOOH}]} = \frac{K_M}{2} t \quad 1.XI$$

$$\log_e \frac{[\text{LOOH}]}{1 - [\text{LOOH}]} = K_B t \quad 1.XII$$

According to Semenov *et al.*, the bimolecular initiation reaction is thermodynamically favored by a hydrogen bond between the two peroxides [21, 22], which is interesting in foods, as this

bimolecular reaction is slower in more polar solvents, or in other words foods or systems with an increased a_w -value (water activity). As water can also mobilize trace metals, the monomolecular initiation is contrary increased, therefore in combination with the bimolecular reaction, the relation of water activity and oxidation is marked with a minimum, which is commonly known as Labuza relation or curve.

However, these calculations are not able for the calculation of the formation and decomposition rate of lipid hydroperoxides. For this purpose, the differential equation for a monomolecular autocatalyzed and a bimolecular decomposition reaction can be written as in equation 1.XIII, which can only be solved numerically [41]. Interesting to note is here, that the bimolecular decomposition reaction rate of the peroxides contains the small amount of bimolecular formation rate of lipid hydroperoxides.

$$\frac{d(\text{LOOH})}{d(t)} = k_{\text{formation}}[\text{LOOH}] - k_{\text{decomposition}}[\text{LOOH}]^2 \quad 1.XIII$$

However, in common the point of rapidly increasing lipid oxidation is attributed to a critical concentration, where the auto-catalyzation gets the determinant factor. As oxidation of lipids is accompanied by the introduction of oxygen atoms, lipid oxidation products are somewhat more hydrophilic, which leads to the production of products with an amphilic behavior. This leads to the formation of micelle-like supramolecular structures [23]. Lipid hydroperoxides and other compounds are firstly slowly formed until they arrive their critical micelle concentration, which is also influenced by surrounding molecules like emulsifiers. Thereafter reversed micelles are formed, whereby lipid hydroperoxides are concentrated at the surface and induce the propagation phase of lipid oxidation [24].

1.2.2.3 Secondary Lipid Oxidation Products

Secondary lipid oxidation products are formed by fragmentation of hydroperoxides. Linoleic acid autoxidizes initially to either the 13- or the 9-hydroperoxide derivative, as this provides a conjugated diene system, which lowers the absolute energy. Concerning the volatiles, these hydroperoxides dissociate forming alkoxy radicals and hydroxyl radicals (equation 1.II). In the following, the alkoxy radicals undergo a β -scission, which can lead to scission on both sites of the fatty acid chain to hexanal and 2,4-decadienal (see Figure 1.2). As 2,4-decadienal oxidizes further to hexanal, hexanal is the most abundant volatile compound in oxidized linoleic acid rich oils. Besides aldehydes, which contribute due to their volatility most to the rancid flavor, many other classes of compounds like alkanes, alkenes, alcohols, ketones, acids, and epoxides are formed [1, 35, 42].

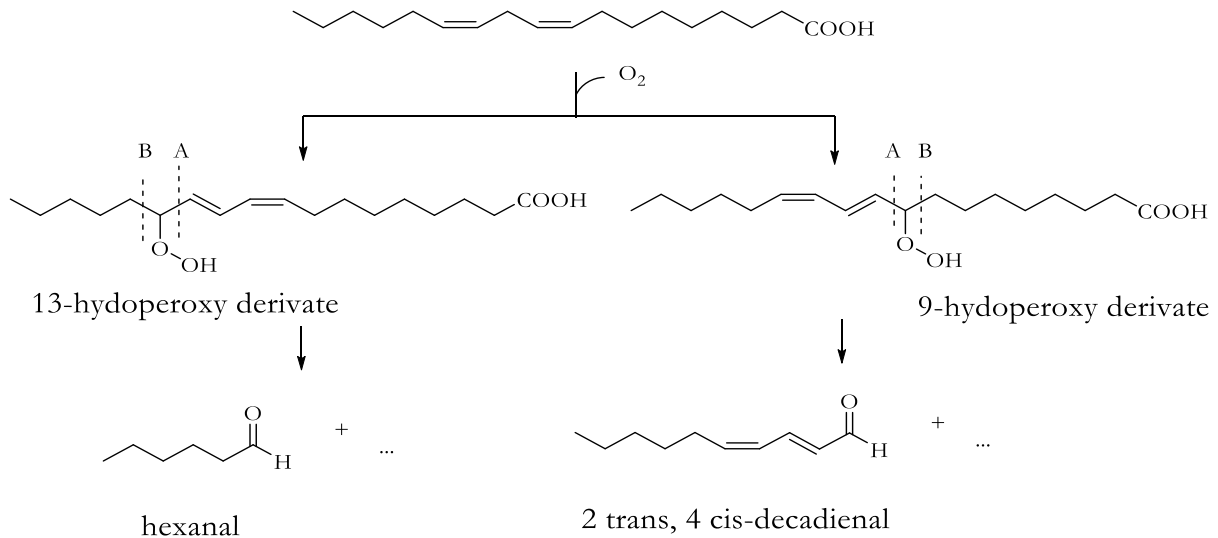


Figure 1.2: β -scission of monohydroperoxides, example of linoleic acid [42].

1.2.3 Proteins

Proteins are the main tools of living cells and fulfill lots of tasks of living activity. For this purpose, proteins are assembled of 20 types of amino acids. Each amino acid consists of an amino group, a carboxyl group and a specific residue. With the amino group and carboxyl group, amino acids function as chain links, which are connected by amide, or more protein specific, peptide bonds. Peptide bonds are relatively stable and resistant for cleavage. Each amino acid in the sequence carries a specific residue. Due to the large amount of possibilities to connect the basic types, this sequence is called the primary structure. There are lipophilic, hydrophilic, acid and basic residues, which forces the primary sequence in aqueous environment in many times to distinct forms, which are α -helices, β -sheets and β -turns and are called secondary structure. Otherwise this is also stated as random coil structure. The arrangement of the second order structure is called tertiary structure. This structure can be seen as the native structure of a single protein, but often proteins are complexed to multimers or with other proteins, too, which is called quaternary structure [1, 2]. Structures of proteins are stabilized mostly by hydrogen bonds and London forces, but are also stabilized disulfide bonds (R-SS-R) of cysteine (R-SH) residues or by ionic forces (R-COO⁻ +H₄N-R). Lipids can vary the structure of proteins, which can lead to conformation changes of sulfide bonds [2, 43].

1.2.4 Protein Oxidation

Lipid induced modifications to proteins has been recognized long ago. Early studies report changes in general behavior (texture, crosslinking, scission, loss of nutritional value), molecular functionality (enzyme activity, browning) and cell activity hindrance up to apoptosis. [12]

Facilitated by advances in chromatography and mass spectrometry and studies on single amino acids, more detail on the oxidation of specific protein sites and typical modifications has been figured out. [12].

1.2.4.1 Primary Lipid Oxidation Product induced Protein Modifications

The lipid oxidation Modifications on proteins can be divided by the oxidation caused by their inner oxygen species classes. Hydroperoxides can bond to proteins and induce the decomposition leading to hydrogen atom abstraction or radical addition to proteins. Peroxyl and alkoxy radicals can transfer radicals to the protein, which can result in crosslinking or scission and a variety of oxidations. Therefore, the radical hydrogen abstraction of residues like tyrosine leads to dityrosine and the oxidation of tryptophan to *N*-formylkynurenine (NFK), which both are fluorescent and are associated with age pigment formation (lipofuscin) [12, 44, 45] (Figure 1.3). Initially by tyrosine a hydrogen atom is abstracted, which forms a mesomeric stabilized tyrosyl radical. Two of the tyrosyl radicals then combine and form dityrosine. The initial radical attack on tryptophan is similar, which leads to a mesomeric stabilized radical (the tryptophyl radical), too. To the tryptophyl radical, which is mostly stabilized on the tertiary C atoms, oxygen adds like to lipid radicals, forming a hydroperoxide derivative, which undergoes a rearrangement and β -scission to NFK. Further reaction of NFK leads to the release of formic acid and the formation of kynurenine [44].

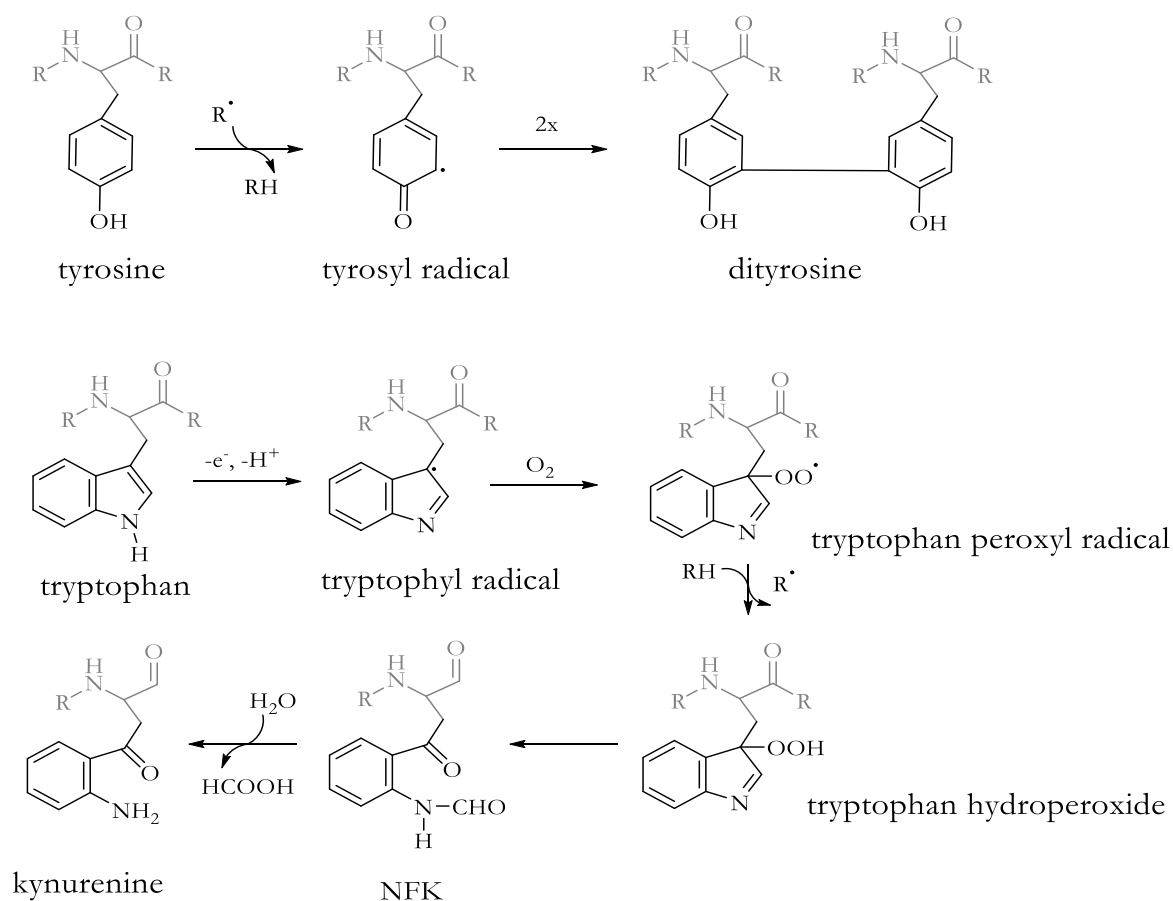


Figure 1.3: Oxidation of tyrosine and tryptophan, which produces the fluorescent products dityrosine and *N*-formylkynurenine according to [44, 45].

Beside the oxidation of residues, the protein backbone can be also a target of radical attacks, which leads to scission, which not only introduce new amino groups, but also increase the content of carbonyl groups in the protein (see Figure 1.4) [34, 46]. However, despite hydroxyl radicals are not quite selective, it was not random and not necessarily on the protein surface. It was shown that proline, valine, leucine, (glutamate) and isoleucine have the highest yields of protein hydroperoxides by radiation (G values of 0.8 – 1.4), where another four (alanine, arginine, glutamine, and tryptophan) have a lower yield (G values of 0.3 – 0.5) [47]. These amino acids are mainly hydrophobic and it was revealed that a tertiary carbon atom or a segment, that contain at least two methylene groups, were necessary to stabilize the required initial radical through hyperconjugation. In addition, the protein radical, which can be generated at the protein surface, can migrate along the protein backbone to glycine residues, where they are stabilized [48]. Other alkyl amino acids may similarly provide electron sink sites, where radicals are stabilized.

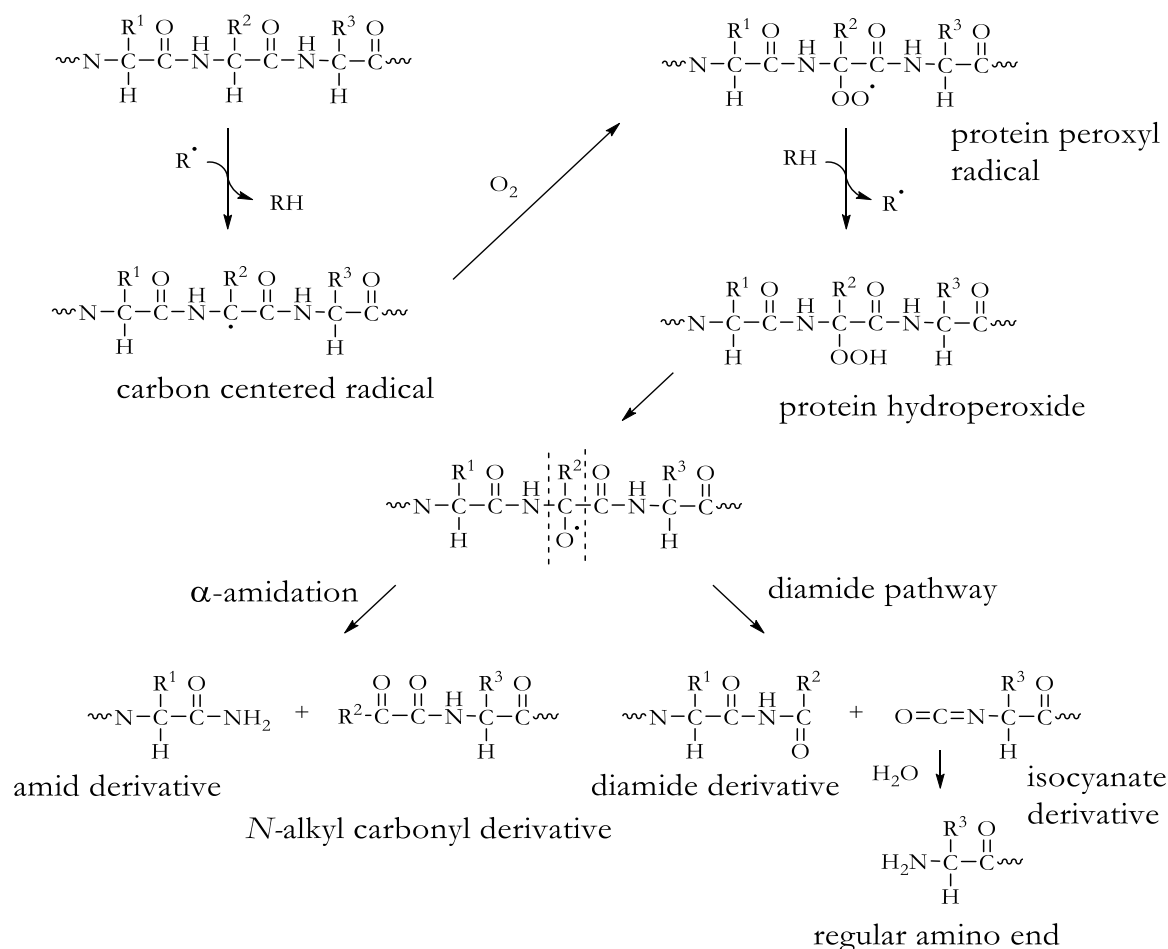


Figure 1.4: Scission of the protein backbone and introducing of amino acids and carbonyls according to [34, 46].

From lipid oxidation it is known, that the formed carbon centered radicals react rapidly with oxygen. However, since this reaction is bimolecular, the intramolecular radical migration should be faster. This should lead also to protein hydroperoxides, which are located at the hydrophobic amino acids as stated above. The further reaction mechanism is very similar to the β -scission of lipid hydroperoxides (see section 1.2.2.3 Secondary Lipid Oxidation Products). The protein alkoxyl radical underlies a β -scission either in the direction of the N-terminus or C-terminus, in which the first is called α -amidation and the second diamide pathway. Interestingly, the isocyanate protein derivative from the diamide pathway further fragment to a regular amino acid ending, as isocyanates are not stable in water [34, 46].

1.2.4.2 Secondary Lipid Oxidation Products induced Protein Oxidation

Secondary lipid oxidation products, especially epoxides and carbonyls, are able to bind to the protein as well. The resulting products can be fluorescent and introduce new carbonyls to the protein as Michael addition leads to maintain the carbonyl group (see Figure 1.6 top). In this reaction a protein amino group attack nucleophilic on the double bond of 2-alkenals, which leads to secondary amine, which in turn can react with a second 2-alkenal. As the two carbonyl groups

maintained, the product reacts further by an aldol condensation and form, in case of lysine and croton aldehyde, formyl dehydropiperidino lysine [12, 32]. Micheal reaction of alkanals could also be indirectly, as two alkanals can Aldol condensate to alkenals, too (see Figure 1.5).

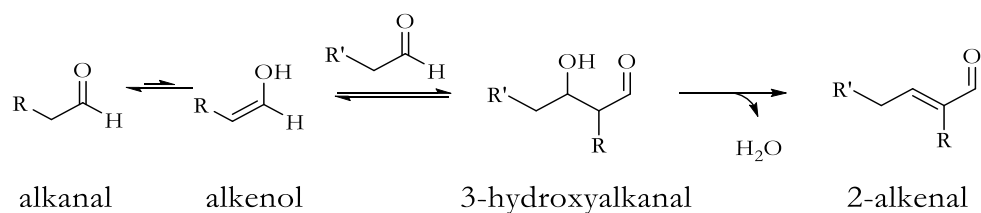
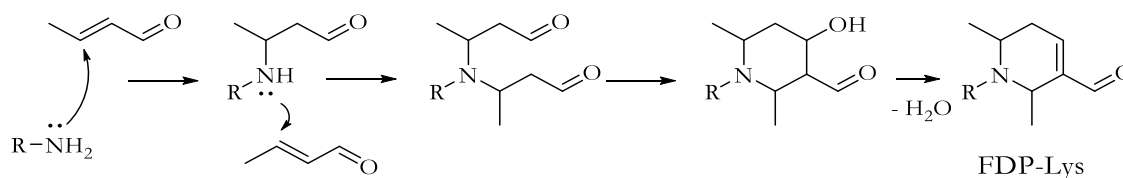


Figure 1.5: Aldol reaction of an aldehyde (alkanal) to 3-hydroxyalkanal and aldolcondensation to the 2-alkenal.

If the first reaction with the alkenal is a Schiff base formation (see Figure 1.6 bottom) and a second 2-alkenal is added similarly, an aromatization takes place after a cyclization, where the aromatic ethylmethyl peridinium is fluorescent [33]. As many of the lipid oxidation compounds are bifunctional, crosslinking of the protein is also present [12]. Bifunctionality is also a condition for the formation of fluorescence of Schiff base adducts since an electron-donating in conjugation with the imine is required [49]. However, initial adducts rearrange to further to other products like pyrrole- and pyridinium- derivatives, which are often fluorescent, too [12, 50–59].

1,4 addition, Micheal pathway



1,2 addition, Schiff base pathway

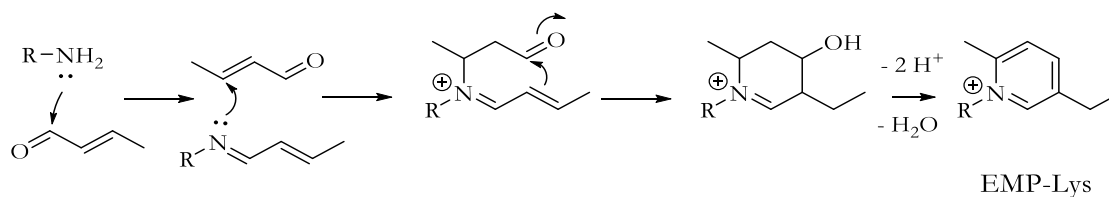


Figure 1.6: Formation of cyclic products by addition on lysine residues by 2-alkenals, e.g. the formation of formyl dehydropiperidino lysine (FDP-Lys) via 1,4 addition Michael addition pathway and the fluorescent ethylmethylpyridinium lysine (EMP-Lys) via the 1,2 addition Schiff base pathway [12, 32, 33].

1.2.5 Oleogels

1.2.5.1 Texture of Colloidal Fat Crystal Networks

The melting behavior of fats and oil is largely determined by the crystallization of fatty acids. The inner structure of fat can therefore be imagined like schemed in Figure 1.7. Single triglyceride molecules stick together and form lamellas, which pile up to domains. These domains in turn form single crystallites, which stack together to cluster. These clusters aggregate to flocs, which then build a colloidal network of fat crystals in the fluid bulk fat. The interlocking of the fat crystals with each other ultimately results in an increased consistency [60].

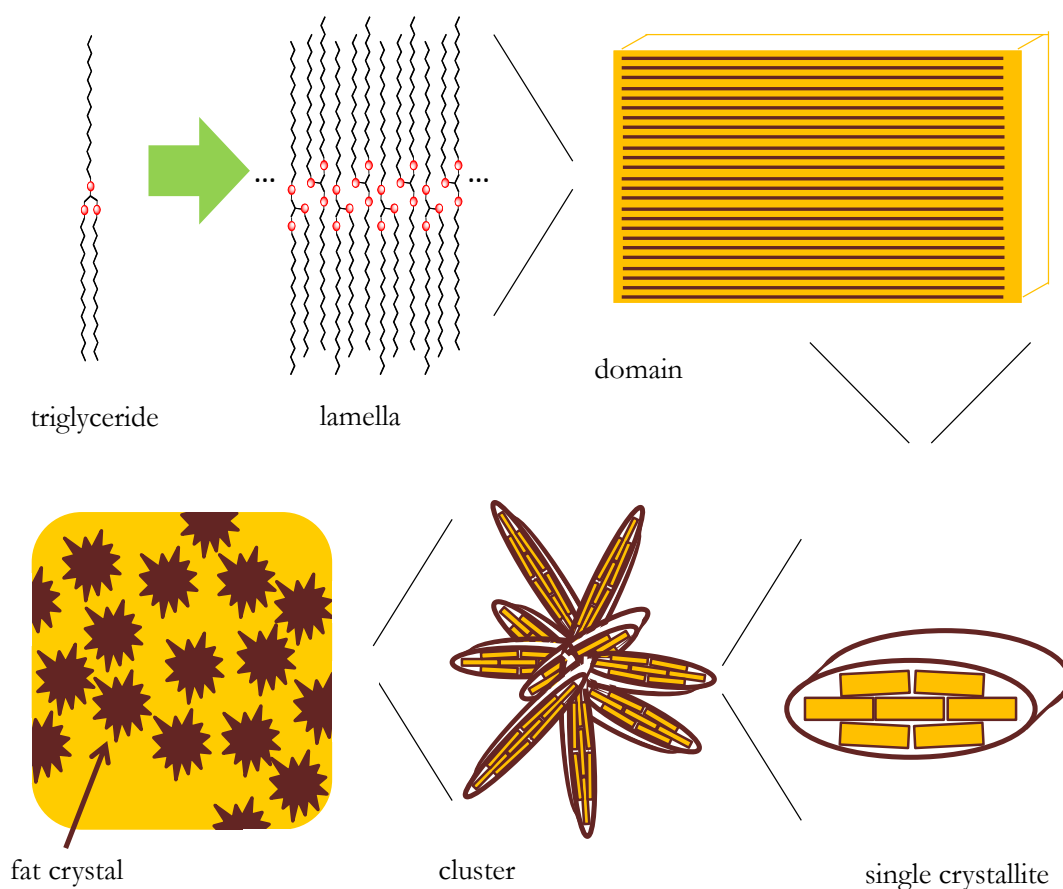


Figure 1.7: Scheme of the colloidal network of fat crystals in fat.

1.2.5.2 Oleogelators

Association of single molecules to a greater extent, forming a network, which traps liquid, is typical for gel. Thus, the idea to oleogels looks very natural: just replace fat crystals with compounds, which have similar properties (see Figure 1.8). These network building blocks, so called oleogelators, can be similar to common water gelling compounds, but they must be finely dispersible in fat. One can distinguish between several classes, which contain crystalline particles

(e.g. natural waxes, mono- and diacylglyceride), self-assembled structures (e.g. 12-hydroxy stearic acid, sphingolipids), inorganic particles (fumed silica), high internal phase emulsions (HIPEs) and polymeric strands (e.g. carbohydrates, proteins) [61]. In the ideal case, saturated fatty can be fully avoided and replaced with minor amounts of gelators, which leads to the healthy properties of the unsaturated oils, and the avoidance of *trans*-fatty acids loaded hydrogenated oils. For the utilization in foods, oleogelators have also to be edible, tasteless, easy to use, minor concentrated, tolerating water contact and higher temperatures (e.g. to be also thermoreversibel), cheap, easily available, and similar behavior when used as shortening or baking margarine (oral sensation by melting in the mouth). However, all conditions are not fulfilled by either of the classes [61].

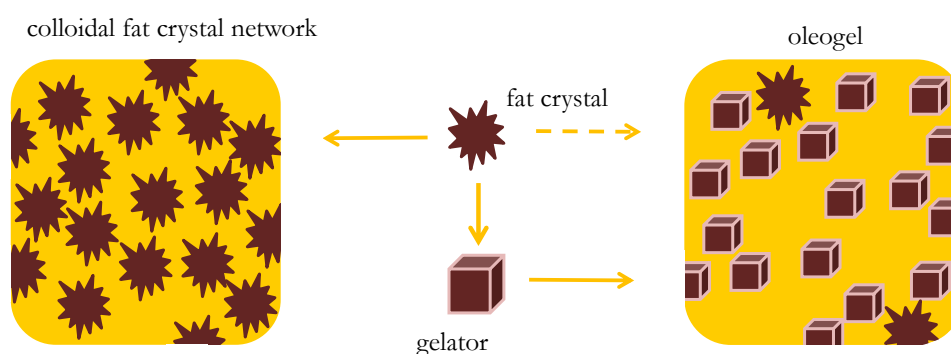


Figure 1.8: Scheme of the colloidal network of fat crystals in fat and oleogelators in liquid oil.

One distinguishes by the oleogel preparation between the direct and the indirect method. In the direct method the gelator like waxes, or ethyl cellulose are simply dispersed in the oil and heated until the fully solubilization, whereas the end temperature is dependent on the specific gelator [62–64]. In contrast, in the indirect method the structuring properties of hydrophilic structures, e.g. polymers (with surface active properties), are exploited with following water abstraction [61, 65].

1.2.5.3 Whey Protein based Oleogels

The protein oleogels used in this thesis were based on heat induced whey protein aggregates, transferred into oil. This oleogels belong to the indirect preparation type and were developed by de Vries and coworkers [65–67]. These aggregates are generated by 85 °C in water (pH 5.7) form a weakly gel and can count sulfide bridges mediated. These aggregates are then transferred into liquid oil using a solvent exchange process, which is achieved by several centrifugation and resolving steps using solvents with decreasing polarity and finally oil [66]. However, protein aggregates can also freeze dried and dispersed in liquid oil, but special care must be taken to avoid further agglomeration by the freezing process, as ice crystals can stick protein aggregates

together (freeze casting) [68, 69]. In both processes, smaller protein fragments are removed and a network of protein aggregates in oil is established. These aggregates are bound by hydrogen bonds, water capillary forces and van der Waals interactions and form paste like gels, whereas water addition increase gel strength [68].

In relation to this thesis about protein lipid co oxidation, this kind of system is chosen in the early stages of this work (Chapter II), as the resulting gels have advantages over emulsion and suspensions:

- The gels need ideally no third component (emulsifier or filler) to stabilize the physical stability over the experiment time, which can be several weeks as 40 °C was chosen as moderate oxidation temperature,
- water can be added and incorporated, or excluded,
- and Oxidation will be independent from micelles sizes in emulsions.

In addition, the oil type is undefined and can be changed from oxidizable to non oxidizable oils and whey protein contains mainly beta lactoglobulin, a well characterized protein.

1.3 Experimental Approach

This section aims to provide more detailed information of the methods that has been used, as given in each paper based chapter and provide background characteristics of the methods. Unless otherwise noted, all measurements have been prepared in triplicate and results are given as mean with sample standard deviation.

1.3.1 Pretreatment of Oils

Vitamin E is essential for the human nutrition, as it inhibit the lipid oxidation in cells and it prolongs the shelf life of liquid oil [1]. Natural oils contain up to over 100 mg/100 g oil of tocopherols, which are also known as vitamin E (see Figure 1.9) [70]. The used safflower oil of this thesis contains about 44 mg/ 100 g oil.

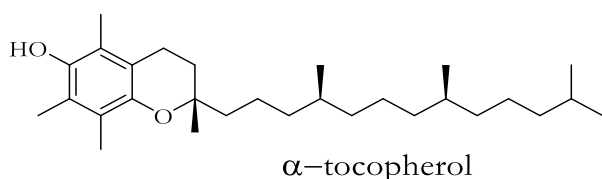


Figure 1.9: Vitamin E – a class of different methylated tocopherols.

Lipid oxidation experiments with oils, which contain tocopherols, are therefore delayed. In order to equalize the experiments for reasons of comparability, tocopherols besides sterols, trace metals and free fatty acids are removed from the oil by column chromatography, which is also called stripping the oil. As those compounds are more polar than the oil, they absorb on polar materials like activated alumina (Al_2O_3).

The method used in this thesis is based on the method by Lampi & Kamal-Eldin [71]. A glass column is prepared with a piece of wool and filled with a sufficient amount of hexane to cover the wool and to remove any air in the tip of the column. Then alumina is added, which was prior activated through heating at 100 °C for 8 h and 200 °C for 12 h. Therefore, the alumina is suspended in hexane, which provides the possibility to transfer the alumina as slurry air bubble free in the column assisted with knocking on the column. Another piece of wool is added, to prevent moving of the alumina and the column is covered with aluminum foil for inhibition of light induced oxidation. A mixture of oil and hexane (<500 mL/500 mL) is now passed through the column, where the first 250 mL (~ the volume of activated alumina) are discarded. The following eluate and the eluate after addition of another 250 mL of hexane to flush the remaining mixture from the alumina are collected in a brown ice water cooled glass flask and stored at -20 °C until further use. The evaporation of hexane was achieved on a rotary evaporator in a 3 cycled procedure. In each cycle the mixture was flushed initially for 10 min with nitrogen to remove any oxygen. Then the pressure was carefully adjusted to 150 mbar in 3 steps, each 15 min long. The first cycle is conducted at 65 °C and the last two cycles at 90 °C, which was followed finally by a cooling down and flushing with nitrogen step. The received oil was tested of residual tocopherols (HPLC, < 0.5 ppm, method DGF F-II 4a) and used for all experiments.

It has to be noted, that the used evaporator needs a gas entrance and air inlet. In addition, flushing the oil with nitrogen in vacuo has to be carefully started and the air inlet has to be opened when normal pressure is reached. In pressure decreasing steps it has to be mentioned, that the air inlet has to be closed first to avoid oxygen entrance.

1.3.2 Preparation of Oleogels

There are two possibilities to prepare oleogels with whey protein, which are based on the work of de Vries and colleagues [66, 67]. This preparation was slightly modified and simplified. Initially whey protein is solved in demineralized water (4 % w/v), stirred for 2 h and stored overnight at 4 °C to guarantee full hydratization of the protein. This solution was then adjusted with HCl (1 M) properly to pH 5.7, which is important, since it is near the isoelectric point of the protein and facilitates agglomeration. 25 mL aliquots were heated in 50 mL closed centrifuge tubes at

85 °C for 15 min in a water bath. Afterwards, the solution was carefully transferred to an ice bath to initiate gel formation. The formed weak gel is now broken by hand shaking and vortexing. The suspension was afterwards further homogenized by using an Ultra Turrax (13.000 rpm) for about 3 min. The achieved protein aggregates were separated from smaller peptide and protein fragments by centrifugation 25 mL aliquots at 3900 g for 20 min and discarding of the supernatant. This was repeated twice by suspension of the pellet in demineralized water. These Protein aggregates can now function as structure template in liquid oil. The limitation is to transfer this aggregates from the water to lipid phase. There are two further methods to remove the water, the solvent exchange route and a freeze drying procedure. The solvent exchange route needs solvents and oil in excess, but is able to generate relatively large amount of gel, whereas the freeze drying procedure provide a route to add water to different concentrations. Furthermore to our intended purpose, the protein is not contaminated with acetone in the freeze drying technique, which may induce protein carbonyl formation, which is of interest.

1.3.3.1 Solvent Exchange Route

This route is according the method described in [66] and based on the idea to extract solvents with decreasing polarity stepwise. The aquatic pellet was collected and homogenized in the 10 fold amount of acetone by an Ultra Turrax (13.000 rpm) for about 3 min. The achieved protein aggregates were separated from the solvent by centrifugation 25 mL aliquots at 3900 g for 20 min and discarding of the supernatant. This was repeated once by suspension of the pellet in acetone and twice with oil. Thereafter, the lipophilic protein pellet was suspended in the 10 fold amount of oil and stored overnight. Finally, the aggregates were centrifuged again at 4000 g for 20 min, with discarding the supernatant.

1.3.3.2 Fast freezed followed Lyophilization

To transfer the protein aggregates to dryness it is important to know that simple freezing of the aquatic protein aggregates leads to agglomeration and greater sized conglomerates, which are not able to form a network in liquid oil [68]. To prevent slow freezing and the formation of large ice crystals, which pressing proteins together, the aquatic protein aggregates were diluted (1% in reference to the original whey protein solution) and dropped in liquid nitrogen (-196 °C). The frozen droplets were then collected in a round-bottom flask with the addition of some spoons of liquid nitrogen to prevent thawing, stored at -80 °C overnight and finally freeze dried. The protein aggregate size was the controlled by resolving a small amount in water and using static light scattering (Horiba, Retsch Technology GmbH, Haan, Germany). The particle size is bimodal distributed with a second minor peak, which is from further agglomerated protein.

However, it was checked that the main peak is over 80%. To mimic the 6.8 % of protein in solvent exchange oleogels [66], the dry whey protein aggregates (6.8 %) were then combined with liquid stripped oil. This mixture was premixed and stirred (300 rpm) for 10 min using a larger stir bar, which is only slightly smaller than the beaker. When water has to be added to an experiment, the specific amount was carefully added dropwise after 5 min, to provide a fully networking of the protein in the oil before. The resulting liquid protein paste was then centrifuged for 20 min at 4000 g to remove the liquid oil by decanting the tubes for 10 min. In each of the steps the weight is carefully measured and the final protein concentration was measured as stated in equation 1.XIV. As the mixture cannot be fully transferred to the centrifuge tube, the amount of protein centrifuged in the resulting oleogel was corrected. It was assumed, that water is fully absorbed by the protein and integrated in the gel, but to give precise information, the water concentration was referred to the initial oil protein mixture. The approximate oil content was then given as the difference to 100 %. 200 mg of oleogel were taken for incubation in 20 mL either in brown screw capped headspace vials or for later extractions in closed 20 mL centrifuge tube, wrapped additionally with para film. These incubation vessels were stored for the certain time at 40 °C and used each for analysis.

$$\beta(\text{Protein}) = \frac{m_{\text{protein}} \cdot \frac{m_{\text{mixture in c tube}}}{m_{\text{mixture}}}}{m_{\text{Oleogel}}} \cdot 100 \% \quad 1.XIV$$

$$= \frac{m_{\text{protein}} \cdot \frac{m_{\text{c. tube, before}} - m_{\text{c. tube, before, empty}}}{m_{\text{oil}} + m_{\text{protein}} + m_{\text{water}}}}{m_{\text{c. tube, after decanting}} - m_{\text{c. tube, before, empty}}} \cdot 100 \%$$

1.3.3 Extraction of Protein and Lipids

Lipid containing experiment systems in this thesis are simple structured, whereby only systems are taken, where the oil is mixed with different substances. As this is the case, no fatty acid esters with carbohydrates and proteins have to be expected, which make it easy to extract the lipids by simple solvent extraction.

1.3.3.1 Powder Model Systems

In powder model systems, which contain about 10 % oil, ~10 g were taken and extracted with 25 mL of cyclohexane with sonification for 20 s (Bandolin SONOPULS HD 2200, 50 % power, 9 cycles,) in centrifuge tubes. Sonification was established to facilitate the solubilization of lipid in clusters and aggregates of the suspension. After centrifugation (Hettich Zentrifugen Universal 32) for 5 min (4500 rpm), the supernatant of the samples was filtered through a filter paper and

collected. This procedure was repeated twice with 20 mL of cyclohexane. Finally, the combined filtrates were evaporated in a rotary evaporator to dryness (250 mbar at 65 °C).

1.3.3.2 Oleogel Model Systems

Oleogels were extracted *vice versa* to the solvent exchange production procedure for whey protein aggregate oleogels. Whey protein aggregates are insoluble in cyclohexane, isopropyl alcohol and distilled water, which make them easily extractable and cleanable by solvents. Lipids were extracted 3 times with 3 ml of cyclohexane, 2 times with 5 mL of isopropyl alcohol and 5 mL of water (MS grade). Each time, the suspension was rigorously shaken to fully destroy the gel/ pellet and centrifuged at 4000 g (Allegra X-30R, Beckmann Coulter, Krefeld, Germany) for 5 min. The supernatant of each solvent were combined and used for further measurements. 1 mL of cyclohexane extract (~20 mg fat) was dried by flushing with nitrogen for about 20 min, reweighted and used for further analysis. The protein pellet was suspended in 3 mL of water (MS-grade) and used for further analysis as protein extract. All extracts has been frozen after analyses by at least -20 °C. It has to noted, that isopropyl alcohol has been chosen to avoid modification of nucleophiles with the carbonyl containing acetone, because this is of interest especially in the determination of carbonyl content (see section 1.2.4 Protein Oxidation and 1.3.5 Measurement of Protein Properties and Protein Oxidation).

1.3.4 Measurement of Lipid Properties and Lipid Oxidation

Lipid oxidation products are classified to primary and secondary oxidation products. To primary lipid oxidation products belong alkyl, alkoxy, and peroxy radicals and lipid hydroperoxides. To measure them, their oxidative potential or their ability to absorb ultra violet light (UV) through the conjugated double bond is used (in case of linoleic and linolenic acid, see Figure 1.2). Secondary lipid oxidation products are mainly measured by their volatility.

1.3.4.1 Primary Lipid Oxidation Products

Conjugated dienes

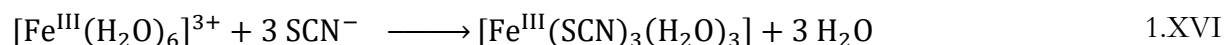
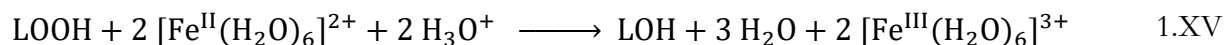
In case of measurement of conjugated dienes by UV, ~20 mg of the extracted, dried and reweighted fat was solved in 5 mL of isopropyl alcohol, vortexed for at least 10 s and diluted if necessary. Conjugated dienes were then measured directly by UV light absorption at 234 nm in quartz cuvettes [72, 73]. To determine the concentration of lipid hydroperoxides, the absorption coefficient of methyl linoleate hydroperoxide was used as estimate for all lipid hydroperoxides (26,000 M⁻¹cm⁻¹) [74]. This assumption can be made for two reasons: oxidative sensibility is increased dramatically with the number of double bonds [1, 35] and linoleic acid is the main

unsaturated fatty acid in the used oil (safflower, ~15 %). It has also to be noted, that quartz cuvettes are essentially, as plastic cuvettes are commonly not transparent to UV light. In addition, the absorption should be measured below 1.6 a.u., as the spectrometer calculates the absorption by the transmission of light. If the absorption is too high, the transmission is relatively low, that residual light increase the standard deviation dramatically.

To measure lipid hydroperoxides by their oxidative potential, many methods has been used. In this thesis mainly the thiocyanate method [72, 73, 75] and a modified iodometric method after Wheeler [76, 77] hast been used.

Thiocyanate method

In case of the thiocyanate method, ~20 mg of the extracted, dried and reweighted fat was solved in 5 mL of distilled isopropyl alcohol and vortexed for at least 10 s. Thereafter, 50 μ L of I (thiocyanate solution) were added and vortexed and 50 μ L of II (Fe^{2+} solution) were added and vortexed. The samples were then incubated for exactly 30 min at 60 °C in a water bath and covered to avoid contamination with condense water. Finally, the samples were cooled in a water bath for exactly 1 min and the formed Fe^{3+} thiocyanate complex (see reaction equation 1.XV and 1.XVI) is measured at 485 nm against blank.



It has to be noted, that distilled isopropyl alcohol is necessary, as purchased isopropyl alcohol is commonly partly oxidized and form peroxides over time [78]. Therefore always a blank as to be measured simultaneously, clean storage bottles have to be used for the distilled isopropyl alcohol and all reactants and the distilled isopropyl alcohol are cooled between measurements, but to provide equal conditions in the measurements, they have to be at room temperature. For solution I 30 g of ammonium thiocyanate are solved in 100 mL distilled water. Solution II, an iron(II)chloride solution, is prepared the combination by two solutions. The first solution is 0.5 g $\text{FeSO}_4 \cdot 7 \text{H}_2\text{O}$ in 50 mL of distilled water. The second solution is 0.4 g $\text{BaCl}_2 \cdot 2 \text{H}_2\text{O}$. Both solutions are combined slowly with stirring and under addition of 3 mL of HCl solution (25 %) and stored overnight in a fridge. The formed fine precipitate of BaSO_4 is filtered with 2 filters and the filtrate is protected from light and used for further analysis.

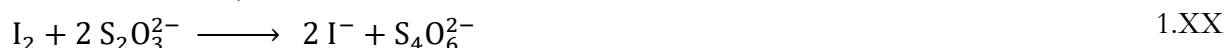
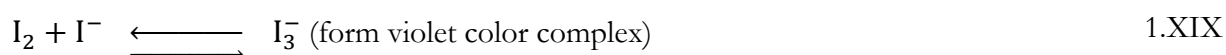
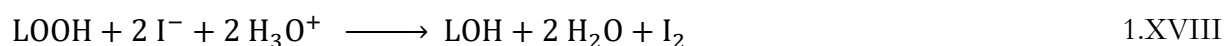
This procedure is preferred as iron chloride is hygroscopic, why different hydrates are formed and an exact amount could not accessed by weighting. Thereby, the HCl provides an acid environment, which prevents iron to precipitate to iron hydroxide. Iron sulfate could not be

used, because it would be less soluble in the resulting hydrophobic solvent. It also has to be noted, that the reaction starts with addition of the iron solution, why the thiocyanate is added firstly. In addition, the ammonium slightly buffers the hydrochloric acid, which can destroy hydroperoxides. Also the time has to be equal and exact in each measurement, as air oxygen provides iron oxidation. For the calculation of hydroperoxides a calibration function with FeCl_3 and thiocyanate has to be used to determine the iron thiocyanate complex absorption coefficient (in our case: $c(\text{Fe}^{\text{III}}) = 20.351 \cdot (A_{485} - A_{485, \text{Blank}}) - 0.0514$). The iron concentration can now be transformed to determine the lipid hydroperoxide concentration and peroxide value by equation 1.XVII, where the 55.84 g/mol is the molar mass of an iron ion [75].

$$\text{PV} = c(\text{LOOH}) \left[\frac{\text{mmol}}{\text{kg oil}} \right] \longrightarrow \frac{c(\text{Fe}^{\text{III}}) \left[\frac{\mu\text{g}}{5 \text{ mL}} \right]}{m(\text{oil})[\text{g}] * 55.84 \text{ g/mol}} \quad 1.\text{XVII}$$

Lipid hydroperoxide determination by the method by Wheeler, modified

The dried oil (~ 1g) was reweighted and solved in a 40 mL of solution of acetic acid/isooctane (60:40 v/v) in Erlenmeyer flasks and 0.5 mL of a saturated KI solution was added. Flasks were then shaken for 1 min, where iodine is formed (see equations 1.XVIII-XIX). The reaction was then stopped by addition of 30 mL of distilled water. The formed, red colored triiodide was then titrated and reduced with sodium thiosulfate (0.1 N or 0.01 N) against a blank test, where tetrathionate is formed (equation 1.XX). For the color change point, 1 mL of a starch solution was added, which form with triiodide ions a bright violet color complex.



It has to be mentioned that the starch has to be fully solved, which is reach by heating the solution up to the boiling point. Also, it is *not* recommended to add them initially to high concentrations of iodine, because starch can form strong complexes with triiodide, which relays the titration point and leads to overestimation. The final peroxide value can now be calculated on the basis of equation 1.XXI:

$$\text{PV} = c(\text{LOOH}) \left[\frac{\text{mmol}}{\text{kg oil}} \right] \longrightarrow \frac{(V - V_{\text{Blank}}) * c}{m(\text{oil})} \quad 1.\text{XXI}$$

It is known, that the determination by the iodometric method differs from the thiocyanate method, which belongs to the difference between the oxidation potential of active oxygen species in lipids with hydrogen iodide (HI) and ferrous ion (2+) [79, 80]. Therefore the determination of

the peroxide value with the thiocyanate based methods results in about 2-3 higher values by the autoxidation of methyl oleate/ methyl linoleate and methyl linolenate at 37 °C [79, 81].

1.3.4.2 Secondary Lipid Oxidation Compounds

Secondary Lipid oxidation compounds, which are mostly volatile, could be measured directly either by static or dynamic headspace, whereas static headspace is most simple. In a vessel, which is incubated an appropriate amount of time by a distinct temperature, an equilibration of compounds between the gaseous and solid/liquid phase is employed. That is way the concentration of the compounds in aliquot of the “head space” correlate directly with the amount in the oil of the sample [82].

Static head space was conducted for the measurement of hexanal, propanal and other compounds according to [83], which could be easily identified by retention time using authentic standards. Therefore either 1 g of a low and medium moisture suspensions or 200 mg of oleogel were incubated in 20 mL headspace vials for 15 min at 70 °C. 1 mL was taken in a sample loop (120 °C) and transferred (150 °C) to the GC Agilent 6890 Series GC (Injection temp. 220 °C, DB-1701 column 60 m x 320 µm x 1 µm, split 1:4, flow 12.7 mL/min). The column flow was 2.0 mL H₂ and a temperature program was used (initially hold 45 °C for 2 min, 15 °C/min to 85 °C hold for 4 min, 15 °C/min to 220 °C hold for 3 min). A flame ionization detector (FID) was used (250 °C, 40 mL/min H₂, 450 mL/min Air, make up gas N₂ 45 mL/ min).

To identify unknown compounds GC mass spectrometer (MS) measurements were conducted using electron ionization (EI, also known as electron impact ionization) fingerprints, which are compared automatically to standards of the NIST Database. For identification a minimum probability of 25 % was taken for a match. As EI of a GC MS system and following detection, is less effective than the FID, in GC MS measurements the dynamic headspace technique is used to increase the compound concentrations [82]. It is called dynamical, because the entire headspace is flushed during the whole incubation with a carrier gas to a trap, why this method is called “purge and trap” technique, too. This provides an accumulation of compounds on the absorbent material (Tenax TA), which is located in a small glass capillary. Thereafter, the compounds were desorbed thermally in a small oven and flushed to a cryo trap, which refocus the compounds by desorbing the compounds in a small cooled area and can rapidly heated to inject sharp substance spots [82].

In detail, 200 mg oleogel in a 20 mL brown screw capped headspace vial were analyzed using a Gerstel multipurpose sampler (MPS2 XL) equipped with a Gerstel dynamic headspace system (DHS), which was mounted on a SIM GC 6890N Series coupled with an Agilent 5975 EI mass

spectrometer. The sample was incubated for 4 min at 70 °C (agitation every 10 s, 500 rpm) and then purged with 500 mL of N₂ by a flow rate of 50 mL/min. The trap temperature was 30 °C, which was dried afterwards by 100 ml at 25 °C and 50 mL/min. Compounds were desorbed thermally (initial temp. 25 °C for 1 min, delayed by 1 min, 120 °C/min to 250 °C hold for 5 min, 25°C/min to 70 °C hold for 3 min) and refocused using a liquid carbon dioxide cryo trap (cooled injection system, Gerstel, initial -30 °C, equilibration 1 min, initial time 1 min, ramped 10 °C/s to 240 °C and hold 1 min) and transferred splitless to the GC inlet (split 50:1, DB-5MS column 60 m x 320 µm x 0.25 µm, flow 39,7 mL/min). The column flow was 0.7 mL He and a temperature program was used (initially hold 45 °C for 2 min, 15 °C/min to 85 °C hold for 4 min, 15 °C/min to 220 °C hold for 8 min, 30 °C/min to 250 °C hold for 5 min). The EI ionization was set to 70 eV for spectral database searches (AMDIS 2.62, NIST Mass spectral search Program) and the quadrupole was adjusted from 30 to 300 Da.

1.3.4.3 Fatty Acid Composition

There are many of international standard methods to measure the fatty acid composition of oil. All of them contain the derivatization of the acids into their methyl esters (FAME), which provides a preferred change in volatility, improves the peak shape and better separation [84]. These methods are mainly based either on acidic (e.g. HCl, BF₃) or alkaline types (e.g. NaOCH₃, KOH) of catalysts and include hydrolysis, transesterification/methylation, and neutralization, washing with water and other time consuming steps. In addition, there are often cautious and expensive [84]. In relation to these methods, the direct transesterification/methylation of oils by trimethylsulfonium hydroxide (TMSH) can be conducted without further preparation and proceed at room temperature [85]. In addition, this method becomes a standard method for fats and oils (milk fat excluded) in the meanwhile as well (ISO 12966-3:2016). TMSH in MeOH is strongly basic and able to attack triglycerides. The fatty acid trimethylsulfonium salt easily rearrange, as the volatile dimethyl sulfide is formed [86] (see Figure 1.10).

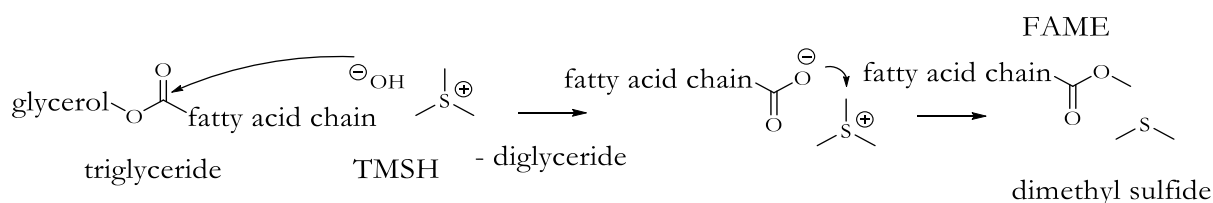


Figure 1.10: Mechanism of fatty acid methyl ester formation with TMSH.

In this thesis, ~50 mg of oil were solved in 2.5 mL of Methyl *tert*-butyl ether. An aliquot of 50 µL was mixed with 25 µL TMSH solution (0.2 M in MeOH), incubated for at least 1 h at room temperature and directly injected in and Agilent 6890 Series GC (Injection temp. 250 °C, DB-23

column 60 m x 250 μm x 0.25 μm , split 1:100, flow 141 mL/min). The column flow was 1.3 mL H_2 and a temperature program was used (80 $^\circ\text{C}$, 25 $^\circ\text{C}/\text{min}$ to 180 $^\circ\text{C}$ hold for 2 min, 2 $^\circ\text{C}/\text{min}$ to 182 $^\circ\text{C}$ hold for 16 min, 6 $^\circ\text{C}/\text{min}$ to 197 $^\circ\text{C}$ hold for 15 min and finally 10 $^\circ\text{C}/\text{min}$ to 240 $^\circ\text{C}$ hold for 3 min). A flame ionization detector was used (300 $^\circ\text{C}$, 40 mL/min H_2 , 450 mL/min Air, make up gas N_2 45 mL/min). An authentic standard of 37 FAMES was used to identify the fatty acids by their retention time.

1.3.5 Measurement of Protein Properties and Protein Oxidation

1.3.5.1 Protein Content

Measuring of the protein content of oxidized and modified protein is an easy done, but complex when the precision is questioned. All methods are based on the measurement either of structure elements, redox activity or individual amino acids and mostly a combination of them [87], which are more or less influenced by the lipid oxidation. There are several dye-based assays like the Bradford or Lowry assay and spectroscopic methods (UV absorption or fluorescence). The dye-based assays are based on (metal) complexes with protein structures and also depend on tryptophan and other amino acids to redox reactions. Furthermore these dye protein complexes can be disturbed by solvents/ detergents (e.g. lipids) [87]. As lipid protein co oxidation should introduce many redox active compounds and change the protein structure, the spectroscopic method has been chosen. As the fluorescence of tryptophan is also susceptible for structure changes [88], the absorption of aromatic amino acids has been chosen for protein concentration measurement. The only disadvantage is that tryptophan is partly oxidized during incubation, however the great advantage is, that the method is nondestructive and the sample can be used for further analysis. This point is important as the achieved protein suspension could not be aliquoted to volume with equal concentrations.

The protein concentration was measured by absorption at 278 nm and the absorption coefficient of β -lactoglobulin (βLG , $\epsilon = 17,600 \text{ M}^{-1} \text{ cm}^{-1}$), the main protein of whey (~75 %), is used in combination with its molar mass (M) of 18,300 g/mol to calculate the protein concentration [1, 89]. In the protein carbonyl content measurement, all DNPH (2,4-dinitrophenylhydrazine) treated samples, the absorption at 278 nm of the protein has to be corrected for the absorption of the yellow DNPH at 278 nm, which corresponds to 43 % of its maximum absorption at 370 nm [26]. The protein mass is therefore calculated as followed (1.XXII):

$$m(\text{Protein}) = \frac{M_{\beta\text{LG}}}{\epsilon_{\beta\text{LG}}} \cdot (A_{278 \text{ nm}} - 0.43A_{370 \text{ nm}}) \quad 1.XXII$$

1.3.5.2 Protein Carbonyl Content

Beside the measurement of protein oxidation conducted over the spectroscopic method (tryptophan decrease), dye-based assays are even more common. These methods are the determination of the protein carbonyl content [90] and sulfhydryl content [91]. However, as the aggregation the whey protein is achieved through crosslinking of the thiol groups to sulfide bridges, they could not further oxidized. In contrast, protein carbonyls can easily be measured by derivatization with the dye DNPH, which contains a reactive hydrazine group towards carbonyls (aldehydes and ketones), which form a hydrazone derivative (see Figure 1.11) [26].

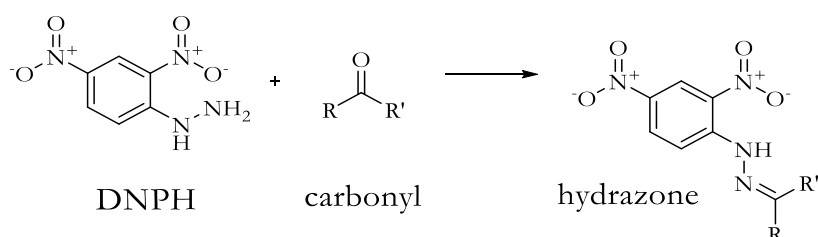


Figure 1.11: Reaction of DNPH with carbonyl to hydrazone derivatives.

In this thesis, the protein carbonyl content was conducted according to Oliver *et al.* with slight modifications [27]. 0.6 mL of the protein extract was precipitated with 1 mL trichloroacetic acid (20 % w/v), which was facilitated to settle down by centrifuging for 5 min at 10,000 g. After discarding the supernatant, the pellet was incubated with 1 mL DNPH solution (0.2 % in 2 M HCl) for 1 h in the dark with agitation in 15 min intervals (DNPH is light sensitive). As not reacted DNPH disturb the absorption measurement, it was removed by an additional precipitation with 1 mL trichloroacetic acid, centrifuged and decanted. Further, the pellet was washed 3 times with 1 L of ethyl acetate/ ethanol (1:1, v/v), each with centrifugation before decanting the supernatant. Finally, the pellet was redissolved in 2 mL guanidine HCl (6 M) phosphate buffer (20 mM, pH 2.3). As the protein only solved slowly, the protein was further incubated at 37 °C for 15 min in a water bath. Still unsolved protein aggregates were removed by centrifuging for 2 min at 10,000 g and if necessary, foam was removed using a plastic spatula. The concentration of hydrazones was measured by the absorption at 370 nm (Helios γ Spectrophotometer, Thermo Electron Corporation, Waltham, USA). The final protein carbonyl content was calculated as followed, using a blank sample to subtract lipid induced modification absorption, whereby in the blank sample the protein was treated with 1 mL HCl (2 M) (see equation 1.XXIII) and an absorption coefficient of 22,000 M⁻¹ cm⁻¹ was used [92].

$$\frac{n(\text{Carbonyl})}{m(\text{Protein})} = \frac{A_{370 \text{ nm}}}{\epsilon_{\text{hydrazone}}} \cdot \frac{\epsilon_{\beta\text{LG}}}{M_{\beta\text{LG}}(A_{278 \text{ nm}} - 0.43A_{370 \text{ nm}})} \left[\frac{\text{nmol}}{\text{mg protein}} \right] \quad 1.\text{XXIII}$$

1.3.5.3 Protein Amino Group Content

The determination of free amines was conducted using a downsized method of [28, 29] with modifications. In this assay, primary amines were derivatized with *ortho*-phthalaldehyde (OPA), whereby the absorption structure (thio-isoindole) is formed (see Figure 1.12), why further cleanup is not necessary like in the protein carbonyl content. Frozen protein extracts were therefore defrosted and vortexed. An aliquot of 500 μL , which leads to a final concentration about 1-20 $\mu\text{g}/\text{mL}$, was added to 150 μL sodium dodecyl sulfate (SDS, 20 wt%) and 2260 μL borate buffer (0.1 M pH 9.3), containing *N*-acetyl-cysteine (0.3 wt%) and incubated for 10 min at 50 $^{\circ}\text{C}$. Thereafter, 90 μL of OPA (3.4 % in MeOH) was added and the sample was incubated for 30 min at 50 $^{\circ}\text{C}$ further. Finally, the sample was cooled down at room temperature for 30 min and the absorbance was recorded at 340 nm. For quantification, a calibration with solutions of L-leucine in a range of 5 μM to 250 μM is used.

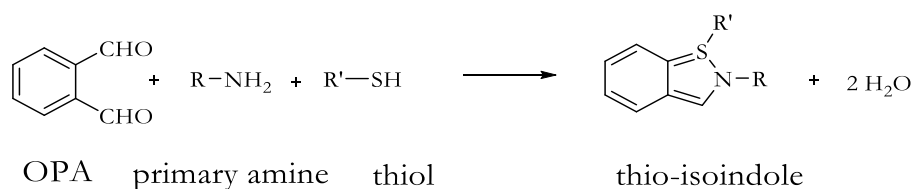


Figure 1.12: Reaction of OPA with primary amine and thiols to thio-isoindole derivatives according to [93].

1.3.5.4 Spectroscopic Methods

Lipidoxidation causes change of the protein structure and modifies proteins (see previous section 1.3.4 Protein oxidation). Therefore spectroscopic methods can be introduced, as electromagnetic waves interact specifically and partly selected with structures behind [25]. In case of infrared waves, structures as molecular groups are excited to rotating and vibrating and their absorption is measured, whereby the strength and frequency of the absorbed wave provide insights to the nature structures. In case of fluorescence spectroscopy, the electromagnetic waves were from higher frequency, which are commonly in the UV-Vis range. Thereby electrons are excited at specific resonance frequencies and emit light of a decreased frequency [25]. In both techniques, a huge amount of data though the complexity of proteins is achieved. In order to detect relevant structures, which are formed or changed by lipid protein co oxidation, partial least squares regression (PLS) was employed (see 1.3.8 Statistical Calculations) using the free statistical software R with the PLS package [94, 95]. This technique provides the detection of correlation of relevant structures and overall oxidation parameters of the sample.

Fluorescence Spectroscopy

The fluorescence formation was recorded using a Cary Eclipse (Varian Agilent, Palo Alto, USA) spectrometer. Two procedures were conducted. The first is the measurement of fluorescence in blank value samples of the protein carbonyl determination, where the protein is precipitated by trichloroacetic acid, incubated in HCl (2 M) and redissolved in guanidine phosphate buffer. Thereby the protein oxidation fluorophores dityrosine and NFK were measured by their known excitation emission combinations (dityrosine: 325 nm, 410 nm [30], NFK 325 nm, 420 nm [31]). In the second procedure, the protein was cut with trypsin to increase the solubility and to provide an equal high hydration of fluorophores. Therefore, 1 mL of protein extract was diluted to a total of 3.2 mL and incubated in 0.05 M TEAA with about 1/20 (w/w) trypsin (160 µg/mL) at 37 °C for 22 h with brief agitating after 20 h. 1 mL was taken from the clear upper phase, diluted with ms-grade water (1/1, v/v) and taken directly for fluorescence measurement. In order to find new fluorophores, fluorescence was recorded in wide range from 400-600 nm (600 nm/min, 5 nm slit) with an extinction from 290-395 nm with 5 nm increment (5 nm slit) by a detector voltage of 600 V. Tyrosine, Phenylalanine and Tryptophan fluorescence was recorded on the same way (emission 260-375 nm, extinction 260-285 nm) by a detector voltage of 500 V in order to follow the oxidation of the aromatic amino acid residues and to determine the solvent environment of the fluorophores, which are known to be influenced by polar solvents [96] and oxidation [97]. All measurements were against blank, containing buffer and trypsin. From the achieved excitation emission fluorescence matrix the known protein oxidation fluorophores are extracted.

Attenuated Total Reflection Fourier Transformation Spectroscopy

ATR-FT-IR spectroscopy was conducted to measure changes in the protein conformation and its modifications. Thereby the ATR technique provides the measurement even of turbid samples like the whey protein oleogels as the IR beam is only reflected at the crystal oleogel surface, which allows the beam to interact with the sample. In advantage to continuous wave techniques, the Fourier transformation (FT) provides a faster measurement, as the measurement beam can be time resolved including all frequencies of the spectrum range. The FT is a calculation, which transfer time resolved data (interferogram) to common frequency resolved data. The used spectrometer was a Confocheck™ Bruker Tensor 2 System (Bruker Optik GmbH, Ettlingen, Germany) optimized for protein analysis in liquids with a thermally controlled BioATR II unit. The spectra were acquired at 20 °C against a stripped oil sample and averaged over 120 scans at a resolution of 4 cm⁻¹. Samples were stored at 4 °C after incubation until measurement. For each time point one sample was measured with 2 technical replicates. Between each measurement, the crystal was washed 10 times by a SDS solution using two syringes and 10 times with a fresh SDS

solution again. A soft tissue was used to dry crystal surface before analysis of the next sample. Data was stored in the .xml format to transfer it into R using the OPUS software (Version 7.5.18 Bruker Optik GmbH)

1.3.6 Chromatography and Mass spectrometry

1.3.6.1 Chromatography

During this thesis liquid and gas chromatography was conducted as it provides the possibility to separate compounds in complex mixtures. Modern chromatography is continuously improved, which increase the resolution power between compounds by decreasing analysis time. However, since the first mention by Field and Tswett before one to two hundred years the principle not changed [98, 99]. A mixture of compounds is transferred (in many times by injecting) to a mobile phase, which can be liquid or gaseous. This phase flows over a mostly solid stationary phase, which is able to retain compounds of the mixture by miscellaneous forces. As these forces on the compounds differs though the structural diversity of the compounds and the compounds are retained differently, the mixture is separated by time. The so called retention time of compound is a constant in a defined system and can used to prove the authenticity of a compound.

1.3.6.2 Mass Spectrometry - Ionizer

Every mass spectrometer consists of three parts: the ionizer, the analyzer and the detector, which principles are mostly easy.

The ionizer is the first part and has the task to ionize molecules, which provide the possibility to manipulate the flow of compounds by magnetic and electric fields. One distinguish between hard and soft ionization. In this thesis hard ionization in form of electron ionization (EI) and soft ionization as electron spray ionization (ESI) has been used. The principle of EI, also known as electron impact ionization, is to transfer molecules through an electron beam, which is generated by heating filaments in the vacuum. In 1 of 10^5 cases, an electron of the beam abstracts an electron of the molecule and generates a radical cation, which are mostly unstable [100]. Thereby, unstable radical cations fragment similar to alkoxy radicals in the lipid oxidation (α -scission) as radicals are mostly generated at atoms with high electron density (e.g. oxygen atoms). In general molecules fragment relatively unselective, but several fragmentation are preferred and form higher amounts of fragments due hyperconjugation of radicals and a lower ionization energy (Stevenson rule) [100]. However, a constant electron beam energy, which is commonly at 70 eV, leads to constant fragmentation patterns. This pattern is used as fingerprint to identify compounds though comparison of fragmentation data bases.

EI is used in GC-MS, where mostly single compounds are ionized at the same time and the eluent is gaseous. In liquid chromatography, the eluent is liquid, which precludes the utilization of EI. Further, mixtures are present, especially in so called shot gun methods, where ionization of many compounds is present at once. That is way, why ESI is used as soft ionization. ESI ionize molecules by protonation or deprotonation, which do not fragment. In more detail, the end of the column ends in a syringe, which is connected to a highly charge electrode. Thereby, the eluent is charged and is sprayed to small liquid droplets at the end of syringe tip. These droplets are dried though dry gas in the chamber (at ambient pressure), coulomb explosion and coulomb fission. Finally, single ion molecules can be formed though evaporation out of a droplet (ion evaporation model) or as charge residue (charge residue model). ESI is much more efficient in the ionization process than EI, and leads to unfragmented molecule ions, which are simpler to interpret. A disadvantage of this technique is, that ESI generate also multicharged compounds, which is especially always the case in proteins as they have many acid residues, and it is sensitive to solved alkali and alkaline earth metals, which leads to positive ion adducts in addition to the proton adducts in the positive ionization mode [101].

1.3.6.3 Mass Spectrometry - Analyzer

Once ionized, molecules are separated from non-ionized compounds though vacuum. Several ion optics, which transfer, focus and accelerate the ions, are also introduced to clean up the ion beam and to transfer it to the analyzer. The task of the analyzer is to manipulate the ion beam ion mass specific, which provides the information which ions are detect later. During this thesis, three kinds of analyzers have been used, which are time of flight (TOF), quadrupole (Q) and FT- ion cyclotron resonance (FT-ICR). The principle of the TOF is well comprehensible. A small sample of the ion beam is accelerated by pulsed electric field with known strength (Voltage U). As all molecules get the same kinetic energy ($E = q \cdot U$) with a charge (q), their velocity differs as they have different masses ($E_{kin} = 0.5 \cdot m \cdot v^2$). Finally, the time of flight is measured for a known distance, which allows calculating the m/z ratio. Another analyzer is a quadrupole, which consist of four parallel bar electrodes [101]. To use the quadrupole as analyzer, electrodes are connected to a direct (DC) and an alternating current (AC), where the opposite electrodes are connected together. By transferring the ion beam through the quadrupole, they are influenced by the oscillating electric field of the bar electrodes and forced to a circular flight though the bars. The underlying function to calculate the exact flight route is complex. However, the alternating current can be seen as filter for low masses, as low masses are too strongly accelerated, collide with the electrodes and get discharged. Contrary, the direct current is a high mass filter, as high masses more influenced by the direct current and get discharged. The AC/DC ration is therefore

adjusted to let only one mass pass the quadrupole, which is detected later. This is different to the before mentioned TOF, which have the same resolution of mass ($R = m/\Delta m$) over the whole spectrum. However, this resolution of the quadrupole is therefore called unity resolution, as the Δm is set to 1 Da over the whole spectra. An exact measurement of the molecule with quadrupoles is therefore not available, but it is sufficient to measure fragment patterns, like by EI ionization. In ESI MS, a quadrupole is very often also used as fragmentation space, to imitate the fragmentation pattern in EI. This case is often called QQQ, triple quadrupole or tandem quadrupole (TQ), as three quadrupole are arranged in a series. The first quadrupole selects a mother ion, which collides with inert gas (mostly N_2 or Ar) and fragments in the second quadrupole. The fragmentation ions, so called daughter ions, are then analyzed by the third quadrupole. This double step process is in advantage to the EI, because it leads to highly selective measurements, which are very sensitive though the effective ESI ionization. Quadrupole and TOF techniques can be also combined. A TQ apparatus, in which the third quadrupole is replaced with a TOF, is called QTOF, which have the advantage of a higher resolution of the daughter ions [101].

The resolution of a TOF apparatus is limited to their flight range. Therefore the first evolution of TOFs is a reflectron, which doubles this range. However, a consequent evolution is to force ions in a circle path. This is the case in an ICR MS, where ions are forced by a strong magnetic field (~ 7 T, in this thesis) into an orbit in an ICR cell (see Figure 1.13). This orbit is expanded, when the mass dependent frequency of the orbit excited by the oscillating excitation plate by a resonance frequency. As the molecules travels in a so called cyclotron motion (nearly circular), they achieve large distances (~ 30 km/s), which gives ICR MS a very high resolution power to about 6 places after the decimal point [102]. This provides the possibility to distinguish between different isotopes of elements and to the determination of the isotopic pattern. This isotopic pattern can be used to verify and predict the sum formula of a compound, which is an additional information besides already high selective precise the molar mass. In addition, ICR excitation is conducted at each compound at once, which can give time and sensitivity advantage [102].

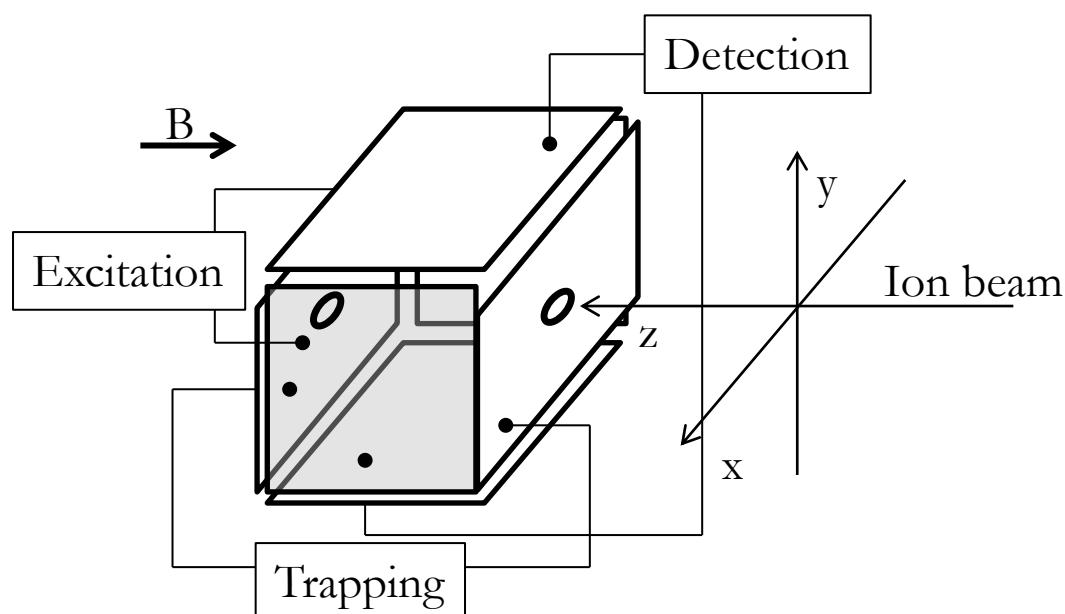


Figure 1.13: ICR cell, ions trapped in a cube of 3 pairs of electric plates, with specific functions.

1.3.6.4 Mass Spectrometry - Detector

The task of the detector is to convert the physical information of upcoming ions into electrical signals. In quadrupole and TOF apparatus therefore electron multiplier are used to amplify the signal, as the amount of charge of ions do not be sufficient alone. Thereby, the signal is multiplied by impacts of the ions on an electron emissive material in a serial structure, as emitted electrons will lead to further emitted electrons, too. Consequently, the signal is increased exponentially and can detect. This type of detection can be seen as direct and destructive. In contrast the detection in ICR-MS is indirect and nondestructive. Here, the ions are forced in a circular motion between the two detector plates. By excitation, a broad spectrum of masses is excited at once like in NMR measurements. Compounds are excited to their mass specific orbits with given mass dependent frequencies. Each compound, with its own mass dependent frequency, induced an electric current in the detector plates. As the ions fly in a circular motion, the signal of the current is the sum of sinus waves for all compounds. This signal is time depended, which looks like a noise on a music oscillator and is similar as the free induced decay (FID) in NMR spectroscopy. This time dependent signal (signal vs time) is in the end translated to a frequency based spectrum (intensity vs frequency) by Fourier transformation. In brief, the factors of a series of sinus waves are fitted to the signal. Thereby, the sum of the different sinus waves results in the shape of the “noise” and the factors of the sinus wave represent the different frequencies [102].

1.3.7 Measurement of Oleogel Properties

1.3.7.1 Rheology

Oleogels prepared in this thesis differ in their consistency, which belongs to several reasons. On the one hand it is known, that water addition leads to connection of protein aggregates by capillary forces, which strengthen the gel [67]. On the other hand, it was observed that the whey protein aggregates, which were prepared by the freeze drying technique, usually produce somewhat softer gels, which most likely relies on greater protein aggregates produced during the freezing process. To quantitate these findings, oscillation rheology was conducted to measure the robustness and strength of gels. Therefore a frequency sweep test was carried out ($\omega = 1 - 100$ 1/s) at a deformation of 1 %, which is safely in the linear viscoelastic region [67], on a plate-plate system (diameter 25 mm) with a gap of 1 mm at 20 °C (Modular Compact Rheometer MCR 302, Anton Paar GmbH). Measurements were repeated in duplicate with two technical duplicates for each sample. This measurement allowed a direct comparison to the macroscopic properties of the gels obtained from snap frozen lyophilized protein and the gels obtained by solvent exchange gels by de Vries *et al.* [67] and is especially useful to account water droplets in the gel, which are crucial for lipid oxidation.

1.3.7.2 Water Activity

The water activity (a_w) of the samples was determined with an electronic measuring instrument for water activity (AW SPRINT TH-500, novasina). A sufficient amount of substance milled with in little plastic cups and used for the determination. The temperature during a_w measurement was at 25 °C and an 1 min stable time was used as end condition.

1.3.7.3 Water Content

Water content of oleogels were determined gravimetrically by the dry mass [76]. 2 ± 0.1 g were placed in aluminum caps with known weight, dried for 4 h at 105 °C and reweighted after cooling down in a desiccator for 30 min. This procedure was repeated for 1 h to guarantee mass constancy. Water content was now calculated as mass difference in relation to the original mass (water content [%] = $100\% * [m_0 - m(\text{constancy})] / m_0$).

1.3.8 Statistical Calculations

1.3.8.1 Multivariate Analysis

Lipid oxidation as well as lipid protein cooxidation is a complex process, in which manifold compounds and pathways exist. This phenomenon is commonly handled on the one side by products, which represents causative reactions, e.g. lipid hydroperoxides or protein carbonyls, which can be measured as a whole class of products and on the other side by specific products, which are more or less specific, e.g. break down products like hexanal or protein modifications like EMP-Lysine. This both ways of handling presuppose a specific knowledge of the processes, which could make it difficult to interpret results further, as no new compounds are involved and relations are postulated before. Multivariate data analysis provides here a powerful tool, as this is independent of the relation between variables and knowledge and which can also handle the full information given by modern spectroscopic and spectrometric methods. In addition, modern computer power and free statistical software (R) [94] make it easy to calculate also with very large data sets. Therefore, the multivariate data analysis of complex lipid protein cooxidation should be in advantage, as specific and common reaction markers are sometimes lacking. Furthermore, the statistic provides new insights into the relation and importance of single products in a network of other compounds, which can be used to cluster samples or even predict attributes and can also be used to interpret the whole lipid protein cooxidation.

Two common multivariate statistics are principal component analysis (PCA) and partial linear least squares regression (PLS), which both are cognate methods. An in-depth mathematical explanation lies outside of space of this thesis and the interested reader is referred elsewhere [103]. All determinations are done with the free statistical software R, which provides access to PCA functions without further software [94], and PLS function is available in the free R package PLS [95] with default parameters, unless otherwise noted. This would mean that the data is centered (abstraction of the mean).

In brief, when the original data is given as a matrix X for PLS, this matrix can be described by a product of two other matrixes, which are called loading and score matrix. This both matrixes are similar as used in PCA, whereas the loadings represent the weight of each variable in the principal components, which is important for interpretation. The score matrix represents the original data in a rotated coordinate system with the principal components as axes. In the PLS algorithm the covariation of the scores of X and the scores of Y (second data input, which one tries to correlate) is maximized. Therefore, the algorithm filters relevant variables of X and Y that are causative for correlation.

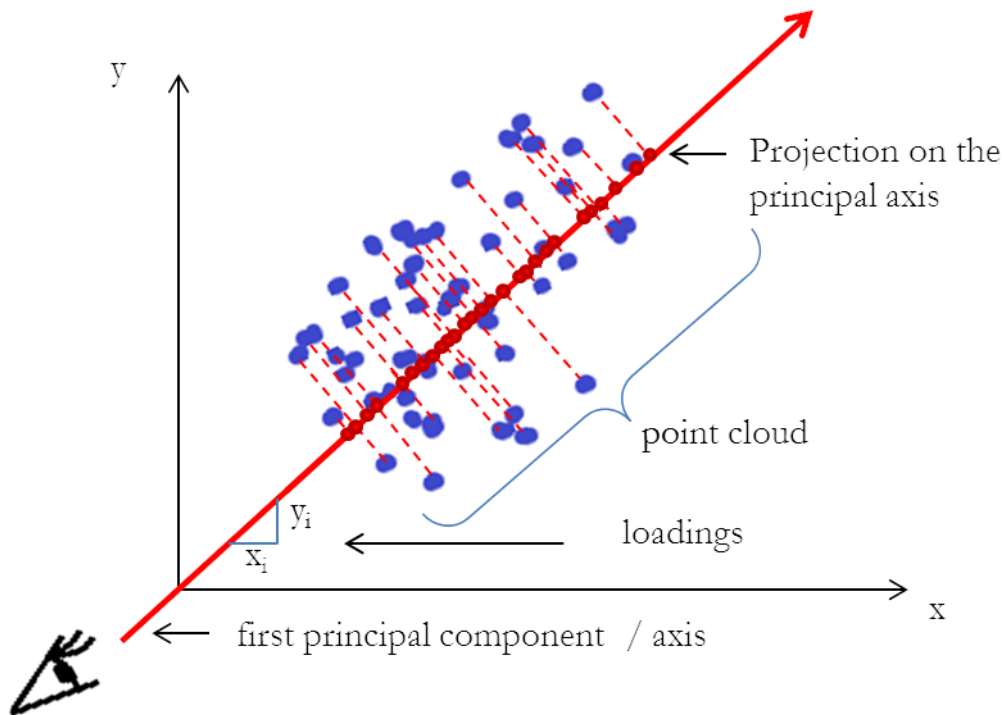


Figure 1.14: first principal axis/ component in a 2D coordinate system.

PCA and PLS are based on finding eigenvectors with highest eigenvalues (explain most of variation) and these are defined orthogonal to each other. This makes a concept to explain it non mathematical by projections (see Figure 1.14). In the given data set with n variables, each variable represent an axis of a coordinate system with n axes. The measured samples will lead to a cloud of points. The trick is to find a new angle of view, whereas most of the information is seen at once, or in other words: the cloud is looking the smallest and densest. In this case, projections of the points on the new axis are distributed most greatly. This direction can also be interpreted as a vector, which is a linear combination of all other axes/ variables and will be called the first principal component. The second component is orthogonal to the first, which means that we now searching for the smallest and densest cloud of points by looking orthogonal to a rotating first principal axis and so on. In case of PLS, the resulting rotated coordinate system is related to the target rotated coordinate system (or single variable vector), which provides the possibility to “translate” original data to the target, which one would like to correlate, as the ways to move data from one coordinate system to another a known in the loadings.

1.3.8.2 Regression of Nonlinear Functions

Nonlinear regressions can easily done in the free software R with the package `minpack.lm` [104], which is based on the method of least squares using the Levenberg-Marquardt algorithm. The interested reader is directed to the literature. Thereby, parameters are fitted to minimize the difference between the expected values and values obtained by the model function. This usually

provides good estimates of the parameters, but no information about the certainty is given. This could be achieved by a linear regression of expected values vs. fitted values, where the calculated slope is checked for significance to the difference to 1. This T-test provides a probability (the p-value), by which the fit can safely be rejected. However, this does not provide direct information of the quality of the fit. Therefore, a parameter free method is used for estimating the standard deviation, which is called Jack knife delete one procedure [105], where each data point's relevance is considered by a bootstrapping technique. In the data with n points n subsets were created with each missing another one of the n points. Jack knife estimation of the standard deviation is now calculated based on the standard deviation of the fitting results of all n subsets, which is corrected by the factor of $(n-1) / \text{square root}(n)$ for reasons, which belong to the decreased degrees of freedom.

References

- [1] Belitz, H. D., Grosch, W., Schieberle, P., *Lehrbuch der Lebensmittelchemie*, Springer, Garching 2007.
- [2] Berg, J. M., Tymoczko, J. L., Stryer, L. (Eds.), *Stryer Biochemie*, Springer Berlin Heidelberg, Berlin, Heidelberg 2013.
- [3] Narayan, B., Miyashita, K., Hosakawa, M., Physiological Effects of Eicosapentaenoic Acid (EPA) and Docosahexaenoic Acid (DHA)—A Review. *Food Reviews International* 2006, 22, 291–307.
- [4] Gunstone, F. D., Hilditch, T. P., 220. The union of gaseous oxygen with methyl oleate, linoleate, and linolenate. *Journal of the Chemical Society (Resumed)* 1945, 836–841.
- [5] Holman, R. T., Elmer, O. C., The rates of oxidation of unsaturated fatty acids and esters. *J. Am. Oil Chem. Soc.* 1947, 24, 127–129.
- [6] Gardner, H. W., Lipid hydroperoxide reactivity with proteins and amino acids: A review. *J. Agric. Food. Chem.* 1979, 27, 220–229.
- [7] Davies, M. J., The oxidative environment and protein damage. *Biochimica et biophysica acta* 2005, 1703, 93–109.
- [8] Jackson, L. S., Chemical food safety issues in the United States: Past, present, and future. *Journal of agricultural and food chemistry* 2009, 57, 8161–8170.
- [9] Hidalgo, F. J., Zamora, R., Amino acid degradations produced by lipid oxidation products. *Critical reviews in food science and nutrition* 2016, 56, 1242–1252.
- [10] MacGregor, J. T., Wilson, R. E., Neff, W. E., Frankel, E. N., Mutagenicity tests of lipid oxidation products in *Salmonella typhimurium*: Monohydroperoxides and secondary

- oxidation products of methyl linoleate and methyl linolenate. *Food and Chemical Toxicology* 1985, 23, 1041–1047.
- [11] Martinet, W., Kockx, M. M., Apoptosis in atherosclerosis: Focus on oxidized lipids and inflammation. *Current opinion in lipidology* 2001, 12, 535–541.
- [12] Schaich, K. M., in: Kamal-Eldin, A., Min, D. B. (Eds.), *Lipid oxidation pathways*, AOCS Press, Urbana, Ill. 2008.
- [13] Papuc, C., Goran, G. V., Predescu, C. N., Nicorescu, V., Mechanisms of Oxidative Processes in Meat and Toxicity Induced by Postprandial Degradation Products: A Review. *Compr. Rev. Food Sci. Food Saf.* 2017, 16, 96–123.
- [14] Friedman, M., Cuq, J. L., Chemistry, analysis, nutritional value, and toxicology of tryptophan in food. A review. *J. Agric. Food. Chem.* 1988, 36, 1079–1093.
- [15] Waraho, T., McClements, D. J., Decker, E. A., Mechanisms of lipid oxidation in food dispersions. *Trends in Food Science & Technology* 2011, 22, 3–13.
- [16] Stadtman, E. R., Oxidation of free amino acids and amino acid residues in proteins by radiolysis and by metal-catalyzed reactions. *Annual review of biochemistry* 1993, 62, 797–821.
- [17] Hensley, K., Floyd, R. A., Reactive Oxygen Species and Protein Oxidation in Aging: A Look Back, A Look Ahead. *Archives of Biochemistry and Biophysics* 2002, 397, 377–383.
- [18] Ingold, K. U., Pratt, D. A., Advances in Radical-Trapping Antioxidant Chemistry in the 21st Century: A Kinetics and Mechanisms Perspective. *Chemical Reviews* 2014, 114, 9022–9046.
- [19] Shahidi, F., Wanasundara, U. N., Methods for measuring oxidative rancidity in fats and oils. *Food lipids: Chemistry, nutrition and biotechnology* 2002, 17, 387–403.
- [20] Viljanen, K., Kivikari, R., Heinonen, M., Protein-lipid interactions during liposome oxidation with added anthocyanin and other phenolic compounds. *J. Agric. Food. Chem.* 2004, 52, 1104–1111.
- [21] Labuza, T. P., Dugan, L. R., Kinetics of lipid oxidation in foods. *C R C Critical Reviews in Food Technology* 1971, 2, 355–405.
- [22] Semenov, N. N., *Some problems in chemical kinetics and reactivity, Volume II* 1959.
- [23] Budilarto, E. S., Kamal-Eldin, A., The supramolecular chemistry of lipid oxidation and antioxidation in bulk oils. *European Journal of Lipid Science and Technology* 2015, 117, 1095–1137.
- [24] Brimberg, U. I., Kamal-Eldin, A., On the kinetics of the autoxidation of fats: Influence of pro-oxidants, antioxidants and synergists. *European Journal of Lipid Science and Technology* 2003, 105, 83–91.
- [25] Atkins, P. W., Paula, J. de, Bär, M., Schleitner, A., Heinisch, C., *Physikalische Chemie*, Wiley 2006.
- [26] Keyse, S. M., *Stress response: Methods and protocols*, Springer Science & Business Media 2000.

- [27] Oliver, C. N., Ahn, B. W., Moerman, E. J., Goldstein, S., Stadtman, E. R., Age-related changes in oxidized proteins. *Journal of Biological Chemistry* 1987, 262, 5488–5491.
- [28] Rade-Kukic, K., Schmitt, C., Rawel, H. M., Formation of conjugates between β -lactoglobulin and allyl isothiocyanate: Effect on protein heat aggregation, foaming and emulsifying properties. *Food Hydrocolloids* 2011, 25, 694–706.
- [29] Roth, M., Fluorescence reaction for amino acids. *Analytical Chemistry* 1971, 43, 880–882.
- [30] Prütz, W. A., Butler, J., Land, E. J., Phenol Coupling Initiated by One-electron Oxidation of Tyrosine Units in Peptides and Histone. *International Journal of Radiation Biology and Related Studies in Physics, Chemistry and Medicine* 1983, 44, 183–196.
- [31] FUKUNAGA, Y., KATSURAGI, Y., IZUMI, T., SAKIYAMA, F., Fluorescence Characteristics of Kynurenine and N'-Formylkynurenine, Their Use as Reporters of the Environment of Tryptophan 62 in Hen Egg-White Lysozyme 1. *jb* 1982, 92, 129–141.
- [32] Uchida, K., Kanematsu, M., Sakai, K., Matsuda, T., Hattori, N., Mizuno, Y., Suzuki, D., Miyata, T., Noguchi, N., Niki, E., Osawa, T., Protein-bound acrolein: Potential markers for oxidative stress. *Proceedings of the National Academy of Sciences of the United States of America* 1998, 95, 4882–4887.
- [33] Ichihashi, K., Osawa, T., Toyokuni, S., Uchida, K., Endogenous formation of protein adducts with carcinogenic aldehydes: Implications for oxidative stress. *The Journal of biological chemistry* 2001, 276, 23903–23913.
- [34] Garrison, W. M., Reaction mechanisms in the radiolysis of peptides, polypeptides, and proteins. *Chemical Reviews* 1987, 87, 381–398.
- [35] Frankel, E. N., *Lipid oxidation*, Elsevier 2014.
- [36] Newman, E. S.R., Rice-Evans, C. A., Davies, M. J., Identification of initiating agents in myoglobin-induced lipid peroxidation. *Biochemical and Biophysical Research Communications* 1991, 179, 1414–1419.
- [37] Bolland, J. L., Kinetics of olefin oxidation. *Q. Rev., Chem. Soc.* 1949, 3, 1.
- [38] Bolland, J. L., Gee, G., Kinetic studies in the chemistry of rubber and related materials. III. Thermochemistry and mechanisms of olefin oxidation. *Trans. Faraday Soc.* 1946, 42, 244.
- [39] MALONEY, J. F., Labuza, T. P., WALLACE, D. H., KAREL, M., Autoxidation of Methyl Linoleate in Freeze-Dried Model Systems. I. Effect of Water on the Autocatalyzed Oxidation. *Journal of Food Science* 1966, 31, 878–884.
- [40] Labuza, T. P., Tsuyuki, H., Karel, M., Kinetics of linoleate oxidation in model systems. *Journal of the American Oil Chemists Society* 1969, 46, 409–416.
- [41] Crapiste, G. H., Bredvan, M. I. V., Carelli, A. A., Oxidation of sunflower oil during storage. *Journal of the American Oil Chemists Society* 1999, 76, 1437.

- [42] Badings, H. T., *Cold-storage defects in butter and their relation to the autoxidation of unsaturated fatty acids*, Wageningen 1970.
- [43] Howell, N. K., Herman, H., Li-Chan, E. C. Y., Elucidation of Protein–Lipid Interactions in a Lysozyme–Corn Oil System by Fourier Transform Raman Spectroscopy. *J. Agric. Food. Chem.* 2001, *49*, 1529–1533.
- [44] Gießauf, A., van Wickern, B., Simat, T., Steinhart, H., Esterbauer, H., Formation of N-formylkynurenine suggests the involvement of apolipoprotein B-100 centered tryptophan radicals in the initiation of LDL lipid peroxidation. *FEBS Letters* 1996, *389*, 136–140.
- [45] Kikugawa, K., Kato, T., Hayasaka, A., Formation of dityrosine and other fluorescent amino acids by reaction of amino acids with lipid hydroperoxides. *Lipids* 1991, *26*, 922.
- [46] Berlett, B. S., Stadtman, E. R., Protein Oxidation in Aging, Disease, and Oxidative Stress. *Journal of Biological Chemistry* 1997, *272*, 20313–20316.
- [47] Simpson, J. A., Narita, S., Gieseg, S., Gebicki, S., Gebicki, J. M., Dean, R. T., Long-lived reactive species on free-radical-damaged proteins. *The Biochemical journal* 1992, *282 (Pt 3)*, 621–624.
- [48] Schaich, K. M., Pryor, W. A., Free radical initiation in proteins and amino acids by ionizing and ultraviolet radiations and lipid oxidation — part I: Ionizing radiation. *C R C Critical Reviews in Food Science and Nutrition* 1980, *13*, 89–129.
- [49] Malshet, V. G., Al Tappel, L., Fluorescent products of lipid peroxidation: I. Structural requirement for fluorescence in conjugated schiff bases. *Lipids* 1973, *8*, 194–198.
- [50] Kikugawa, K., Ido, Y., Studies on peroxidized lipids. V. Formation and characterization of 1,4-dihydropyridine-3,5-dicarbaldehydes as model of fluorescent components in lipofuscin. *Lipids* 1984, *19*, 600–608.
- [51] Kikugawa, K., Ido, Y., Mikami, A., Studies on peroxidized lipids. VI. Fluorescent products derived from the reaction of primary amines, malonaldehyde and monofunctional aldehydes. *J Am Oil Chem Soc* 1984, *61*, 1574–1581.
- [52] Amarnath, V., Valentine, W. M., Montine, T. J., Patterson, W. H., Amarnath, K., Bassett, C. N., Graham, D. G., Reactions of 4-hydroxy-2(E)-nonenal and related aldehydes with proteins studied by carbon-13 nuclear magnetic resonance spectroscopy. *Chemical research in toxicology* 1998, *11*, 317–328.
- [53] Liu, Z., Sayre, L. M., Model Studies on the Modification of Proteins by Lipoxidation-Derived 2-Hydroxyaldehydes. *Chemical research in toxicology* 2003, *16*, 232–241.
- [54] Zhu, M., Spink, D. C., Yan, B., Bank, S., DeCaprio, A. P., Formation and Structure of Crosslinking and Monomeric Pyrrole Autoxidation Products in 2, 5-Hexanedione-Treated Amino Acids, Peptides, and Protein1. *Chemical research in toxicology* 1994, *7*, 551–558.

- [55] Hidalgo, F. J., Alaiz, M., Zamora, R., Effect of pH and Temperature on Comparative Nonenzymatic Browning of Proteins Produced by Oxidized Lipids and Carbohydrates. *J. Agric. Food. Chem.* 1999, *47*, 742–747.
- [56] Zamora, R., Alaiz, M., Hidalgo, F. J., Contribution of Pyrrole Formation and Polymerization to the Nonenzymatic Browning Produced by Amino–Carbonyl Reactions. *J. Agric. Food. Chem.* 2000, *48*, 3152–3158.
- [57] Zamora, R., Hidalgo, F. J., Comparative methyl linoleate and methyl linolenate oxidation in the presence of bovine serum albumin at several lipid/protein ratios. *J. Agric. Food. Chem.* 2003, *51*, 4661–4667.
- [58] Zhang, W.-H., Liu, J., Xu, G., Yuan, Q., Sayre, L. M., Model studies on protein side chain modification by 4-oxo-2-nonenal. *Chemical research in toxicology* 2003, *16*, 512–523.
- [59] Zamora, R., Hidalgo, F. J., 2-Alkylpyrrole formation from 4,5-epoxy-2-alkenals. *Chemical research in toxicology* 2005, *18*, 342–348.
- [60] Tang, D., Marangoni, A. G., Quantitative study on the microstructure of colloidal fat crystal networks and fractal dimensions. *Advances in Colloid and Interface Science* 2006, *128-130*, 257–265.
- [61] Patel, A. R., *Alternative Routes to Oil Structuring*, Springer International Publishing 2015.
- [62] Gravelle, A. J., Barbut, S., Marangoni, A. G., Ethylcellulose oleogels: Manufacturing considerations and effects of oil oxidation. *Food Research International* 2012, *48*, 578–583.
- [63] Jang, A., Bae, W., Hwang, H.-S., Lee, H. G., Lee, S., Evaluation of canola oil oleogels with candelilla wax as an alternative to shortening in baked goods. *Food Chemistry* 2015, *187*, 525–529.
- [64] Daniel, J., Rajasekharan, R., Organogelation of plant oils and hydrocarbons by long-chain saturated FA, fatty alcohols, wax esters, and dicarboxylic acids. *Journal of the American Oil Chemists Society* 2003, *80*, 417–421.
- [65] Vries, A. de, Hendriks, J., van der Linden, E., Scholten, E., Protein Oleogels from Protein Hydrogels via a Stepwise Solvent Exchange Route. *Langmuir* 2015, *31*, 13850–13859.
- [66] Vries, A. de, Wesseling, A., van der Linden, E., Scholten, E., Protein oleogels from heat-set whey protein aggregates. *Journal of Colloid and Interface Science* 2017, *486*, 75–83.
- [67] Vries, A. de, Jansen, D., van der Linden, E., Scholten, E., Tuning the rheological properties of protein-based oleogels by water addition and heat treatment. *Food Hydrocolloids* 2018, *79*, 100–109.
- [68] Vries, A. de, Lopez Gomez, Y., Jansen, B., van der Linden, E., Scholten, E., Controlling Agglomeration of Protein Aggregates for Structure Formation in Liquid Oil: A Sticky Business. *ACS Applied Materials & Interfaces* 2017, *9*, 10136–10147.

- [69] Lee, J., Cheng, Y., Critical freezing rate in freeze drying nanocrystal dispersions. *Journal of Controlled Release* 2006, 111, 185–192.
- [70] Souci, S. W., Fachmann, W., Kraut, H., Scherz, H., Senser, F. (Eds.), *Food composition and nutrition tables: Die Zusammensetzung der Lebensmittel, Nährwert-Tabellen*, MedPharm Scientific Publishers, CRC Press, Stuttgart 2000.
- [71] Lampi, A.-M., Kamal-Eldin, A., Effect of α - and γ -tocopherols on thermal polymerization of purified high-oleic sunflower triacylglycerols. *J. Amer. Oil Chem. Soc.* 1998, 75, 1699–1703.
- [72] Stöckmann, H., Schwarz, K., Huynh-Ba, T., The influence of various emulsifiers on the partitioning and antioxidant activity of hydroxybenzoic acids and their derivatives in oil-in-water emulsions. *J. Amer. Oil Chem. Soc.* 2000, 77, 535–542.
- [73] Thiyam, U., Stöckmann, H., Schwarz, K., Antioxidant activity of rapeseed phenolics and their interactions with tocopherols during lipid oxidation. *J. Amer. Oil Chem. Soc.* 2006, 83, 523–528.
- [74] Chan, H. W.-S., Levett, G., Autoxidation of methyl linoleate. Separation and analysis of isomeric mixtures of methyl linoleate hydroperoxides and methyl hydroxylinoleates. *Lipids* 1977, 12, 99–104.
- [75] Loftus Hills, G., Thiel, C. C., 338. The ferric thiocyanate method of estimating peroxide in the fat of butter, milk and dried milk. *Journal of Dairy Research* 1946, 14, 340–353.
- [76] Matissek, R., Steiner, G., *Lebensmittelanalytik*, Springer Berlin Heidelberg New York, Berlin, Heidelberg 2006.
- [77] Wheeler, D. H., Peroxide formation as a measure of autoxidative deterioration. *J. Amer. Oil Chem. Soc.* 1932, 9, 89–97.
- [78] Redemann, C. E., Peroxides in Isopropanol. *Journal of the American Chemical Society* 1942, 64, 3049–3050.
- [79] Lea, C. H., Methods for determining peroxide in lipids. *Journal of the Science of Food and Agriculture* 1952, 3, 586–594.
- [80] Bolland, J. L., Kinetic studies in the chemistry of rubber and related materials. I. The thermal oxidation of ethyl linoleate. *Proceedings of the Royal Society of London. Series A. Mathematical and Physical Sciences* 1946, 186, 218–236.
- [81] Drusch, S., Serfert, Y., Scampicchio, M., Schmidt-Hansberg, B., Schwarz, K., Impact of Physicochemical Characteristics on the Oxidative Stability of Fish Oil Microencapsulated by Spray-Drying. *J. Agric. Food. Chem.* 2007, 55, 11044–11051.
- [82] Hübschmann, H.-J., *Handbuch der GC/MS: Grundlagen und Anwendung*, Wiley Online Library 1996.

- [83] Frankel, E. N., Formation of headspace volatiles by thermal decomposition of oxidized fish oils vs. oxidized vegetable oils. *J. Amer. Oil Chem. Soc.* 1993, *70*, 767–772.
- [84] Liu, K.-S., Preparation of fatty acid methyl esters for gas-chromatographic analysis of lipids in biological materials. *J. Amer. Oil Chem. Soc.* 1994, *71*, 1179–1187.
- [85] Butte, W., Rapid method for the determination of fatty acid profiles from fats and oils using trimethylsulphonium hydroxide for transesterification. *Journal of Chromatography A* 1983, *261*, 142–145.
- [86] Yamauchi, K., Tanabe, T., Kinoshita, M., Trimethylsulfonium hydroxide: A new methylating agent. *The Journal of Organic Chemistry* 1979, *44*, 638–639.
- [87] Noble, J. E., Bailey, M. J.A., in: Burgess, R. R., Deutscher, M. P. (Eds.), *Methods in Enzymology : Guide to Protein Purification, 2nd Edition*, Academic Press 2009, pp. 73–95.
- [88] Chen, Y., Barkley, M. D., Toward understanding tryptophan fluorescence in proteins. *Biochemistry* 1998, *37*, 9976–9982.
- [89] Keppler, J. K., Koudelka, T., Palani, K., Stuhldreier, M. C., Temps, F., Tholey, A., Schwarz, K., Characterization of the covalent binding of allyl isothiocyanate to β -lactoglobulin by fluorescence quenching, equilibrium measurement, and mass spectrometry. *Journal of biomolecular structure & dynamics* 2014, *32*, 1103–1117.
- [90] Levine, R. L., Garland, D., Oliver, C. N., Amici, A., Climent, I., Lenz, A.-G., Ahn, B.-W., Shaltiel, S., Stadtman, E. R., in: *Methods in enzymology*, Elsevier 1990, pp. 464–478.
- [91] Sedlak, J., Lindsay, R. H., Estimation of total, protein-bound, and nonprotein sulfhydryl groups in tissue with Ellman's reagent. *Analytical Biochemistry* 1968, *25*, 192–205.
- [92] Johnson, G. D., Correlation of color and constitution. I. 2, 4-Dinitrophenylhydrazones. *Journal of the American Chemical Society* 1953, *75*, 2720–2723.
- [93] Simons Jr, S. S., Johnson, D. F., The structure of the fluorescent adduct formed in the reaction of o-phthalaldehyde and thiols with amines. *Journal of the American Chemical Society* 1976, *98*, 7098–7099.
- [94] Team, R. C., R: A Language and Environment for Statistical Computing 2015, Vienna, Austria, <https://www.R-project.org/>.
- [95] Mevik, B.-H., Wehrens, R., Liland, K. H., pls: Partial Least Squares and Principal Component Regression 2018, <https://CRAN.R-project.org/package=pls>.
- [96] Eftink, M. R., *Fluorescence Techniques for Studying Protein Structure* 1991.
- [97] Estévez, M., Kylli, P., Puolanne, E., Kivikari, R., Heinonen, M., Fluorescence spectroscopy as a novel approach for the assessment of myofibrillar protein oxidation in oil-in-water emulsions. *Meat Science* 2008, *80*, 1290–1296.

- [98] Field, G., *Chromatography, Or, A Treatise on Colours and Pigments, and of Their Powers in Painting*, *etc.*, Charles Tilt 1835.
- [99] Abraham, M. H., 100 years of chromatography—or is it 171? *Journal of Chromatography A* 2004, *1061*, 113–114.
- [100] McLafferty, F. W., Tureček, F., Turecek, F., *Interpretation of mass spectra*, University science books 1993.
- [101] Hesse, M., Meier, H., Zeeh, B., *Spektroskopische Methoden in der organischen Chemie*, Georg Thieme Verlag, Stuttgart 2005.
- [102] Marshall, A. G., Hendrickson, C. L., Jackson, G. S., Fourier transform ion cyclotron resonance mass spectrometry: A primer. *Mass Spectrometry Reviews* 1998, *17*, 1–35.
- [103] Geladi, P., Kowalski, B. R., Partial least-squares regression: A tutorial. *Analytica Chimica Acta* 1986, *185*, 1–17.
- [104] Elzhov, T. V., Mullen, K. M., Spiess, A.-N., Bolker, B., minpack.lm: R Interface to the Levenberg-Marquardt Nonlinear Least-Squares Algorithm Found in MINPACK, Plus Support for Bounds 2015.
- [105] Quenouille, M. H., Notes on Bias in Estimation. *Biometrika* 1956, *43*, 353.

Chapter 2

Protein Amino Acid Lipid Co Oxidation – Low Moisture Suspensions and Oleogels – Preliminary Investigations

2.1 Introduction

Low moisture suspensions are common components or ingredients our daily nutrition. Therefore they contain lipids among other compounds like proteins, carbohydrates and other minor compounds. As lipids in those low moisture suspensions are very prone to oxygen, these suspensions usually contain unsaturated lipids in only small amounts or the lipid is accompanied with antioxidants. However, oxidization can never fully prohibited since oxidation of lipids is an autocatalyzed process [1]. In addition, due the complexity ingredients, lipid oxidation is influenced by all of the compounds in the food. Thereby, typical oxidation marker compounds of lipids underlie further decomposition reactions with e. g. amino acids in these dry foods. Therefore, it can be difficult to determine the state of the “true” oxidation of an unknown sample. The aim of the present study is to investigate such influences on lipid oxidation in “complex” system and especially the influence of amino acids. It is known, that lipid oxidation occurs is catalyzed on surfaces and interfaces, especially in emulsions [2]. We therefore hypothesize, that lipid oxidation in low moisture suspensions occurs on different reaction regions in complex food mixtures, too. Further, these reaction sites are physical separated in powdered samples and will have different oxidation characteristics. As water is known to have a distinct impact on lipid oxidation [1], water is especially relevant and is used in changing amounts and complexation types, which is conducted using water activity implementing substances. To special interest are also amino acids. Free amino acids have mostly an amphilic character and are introduced in all of these interfaces. Further, oxidation of leucine have one of the highest interactions rates with lipid hydroperoxides [3] and is oxidized to the Strecker aldehyde 3-methylbutanal (3MB, also known as isovaleraldehyde), which could easily be determined beside the lipid oxidation volatiles. Therefore, leucine is an interesting candidate for the determination of influence of the lipid oxidation in interfaces on amino acids and proteins.

To focus on the lipid protein co oxidation, which could be also bidirectional, a simple two compound system of lipids and proteins is used. Protein network structured lipids, which are introduced to avoid *trans* fatty acids related hydrogenated fats [4], are foods of interest. In such gels, so called organogels or oleogels, lipid oxidation is less investigated and no studies especially to the modification on the proteins in such gels is done so far (known by the author at start of this study). In comparison to emulsions, oleogels are free of lipid droplets and emulsifiers; lacking physical instability and accompanied complex influences by all them knowing as polar paradox [2]. We therefore hypothesize, that the lipid protein interface in such a system is the dominating

structure and therefore the underlying reaction site of lipid oxidation in such systems, whereby proteins were modified through lipid oxidation products. Such modifications may result in the formation of fluorescent products due radicals like dityrosine and *N*-Formylkynurenine and carbonylation through the addition of lipid oxidation carbonyl compounds [5].

2.2 Material & Methods

Al₂O₃, CaCl₂, FeSO₄, guanidine hydrochloride, hydrochloric acid, trichloroacetic acid, L-Lysine and silica gel (60, 0.04-0.063 mm) were purchased from Roth, (Karlsruhe, Germany). L-Leucine was applied from AppliChem (Darmstadt, Germany) and Methylcellulose, (Metolose, MCE 4 /15) were purchased from Shin Etsu Chemical Co. Ltd. (Wiesbaden, Germany). Sea sand was from Merck (Darmstadt, Germany) DNPH was from Sigma Aldrich (Steinheim, Germany). Corn starch (C* gel 03401) was achieved from Cargill (Krefeld, Germany). Whey protein isolate (BiPro) was obtained from Davisco Foods International with 97.7 % protein and 75 % β-lactoglobulin in dry matter according to [6]. Oleic acid rich safflower oil was purchased in a local supermarket (fatty acid composition according to [7] using authentic standards for calibration (supelco 37 FAME Mix): C16:0= 4.65 ± 0.02 %, C18:0= 2.38 ± 0.02 %, C18:1= 76.7 ± 0.2 %, 18:2= 14.7 ± 0.03 %, 18:3= 0.14 ± 0.01 %). All solvents were from VWR (Fontenay-sous-Bois, France). All chemicals were at least from high purity. Water (>18.2 MΩ) was purified by an Elga Veolia system (Celle, Germany) and was used for all the experiments. All chemicals were at least from high purity.

Purification of Safflower Oil

The purification of safflower oil from natural antioxidants and trace metals was based on the method described by Lampi & Kamal-Eldin [8]. A glass column, wrapped with aluminum foil to prevent light induced oxidation, was packed with 250 g of activated alumina (100 °C for 8 h followed by 200 °C for 12 h) suspended in hexane. 500 mL of oil were dissolved in equal volume of hexane and then passed through the column. Afterwards the column was with 250 mL of hexane. The first 250 mL eluate was discarded and the remaining eluate was collecting in a brown ice water cooled glass flask. The collected oil-hexane mixture was gassed with nitrogen for 10 min and stored at -20 °C until evaporation of hexane. Evaporation of hexane was achieved on a rotary evaporator with carefully adjusted vacuum down to 150 mbar in 3 steps, each 15 min long and starting and followed by 10 min of gassing with nitrogen. The first step was by 65 °C and the last two steps by 90 °C. The oil was tested of residual tocopherols (< 0.5 ppm, method DGF F-II 4a).

Sample Preparation

Powder model samples were premixed with spoon and then finally mixed with an analysis mill (IKA *Analysemmühle Typ A11-basic*) for about 10 s. As suspension ground substances MC (MCE 4) and CaCl₂ were used and in the open system model the amount of safflower oil was 10 w% and of deionized water 5 w%. In case of adding an amino acid, 0.25 w% of L-leucine or equimolar amount of L-lysine were used. The suspensions were finally filled in airtight 1 L flask and stored by 40 °C in the dark and frequently opened for taking aliquots. In case of the closed model, CaCl₂ and MCE 15 MC was used and the amount of oil were varied (10 %, 13.33 %, 19.05 %), but the ratio of oil/water/amino acid were remain constant (see Table 2.1). Here samples were stored in 1 g aliquots in brown 20 mL screw cap closed headspace vials and were used as it is for analyzing volatiles. Kinetic measurements of open model samples were single spot measurements, where samples of closed models were analyzed in duplicate.

Table 2.1: Composition of low moisture model systems with changing water activity

Model	Powder [g]([%])	Leucine [g]	Oil [g] ([%])	H ₂ O [g]	aw value
MC 71	149 (71.0)	1	40 (19.0)	20	0.770
MC 80	239 (80.0)	1	40 (13.3)	20	0.619
MC 85	339 (85.0)	1	40 (10.0)	20	0.515
CaCl ₂ 80	239 (80.0)	1	40 (13.3)	20	0.033
CaCl ₂ 85	339 (85.0)	1	40 (10.0)	20	0.033

Oleogels were prepared by the solvent exchange method according to [9] as described in chapter I. The protein oil suspension was intended to mimic the protein concentration. Therefore 6.8 % whey protein isolate (WPI) was mixed with stripped safflower oil and mixed with an Ultra Turrax (2 min, 13000 rpm).

Extraction

An aliquot of the powdered sample containing ~ 1g of fat was weighted in a 50 mL centrifuge tube with the addition of 25 mL of cyclohexane and sonification (Bandelin sonoplus HD 2200) where following parameters were set: cycle: 9, power: 50% and time: 20 seconds. Thereafter the powder was centrifuged (Hettich Zentrifugen Universal 32) at 4500rpm for five minutes and the supernatant of the samples was filtered through filter paper and the filtrate was

collected in Erlenmeyer flasks. This procedure was repeated twice with 20 mL of cyclohexane. Afterwards cyclohexane was evaporated at 250 mbar at 65 °C. In case of the extraction of inner fat, an aliquot of the powdered sample containing ~ 1g of fat was weighted in; 40 mL of petroleum ether was added, closed and shaken for 10 min at 150 rpm. Afterwards, the sample was filtered and the powder in the filter was washed twice with 2 mL of petroleum ether. To fully evaporate the petroleum ether, the filtrate was first evaporated at 300 mbar at 65 °C and dried 105 °C for 20 min. The inner fat was extracted like described above with cyclohexane and the drying step was done, too.

Oleogels are extracted as described in the General Introduction section (chapter I).

Lipid hydroperoxides

Lipid hydroperoxides were measured as described in the General Introduction section using the iodometric method according to Wheeler [10, 11] in powder model systems and using the thiocyanate method [12–14] in oleogel systems.

To measure the influence of the added drying step in the extraction of inner fat and measurement of peroxide according to Wheeler, fat was oxidized overnight (18 h) at 70 °C and 90 °C. Aliquots of 0.2 - 1.2 g were mixed with petroleum ether and dried and measured as described. Finally, linear correction functions for the fat was determined by fat weighted vs. reweighted after drying (slope = 1.1634, intercept = -0.0421 g, $R^2 = 0.992$) and for the peroxide values by fat weighted vs. peroxide value divided by the mean (slope = -0.2017, intercept = 1.157 g, $R^2 = 0.7262$). In the inner fat peroxide determination the peroxide values were then calculated on the basis of fat, which was calculated by using the reweighted fat after drying and finally adjusted using the second correction function for peroxides.

Water Activity (a_w)

The water activity of the samples was a single measurement with an AW SPRINT TH-500 (Novasina) at 25 °C.

Measurement of Volatiles.

Approximately 1 g of suspension was weighted into an airtight 20 mL headspace vial, sealed, and measured according to Serfert et al. [15]. In brief, an aliquot (1 mL) of the head space was injected into an Agilent 6890 series gas chromatograph running in split mode (4:1) equipped with a J&W DB-1701 column (60 m × 0.32 mm × 3 μm). The injection port was heated to 220 °C and volatiles were detected with a flame ionization detector (FID) at 250 °C. Initially Oven

temperature (45 °C) was held for 2 min then raised up to 220 °C at 15 °C min⁻¹ with a break time at 85 °C for 4 min and a holding time of 3 min at the end. Substances were qualified by their retention time and analyzed by their area under the curve.

Protein Oxidation

Protein oxidation was measured according to the general introduction section, with small differences. For the measurement of protein carbonyls, the pellet was centrifuged at 5000 g, washed twice with 1 mL EtOH/ EtAc (1:1, v/v), and finally solved in guanidine (6 M) phosphate buffer (9.6 mM pH 6.5) and centrifuged at 5000 g for 2 min to remove insoluble particles [16]. HCl treated samples for blank measurement were used for fluorescence measurement, too. Proteins on the surface were removed using a plastic spatula.

Statistical Analysis

ChemStation (Agilent) was used for GC data collecting and converting in .csv files. All other data preparation and visualization was done with Excel and R-Script [17] including the minpack.lm-package [18], which uses a modification of the Levenberg-Marquardt algorithm. Upper and lower limits are carefully chosen to avoid artifacts and lists of initial parameters as obtained by fitting all volatiles one time are employed. Standard deviation was estimated using the jack-knife delete-1 procedure (see general introduction).

2.3 Results & Discussion

2.3.1 Lipid induced Oxidation of Leucine in Low Moisture Suspensions

2.3.1.1 Hydroperoxides in Low Moisture Suspensions

To evaluate the formation of primary lipid oxidation compounds in the various substance mixtures (methylcellulose (MC), starch, CaCl₂, sea sand, silica gel) at 40 °C, lipid hydroperoxides was analyzed at different time points. Thereby, the suspension base material had a crucial influence on the formation of lipid hydroperoxides (see Figure 2.1). Highest oxidation rates were observed in sea sand models (not shown) and CaCl₂, whereas in starch and silica gel the oxidation rate was slow. MC had an average oxidation rate. In CaCl₂ based models the water activity is very small (see section 2.3.2) as CaCl₂ introduce water in the crystal lattice, why no water monolayer of the lipid could be formed, which prevents lipid oxidation. Contrary, in the sea sand model, the water could not be absorbed by the base material, the water in these systems therefore is very

moveable and can solve and transfer trace metals, which induce the decomposition of lipid hydroperoxides and lipid oxidation in general [19]. In starch and methylcellulose based systems the water activity should be medium moisture (see section 2.3.2), which therefore prevent lipid oxidation. However, the oxidation in the starch based systems is lower than in MC based systems. This might be due an advantageous even lower water activity than MC, but this fact will not explain the large prohibition of oxidation. Both base materials are carbohydrates, which differs besides the methylation in the formation of secondary structures. Starch is known to consists as mixture of the two polymers amylopectin and amylose, in which the latter form left-handed helices with a hydrophobic cavity, which are able to complex compounds like free fatty acids, linear alcohols (see next section, formation of volatiles) or triiodide [20]. It was demonstrated, that the formation of reversed micelles of lipid hydroperoxides initiate the autocatalyzed propagation phase in lipid oxidation by reaching a critical micelle building concentration (CMC) of oxidation compounds [21, 22]. Therefore, helices of starch, which complex oxidation compounds, should prevent the oxidation compounds reaching their CMC and overall prevent the propagation phase as antioxidant though complexation. In addition, this antioxidative effect may also visible in silica gels, as silica gel is generally known for his adsorption abilities in term of normal phase chromatography. In silica gel suspensions, lipid hydroperoxides were very low (not shown), but oil extraction was about 10 times worse than other models, too.

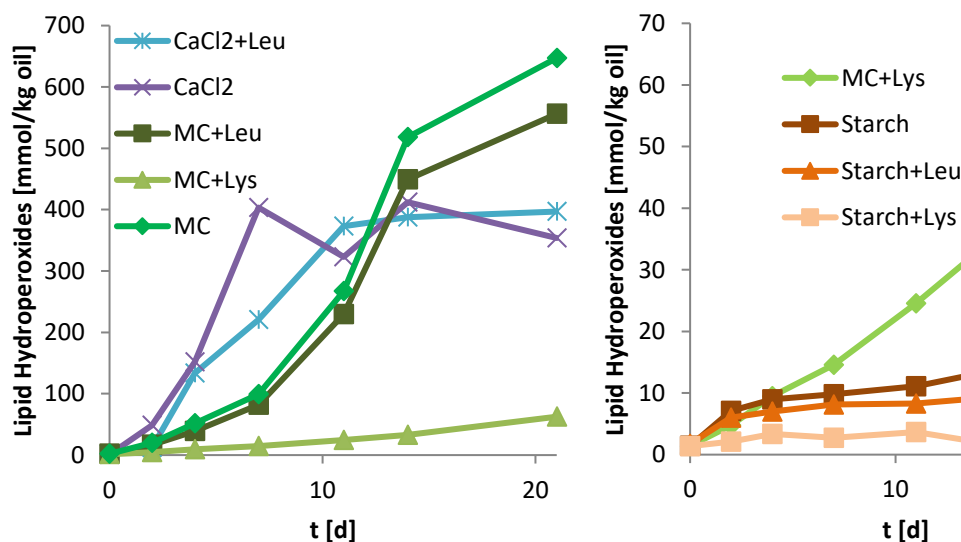


Figure 2.1: Formation of lipid hydroperoxides in open low moisture models of mixtures (10 % oil, 5 %, (0.25 %

Leucine or Lysine)) during the first 3 weeks of incubation at 40 °C. Each point was a single measurement.

Each model was repeated with the addition of 2.5 wt% (vs oil) of the amino acid leucine or lysine. In each of these amino acids enriched suspensions, the amino acids decreased the

oxidation rate in the first 3 weeks in manner of lipid hydroperoxides. Furthermore, lysine had a higher influence in decreasing the oxidation rate than leucine. Amino acids, hydrolysates and protein have been shown to be antioxidative [23, 24], which is due several reasons: they are capable to complex trace metals, which catalyze the oxidation and radical scavenging.

2.3.1.2 Formation of Volatiles

The lipid oxidation products hexanal and propanal of the used safflower oil were identified using authentic standards and the GC flame ionization detection technique. In accordance to the literature these were highly characteristic and abounded compound of the degradation of linoleic (14.7 ± 0.03) and linolenic acid ($18:3 = 0.14 \pm 0.01\%$), which would be oxidized first [1] (see chapter I). To further identify characteristic compounds of oxidized safflower oil at incubation at 40°C with the influence of protein dynamic headspace GC MS was conducted (see Figure 2.2). Smaller compounds than hexanal were not measured, which could belong to increased water solubility and therefore a higher decomposition and reaction rate with proteins (see chapter 3, 4).

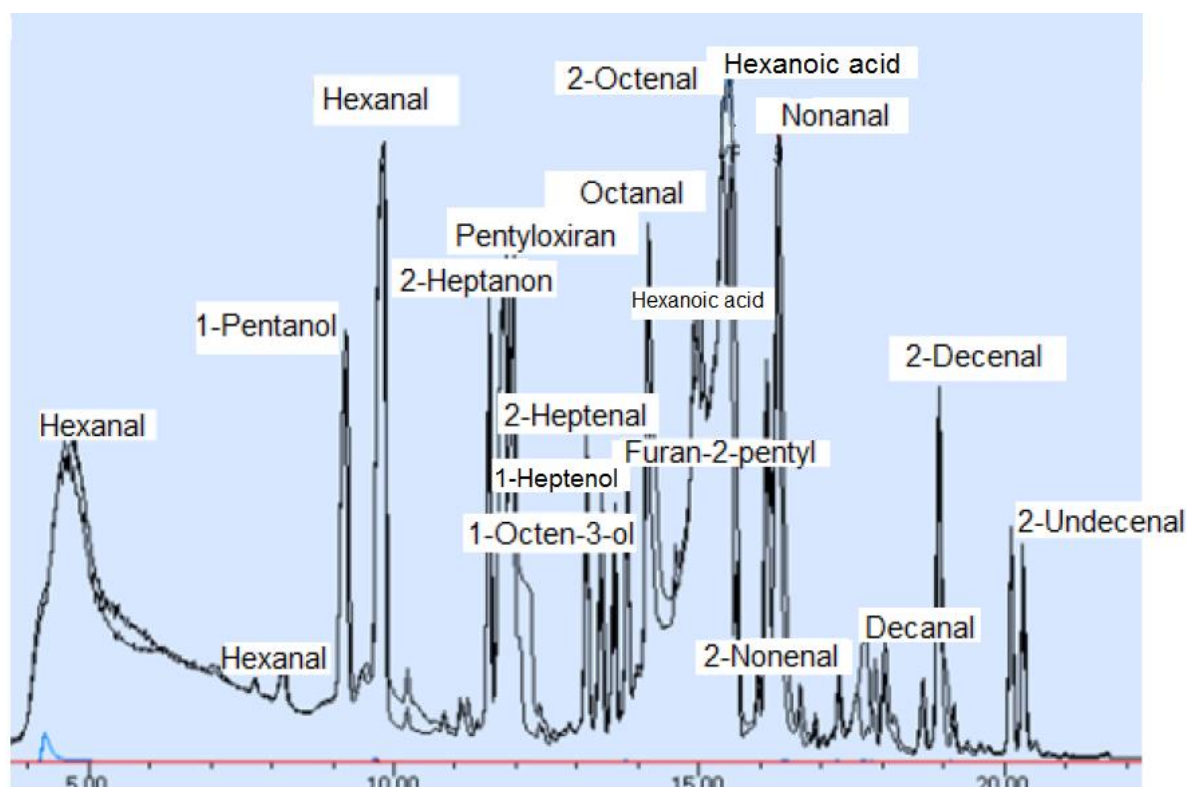


Figure 2.2: Volatile compounds of two oxidized safflower oils with 6.8 % whey protein identified with dynamic headspace gas chromatography mass spectrometry. Hexanal was eluted twice due high concentration and limited cryo focusing.

However, this preparation technique suffers to the limited absorbance ability of trapping material, which was stressed by the high amounts of hexanal. In addition, smaller molecules have a

decreased boiling point, which made them even worse to cryo trap than the hexanal. Among hexanal, typical other lipid oxidation compounds (chapter I) like aldehydes, alcohols and acids were identified using the EI Mass Spectra NIST Database (Probability > 25 %). Many of the identified compounds contained an additional double bond to the main group. This indicate, that those compounds, which often contained a carbonyl group as main group, formed in this systems were able to modify proteins by either 1,2 addition (Schiff base formation) or 1,4 addition (Micheal addition) (see chapter I) [5, 25]. However, as hexanal and propanal were the first decomposition products of lipid hydroperoxides and isovaleraldehyde was the oxidation products of leucine, those compounds were mainly focused in the following sections, but full range of secondary lipid oxidation compounds have to be kept in mind by the measurement of the formation of fluorescence among other protein modifications or self-influenced lipid oxidation.

Formation of Selected Compounds

The formation of volatiles was highly influenced by the suspension base material (see Figure 2.3). In general, the formation of secondary lipid oxidation compounds was in accordance to the formation of lipid hydroperoxides (see Figure 2.1), whereby the formation of hexanal and propanal was the highest in inorganic materials except silica gel. In contrast, the formation of hexanal and propanal was the lowest in starch based systems and silica gel, which should be due the lower lipid hydroperoxide formation. In comparison of amino acid containing to non-containing suspension, systems with amino acids had a decreased concentration hexanal and propanal during the first 3 weeks(see Figure 2.4), attributed to the lower lipid hydroperoxide formation in those models. However, thereafter an increased concentration after the maximum concentration was remained. This may be due the amino group of the amino acids, which is able to react via Micheal addition and formation of Schiff bases (see chapter I, III, IV). Among them, Schiff base formation is especially known to be reversible [25], which finally leads to compounds, which are prevented from further decomposition by other reactions, but are not stable enough at the measurement. This effect will be doubled in case of lysine, but as all lysine models shows a very slow oxidation rate, this systems are never reaching the maximum concentration. Nevertheless, these reactions should be present, too. In the CaCl₂ model a second maximum concentration of propanal is reached after 100 d. As most of the oxidizable material in this system is already oxidized, this could imply that polymers began to decompose and release the aldehydes or that a certain amount lipid oxidizes at a slower oxidation rate on a different region

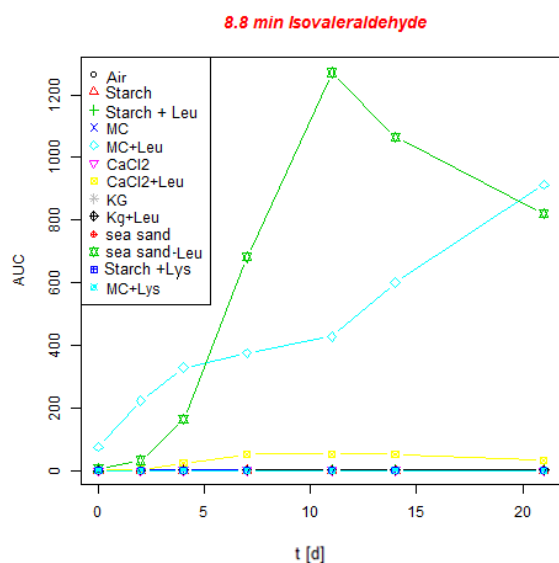
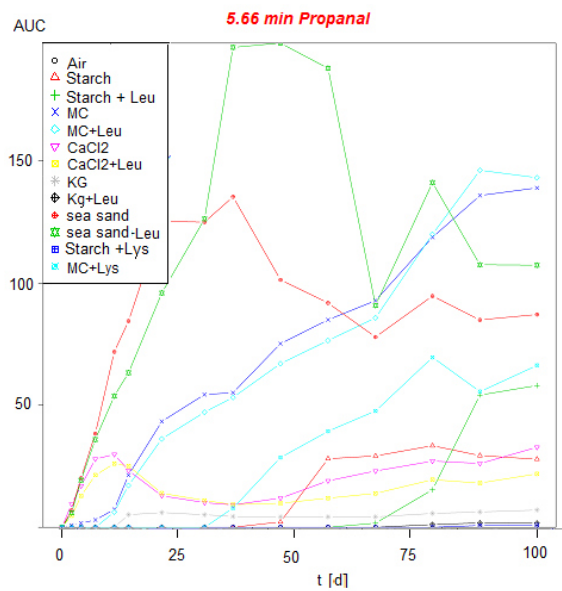
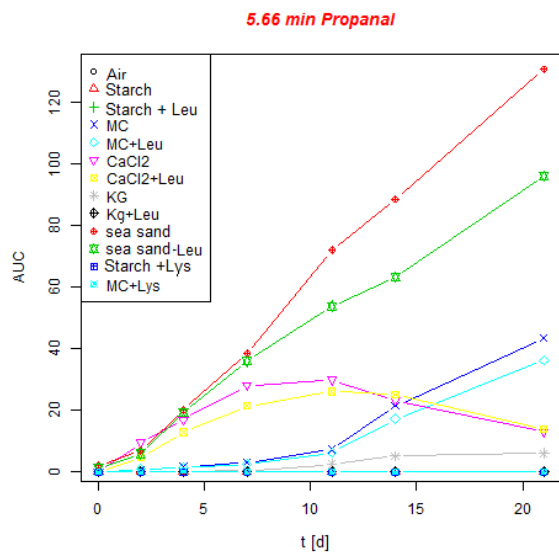
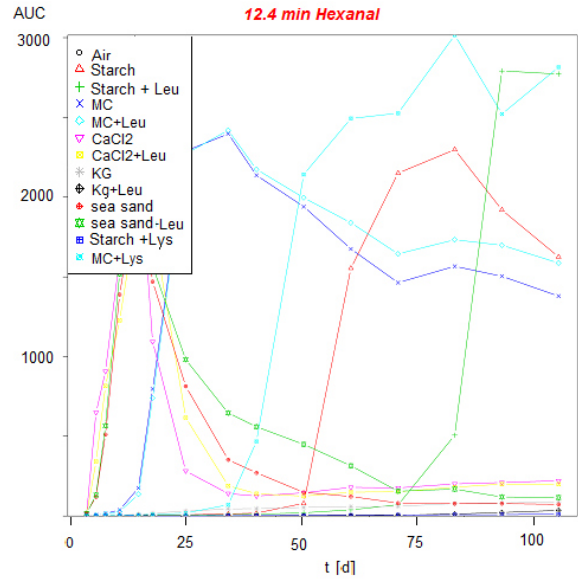
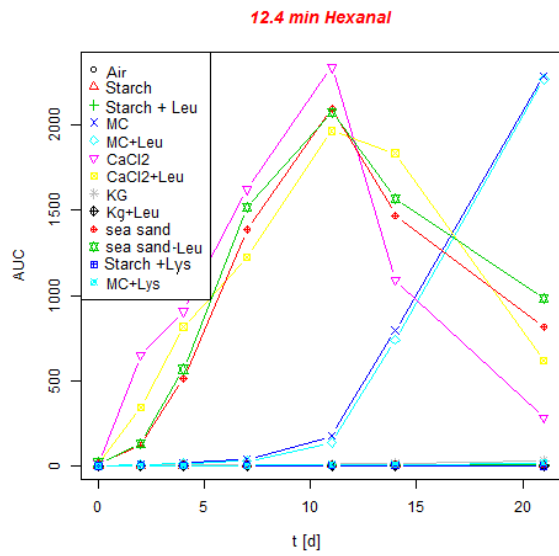


Figure 2.3: Formation of volatiles (Hexanal, propanal and isovaleraldehyde) in open low moisture models (Starch, Methylcellulose (MC), CaCl₂, silica gel (KG) and sea sand) of mixtures (10 % oil, 5 % water, (0/0.25 % Leucine or Lysine)) incubated at 40 °C. Left the first 3 weeks, right : formation until week 14. . Each point was a single measurement.

in the system under different conditions (see next section 2.3.2.2 Volatiles). However, as the formation rate of polymers should be greater than their formation (otherwise there is no polymer accumulation), the compound release reaction should be slow. In addition, these second formation region can underlie the kinetic in MC based systems, too, where the oxidation rate was slower. In case of leucine containing systems isovaleraldehyde was detected in sea sand, methylcellulose and CaCl_2 models, where the amount of maximum concentration correlate to their water activity, which should be in sea sand very high in MC at a medium aw value and in CaCl_2 at a very low value, as water is introduced in the crystal lattice. This may due the ability of free water at higher water activity to solve leucine, whereby leucine could be decomposed faster. Further, water provides a protic solvent, which is able to catalyze acid base dependent reactions [25].

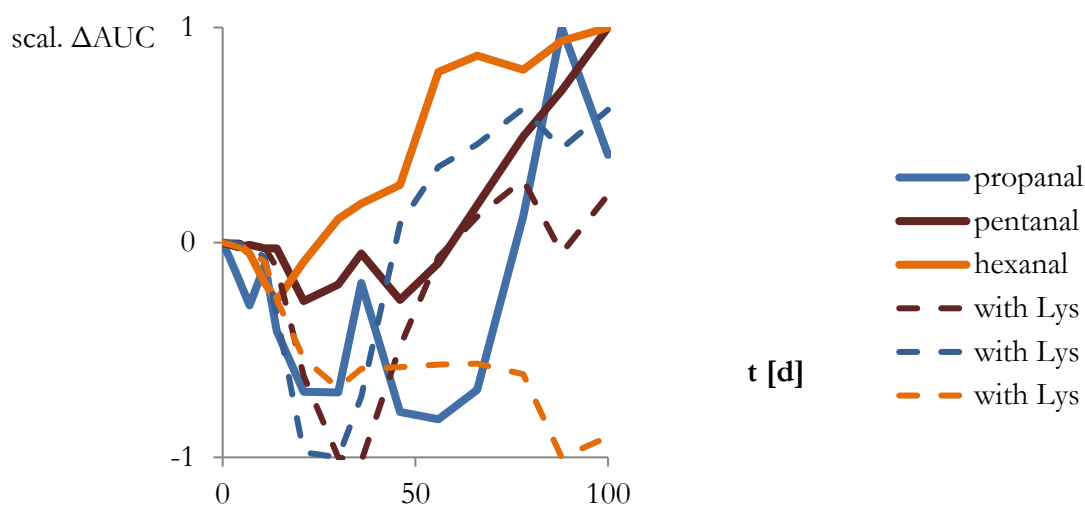


Figure 2.4: Formation of volatiles (Hexanal, propanal and pentanal) in open low moisture methylcellulose, leucine models (MC + Leu, 10 % oil, 5 % water, (0/0.25 % Leucine or Lysine)) incubated at 40 °C as difference to the MC system and scaled to compare the different compounds.

Differences in Volatile Composition of Low Moisture Systems

To consider the whole complexity of the low moisture systems, the use entire spectrum of volatiles may describe a system better than the selected compounds alone. Therefore MC with leucine and CaCl_2 with leucine had been used as example and for the purpose of using all volatiles; their concentration over time was followed (see Figure 2.5). In according to the selected aldehydes, the most compounds were firstly detected between 10 and 20 days of incubation, but in the CaCl_2 system earlier. Further, in the CaCl_2 system the yellow color in the figure dominate,

whereas in the MC system blue and green colors are mostly present. This may be due to the different water activities in both systems. A higher water activity leads to reactions where water can be involved and oxygen atoms introduced. This leads to more polar compounds, which have a decreased retention time. In contrast, in CaCl_2 based models no water is involved, which leads to the decomposition of relatively lipophilic compounds. In addition, CaCl_2 as an ionic salt can adsorb acids and polar substances on the surface through ion induced dipole forces, too.

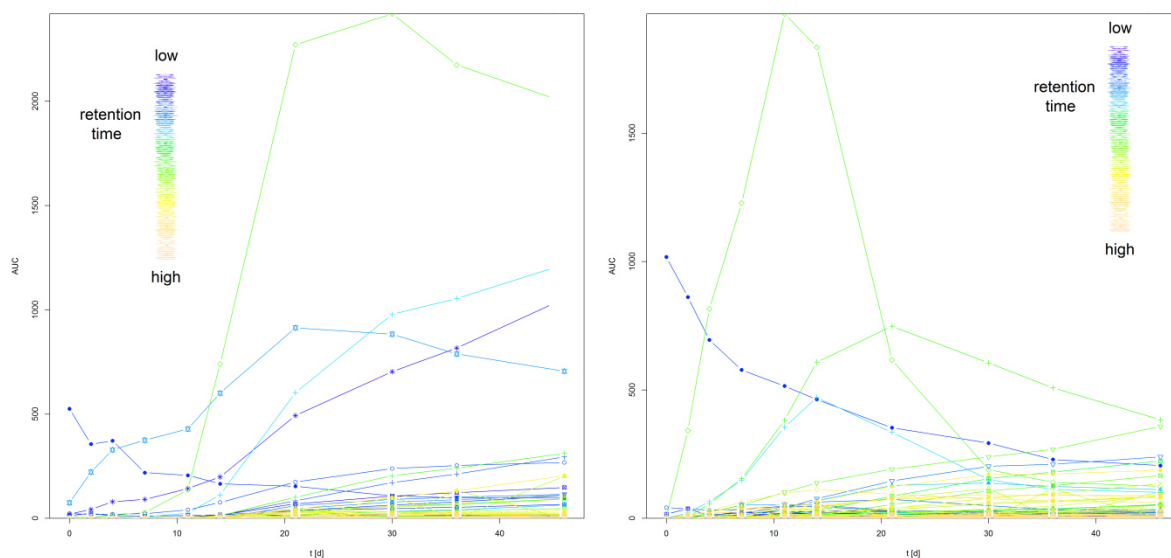


Figure 2.5: Formation of volatiles in see first 6 weeks of incubation at 40 °C; left MC + Leu; right: CaCl_2 + Leu.

Peaks volatiles are colored according to their retention time. Each measurement was conducted twice.

To qualify the color observations by the naked eye more precisely, a principal component analysis (PCA) was conducted using all volatiles after 3 weeks of incubation (see Figure 2.6). At this time point systems with a slow oxidation rate (starch based and MC + Leu) was most similar to air of the laboratory, whereas highly oxidized systems was distributed. However, leucine containing systems were closely to their lacking amino acid models, whereby sea sand had the greatest distance. This indicates that leucine have minor influence of the variance of compounds formed in the systems. The only difference is the additional oxidation of leucine, which forms isovaleraldehyde (see Figure 2.3), which explains the shift of the shift for silica gel + leucine (SG + LEU), sea sand + Leu and MC + Leu in the direction of isovaleraldehyde. As the formation of isovaleraldehyde in sea sand was highest, there is the shift at maximum, whereas in CaCl_2 only a low amount was form, which results in neglected shift.

The silica gel models, which had a slow oxidation rate, are in the same direction in PCA plot as CaCl_2 , whereas MC systems are on the opposite site. This distribution in the plot may correlate to the ability to adsorb polar oxidation compounds, discussed before, as CaCl_2 is nearest to the silica gels, which are definitely adsorptive. Sea sand in turn, is chemical identical with silica gel

(silicon dioxide). The difference is in the surface area density. Sea sand (0.1 - 0.3 mm) has larger particles than silica gel (60, 0.02 - 0.045 mm) and therefore about 1000 times smaller surface.

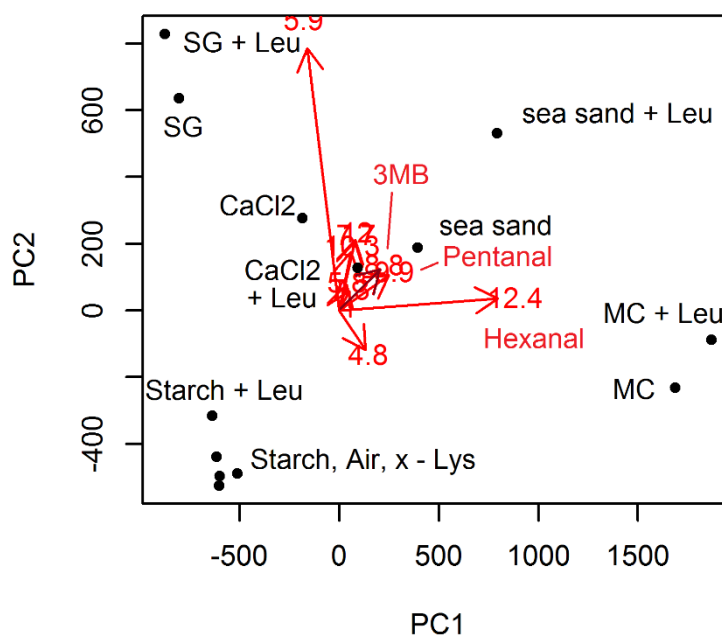


Figure 2.6: Principal component analysis of the models with the volatiles formed after 3 weeks of incubation at 40 °C. The first principal component most influencing compounds are printed and highlighted in red and isovaleraldehyde (3MB) in dark red.

2.3.2 Lipid and Amino Acid Oxidation Varied by Water Activity

In the following section, an experiment was carried out to further investigate the influence of water and water activity on lipid oxidation in the suspensions. For that purpose the amount of the base substance was varied to adjust another water activity. In methylcellulose based models (MC 71, MC 80, MC 85) the amount of base material was varied from 71 to 85 % and in CaCl₂ based models (CaCl₂ 80, CaCl₂ 85) from 80 to 85 %. This variation changed the water activity of MC models to 0.77, 0.619, 0.515, but both CaCl₂ models remained to 0.033.

2.3.2.1 Lipid Hydroperoxides

Lipid hydroperoxide formation in the MC based systems was very similar in the first 3 weeks (see Figure 2.7), but thereafter, in the Mc 71 model lipid hydroperoxides decreased further, whereas in the other both MC models the PV began to stagnate. It is striking, that the overall lipid hydroperoxide content from day 60 to day 90 was increasing with increasing water concentration and water activity, which can be attributed to the facilitated auto catalyzation by water though decomposition of peroxides and to the transport of oxidative trace metals like iron [19, 26]. In

contrast to MC, CaCl_2 had a fast initially oxidation rate and the system with higher water content had a higher maximum of lipid hydroperoxide concentration. This can be attributed to a missing water mono layer as described in the previous section, which prevents lipids to contact with oxygen [19, 26].

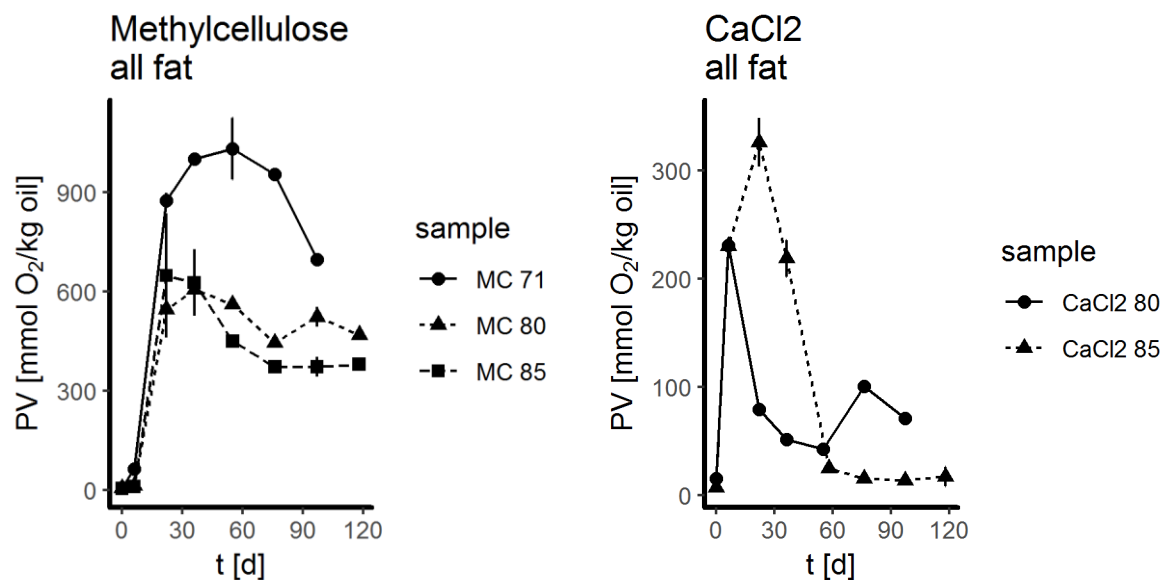


Figure 2.7: Lipid hydroperoxide value (PV) vs. time; formation of lipid hydroperoxides in methylcellulose (left) and CaCl_2 (right) Systems at 40 °C. Each measurement was conducted twice.

In the first section of low moisture suspension it was noted that the volatiles concentration over time could be polymodal, as oxidation is present at different regions. This implied an oxidation in certain regions, which were locally independent. Such physical separation may be induced to the formation of lipid complexes with the base substance. As this kind of fat will be enclosed, this fat was called in the following the inner fat (IF), whereas the remaining fat was called free fat (FF). To extract the free and inner fat an extraction procedure was developed, where the free fat was extracted using petroleum. In the MC based system the inner fat increased with the base material concentration (~31 %, ~35 %, ~39%), whereas in the CaCl_2 systems the inner fat concentration was very similar (~27 %, 28 %). In all models, the lipid hydroperoxide formation kinetic of inner, free and whole fat (GF) was very similar (see Figure 2.8 for example of methylcellulose 71.4 %), which indicates that the oxidation of the oil is not influenced by this kind of physical separation in these systems. Another assumption was that the free fat is oxidized first, as this is more prone to oxygen. In the first instance, the data signals differences in these kinds of oil, but recalibration of the measuring method showed that there is no difference. This recalibration was necessary, as in the extraction procedure heating and evaporation was involved, which influenced the extracted oil in linear dependence on their mass. Thereby, the linear correction functions for the true fat

weight vs. the reweighted fat in experiment after drying was quite mass dependent (slope = 1.1634, intercept = -0.0421 g, $R^2 = 0.992$), which may be due petroleum ether, which is less effectively evaporated in higher amounts of oil. The peroxide correction function was less dependent of the mass (peroxides values by true fat vs. peroxide value divided by the mean, slope = -0.2017, intercept = 1.157 g, $R^2 = 0.7262$), which can be due the small amount of oil, that had a relatively small absolute heat capacity, why every oil sample is heated relatively in the same time.

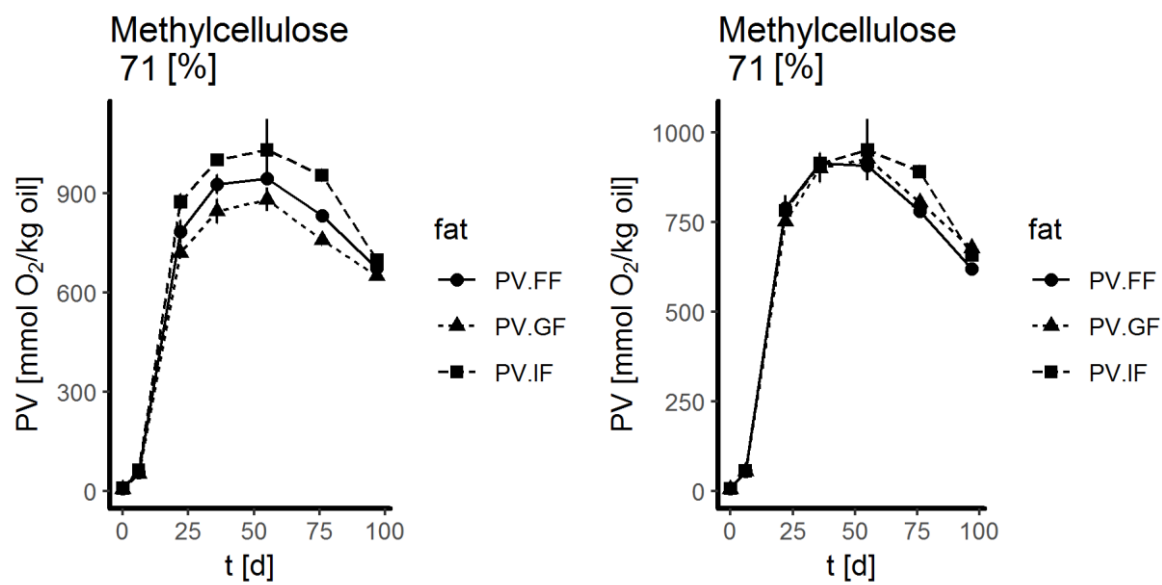


Figure 2.8: Peroxid value vs. time; formation of lipid hydroperoxides in petroleum ether extracted fat (“free fat” FF), remaining fat (“inner fat” IF) and a whole fat sample (GF) in the 71 methylcellulose model; left: data uncorrected, right: corrected to oil mass gain after 20 min of drying at 105 °C and slightly increased PV.

2.3.2.2 Volatiles

The formation of the two selected volatiles hexanal and propanal were similar between CaCl₂ systems (see Figure 2.9), whereas the maximum of concentration was decreased in CaCl₂ 80 in comparison to CaCl₂ 85 system, which was similar in the MC 85 system. Like in the formation of isovaleraldehyde in open low moisture systems (see above) the formation of isovaleraldehyde in CaCl₂ systems is decreased in comparison to MC based systems, which should be due the same reasons: less accessible leucine as leucine is not solved. Further, as closed vessels are used, the formation of isovaleraldehyde could be more accumulated, which results in are increased difference between CaCl₂ and MC based systems. Also the water activity seems to play a role in isovaleraldehyde formation as the first 2 weeks. As in the systems the lipid hydroperoxides formation rate correlated with the water activity isovaleraldehyde, beside hexanal and propanal, is formed in the same order as they are a product of decomposition of the primary lipid oxidation products. However, thereafter order is turned, which may induced to a faster decomposition

reaction rate, too. Water is able to provide acid base catalyzation, as water is a polar and protic solvent. As all models contain the amino acid leucine, it might be the amino group, which can degrade the aldehydes by Schiff base formation and further reaction, where the Schiff base reaction is known to be acid base catalyzed [25].

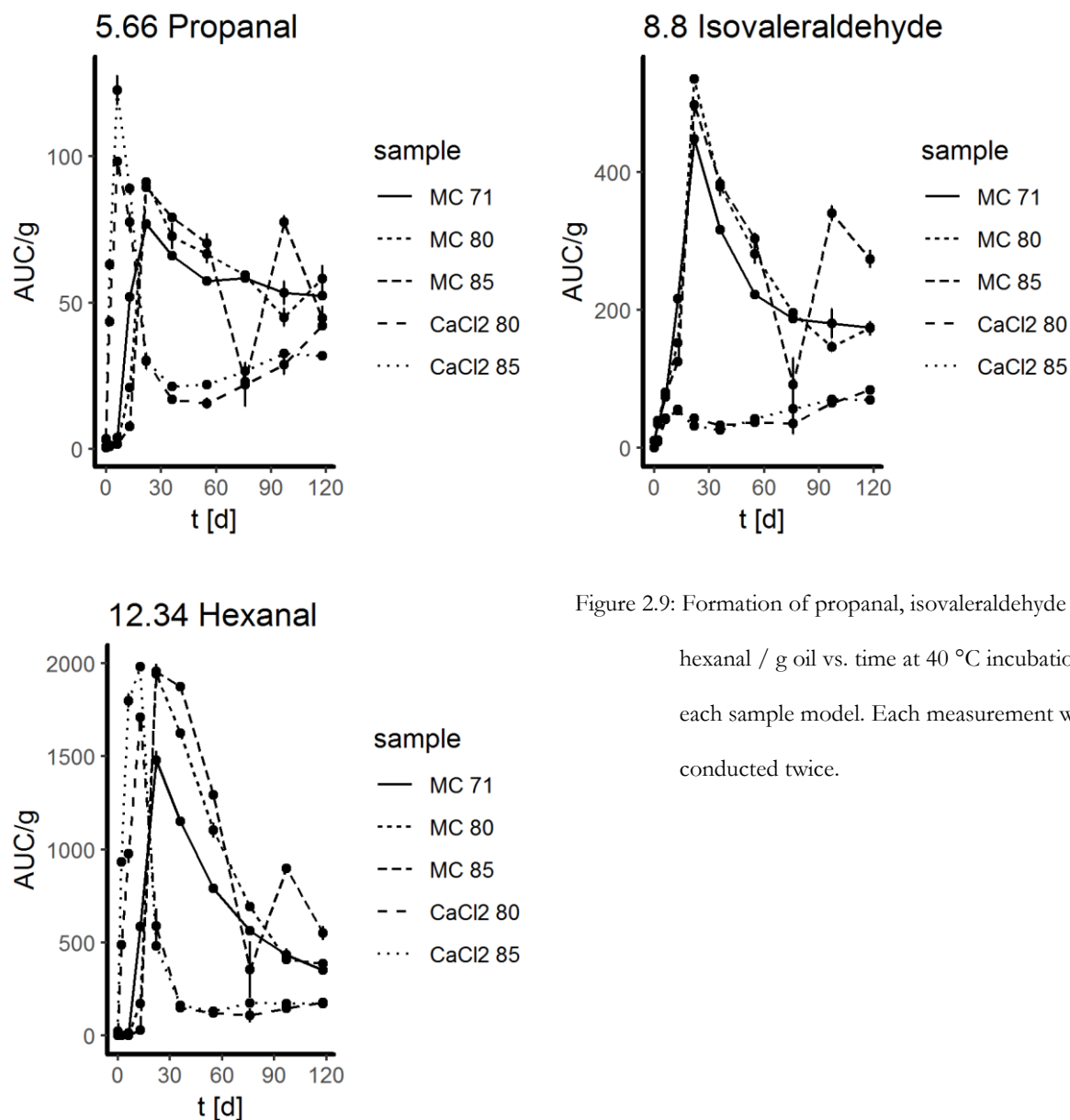
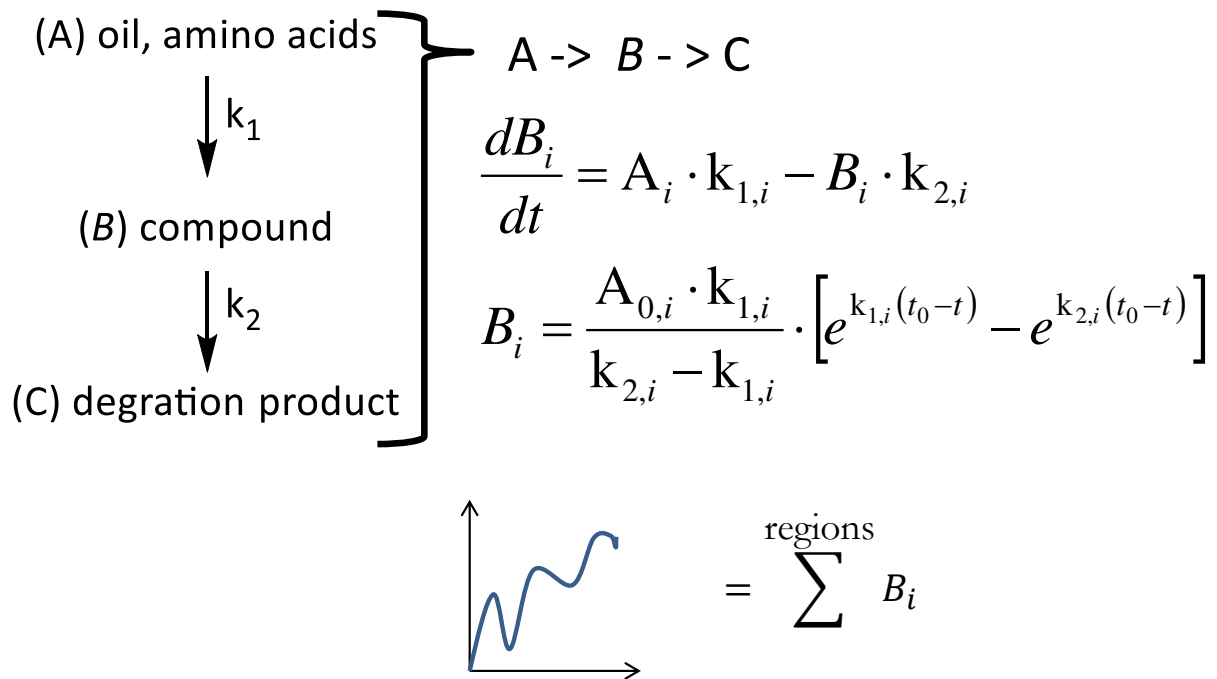


Figure 2.9: Formation of propanal, isovaleraldehyde and hexanal / g oil vs. time at 40 °C incubation in each sample model. Each measurement was conducted twice.

By looking on propanal formation in CaCl₂ systems, a bimodal distribution could be expected. These different oxidation locations or regions were proven by the extraction procedure and lipid hydroperoxides determination (see Figure 2.8) to be not as physical as the base substance complex lipids. However, the selected compound is formed from the lipid in each of the regions, whereas the selected compound is further decomposed. In the simplest kinetic form this behavior can be described as A to B to C (see equation 2.Ia-d). Where the actual concentration of B (the selected compound) is dependent on the formation (k_1) and decomposition rate (k_2) and

on the initial concentration of the starting material, which would be the concentration of the oils linoleic and linolenic acid or their hydroperoxides on the oxidation region. In addition, each region may have its own starting time, due to different lag times of oxidations. However, as volatiles are measured, the sample is incubated at elevated temperature, by which the compound is evaporated in each region. Therefore the measured concentration is the sum of the compounds in all regions.

Equation 2.Ia-d:



Kinetics of the selected compounds were fitted to equation 2d (see Figure 2.10). Thereby a bimodal (regions = 2) and trimodal distribution (regions = 3) was tested, where the trimodal model was better able to fit MC based systems. In addition it was tested if the regions have either the same initial time (t_0) or two (in trimodal it was estimated that two regions have the same t_0). Limits for reactions rate constants were tested from 0.1 d^{-1} to infinity, as a certain amount was necessary to prevent nonphysical simulations. The limit for the starting material was test to up to the 25-times magnified maximum value, which corresponds to highest possible concentration of $\sim 30 \text{ mg/g}$ (linoleic acid $\sim 150 \text{ mg/g}$). The best fits were achieved using one t_0 time for all regions and a limit of 0.5 d^{-1} for rate constants and a limit for the starting material to the 5 or 25-times magnified values (see Figure 2.10).

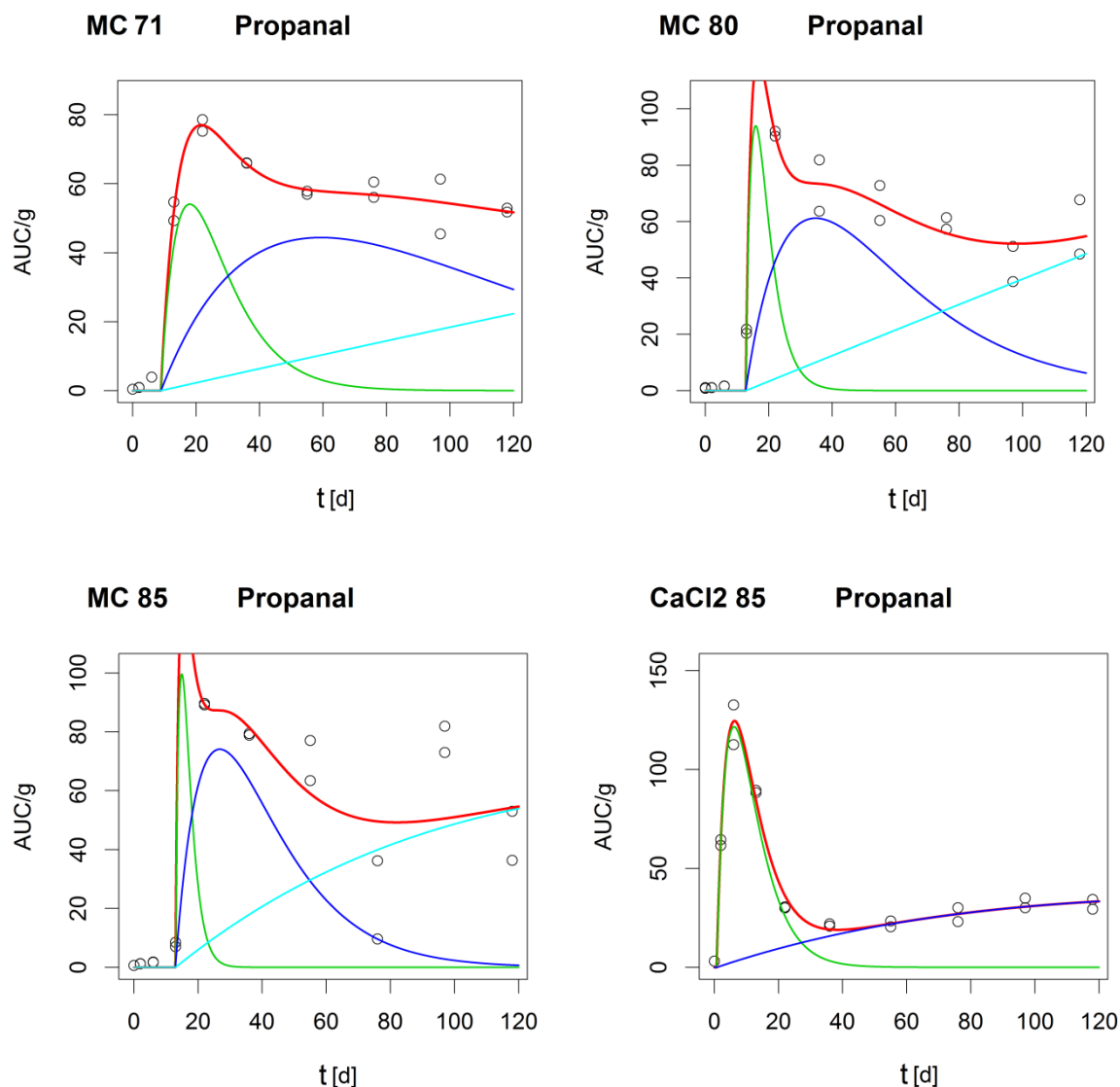


Figure 2.10: Formation of propanal at 40 °C and fitted curve of underlying regions in methylcellulose material with decreasing water activity (MC 45, 80, 85) and CaCl₂. The sum of the regions is marked in red.

Integrated areas (A1-3) of compounds at the certain region as well as the base amounts of starting material (A1_0 to A3_0) were influenced by the water activity (see Figure 2.11). Different regions in the suspensions could be possible. It is known that antioxidants are mostly effective on surfaces as lipid hydroperoxides accumulate on water lipid and air water interface [2, 27]. In this suspensions, the lipid phase form interfaces to air, to water, to the base material and to the reaction vessel. However the surface of the reaction vessel is comparably small, why the region, which were fitted in the models may assigned to the air, water and base material interface. The water activity in CaCl₂ systems is very low, as water is strongly bond into the crystal lattice. This however, leads to no free water, which can build up a lipid water interface in CaCl₂ systems. Therefore, the two regions in CaCl₂ systems have to be the air and the base

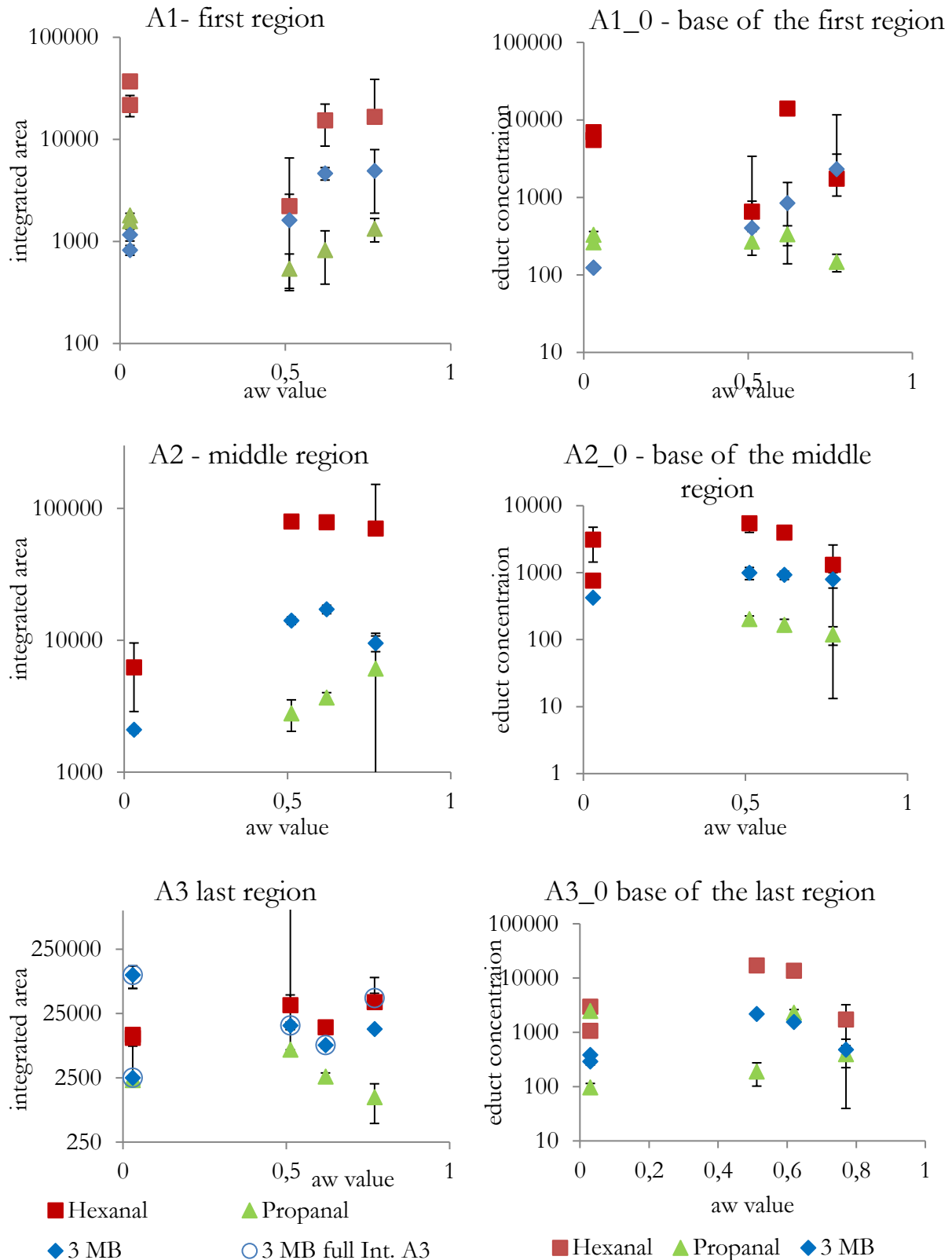


Figure 2.11: Integrated areas (A1-3) of compounds at the certain regions as well as the base amounts of starting material (A1_0 to A3_0) in models using the same t_0 . Integrals are from t_0 to infinity or to the last day of the experiment. The logarithmic scale was used to make the 3 compounds comparable.

material interface. These both interfaces have to be also in the MC systems. By comparing the uncovered contribution of each region (see Figure 2.10), it can be concluded that the region with average oxidation speed is the lipid water interface, because it only occurs in the MC based systems. Further evidence therefore is given in the bases of the middle region (A2_0). As the water lipid ratio was held constant, the water lipid interface may also constant, leading to the same amounts of starting material in the oxidation to the selected compounds in MC systems. In addition this leads to the same formation of hexanal and isovaleraldehyde (A2). However, propanal is more formed with increasing water activity, which might be attributed to the condition of more moveable water [19]. This is also indicated in CaCl_2 systems, where they have the same base and therefore the same potential to oxidation, but the oxidative formation of the compounds is slowed or even prohibited in case of propanal, as the water is strongly bond to CaCl_2 .

The assigning of the first region may be more difficult, but as this region rapidly oxidized this should be the lipid air interface. Lipid oxidation is the reaction of lipids with oxygen in the air. Therefore the concentration of oxygen, and thereby the reaction rate with oxygen, will be high. On the basis of the fitted starting material (A1_0) this can be seen, as the basis is more or less constant. This is because of physical forces of the oil droplets and the equal preparation. Independent from the base material amount, the oil will be form droplets, which smallest size is limited by the surface energy, thus the droplet size and lipid air interface in each suspension is comparable. The base of isovaleraldehyde may increase due the increased water activity, which leads to a higher amount of solved leucine, which can than transferred to the lipid air interface. The entire formation of the selected compounds (A1) in turn should be classical dominated by the decomposition of lipid hydroperoxides, which will be facilitated by accessible water from the air with increasing water activity. Further, in CaCl_2 the monolayer of water is lacking, which leads to higher oxidation rates, too [1, 19].

The interface between the base material and lipid differ to the other interfaces as the base material is solid. Therefore this interface may be described best with adsorption characteristics on the base material. CaCl_2 is an ionic salt, where ionic interactions and ion induced dipole forces should determine the adsorption of a compound. Ionic lipid oxidation compounds like acids and polar compounds of oxidation will so adsorbed preferably. In MC based systems, the surface consists of methylated and free hydroxyl groups and acetals. Methyl groups will provide hydrophobic interactions through Van der Waals forces, where hydroxyl and acetals can lead to adsorption by dipole-dipole forces and hydrogen bonding. Therefore water can adsorb on the base materials well, as it is protic and polar. However, only in MC based systems water may be

moveable, which induces the formation of a layer of water, which disturbs the adsorption of primary lipid oxidation compounds and their decomposition (see A3 propanal in MC systems, hexanal, isovaleraldehyde A3_0). However, water will also act as solvent for trace metals in the base material, which catalyzes the decomposition of lipid hydroperoxides, which induce lipid oxidation [1, 19, 26].

2.3.3 Lipid Protein Co Oxidation in Oleogels

The oxidation of the low moisture suspensions was greatly influenced by their different interfaces. However, it was shown, that leucine had an impact on the formation of volatiles. Therefore, a system with one dominating interface of lipid to protein should be established. As the interface is a crucial parameter, changes during the incubation should be prevented. In lipid protein studies, often emulsions are used [5], which provide a large protein lipid interface as proteins are located at the water oil interface. This will lead to always accessible water in those systems, which they make different to protein lipid interactions in dry foods. In addition, emulsions are accompanied by droplet size changing processes like coalescence. These changes may lead to difficult interpreting results as oxidation parameters change during the experiment. Mainly two procedures are conducted to prevent these changes. On the one hand, the droplets were prepared smaller by homogenization, why it took longer to coalescence. However, even if the coalescence is not visible or small, changes of droplets diameter results in a cubic decreased surface. On the other hand, emulsifiers are used, which stabilize the lipid protein interface. However, it is known that emulsifier have distinct influence on the activity of antioxidants [14, 28] and therefore will also alter the interface in terms of accumulation of lipid hydroperoxides on the interface. To circumvent this hindrance, it was decided to use the protein as emulsifiers self. This kind of lipid protein matrix was developed from de Vries *et al.* [9] as an alternative to hydrogenated fat. In this matrix, aggregated denaturated whey protein isolate forms a network, which is able to capture the oil. However, this so called oleogel would be an ideal candidate to investigate the lipid protein co oxidation in the purpose of this work, as the lipid protein interface is strengthened to the formation of the network in the oil and will not change during the experiment. For a comparison, beside the oxidizable gel, a suspension of the same constituents is created without prior denaturation of the protein and a gel with stable middle chain triglyceride oil (mct-oil) was taken.

2.3.3.1 Lipid Oxidation in Oleogels

Primary lipid oxidation products were measured in form of lipid hydroperoxides by the thiocyanate method. A logarithmic scale for the lipid hydroperoxides was used to demonstrate the large differences in Figure 2.12 between the models and the strong increase of lipid hydroperoxides. There was no oxidation in the mct oil gel, which was expected as the mct-oil is stable versus lipid oxidation having no unsaturated lipids. The formation of lipid hydroperoxides was greatest in the suspensions, where the lipid hydroperoxides raised quickly after 8 d of incubation at 40 °C. Contrary safflower oil gel (s-gel) oxidized slower and began the propagation phase after 24 d of incubation. This may due two reasons: 1. lipid protein interface is in the suspension decreased, which decrease the amount of antioxidative groups presented to the oil; 2. the suspension contained water, which is able to increase the lipid oxidation rate. To the first, the native WPI in the suspension did not solve in the oil, which leads to the separation of oil and protein. In addition, air was adsorbed at the protein surface, which even more decreases the lipid protein interface. Furthermore, the protein in the gel was denaturated, which may leads to the presentation of lipid oxidation antioxidative or side reaction active groups. The whey protein used in this study contains about 4.4 % moisture, whereas the gel prepared with denaturated whey protein aggregates and the solvent exchange procedure contains about 0.8 % water [9]. As described by the previous lipid hydroperoxide section of low moisture suspensions, water facilitates the lipid auto catalyzation by solving trace metals, which are able to decompose lipid hydroperoxides to radicals.

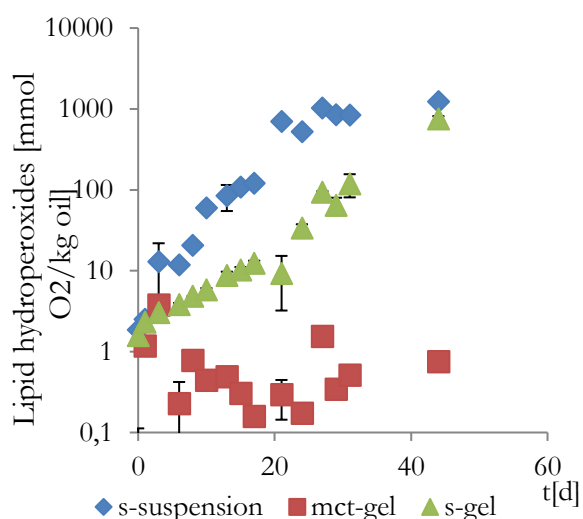


Figure 2.12: Formation of lipid hydroperoxides (PV) in solvent exchange mct oil and safflower gel (mct-gel, s-gel) and a whey protein isolate suspension in safflower oil (s-suspension) during incubation at 40 °C. A logarithmic scale was chosen to demonstrate the huge differences between the models.

In all models hexanal was detected since the beginning even in mct-oil. This was unexpected, as the oil was not oxidized and in mct-oil is even no starting material to produce hexanal. As other lipid oxidation measurements are conducted during the preparation of the gels, we assume that this initial hexanal concentration is due contaminated vessels. Besides hexanal, pent-3-en-2-on, 4-methyl-pent-3-en-2-on were identified using dynamic headspace GC-Ms in high amounts and hexen-3-en-2,5-diol and 3,5-dimethylcyclohex-2-enone in low concentrations. These compounds can all be attributed to acetone, which were used in high amounts in the solvent exchange procedure. Thereby 4-methylpent-3-en-2-on is formed through an aldol condensation of two acetone molecules (see

Figure 2.13). Therefore these compounds are either formed initially in the acetone protein network or are present at contamination since the manufacture of acetone. However, in these compounds may especially be accumulated in protein aggregates through lipophilic cavities formed by lipophilic amino acids.

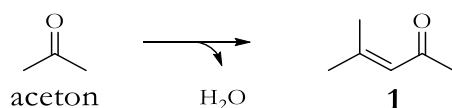


Figure 2.13: Aldol condensation of acetone to 4-methylpent-3-en-2-on (1).

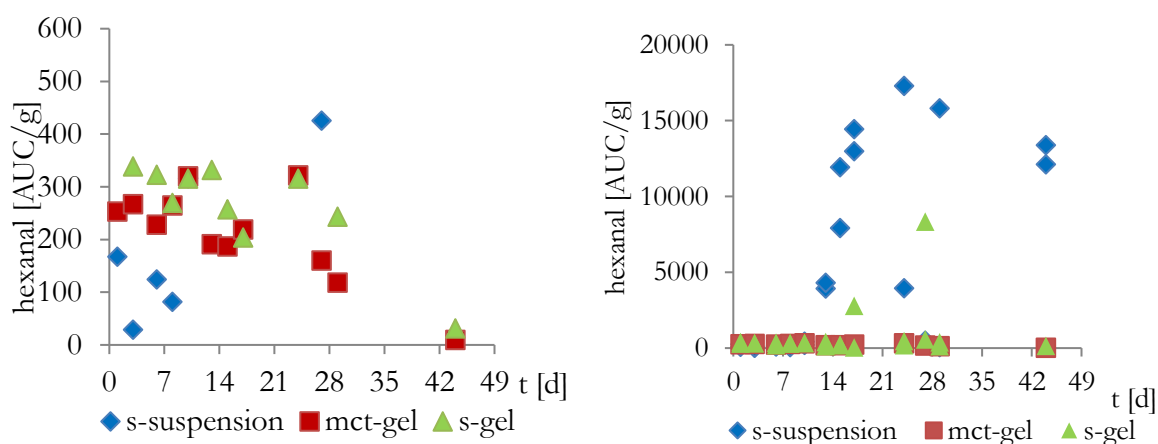


Figure 2.14: Formation of hexanal in solvent exchange mct oil and safflower gel (mct-gel, s-gel) and a whey protein isolate suspension in safflower oil (s-suspension) during incubation at 40 °C. Two scales are given to show the large differences. Left: zoom to the mct-oil and low concentration gel samples. Right: concentration of hexanal in suspension to comparison with the gel, where one point equals one measurement. All measurements were conducted as duplicate.

Lipid induced formation of hexanal is evident only in the suspension after 13 d of incubation and in the safflower oil gel after 17 d of incubation at 40 °C. However, hexanal was only increased in

two samples of s-gel, in all other samples the concentration of hexanal is decreasing over time like in the mct-oil gel samples. This may be explained by side reactions of the initial, formed hexanal and its precursors with free amines and the protein in general [29–32]. Thereby, the carbonyl group of the aldehyde easily reacts with the amino groups either from lysine or the N-terminal amino group. It is known, that the Schiff bases are able to condense with further aldehydes to form polymers [1]. Thereby this reaction may be driven through the ability of proteins to complex formed water [33, 34].

2.3.3.1 Modification of Protein in Co Oxidizing Oleogels

Protein Carbonyl Content

Protein carbonyl concentration during the incubation at 40 °C is shown in Figure 2.15. There is a huge standard derivation by the oleogel system due the low solubility of protein aggregates. However, some trends might be observable. Initially there is a higher carbonyl concentration in oleogels (17.5 ± 2.5) in comparison to the suspension (1.1 ± 0.3 , 3rd day). This might be to several reasons. The protein in the oleogel is denaturated in comparison to the protein in the suspension. Therefore, the protein absorption factor may be changed, whereby the result is shifted. In addition, the protein in oleogels is thermal processed in the preparation at 85 °C for 20 min, which might induced initially carbonyl formation, too. For example it was investigated, that cooking increase the protein carbonyl content in beef [35]. However, in this experiment the protein is cooked besides lipids even in the control with no added unsaturated lipids.

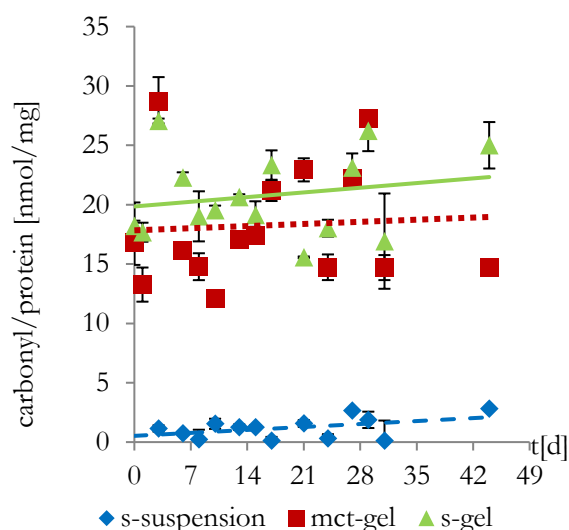


Figure 2.15: Concentration of protein carbonyls in solvent exchange mct oil and safflower gel (mct-gel, s-gel) and a whey protein isolate suspension in safflower oil (s-suspension) during incubation at 40 °C. Linear fitting curves were added to indicate the overall trend.

Formation of Characteristic Fluorescence

Formation of protein fluorescence formation is shown in Figure 2.16 for the models incubated at 40 °C. All measurements were taken out at pH to 6.5 comparisons. In mct-oil samples no dityrosine or NFK fluorescence was observed. This could be seen as expected, when no own protein oxidation takes place. Therefore, NFK and dityrosine formation in other models have to belong to lipid oxidation induced protein modifications. Dityrosin formation was evident in the safflower oil and suspension after a specific time. This specific time correlates well with the beginning of the propagation phase of lipid hydroperoxide formation (see Figure 2.12), which is in accordance to the formation mechanism. Despite the likely different protein absorption factors, it is interesting to note, that the dityrosine levels of the gel exceed the levels of the suspension after 4 weeks of incubation. This is also the case in NFK measurements after 3 weeks, where the formation of NFK in the suspension is even not visible. This both observations can be explained with an increased protein lipid interface. Further, as in the suspension the protein is native, one of the tryptophan residues will be buried in the globular protein [36].

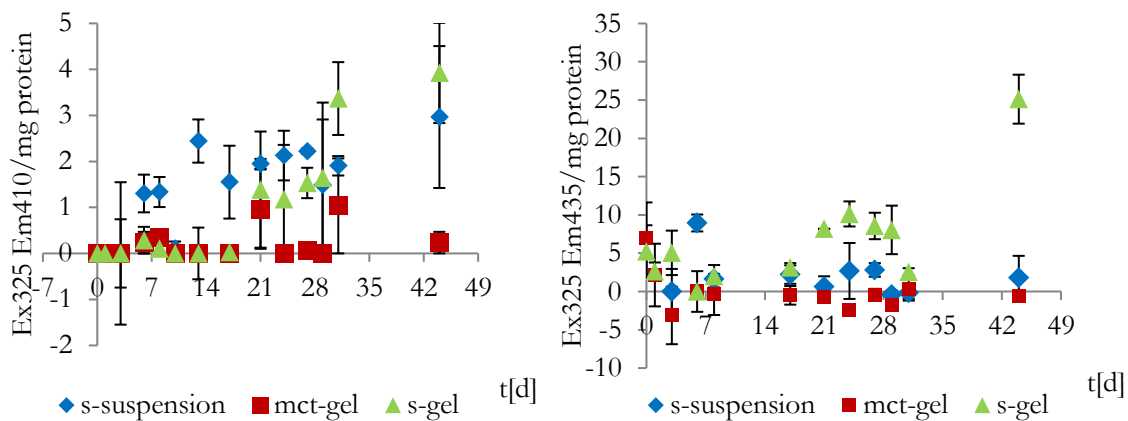


Figure 2.16: Formation of protein fluorescence of protein extracts from solvent exchange mct oil and safflower gel (mct-gel, s-gel) and a whey protein isolate suspension in safflower oil (s-suspension) model during incubation at 40 °C. The fluorescence at 410 nm (325 excitation) is characteristic for dityrosine and 435 nm (325 excitation) for NFK.

2.4 Conclusion

In low moisture suspensions, lipid oxidation is enhanced through the general high availability of oxygen and the distribution of lipid hydroperoxides on different interfaces. These include the lipid air, lipid water and lipid base substance interface and the oxidation and further fragmentation on these surfaces is influenced by the water activity. Water has a decent influence on the oxidation of leucine. Furthermore, it was proposed, that the amino acids leucine and lysine are able to bind lipid aldehydes as those were initially lowered, but then in increased amounts. This decomposition of aldehydes was also observed in oleogels, which were introduced to focus on the lipid protein interface. Furthermore, the protein modifications in the oleogels were lipid oxidation induced, as they do not occur in non-oxidizing mct-oil gels. Like in the suspensions, these modifications are enhanced through a high interface as those reactions likely takes place on the surface of the protein. As the lipid hydroperoxide formation in suspension and safflower gel was different, it could be concluded that in the gels water content and activity have a decent role to. Beside a testing of different water activities in gels, the investigation of the decomposition of aldehydes and the protein modifications should be worth to conduct further experiments.

2.5 References

- [1] Belitz, H. D., Grosch, W., Schieberle, P., *Lehrbuch der Lebensmittelchemie*, Springer, Garching 2007.
- [2] Waraho, T., McClements, D. J., Decker, E. A., Mechanisms of lipid oxidation in food dispersions. *Trends in Food Science & Technology* 2011, 22, 3–13.
- [3] Simpson, J. A., Narita, S., Gieseg, S., Gebicki, S., Gebicki, J. M., Dean, R. T., Long-lived reactive species on free-radical-damaged proteins. *The Biochemical journal* 1992, 282 (Pt 3), 621–624.
- [4] Patel, A. R., Dewettinck, K., Edible oil structuring: An overview and recent updates. *Food Funct.* 2016, 7, 20–29.
- [5] Schaich, K. M., in: Kamal-Eldin, A., Min, D. B. (Eds.), *Lipid oxidation pathways*, AOCS Press, Urbana, Ill. 2008.
- [6] Wilde, S. C., Keppler, J. K., Palani, K., Schwarz, K., β -Lactoglobulin as nanotransporter for allicin: Sensory properties and applicability in food. *Food Chem.* 2016, 199, 667–674.

- [7] Butte, W., Rapid method for the determination of fatty acid profiles from fats and oils using trimethylsulphonium hydroxide for transesterification. *Journal of Chromatography A* 1983, 261, 142–145.
- [8] Lampi, A.-M., Kamal-Eldin, A., Effect of α - and γ -tocopherols on thermal polymerization of purified high-oleic sunflower triacylglycerols. *J. Amer. Oil Chem. Soc.* 1998, 75, 1699–1703.
- [9] Vries, A. de, Wesseling, A., van der Linden, E., Scholten, E., Protein oleogels from heat-set whey protein aggregates. *Journal of Colloid and Interface Science* 2017, 486, 75–83.
- [10] Wheeler, D. H., Peroxide formation as a measure of autoxidative deterioration. *J. Amer. Oil Chem. Soc.* 1932, 9, 89–97.
- [11] Matissek, R., Steiner, G., *Lebensmittelanalytik*, Springer Berlin Heidelberg New York, Berlin, Heidelberg 2006.
- [12] Loftus Hills, G., Thiel, C. C., 338. The ferric thiocyanate method of estimating peroxide in the fat of butter, milk and dried milk. *Journal of Dairy Research* 1946, 14, 340–353.
- [13] Thiyam, U., Stöckmann, H., Schwarz, K., Antioxidant activity of rapeseed phenolics and their interactions with tocopherols during lipid oxidation. *J. Amer. Oil Chem. Soc.* 2006, 83, 523–528.
- [14] Stöckmann, H., Schwarz, K., Huynh-Ba, T., The influence of various emulsifiers on the partitioning and antioxidant activity of hydroxybenzoic acids and their derivatives in oil-in-water emulsions. *J. Amer. Oil Chem. Soc.* 2000, 77, 535–542.
- [15] Drusch, S., Serfert, Y., Scampicchio, M., Schmidt-Hansberg, B., Schwarz, K., Impact of Physicochemical Characteristics on the Oxidative Stability of Fish Oil Microencapsulated by Spray-Drying. *J. Agric. Food. Chem.* 2007, 55, 11044–11051.
- [16] Estévez, M., Ollilainen, V., Heinonen, M., Analysis of Protein Oxidation Markers α -Aminoadipic and γ -Glutamic Semialdehydes in Food Proteins Using Liquid Chromatography (LC)–Electrospray Ionization (ESI)–Multistage Tandem Mass Spectrometry (MS). *Journal of Agricultural and Food Chemistry* 2009, 57, 3901–3910.
- [17] Team, R. C., R: A Language and Environment for Statistical Computing 2015, Vienna, Austria, <https://www.R-project.org/>.
- [18] Elzhov, T. V., Mullen, K. M., Spiess, A.-N., Bolker, B., minpack.lm: R Interface to the Levenberg-Marquardt Nonlinear Least-Squares Algorithm Found in MINPACK, Plus Support for Bounds 2015.
- [19] Frankel, E. N., *Lipid oxidation*, Elsevier 2014.
- [20] Putseys, J. A., Lamberts, L., Delcour, J. A., Amylose-inclusion complexes: Formation, identity and physico-chemical properties. *Journal of Cereal Science* 2010, 51, 238–247.

- [21] Brimberg, U. I., Kamal-Eldin, A., On the kinetics of the autoxidation of fats: Substrates with conjugated double bonds. *European Journal of Lipid Science and Technology* 2003, 105, 17–22.
- [22] Brimberg, U. I., On the kinetics of the autoxidation of fats. *J. Amer. Oil Chem. Soc.* 1993, 70, 249–254.
- [23] Hu, M., McClements, D. J., Decker, E. A., Lipid Oxidation in Corn Oil-in-Water Emulsions Stabilized by Casein, Whey Protein Isolate, and Soy Protein Isolate. *J. Agric. Food. Chem.* 2003, 51, 1696–1700.
- [24] Sakanaka, S., Tachibana, Y., Ishihara, N., Raj Juneja, L., Antioxidant activity of egg-yolk protein hydrolysates in a linoleic acid oxidation system. *Food Chem.* 2004, 86, 99–103.
- [25] Vollhardt, K. P. C., Schore, N. E., Butenschön, H., *Organische Chemie* 2011.
- [26] Labuza, T. P., Dugan, L. R., Kinetics of lipid oxidation in foods. *C R C Critical Reviews in Food Technology* 1971, 2, 355–405.
- [27] Frankel, E. N., Huang, S.-W., Kanner, J., German, J. B., Interfacial Phenomena in the Evaluation of Antioxidants: Bulk Oils vs Emulsions. *J. Agric. Food. Chem.* 1994, 42, 1054–1059.
- [28] Oehlke, K., Heins, A., Stöckmann, H., Schwarz, K., Impact of emulsifier microenvironments on acid–base equilibrium and activity of antioxidants. *Food Chem.* 2010, 118, 48–55.
- [29] Fletcher, B. L., Tappel, A. L., Fluorescent modification of serum albumin by lipid peroxidation. *Lipids* 1971, 6, 172–175.
- [30] Iio, T., Yoden, K., Formation of fluorescent substances from degradation products of methyl linoleate hydroperoxides with amino compound. *Lipids* 1988, 23, 1069–1072.
- [31] YAMAKI, S., KATO, T., KIKUGAWA, K., Characteristics of Fluorescence Formed by the Reaction of Proteins with Unsaturated Aldehydes, Possible Degradation Products of Lipid Radicals. *CHEMICAL & PHARMACEUTICAL BULLETIN* 1992, 40, 2138–2142.
- [32] MONTGOMERY, M. W., DAY, E. A., Aldehyde-Amine Condensation Reaction: A Possible Fate of Carbonyls in Foods. *J. Food Sci.* 1965, 30, 828–832.
- [33] Kinsella, J. E., Fox, P. F., Water sorption by proteins: Milk and whey proteins. *Crit. Rev. Food Sci. Nutr.* 1986, 24, 91–139.
- [34] Bull, H. B., Breese, K., Protein hydration. *Archives of Biochemistry and Biophysics* 1968, 128, 488–496.
- [35] Gatellier, P., Kondjoyan, A., Portanguen, S., Santé-Lhoutellier, V., Effect of cooking on protein oxidation in n-3 polyunsaturated fatty acids enriched beef. Implication on nutritional quality. *Meat Sci.* 2010, 85, 645–650.

- [36] Albani, J. R., Vogelaer, J., Bretesche, L., Kmiecik, D., Tryptophan 19 residue is the origin of bovine β -lactoglobulin fluorescence. *Journal of Pharmaceutical and Biomedical Analysis* 2014, *91*, 144–150.

Chapter 3

Influence of Water Addition on Lipid Oxidation in Protein Oleogels

Abstract

The aim of the present study is the investigation of lipid oxidation in protein based oleogels. For this purpose, oleogels are prepared by suspension of freeze dried whey protein isolate aggregates and small amounts of water (<10%) in purified oleic rich safflower oil. The formation of conjugated dienes positively correlates with the addition of water. In contrast, a lower concentration of aldehydes is measured by headspace gas chromatography in oleogels with higher water addition, indicating a water facilitated degradation of aldehydes reacting with proteins. Determination of water activity indicates the presence of water droplets at higher water addition to oleogels. Furthermore, changes in the surface appearance (greasy-glossy to dull) and the texture (consistent gel vs. crumbly) structure are indicative of microstructural changes due to increased water addition. The study suggests that water droplet formation is responsible for the marked increase in lipid oxidation. However, cross reaction of aldehydes with proteins is suggested to result in lowering the levels of secondary lipid oxidation products hexanal and propanal in oleogel.

Practical Applications: The practical applications of the present work are related to the fabrication, processing, storage and consumption of oleogels and other protein-lipid-matrices. The results clearly indicate oleogels are prone to oxidation and proteins are involved by cross-reaction resulting in visible browning during storage. Oxidation products such as hexanal (marker for secondary lipid oxidation) may not reflect the level of oxidation due to degradation by cross-reactions with proteins.

Keywords: lipid oxidation, oleogel, organogel, oxidation, protein

3.1 Introduction

The production of oleogels is an innovative way of structuring and plasticizing liquid oils consisting mainly of unsaturated fatty acids. Waxes and polymers are used as gelling and structuring agents [1]. The two main objectives of oil gelling are: Substitution of saturated lipids by unsaturated lipids and the avoidance of *trans* fatty acids, which are also known as unhealthy lipid compounds and mainly introduced by conventionally partially hydrogenated fats [2-4].

Unsaturated fatty acids, however, are prone to lipid oxidation, which is well known as one of the main causes of deterioration and quality loss in food [1, 2]. But only a few papers have been published on lipid oxidation of oleogels, yet. So far, only one study by Chen *et al.* has investigated oxidation of a protein based oleogel, a so called emulgel, consisting of 60 % soybean oil in glycerol stabilized zein [3]. The preparation of the emulgel requires a heating step at 95 °C, which may initiate lipid oxidation, but in fact the protein network retard lipid oxidation in comparison to liquid oil [3]. Thus, it is of particular interest to evaluate the function of protein during lipid oxidation, as proteins as well as hydrolysates are considered to function as effective antioxidants [4, 5]. Further, it is of growing interest as several amino acids including the essential amino acid tryptophan present in proteins or hydrolysate are vulnerable to reactive oxygen species and are therefore affected by oxidation [6]. Also the protein backbone can be attacked by reactive species. Therefore, protein oxidation causes a lower nutritional value and a reduced digestibility, but also toxic products may be formed, which exhibited, in addition to several lipid oxidation products, carcinogenic potential [1, 7].

This paper focuses on whey protein as polymer for structuring the oil. These oleogels contain a high oil content and no heating step that includes the oil phase is needed [8]. Thus, the aim of this study is the evaluation of the oxidative stability of a whey protein based oleogel during storage. The formation of typical lipid oxidation markers will therefore be evaluated. A special focus will be on the influence of the water content on the changes in the oleogels during storage, as the water content is an important factor for the resulting texture of oleogels [9].

3.2 Materials & Methods

Oleic acid rich safflower oil was purchased from a local supermarket (fatty acid composition according to [10] using authentic standards for calibration (supelco 37 FAME Mix): C16:0= 4.65 ± 0.02 %, C18:0= 2.38 ± 0.02 %, C18:1= 76.7 ± 0.2 %, 18:2= 14.7 ± 0.03 %, 18:3=

0.14 ± 0.01 %). Whey protein isolate (BiPro) was obtained from Davisco Foods International with 97.7 % protein and 75 % β -lactoglobulin in dry matter according to Keppler et al. 2017 and 2018. Al₂O₃, BaCl₂ and FeSO₄ are from Carl Roth. Trimethylsulfonium hydroxide (0.25 M in methanol) is from Sigma Aldrich. All solvents were from VWR. Water (<18 M Ω) was purified by an Elga Veolia system and was used for all the experiments. All chemicals were at least from high purity.

3.2.1 Purification of safflower oil

The purification of safflower oil from natural antioxidants and trace metals was based on the method described by Lampi & Kamal-Eldin [11]. A glass column, wrapped with aluminum foil to prevent light induced oxidation was packed with 250 g of activated alumina (conditioned by 100 °C for 8 h followed by 200 °C for 12 h) suspended in *n*-hexane. 500 mL oil were dissolved in an equal volume of *n*-hexane and then passed through the column. Afterwards the column contained 250 mL of *n*-hexane. The first 250 mL eluate was discarded and the remaining eluate was collected in a brown ice water cooled glass flask. The collected oil-hexane mixture was flushed with nitrogen for 10 min and stored at -20 °C until further use. Evaporation of *n*-hexane was achieved on a rotary evaporator with carefully adjusted vacuum down to 150 mbar in 3 steps, each 15 min long and followed by 10 min of flushing with nitrogen. The first step was conducted at 65 °C and the last two steps at 90 °C. The oil was tested of residual tocopherols (HPLC, < 0.5 ppm, method DGF F-II 4a).

3.2.2 Sample preparation

Whey protein aggregates were produced according to de Vries *et al.* by lyophilizing two times with water washed protein aggregates, which were prior frozen by dropping into liquid nitrogen [12]. The mode and median of particle size of protein aggregates was measured after rehydration of dry protein aggregate samples in water using static light scattering (Horiba, Retsch Technology GmbH, Haan, Germany). This was also done to check for constant particle sizes (mode 12-15 μ m, median 12-18 μ m). The particle size is bimodal distributed with a second minor peak. However, it was checked that the main peak is over 80%. Dry whey protein isolate aggregates (6.8 %) were then combined with stripped oil, premixed and stirred for 10 min. In models containing water, the water was added slowly after 5 min. After centrifugation for 20 min by 4000 *g*, superfluous oil was removed by decanting the gel for 10 min.

Except for the measurement of volatiles, 200 ± 10 mg of sample was stored in closed 15 mL plastic tubes, centrifuged by 1000 *g* for 1 min to have an equal surface and additionally wrapped with parafilm. The sample was then incubated in the dark by an elevated and constant storage

temperature of 40 °C in a drying oven until the sample was taken for analysis. This temperature was chosen to moderately accelerate the experiments without inducing new reactions compared to ambient conditions. Lipids were extracted by washing the gel 3 times with *cyclo*-hexane, centrifuging 5 min by 4000 *g* and decanting the fluid. Extracted *cyclo*-hexane fractions were combined in a glass reaction vial, flushed with nitrogen to dryness in 20 min, reweighted and used for further analysis.

3.2.3 Color formation and appearance

Photographs for color formation and appearance were taken with a digital camera (>12 MP). To ensure the same illumination, representative samples for each oleogel type were collected and stored at 4 °C and one picture was taken for all samples together. From this picture identically sized cutouts (224 x 374 px) were assembled in Fig. 6. No further image editing was carried out.

3.2.4 Determination of conjugated dienes

Extracted fat was dissolved in 5 mL distilled isopropyl alcohol, vortexed and diluted if necessary. Conjugated dienes (CD) were measured directly by UV absorption at 234 nm [13, 14] and the absorption coefficient of 26,000 M⁻¹cm⁻¹ for methyl linoleate hydroperoxides was used [15]. All measurements were prepared in triplicate unless otherwise noted and results of CD are given as difference to the unoxidized sample.

3.2.5 Volatiles

Measurement of volatiles was conducted as indicator for secondary lipid oxidation products using headspace gas chromatography (HS-GC) according to the method of Frankel [16]. Approximately 200 mg gels in 20 mL headspace vials, hermetically sealed with PTFE/silicone membrane screw caps, were stored as described above. Periodically, samples were taken and incubated at 70 °C for 15 min, before an aliquot was transferred to the GC. All measurements were prepared in triplicate

3.2.6 Rheology

Oscillation rheology was used to measure the robustness and strength of gels and to compare the macroscopic properties of the gels obtained from snap frozen lyophilized protein in oil in this study to gels obtained by solvent exchange by de Vries *et al.* [9]. Therefore a frequency sweep test was carried out ($\omega = 1 - 100$ 1/s) at a deformation of 1 %, which is safely in the linear viscoelastic region [9], on a plate-plate system (diameter 25 mm) with a gap of 1 mm at 20 °C

(Modular Compact Rheometer MCR 302, Anton Paar GmbH). Measurements were repeated in duplicate with two technical duplicates for each sample.

3.2.7 Determination of water content & water activity

Water content was estimated by heating ~ 2.5 g gel in dry aluminum cups (diameter = 96 mm) for 4 h by 105 °C in an air oven and reweighting of the dry mass. The water activity of ~ 0.9 g samples was measured with an AW SPRINT TH-500 (Novasina) at 25 °C. Measurements were repeated in triplicate.

3.2.8 Statistical analysis and calculations

All results were statistically analyzed with Excel and R (with the R packages ggplot2 and dplyr for imaging), which includes T-test and Shapiro Wilk normality test [17–19]. The R package deSolve was used for calculations with differential equation (formal 1, see below) and minpack.lm for fitting of the parameters (rate constants and initial value, see discussion) with a nonlinear least square regression using the Levenberg-Marquardt algorithm [20, 21]. Standard deviation was estimated using the Jack knife delete one procedure [22], whereas each data points relevance is considered by a bootstrapping technique. Briefly, for data with n points n subsets were created with each missing another one of the n points. Jack knife estimation for standard deviation was used as the standard deviation of the selected parameters calculated for all subsets multiplied with $(n-1) / \text{square root}(n)$, for further validation see in supplementary materials.

3.3 Results/Discussion

3.3.1 Formation of primary lipid oxidation products

To evaluate the formation of primary lipidoxidation products in oleogels the concentration of conjugated dienes was analyzed at three different time points during a storage period of two weeks. Oleogel without water addition (0 %) was compared with oleogels that contained an addition of 1 to 3 % water. A logarithmic scale for the conjugated diene content was used in figure 3.1 to demonstrate on the one hand the strong increase within two weeks and on the other hand the large differences between the individual oleogels. With a water addition of 1 % there was no difference compared to the control (0 % water addition) after 3 days of storage. After 9 days, a significant increase in the formation of conjugated dienes in the oleogel with 1% water addition was observed. The addition of more than 2 % water had a significant influence on the formation of conjugated dienes already after 3 days of storage. After 14 days the content of

conjugated dienes in oleogels with 2 and 3 % water addition had increased to 36 and 101 mmol /kg, respectively, while the increase amounted only to 1.9 and 2.2 mmol /kg in oleogels with the content of 0 and 1 % water addition, respectively. In comparison, in bulk oil incubated at 40 °C dienes raised to about 0.85 mmol /kg within 14 days.

Due to these large differences in oxidation in oleogels, a distinction was made in the further course of the study between oleogels with low water addition (< 1%) and higher water addition (> 2.0 %).

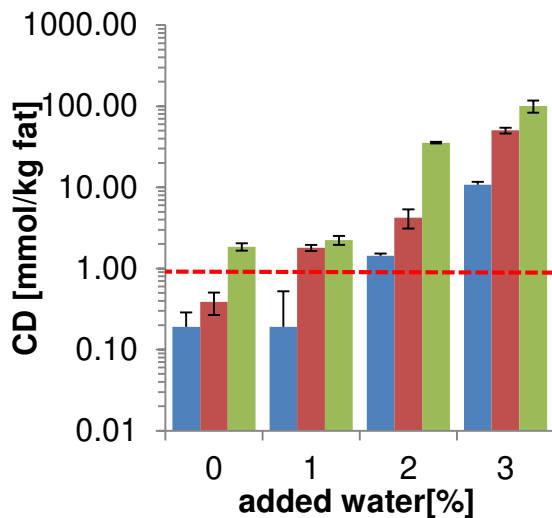


Figure 3.1: Changes of conjugated dienes (CD, 234 nm) in extracted oil of stored gel samples by 40 °C, added 0 to 3 % water, after 3 (blue), 9 (red) 14 (green) days of incubation by 40 °C in comparison to the oxidation of bulk oil stored under same conditions for 14 days (red dashed). All values are listed as mean and standard deviation of three independent replicates.

The formation of conjugated dienes in oleogel without or low addition of water (0 % and 0.23 %) showed a slow and continuous increase reaching an increase by < 6 mmol/kg after 7 weeks (figure 3.2). The oxidation kinetic of oleogel with higher addition of water (2.8 – 8.4 %) was strikingly different. Within 10 to 21 days a maximum increase by 120 mmol/kg oil was reached before exhibiting a plateau followed by a marked decrease after 28 days. A maximum in the formation of primary lipid oxidation products is consistent with other low temperature lipid oxidation kinetic models [23, 24].

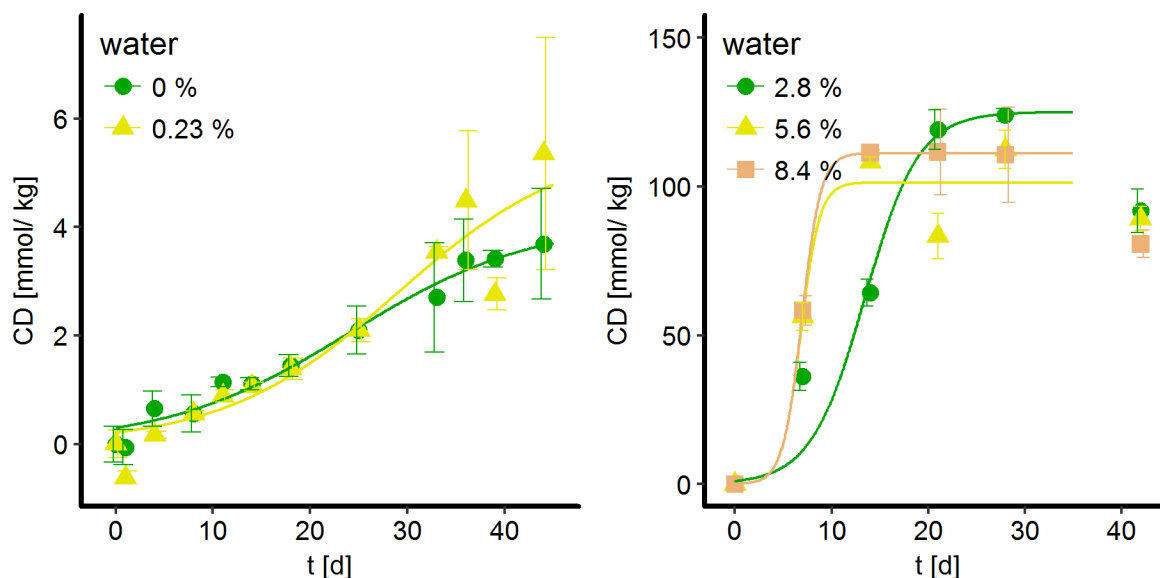


Figure 3.2: Changes of conjugated dienes (CD, 234 nm) in extracted oil of stored gel samples by 40 °C, left: 0 % and 0.23 % water added, right: 2.8 – 8.4 % water added. Fitting lines are according to formula 3.1 using a nonlinear least square regression to the raw data, not to means (standard error of estimates from 0 to 8.4 % water: 0.47, 0.83, 11.9, 10.8 and 8.05 mmol/kg). All values are listed as mean and standard deviation of three independent replicates.

Also, the levels of conjugated dienes in the oleogels fit well to the model proposed by Crapiste *et al.* for lipid hydroperoxide kinetics, which includes a first-order autocatalytic reaction and a second-order decomposition reaction (formula 3.1) [23], despite the model does not include a decrease in the total amount of hydroperoxides. As the model describes the formation and degradation of hydroperoxides, a dynamic equilibrium is formed. However, this reaction kinetic system depends on a constant formation rate, which is consistent as long as the plateau or maximum is not reached. The formation rate depends on the concentration of oxygen and unsaturated lipids. As long as the unsaturated lipid concentration is in excess over oxygen, the formation rate is constant, which is consistent with the used model. If the concentration of unsaturated lipids would be low this assumption is not valid anymore. The formation rate decreases and would result in turn in a decrease in the concentration of lipid hydroperoxides or CD. It is suggested that the CD maximum is the best assumption for the beginning of the plateau. Therefore, a nonlinear regression was only conducted until the day with the observed maximum with initial borders of 0.1 and 1 mmol/kg CD_0 . This borders were estimated, because all gel samples were made of the same oil and low water (0-0.23 %) gels have CD_0 of 0.29 ± 0.10 and 0.21 ± 0.12 mmol/kg (measured CD concentration on day 0 was set to 0, standard derivation was 0.4; 0.3 mmol/kg) and high water gel samples (2.8-8.4 % water added) have a standard derivation of measured values of 0.3, 0.8 and 0.5 mmol/kg. The standard deviation of the

regression parameters and relevance of each data point were estimated by the jack knife delete one procedure [22]. The formation rate constant k_1 increased constantly by water addition from 0.11 ± 0.03 to $1.02 \pm 0.02 \text{ d}^{-1}$ (0 % to 5.6 % water addition), whereas decomposition rate constant k_2 slightly decreased (figure 3.3).

$$\text{(Formula 3.1): } \frac{dCD}{dt} = k_1 CD - k_2 CD^2$$

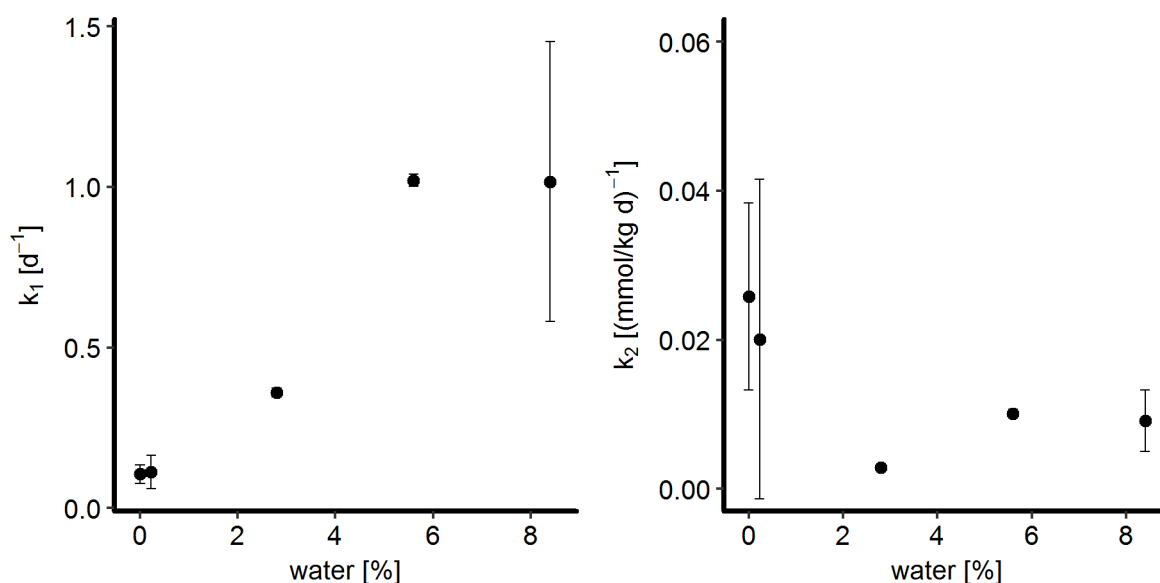


Figure 3.3: left: constant k_1 and right: k_2 in gel samples from 0 % to 8.4 % water addition for fitting curves in figure 3.2. Standard deviation was estimated using the Jack knife delete one procedure [22].

Water appears to play a crucial role in relation to the predominant reaction behavior that governs lipid oxidation, as can be seen by the increasing k_1 rate constant. As the water content increased, the first phase of lipid oxidation was more strongly characterized by the 1st order reaction, whereas the level of CD after 14 days was more characterized by the second order decomposition. However, a low increase of conjugated dienes predominates at very low (0.28 %) or no (0 %) water addition during the first weeks. Water provides enhanced diffusion of oxidation products and facilitates the solubilization. Both effects may be causative for the predominant effect of the 1st order reaction kinetic, i.e. strong formation of CD.

3.3.2 Formation of volatile secondary lipid oxidation products

Figure 3.4 shows the formation of two secondary lipid oxidation products hexanal and propanal. Hexanal was chosen for comparison as this aldehyde is the main degradation product of linoleic acid [25] which amounted to 15% in the oil used for this study. However, as the oil also contained a small amount of α -linolenic acid, propanal was also chosen for comparison as this fatty acid is even more prone to oxidation resulting in propanal as one of its main oxidation

products [25]. For both oxidation products, the formation in oleogels without or with low water addition was lower than with higher water addition. With a higher water addition ($> 2\%$), the formation of both hexanal and propanal increased significantly with the start of storage. On the other hand, at low water content, a distinct lag phase was evident before the formation increased rapidly. These results were in agreement with the formation of conjugated dienes as a function of water content (figure 3.2). If, however, the formation of hexanal and propanal in oleogels was related to the formation in pure bulk oil (without water addition and structuring protein), considerable differences were found. The lag phase for hexanal formation of bulk oil was equally pronounced as in oleogels with a low water content and the maximum laid in a similar order of magnitude. In contrast, the lag phase of propanal formation is shorter than in low water oleogels and the maximum exceeded the maximum of oleogels several times followed by a significant decrease.

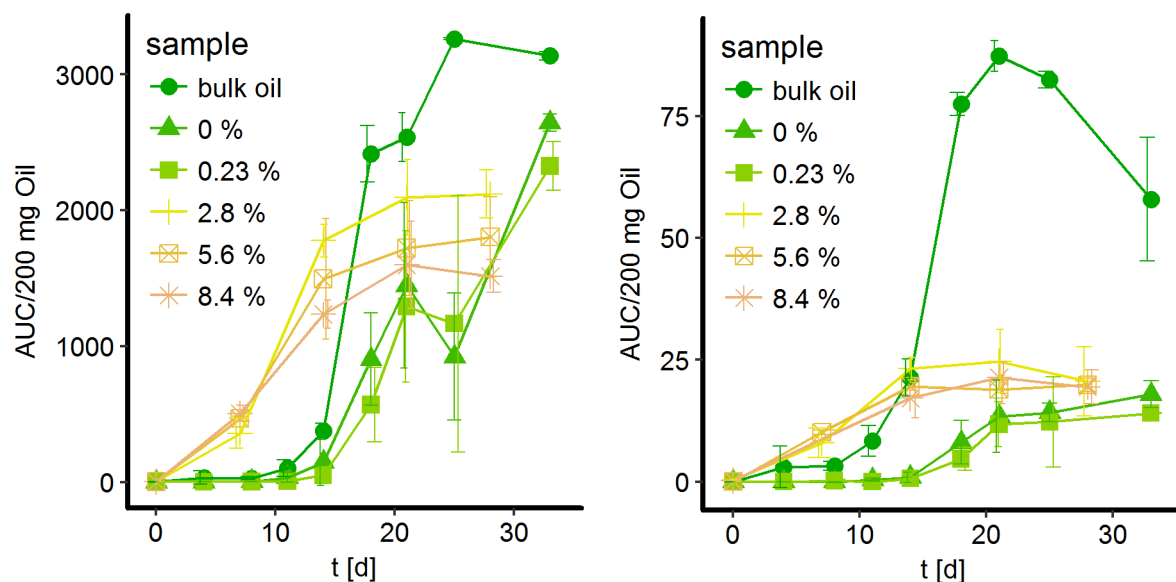


Figure 3.4: Left: Formation of hexanal and right: propanal in gel samples from 0 % to 8.4 % water addition and in bulk oil, lines are added to guide the eyes only.

The differences in the formation of hexanal and propanal in relation to pure bulk oil may be explained by the observed decrease of the degradation reaction rate k_2 , as water can prevent hydroperoxides from fragmentation to secondary oxidation products by a hydration shield and hydrogen bonds. However, since the oleogel with 2.8 % water addition has a significant higher hexanal concentration on most days in comparison to the oleogel with 8.4 % water addition (see below) but a lower degradation rate constant k_2 (0.0029 ± 0.0002 (mmol/kg d) $^{-1}$, 0.0091 ± 0.0042 (mmol/kg d) $^{-1}$), the lack of hexanal could not be explained by a lower degradation rate. It is therefore suggested to attribute the degradation by side reactions of aldehydes or their precursors with proteins in oleogels [26–29]. Carbonyl groups of aldehydes react easily with nucleophiles

such as free amino groups of lysine residues or the N-terminal residues of the protein in oleogels. Schiff bases can be formed which can condense with further aldehydes to form polymers [25]. These reactions can be promoted by removing free water, which is formed during condensation. The hydration of the proteins in the oleogels may play a key role here [30, 31]. Similar findings have been reported for WPI sunflower oil suspension systems stored at 40 °C [32]. In addition, an increase in the water concentration near proteins, due to hydration, in the overall low-water oleogel system could facilitate the hydrolysis of the amino groups. Locating protein-bound amino groups in the vicinity of acidic amino acid residues such as aspartate or glutamate could promote local acid catalysis. This reaction mechanism, of repeated aldol condensation, was proposed by Montgomery et al. for the formation of nitrogen-free pigments using heptanal and L-tyrosine ethyl ester [28] and may also apply during lipid oxidation in the presence of proteins as observed in the present study.

Further, the better water solubility of propanal compared to hexanal could explain the different increase in oleogels in relation to pure bulk oil. Amino-carbonyl reactions are catalyzed by acids in aqueous media by activating the carbonyl group by protonation [33]. This could also explain the significantly lower level of hexanal in oleogels with the highest water addition of 8.4% compared to 2.8% (each measuring point from day 14 to day 28 ($p = 0.002 / 0.06 / 0.006$; figure 3.4) despite higher formation of conjugated dienes (figure 3.2).

3.3.3 Differences in gels appearances and color formation

Photos of oleogels with different water addition are shown in figure 3.5. The appearance of the surface changes with increasing water addition from greasy-glossy to dull and the consistent structure becomes crumbly. Oleogels without added water in this study appeared white-opaque and were similar to oleogels obtained via solvent exchange route [8] instead of freeze-drying with previous dripping of whey protein solutions in liquid nitrogen.

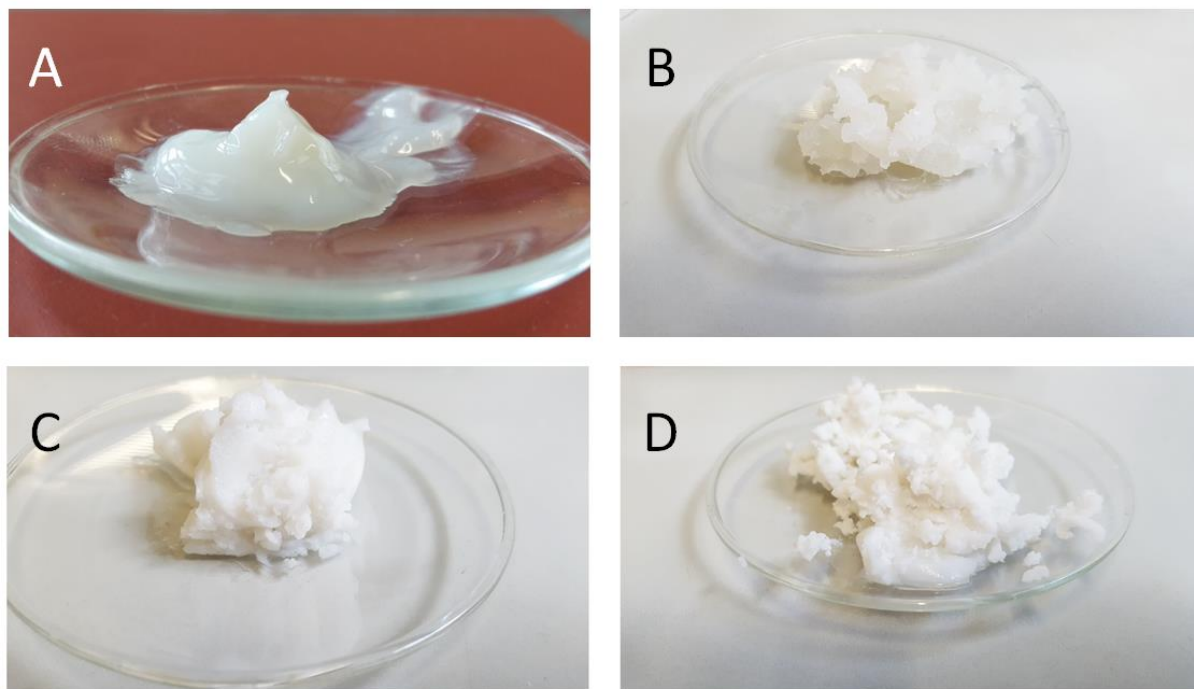


Figure 3.5: Appearances of oleogels with 0 % (A), 2.8 % (B), 5.6 % (C) and 8.4 % (D) water added during preparation.

Figure 3.6 shows the change in color of the oleogels over the entire storage period. A color change from white to yellow-brown was observed. Samples with 2.8 % and more water addition developed a yellow-brownish color after 2-3 weeks of storage at 40 °C. With water additives of 5.6 and 8.4 %, a darker brown tone was observed at the end of storage. Similar color changes were already observed for different lipid-protein mixtures in previous studies [32, 34, 35]. Color changes were associated with the interaction of lipid oxidation products and proteins as well as polymerization or cross-linking [36, 37], cleavage reactions [35, 38], increased hydrophobicity of proteins [36, 39] and the formation of lipid-protein complexes [40]. This is in agreement with the increased formation of primary lipid oxidation products in discolored oleogels in this study and the proposed side reactions of secondary oxidation products with protein aggregates of the oleogels.

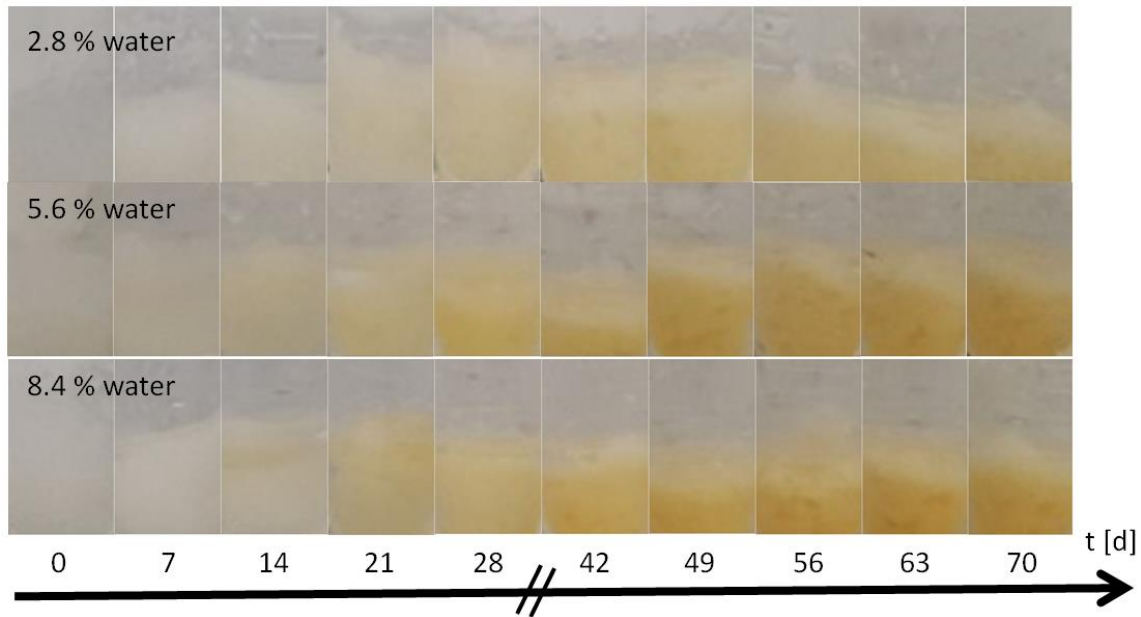


Figure 3.6: Color formation in oleogels with 2.8 to 8.4 % water addition during incubation at 40 °C.

3.3.4 Water content and gelling efficiency

The relation of water addition (to premix) and resulting water content (in the oleogel) is illustrated in figure 3.6 on the left side. Increasing water addition led to a quadratically increase of the resulting water content in the oleogel. During centrifugation, the oleogel precipitates and oil forms a supernatant which is removed by decanting. During centrifugation, not only the hydrated protein is separated but also water droplets present. With increasing addition of water, an increase in free water droplets is to be expected. The disproportionate increase in the water content indicates that the water droplet size [9] and thus the rate of descent during centrifugation increased with higher water addition.

Samples with 100 mg/g water addition exhibited an increase in the water content by a factor of nearly 2. This corresponds to the ratio of premix to oleogel yield (see figure 3.6 right.). Samples with less than 15 mg/g water addition did not seem to build water droplets that were centrifugable and thus formed a linear relationship between water addition oleogel yield.

The water content of oleogel without water addition amounted to 4.8 mg/g which is attributed to residual water strongly bound to freeze dried protein subjected to the oil for oleogel formation. Samples that differed from the linear fit exhibited a water addition of more than 25 mg/g corresponding to a water/protein ratio of 0.37. This ratio is quite close to the findings of de Vries *et al.* for whey protein aggregation in sunflower oil. The authors observed water droplet building

at a water/protein ratio of 0.25 with small water droplets and greater droplets at a water/protein ratio above 0.5 in stained confocal laser scanning microscopy images [9].

Furthermore, the water activity (a_w -value) of 0 % and 0.23 % water addition amounted to 0.52 ± 0.01 and 0.52 ± 0.02 , respectively. These a_w -values were markedly lower than for oleogels with 3 % water addition (0.94 ± 0.02). High a_w -values are indicative for non-bound water such as dispersed water droplets. This water activity found for oleogels with higher water additions is comparable to the water activity of unsalted butters and margarines with water present as dispersed droplets in the continuous oil-fat phase [41].

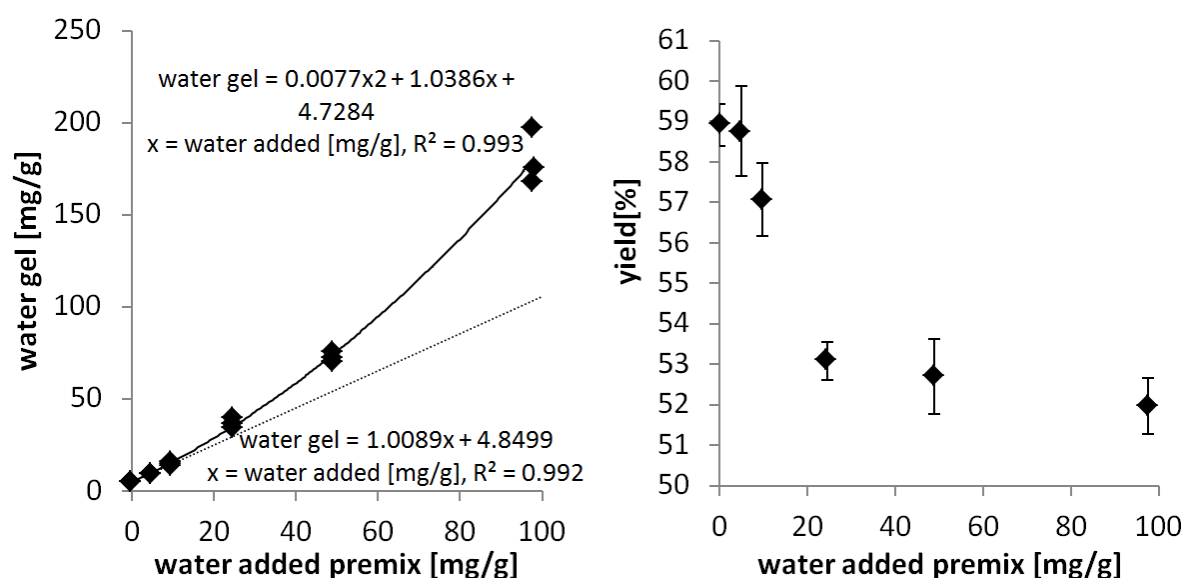


Figure 3.7: Left: water content in gel measured gravimetrically after drying for 4 h over water added in premix, linear fit for first nine values (water added < 10 mg/g, dotted) and second order polynomial (line). Right: relation of gel yield after centrifugation over water added in premix.

The marked difference in water activity is accompanied by a sharp increase in the oxidation rate of oleogels. This effect could be also attributed to the formation of water droplets, which on the one hand led to the formation of interfaces. It is suggested, that with establishing new interfaces, amphiphilic lipid oxidation products are concentrated in this so call pseudophase. [42] As lipid oxidation is an autocatalyzed reaction, a higher concentration strongly affects the reaction rate and accelerates lipid oxidation. This can also be seen by the formation of primary oxidation product part as the k_1 rate constant raise with water addition. On the other hand, weakly bound water increase the diffusion rate of reaction products and catalysts of lipid oxidation, which also promotes lipid oxidation as this is a bimolecular reaction with oxygen. Thus finally, a critical concentration of radicals in oleogels with higher water content would be reached faster and the induction period would be shortened.

3.3.5 Rheological properties

The protein aggregates in this study are introduced as freeze dried material, which was prior frozen by liquid nitrogen. By contrast, de Vries *et. al.* used solvent exchange procedure for oleogels in their rheology study on the effect of water addition [9]. Clustered aggregates in water of the size $\sim 20 \mu\text{m}$ (mean value) were reported before for solvent exchange produced material [8], which is comparable to our freeze dried material (median 12-18 μm). However, the substructure of the aggregates may differ as de Vries *et al.* reported a mean value of 220 nm and 140 nm for material from the freeze dried and the solvent exchange procedure, respectively, after sonification before the particle size measurement [12]. As water influence and droplet formation is of special interest in the present study and influenced by aggregate size, the rheological properties of the system were reported here using oscillatory rheology. It is evident that the elastic modulus is higher than the viscous one for all systems ($G' > G''$) (figure 3.8 left) which indicates that the deformation resembles that of a weak gel in all the observed systems. With an addition of 100 mg/g water in the premix (finally $180 \pm 15 \text{ mg/g}$), the storage modulus G' increased by an order of magnitude. There was no significant frequency dependency evident for G' or G'' . The effect of water addition to the oleogel on the storage modulus is shown in figure 3.8 right, where a saturation effect can be observed after addition of $\sim 50 \text{ mg/g}$ water to the premix.

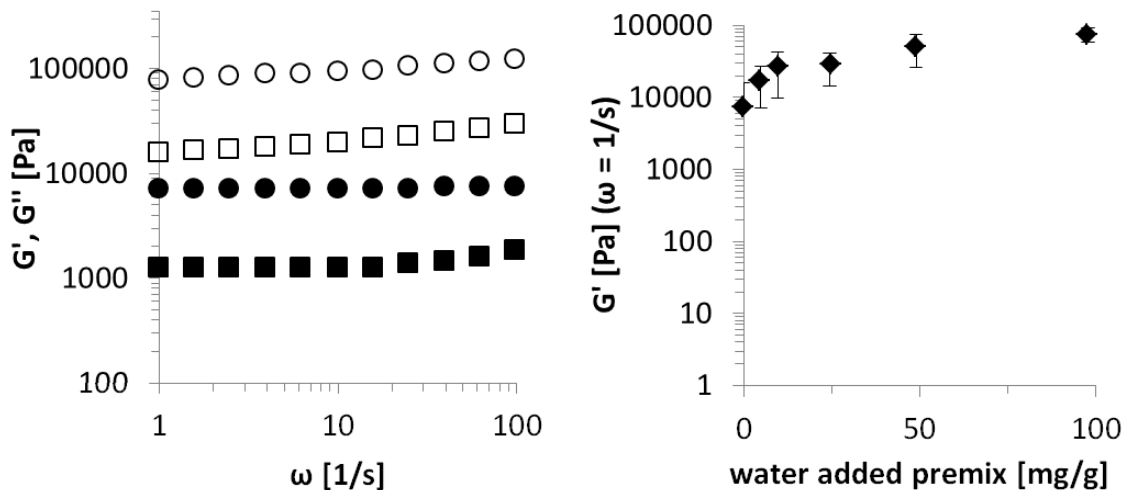


Figure 3.8: Left: frequency sweep plot from gels with no water addition (filled symbols) and water addition about 100 mg/g (open symbols). \circ : G' ; \square : G'' ; right: storage modulus G' as a function of water addition in premix.

The observed G' of the present oleogels fit well with those described previously for a similar gel [9] i.e. that water addition has an impact on gel strength and viscosity. The authors concluded that water forms capillary bridges between protein aggregates in oil, which strengthen the gel network. A saturation of G' was suggested to indicate that a maximum hydration level is reached

where no further water can be incorporated into the protein network [9]. These results are also in line with the results presented in figure 3.7 left: Here, water droplet formation was suggested to occur for the high water systems (>2 % water) and this is reflected in the observed saturation of G' .

Although increased viscosity potentially affects the lipid oxidation kinetics, because the reactions are diffusion controlled this mechanism does not apply for oleogels. As the increase in viscosity is related to the water content which in turn accelerates the autocatalytic lipid oxidation the opposite effect, increase in the degree of lipid oxidation, was found.

3.4 Conclusion

The texture of oleogels prepared by freeze-dried whey protein aggregates can be adjusted by adding water like for solvent exchange prepared oleogels. With increasing water content gel strength increases, but provokes forming of unbound water, which leads to higher lipid oxidation in terms of conjugated dienes. Contrary to higher conjugated diene levels lower levels of hexanal and propanal were found in gel systems with higher water contents. These findings are attributed to the ability of water to catalyze acidic aldol reactions and the Schiff base reaction of that aldehydes with amino groups of the protein, which leads to further degradation. Overall, adjusting oleogel texture with water or combining this oleogel with water-rich food ingredients will provoke lipid oxidation, however, typical lipid secondary oxidation markers, such as aldehydes, are decreased or even lacking.

Abbreviations Used

CD, conjugated dienes

Figure captions

Figure 3.1: Changes of conjugated dienes (CD, 234 nm) in extracted oil of stored gel samples by 40 °C, added 0 to 3 % water, after 3 (blue), 9 (red) 14 (green) days of incubation by 40 °C in comparison to the oxidation of bulk oil stored under same conditions for 14 days (red dashed).

All values are listed as mean and standard deviation of three independent replicates.....83

Figure 3.2: Changes of conjugated dienes (CD, 234 nm) in extracted oil of stored gel samples by 40 °C, left: 0 % and 0.23 % water added, right: 2.8 – 8.4 % water added. Fitting lines are

according to formula 3.1 using a nonlinear least square regression to the raw data, not to means (standard error of estimates from 0 to 8.4 % water: 0.47, 0.83, 11.9, 10.8 and 8.05 mmol/kg). All values are listed as mean and standard deviation of three independent replicates.84

Figure 3.3: left: constant k_1 and right: k_2 in gel samples from 0 % to 8.4 % water addition for fitting curves in figure 3.2. Standard deviation was estimated using the Jack knife delete one procedure [22].85

Figure 3.4: Left: Formation of hexanal and right: propanal in gel samples from 0 % to 8.4 % water addition and in bulk oil, lines are added to guide the eyes only.86

Figure 3.5: Appearances of oleogels with 0 % (A), 2.8 % (B), 5.6 % (C) and 8.4 % (D) water added during preparation.88

Figure 3.6: Color formation in oleogels with 2.8 to 8.4 % water addition during incubation at 40 °C.89

Figure 3.7: Left: water content in gel measured gravimetrically after drying for 4 h over water added in premix, linear fit for first nine values (water added < 10 mg/g, dotted) and second order polynomial (line). Right: relation of gel yield after centrifugation over water added in premix.90

Figure 3.8: Left: frequency sweep plot from gels with no water addition (filled symbols) and water addition about 100 mg/g (open symbols). ○: G' ; □: G'' ; right: storage modulus G' as a function of water addition in premix.91

3.5 References

- [1] Papuc, C., Goran, G. V., Predescu, C. N., Nicorescu, V., Mechanisms of Oxidative Processes in Meat and Toxicity Induced by Postprandial Degradation Products: A Review. *Compr. Rev. Food Sci. Food Saf.* 2017, 16, 96–123.
- [2] Min, D., Jung Kim, H., in: *Food Lipids*, CRC Press 2008.
- [3] Chen, X.-W., Fu, S.-Y., Hou, J.-J., Guo, J., Wang, J.-M., Yang, X.-Q., Zein based oil-in-glycerol emulgels enriched with β -carotene as margarine alternatives. *Food Chem.* 2016, 211, 836–844.

- [4] Hu, M., McClements, D. J., Decker, E. A., Lipid Oxidation in Corn Oil-in-Water Emulsions Stabilized by Casein, Whey Protein Isolate, and Soy Protein Isolate. *J. Agric. Food. Chem.* 2003, *51*, 1696–1700.
- [5] Sakanaka, S., Tachibana, Y., Ishihara, N., Raj Juneja, L., Antioxidant activity of egg-yolk protein hydrolysates in a linoleic acid oxidation system. *Food Chem.* 2004, *86*, 99–103.
- [6] Lund, M. N., Heinonen, M., Baron, C. P., Estévez, M., Protein oxidation in muscle foods: A review. *Mol. Nutr. Food Res.* 2011, *55*, 83–95.
- [7] Friedman, M., Cuq, J. L., Chemistry, analysis, nutritional value, and toxicology of tryptophan in food. A review. *J. Agric. Food. Chem.* 1988, *36*, 1079–1093.
- [8] Vries, A. de, Wesseling, A., van der Linden, E., Scholten, E., Protein oleogels from heat-set whey protein aggregates. *J. Colloid Interface Sci.* 2017, *486*, 75–83.
- [9] Vries, A. de, Jansen, D., van der Linden, E., Scholten, E., Tuning the rheological properties of protein-based oleogels by water addition and heat treatment. *Food Hydrocoll.* 2018, *79*, 100–109.
- [10] Butte, W., Rapid method for the determination of fatty acid profiles from fats and oils using trimethylsulphonium hydroxide for transesterification. *Journal of Chromatography A* 1983, *261*, 142–145.
- [11] Lampi, A.-M., Kamal-Eldin, A., Effect of α - and γ -tocopherols on thermal polymerization of purified high-oleic sunflower triacylglycerols. *J. Amer. Oil Chem. Soc.* 1998, *75*, 1699–1703.
- [12] Vries, A. de, Lopez Gomez, Y., Jansen, B., van der Linden, E., Scholten, E., Controlling Agglomeration of Protein Aggregates for Structure Formation in Liquid Oil: A Sticky Business. *ACS Appl. Mater. Interfaces* 2017, *9*, 10136–10147.
- [13] Thiyam, U., Stöckmann, H., Schwarz, K., Antioxidant activity of rapeseed phenolics and their interactions with tocopherols during lipid oxidation. *J. Amer. Oil Chem. Soc.* 2006, *83*, 523–528.
- [14] Stöckmann, H., Schwarz, K., Huynh-Ba, T., The influence of various emulsifiers on the partitioning and antioxidant activity of hydroxybenzoic acids and their derivatives in oil-in-water emulsions. *J. Amer. Oil Chem. Soc.* 2000, *77*, 535–542.
- [15] Chan, H. W.-S., Levett, G., Autoxidation of methyl linoleate. Separation and analysis of isomeric mixtures of methyl linoleate hydroperoxides and methyl hydroxylinoleates. *Lipids* 1977, *12*, 99–104.
- [16] Frankel, E. N., Formation of headspace volatiles by thermal decomposition of oxidized fish oils vs. oxidized vegetable oils. *J. Amer. Oil Chem. Soc.* 1993, *70*, 767–772.
- [17] Wickham, H., Francois, R., dplyr: A Grammar of Data Manipulation 2016, <https://CRAN.R-project.org/package=dplyr>.

- [18] Wickham, H., *ggplot2: Elegant Graphics for Data Analysis*, Springer-Verlag New York 2009.
- [19] Team, R. C., R: A Language and Environment for Statistical Computing 2015, Vienna, Austria, <https://www.R-project.org/>.
- [20] Elzhov, T. V., Mullen, K. M., Spiess, A.-N., Bolker, B., minpack.lm: R Interface to the Levenberg-Marquardt Nonlinear Least-Squares Algorithm Found in MINPACK, Plus Support for Bounds 2015.
- [21] Soetaert, K., Petzoldt, T., Setzer, R. W., Solving Differential Equations in R: Package deSolve. *J. Stat. Soft.* 2010, 33.
- [22] Quenouille, M. H., Notes on Bias in Estimation. *Biometrika* 1956, 43, 353.
- [23] Crapiste, G. H., Brevedan, M. I. V., Carelli, A. A., Oxidation of sunflower oil during storage. *J. Amer. Oil Chem. Soc.* 1999, 76, 1437.
- [24] Aragao, G. M. F., Corradini, M. G., Peleg, M., A Phenomenological Model of the Peroxide Value's Rise and Fall During Lipid Oxidation. *J. Amer. Oil Chem. Soc.* 2008, 85, 1143.
- [25] Belitz, H. D., Grosch, W., Schieberle, P., *Lehrbuch der Lebensmittelchemie*, Springer, Garching 2007.
- [26] YAMAKI, S., KATO, T., KIKUGAWA, K., Characteristics of Fluorescence Formed by the Reaction of Proteins with Unsaturated Aldehydes, Possible Degradation Products of Lipid Radicals. *CHEMICAL & PHARMACEUTICAL BULLETIN* 1992, 40, 2138–2142.
- [27] Iio, T., Yoden, K., Formation of fluorescent substances from degradation products of methyl linoleate hydroperoxides with amino compound. *Lipids* 1988, 23, 1069–1072.
- [28] MONTGOMERY, M. W., DAY, E. A., Aldehyde-Amine Condensation Reaction: A Possible Fate of Carbonyls in Foods. *J. Food Sci.* 1965, 30, 828–832.
- [29] Fletcher, B. L., Tappel, A. L., Fluorescent modification of serum albumin by lipid peroxidation. *Lipids* 1971, 6, 172–175.
- [30] Kinsella, J. E., Fox, P. F., Water sorption by proteins: Milk and whey proteins. *Crit. Rev. Food Sci. Nutr.* 1986, 24, 91–139.
- [31] Bull, H. B., Breese, K., Protein hydration. *Archives of Biochemistry and Biophysics* 1968, 128, 488–496.
- [32] Potes, N., Kerry, J. P., Roos, Y. H., Protein Modifications in High Protein-Oil and Protein-Oil-Sugar Systems at Low Water Activity. *Food Biophysics* 2014, 9, 49–60.
- [33] Vollhardt, P., Schore, N., *Organic chemistry: Structure and function*, W H Freeman, New York 2010.
- [34] Pokorný, J., El-Zeany, B. A., Kolakowska, A., Janíček, G., Nonenzymic browning. IX. Correlation of autoxidation and browning reactions in lipid-protein mixtures. *Zeitschrift für Lebensmittel-Untersuchung und Forschung* 1974, 155, 287–291.

- [35] ZIRLIN, A., Karel, M., Oxidation Effects in a Freeze-Dried Gelatin-Methyl Linoleate System. *J. Food Sci.* 1969, *34*, 160–165.
- [36] Funes, J., KAREL, M., Free radical polymerization and lipid binding of lysozyme reacted with peroxidizing linoleic acid. *Lipids* 1981, *16*, 347–350.
- [37] LEAKE, L., KAREL, M., Polymerization and Denaturation of Lysozyme Exposed to Peroxidizing Lipids. *J. Food Sci.* 1982, *47*, 737–743.
- [38] Stadtman, E. R., Protein oxidation and aging. *Free radical research* 2006, *40*, 1250–1258.
- [39] Roubal, W. T., Tappel, A. L., Damage to proteins, enzymes, and amino acids by peroxidizing lipids. *Archives of Biochemistry and Biophysics* 1966, *113*, 5–8.
- [40] Howell, N. K., Herman, H., Li-Chan, E. C. Y., Elucidation of Protein–Lipid Interactions in a Lysozyme–Corn Oil System by Fourier Transform Raman Spectroscopy. *J. Agric. Food. Chem.* 2001, *49*, 1529–1533.
- [41] Gómez, R., Fernández-Salguero, J., Water activity and chemical composition of some food emulsions. *Food Chem.* 1992, *45*, 91–93.
- [42] MCCLEMENTS, D. J., DECKER, E. A., Lipid Oxidation in Oil-in-Water Emulsions: Impact of Molecular Environment on Chemical Reactions in Heterogeneous Food Systems. *J. Food Sci.* 2000, *65*, 1270–1282.

Figure captions

- Figure 3.1: Changes of conjugated dienes (CD, 234 nm) in extracted oil of stored gel samples by 40 °C, added 0 to 3 % water, after 3 (blue), 9 (red) 14 (green) days of incubation by 40 °C in comparison to the oxidation of bulk oil stored under same conditions for 14 days (red dashed). All values are listed as mean and standard deviation of three independent replicates.....83
- Figure 3.2: Changes of conjugated dienes (CD, 234 nm) in extracted oil of stored gel samples by 40 °C, left: 0 % and 0.23 % water added, right: 2.8 – 8.4 % water added. Fitting lines are according to formula 3.1 using a nonlinear least square regression to the raw data, not to means (standard error of estimates from 0 to 8.4 % water: 0.47, 0.83, 11.9, 10.8 and 8.05 mmol/kg). All values are listed as mean and standard deviation of three independent replicates.84
- Figure 3.3: left: constant k_1 and right: k_2 in gel samples from 0 % to 8.4 % water addition for fitting curves in figure 3.2. Standard deviation was estimated using the Jack knife delete one procedure [22].85

Figure 3.4: Left: Formation of hexanal and right: propanal in gel samples from 0 % to 8.4 % water addition and in bulk oil, lines are added to guide the eyes only.....86

Figure 3.5: Appearances of oleogels with 0 % (A), 2.8 % (B), 5.6 % (C) and 8.4 % (D) water added during preparation.88

Figure 3.6: Color formation in oleogels with 2.8 to 8.4 % water addition during incubation at 40 °C.....89

Figure 3.7: Left: water content in gel measured gravimetrically after drying for 4 h over water added in premix, linear fit for first nine values (water added < 10 mg/g, dotted) and second order polynomial (line). Right: relation of gel yield after centrifugation over water added in premix.90

Figure 3.8: Left: frequency sweep plot from gels with no water addition (filled symbols) and water addition about 100 mg/g (open symbols).○: G'; □: G''; right: storage modulus G' as a function of water addition in premix.....91

Chapter 4

Cooxidation of Proteins and Lipids in Whey Protein Oleogels with Different Water Amounts

Abstract

Protein- and lipid oxidation were investigated in whey protein based oleogels with varying water addition. Lipid oxidation was low (~ 30 mmol O_2 /kg lipid hydroperoxides after 6 weeks) in gels with $<0.23\%$ water and a high ($>1,000$ mmol O_2 /kg lipid hydroperoxides after 4 weeks) in gels with $>2.4\%$ water addition. In systems with $>2.4\%$ water addition fluorescence (excitation 325 nm / emission 410 nm) as indicator of tyrosine oxidation and carbonyl content significantly increased and remained at low levels in oleogels with $<0.23\%$ water addition. Primary amines as indicator for protein backbone breakage increased in early stages of oxidation in high water oleogels and decreased after 28 days. Degradation has been suggested to occur through interactions with reactive secondary lipid oxidation products and was confirmed by spiking experiments using respective compounds. The results suggest that secondary lipid oxidation markers are masked dependent on water addition in the presence of proteins.

Keywords: lipid oxidation, protein oxidation, oleogel, aldehyde, water

Highlights:

Whey protein oleogels with low ($<0.23\%$) and high ($>2.8\%$) water addition differ in their oxidation profiles.

Fluorescence increases indicate strong protein oxidation levels even with low lipid oxidation

Primary amines and protein carbonyls degrade and only accumulate at high oxidation levels.

Typical lipid oxidation aldehydes decompose in protein oleogels

4.1 Introduction

Oleogels containing structured proteins represent a class of organogels (proteinogen oleogels), where protein aggregates structure liquid oils, resulting in a system with plastic and viscoelastic rheological properties, which are gel-like features (Vries, Lopez Gomez, Jansen, van der Linden, & Scholten, 2017). This system can be further combined with water, which may then called organogelled emulsion beside oleogel (Jimenez-Colmenero et al., 2015). Oleogels are used as substitutes for saturated and hydrogenated fats and they contribute to the reduction of trans fatty acid in the diet (Mozaffarian, Katan, Ascherio, Stampfer, & Willett, 2006; Smith, Robinson, Nam, & Ma, 2009). Whey is considered to be a favorable protein source because it represents one of the most valuable protein sources for human nutrition and is available as a common by-product from the dairy industry (Schaafsma, 2000). Protein oxidation reduces nutritional value and digestibility and may result in the formation of toxic products, which have been classified as carcinogenic (Friedman & Cuq, 1988; Papuc, Goran, Predescu, & Nicorescu, 2017). To estimate the potential deterioration of whey proteins and, thus the loss of nutritional quality, determining the oxidation processes that may occur in the presence of co-oxidizing compounds in oleogels is important.

Polyunsaturated fatty acids, which are present in the liquid oils used for oleogelation, are particularly susceptible to lipid oxidation, which is one of the primary causes of deterioration and quality loss in lipid-containing foods (Min & Jung Kim, 2008; Papuc et al., 2017). Thus, protein oxidation is likely to be involved in a co-oxidation process associated with lipid oxidation. Moreover, proteins and their hydrolysates have been frequently introduced as antioxidants (Sakanaka, Tachibana, Ishihara, & Raj Juneja, 2004), to inhibit lipid oxidation, which may consequently lead to protein oxidation.

At present, only a few papers have studied lipid oxidation in oleogels and only one paper has investigated a protein-containing oleogel (zein, stabilized in glycerol) as a gelling agent (Chen et al., 2016). Lipid oxidation of gelled soybean oil (60%) was retarded compared with lipid oxidation in liquid oil, based on aldehyde formation and oxygen consumption. We recently demonstrated that lipid oxidation is greatly influenced by the water addition in oleogels (gelled with whey protein), due to increased water activity (a_w -value) and water droplet formation, which result in increased water-lipid interfaces (Meissner, Keppler, Stöckmann, Schrader, & Schwarz, 2019): Trace metals can catalyze lipid oxidation, which are dissolved by unbound water at higher water activities. Conjugated dienes are concentrated at water lipid interfaces due to their amphiphilic

character, which accelerates the bimolecular lipid oxidation. In contrast with the increased formation of conjugated dienes, aldehydes that are formed as secondary lipid oxidation products do not follow the same trend.

We, therefore, hypothesize that aldehydes are degraded in the presence of proteins. Several degradation mechanisms may occur, including reactions with free amines or complexation, which can facilitate reactions with other lipid oxidation compounds, such as aldol reactions. Thus, a low aldehyde concentration, which is generally considered to be representative of a low lipid oxidation status, may result from protein modifications caused by the interaction with secondary lipid oxidation products.

Protein modifications can be detected as increases in fluorescence, due to lysine reaction products (e.g., Schiff bases or nitrogen cycles) (Fruebis, Parthasarathy, & Steinberg, 1992; Liu & Sayre, 2003) and radical dimerization products (dityrosine) (Kikugawa, Kato, & Hayasaka, 1991). However, these compounds can be difficult to distinguish, as fluorophores are sometimes similar in their excitation and emission wavelengths. Therefore, complementary approaches are necessary to determine the identities of protein oxidation products, such as the measurement of protein carbonyl content. Two primary mechanisms exist for protein carbonyl formation. On the one hand, carbonyls can be generated by the addition of secondary lipid oxidation carbonyls in a Michael-like reaction, during which the carbonyl group is maintained, and on the other hand, the protein may be modified in a site-specific manner or by fragmentation *via* hydroxyl radical attack and a proton abstraction of the α -C-atom. The latter reaction is either followed by a diamide or α -amidation pathway, including the formation and release of carbonyls, or by the formation of “new” amino groups, caused by the splitting of the backbone (Berlett & Stadtman, 1997). Thus, free and protein bound amino acids are affected by several reactions that are driven by lipid oxidation, and their concentrations were determined using the o-phthalaldehyde (OPA) method. Tyrosine and tryptophan, which are essential for human nutrition, are notably labile amino acid residues for such backbone splitting reactions (Garrison, 1987; Lund, Heinonen, Baron, & Estévez, 2011). The objective of this work is to characterize the interplay of lipid and protein oxidation mechanisms (including formation and degradation reactions) and the resulting protein modification in a well-characterized co-oxidizing system, such as the present oleogels.

4.2 Materials & Methods

4.2.1 Materials

High oleic safflower oil was purchased from a local supermarket. Whey protein isolate (BiPro) was obtained from Agropur Inc. (Appleton, USA) containing 97.7% protein and 75% beta-lactoglobulin in dry matter. Al_2O_3 , BaCl_2 , boric acid, butanol, FeSO_4 , guanidine hydrochloride, hexanol, hydrochloric acid, sodium dodecyl sulfate, trichloroacetic acid and trypsin (5,000 USP-U/mg) were obtained from Carl Roth (Karlsruhe, Germany). *N*-acetylcysteine, 2,4-dinitrophenylhydrazine (DNPH), heptanal (octanol/water partition coefficient, $\log P_{\text{OW}} = 2.8$), hexanal ($\log P_{\text{OW}} = 1.78$), L-leucine, 3-methylbutanal ($\log P_{\text{OW}} = 1.31$), octanal ($\log P_{\text{OW}} = 2.78$), *ortho*-phtaldialdehyde and triethyl ammonium acetate (TEAA) buffer were obtained from Sigma Aldrich (Steinheim, Germany). Propanol was obtained from AppliChem (Darmstadt, Germany), and valeric acid was obtained from Alfa Aesar (Karlsruhe, Germany). All solvents were obtained from VWR (Fontenay-sous-Bois, France). All chemicals were at least high-purity. Water ($>18.2 \text{ M}\Omega$) was purified by an Elga Veolia system (Celle, Germany) and was used for all experiments.

4.2.2 Purification of safflower oil

The purification of safflower oil from natural antioxidants and trace metals was based on a preparative chromatography method using activated aluminum oxide (Lampi & Kamal-Eldin, 1998), with slight modifications (Meissner et al., 2019). The oil was tested for residual tocopherols (high-performance liquid chromatography [HPLC], $< 0.5 \text{ ppm}$, using the DGF F-II 4a standard method).

4.2.3 Sample preparation

Whey protein aggregates were produced using the method described by de Vries *et al.* In brief, a whey protein was dissolved in water (4% w/w), stirred for 2 h and stored overnight, at 4°C , to fully hydrate. The pH value was adjusted to 5.7 (1 M HCl), and the solution was heated for 20 min at 85°C . A weak gel was obtained by cooling the heated solution in an ice bath. The gel was hand-shaken to break the gel apart and homogenized with an Ultra Turrax, for 3 min at 13,000 rpm. This solution was then centrifuged ($3900 \times g$) for 20 min, which was repeated twice for the redispersed protein aggregate pellet. The protein aggregates were finally redispersed (1%), frozen by dropping into liquid nitrogen, and lyophilized (Vries et al., 2017).

Dry whey protein aggregates (6.8%) were then added to stripped oil and stirred for 10 min with a magnetic stir bar. In water containing models, the water was added slowly after 5 min. Two model systems were prepared using two batches of whey protein aggregates (batch 1: 0% and 0.23% of added water; batch 2: 2.8%, 5.6%, and 8.4% of added water. After centrifugation for 20 min by $4000 \times g$ (Allegra X-30R, Beckmann Coulter, Krefeld, Germany), superfluous oil was removed by decanting the gel for 10 min, and the obtained gel was reweighed. For the reweighed gel, the final protein concentration was calculated as the appointed protein mass in the achieved oleogel mass, by assuming no protein content in the upper liquid oil phase (13.9, 16.9, 13.0, 13.6, and 13.2% protein in gels containing 0%, 0.23%, 2.8%, 5.65%, and 8.4% added water respectively). The average aggregate diameter protein aggregates was estimated after rehydration of dry protein aggregate samples with particle light scattering (Horiba, Retsch Technology GmbH, Haan, Germany, in increasing water order, the average diameter: 13.47, 13.47, 14.57, 14.57 μm).

200 mg Samples were then stored in closed 15 mL centrifuge tubes, additionally sealed with a plastic wrap, and stored in the dark, in a drying cabinet at 40°C . After a varying incubation time, the samples were extracted for measurements as described in previous works (Meissner et al., 2019). In brief, the lipid phase was extracted 3 times with 3 mL cyclohexane, followed by centrifugation at $4000 \times g$ for 5 min each time. Combined extracts were used to measure lipid hydroperoxides (see Section 4.2.4). The defatted protein was then washed 2 times with 5 mL isopropanol and 2 times with 5 mL mass spectrometry (MS)-grade water, by decanting the upper phase after centrifugation. The protein pellet was then suspended in 3 mL MS-grade water.

4.2.4 Determination of lipid hydroperoxides

The lipid phase was flushed with nitrogen, at 20°C for 20 min, to evaporate cyclohexane. Then, the reweighed, extracted fat was dissolved in 5 mL isopropyl alcohol and diluted, if necessary, to avoid too high values ($>1,5$) in UV-measurements in the latter. Lipid hydro peroxides were determined using the ferric thiocyanate method (Thiyam, Stöckmann, & Schwarz, 2006). All measurements were prepared in triplicate unless otherwise noted.

4.2.5 Determination of the carbonyl content

The determination of protein carbonyl contents was conducted as described by to Oliver *et al.* with slight modifications (Oliver, Ahn, Moerman, Goldstein, & Stadtman, 1987). Two aliquots (0.6 mL) of protein extract were precipitated with 1 mL trichloroacetic acid (20%, w/v). After centrifuging 5 min at $10000 \times g$ and decanting, 1 pellet was treated with 1 mL 2 N HCl and the

other with 1 mL DNPH (0.2% in 2 N HCl). Both samples were incubated for 1 h, at 20°C in the dark, and vortexed in 15 min intervals. The samples were then precipitated, again, with trichloroacetic acid and, after centrifuging and decanting, washed 3 times with 1 mL ethyl acetate/ethanol (1:1, v/v). Finally, the pellets were redissolved in 2 mL of 6 M guanidine HCl (including a sodium phosphate buffer, pH 2.3, 0.5 M), incubated for 15 min at 37 °C, centrifuged for 2 min at 10000 × g and, if necessary, disturbing foam was removed with a plastic spatula. The solutions were then transferred into cuvettes, and the absorption was measured, at 370 nm for hydrazones and 278 nm for the proteins, was measured versus buffer as a blank (Helios γ Spectrophotometer, Thermo Electron Corporation, Waltham, USA). The concentration was determined in nmol carbonyl/mg protein using the molar absorption coefficient for hydrazones of 22,000 M⁻¹ cm⁻¹ (Johnson, 1953) and the molar absorption coefficient of β -lactoglobulin (17,600 M⁻¹ cm⁻¹), as assumptions for the molar absorption coefficient of whey protein and a molar mass of 18,300 g/mol (Belitz, Grosch, & Schieberle, 2009; Keppler et al., 2014). In DNPH treated samples the absorption at 278 nm was corrected by 43% of the absorption at 370 nm (Keyse, 2000). The final values were given as differences between the DNPH- and HCl-treated samples.

4.2.6 Measurement of free amines

Ortho-phthaldialdehyde (OPA) was used to measure free amines using a downsized method with modifications (Rade-Kukic, Schmitt, & Rawel, 2011). In brief, frozen protein extract samples were defrosted and vortexed. A total of 500 μ L of a protein solution (final concentration 1–20 μ g/mL) was incubated for 10 min at 50°C, with 150 μ L 20 wt% sodium dodecyl sulfate and 2,260 μ L 0.1 M borate buffer, pH 9.3, containing 0.3 wt% *N*-acetyl-cysteine. Then, 90 μ L 3.4% OPA, in methanol, was added, and the sample was incubated 30 min by 50 °C again. Thereafter the sample was cooled at room temperature, for 30 min, and the absorbance was recorded at 340 nm. For calibration, solutions of L-leucine, ranging from 5 μ M to 250 μ M, were used.

4.2.7 Estimation of dityrosine formation

The dityrosine contents were estimated by fluorescence spectroscopy (Cary Eclipse, Varian Agilent, Palo Alto, USA), using an excitation wavelength of 325 nm and an emission wavelength of 410 nm (Prütz, Butler, & Land, 1983), compared against a blank. A total of 1 mL protein extract was diluted and incubated in 0.05 M TEAA with about 1/20 (w/w) trypsin (160 μ g/mL), at 37°C for 22 h. After 20 h of incubation, the samples were briefly agitated. Then, 1 mL was taken from the upper clear phase, diluted with MS-grade water (1/1, v/v), and fluorescence

measurement was performed. Protein concentration was measured as described for carbonyl content.

4.2.8 Degradation of volatiles

Measurement of volatiles was conducted using headspace (HS) gas chromatography (GC, Agilent 6890 Series, Santa Clara, USA) (Frankel, 1993). Approximately 200 mg olegel (with 0% or 0.5% water addition) was placed in in 20-mL headspace vials, hermetically sealed with polytetrafluoroethylene (PTFE)/silicone membrane screw caps, and stored as described above. Periodically, samples were taken and incubated at 70°C for 15 min, before aliquots were transferred for GC measurement.

For the measurement of degradation of volatiles, middle chain triglyceride oil (MCT-oil), containing a typical mix of lipid oxidation alcohols, aldehydes and one acid, was used for gel preparation (propanol, 3-methylbutanal, butanol, valeric acid, hexanol, hexanal, heptanal, octanal). Lipid-oxidation-stable MCT-oil was used to avoid the further formation of lipid oxidation products. The concentration of each compound was adjusted to a HS GC signal of 300–400 area under the curve (AUC, 0.05, 0.065, 0.095, 3.4, 0.38, 0.15, 0.3, and 0.6 mg/g oil). For comparison of concentrations, overall response factors were estimated for hexanal, heptanal, octanal and 3-methylbutanal from HS GC samples at day 0 (0.63, 1.11, 1.75, and 0.43 µg/g/AUC). Measurements were repeated in triplicate.

4.2.9 Statistical analysis

All results were statistically analyzed with excel and R (Student's t-test, Shapiro-Wilk normality test, analysis of variance).

4.3 Results & Discussion

4.3.1 Formation of the primary lipid oxidation products

To evaluate the formation of primary lipid oxidation products the amount of hydroperoxide was analyzed for 50 days, in oleogels with either no or low water contents (0% and 0.23% water addition, respectively) and oleogels with high water contents (2.8%, 5.6%, and 8.4% water addition). The addition of water had a strong influence on the formation of lipid hydroperoxides. In low-water systems, there is a slow and continuous increase in hydroperoxide concentrations was observed, reaching < 30 mmol/kg oil after 7 weeks (see Figure 4.1), whereas oleogels with high addition of water (2.8%–8.4%) the concentration of hydroperoxides increased rapidly within

the first 2 weeks, although the increase was significantly lower in 2.8% water oleogels, than in those with high water contents. However, in all high-water gels, the concentration of hydroperoxides exceeded 1,000 mmol/kg oil within 4 weeks, after which the hydroperoxides concentration did not change any further. Reaching a maximum is consistent with lipid oxidation models for low or moderate temperatures (Aragao, Corradini, & Peleg, 2008; Crapiste, Brevedan, & Carelli, 1999). The results align with those from our previous study for the formation of lipid hydroperoxides (measured as conjugated dienes) in oleogels with different amount of water addition (Meissner et al., 2019), which were explained by the increased catalytic activity of trace metals and bimolecular autocatalyztion.

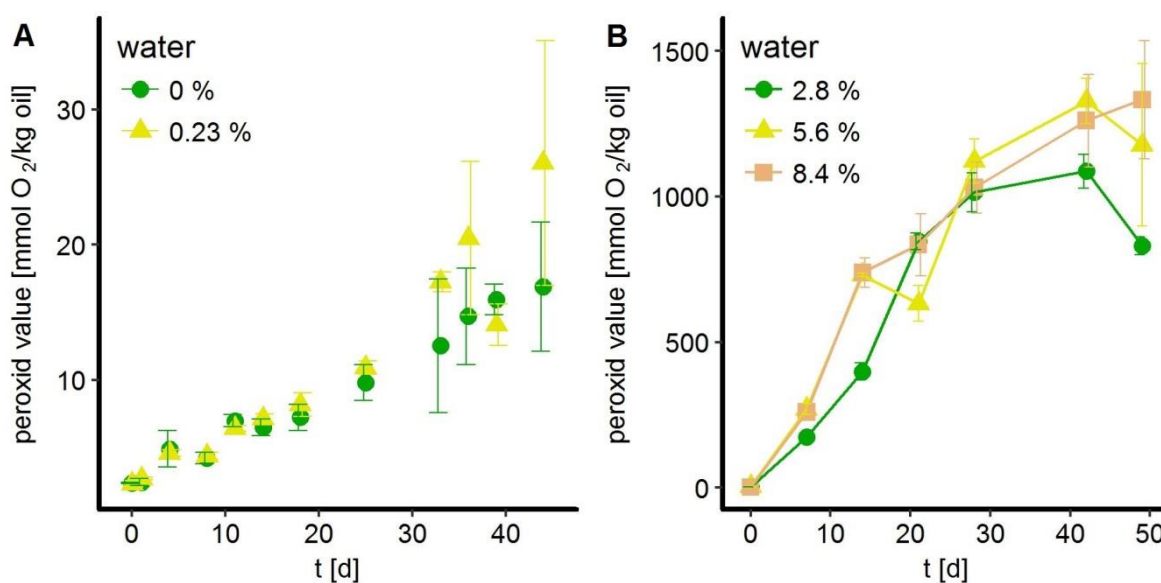


Figure 4.1: Changes in the peroxide value (PV) of oil extracts in gel samples during 7 weeks of incubation at 40°C. A: With no and 0.23% water added. B: with higher water amounts added (2.8-8.4%). Lines were added to guide the eyes, only.

4.3.2 Dityrosine formation estimation using fluorescence analysis

Dityrosine formation was analyzed by measuring the fluorescence of the protein extract. A significant increase in fluorescence at 410 nm was observed for all samples during the first week. In more detail, the fluorescence increased more strongly in oleogels with 2.8-8.4% water addition (Student's t-test, day 0 vs. day 8; $p(2.8\%) = 0.006$, $p(5.6\%) = 0.003$, $p(8.4\%) = 0.006$) than in oleogels with 0 and 0.23% water addition (Student's t-test, day 1 vs. 8; $p(0\%) = 0.04$, $p(0.23\%) = 0.004$) during the first week. The large difference in dityrosine fluorescence observed between high- and low-water aligns with the formation of hydroperoxides (Figure 4.1) in both types of oleogels. Because the dimerization of two tyrosine residues can be forced by lipid radicals derived

from hydroperoxide cleavage (see Section 4.3.1) (Kikugawa et al., 1991), increased dityrosine levels can be regarded as a protein oxidation process that is triggered by lipid oxidation.

In small amounts water may have different effects during the onset of oxidation. By shielding protein residues through hydration, water may inhibit the attack of radicals that originate in the lipid phase and the formation of H-bonds between protein residues and lipid hydroperoxides. During the first 4 days of storage, fluorescence was lower in oleogels with 0.23% water addition (0.0 ± 1.6 a.u./mg) than in the oleogel without water addition (2.5 ± 2.0 ; $p = 0.008$, removed outlier 10.2 a.u./mg). No differences could be determined among all water containing oleogels (0.23%–8.4%) by the analysis of variance ($p = 0.75$) on day 0.

However, the increase in fluorescence may be, at least partly, attributed to the formation of adducts between proteins and aldehydes (carbonyl groups), formed by secondary lipid oxidation, resulting in protein carbonylation in addition to the radical-generated dityrosine (Liu & Sayre, 2003).

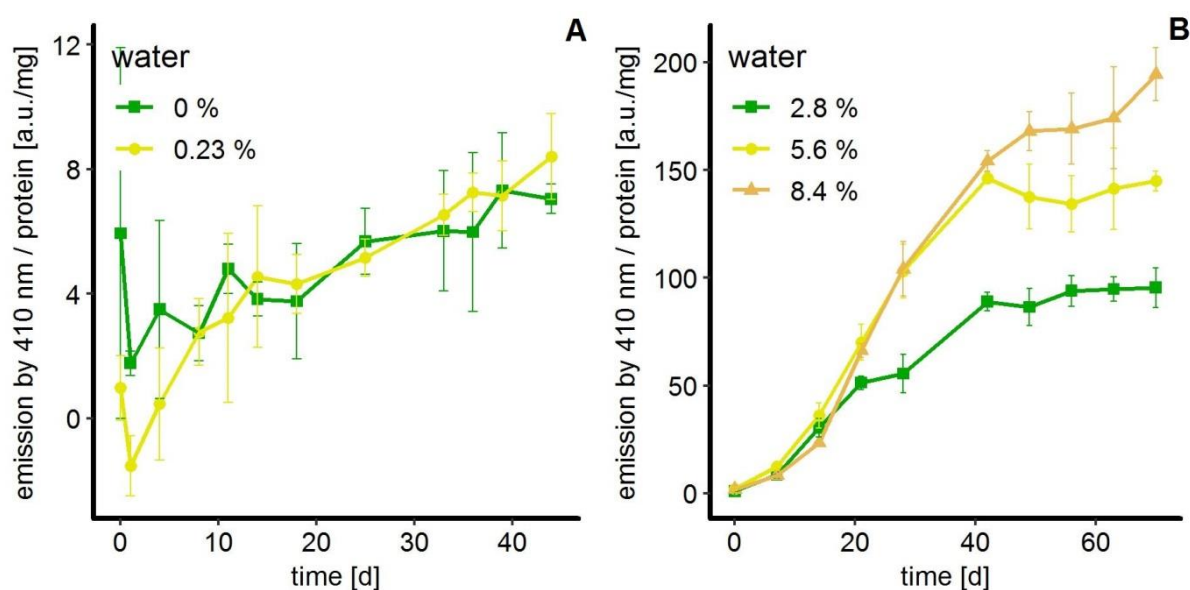


Figure 4.2: Estimation of dityrosine formation, assessed by fluorescence (excitation 325 nm, emission 410 nm) of protein extracts during a 7 weeks incubation at 40°C. A: low-oxidation systems (no and 0.23% water added) and B: high-oxidation systems (2.8-8.4% water added). Lines were added to guide the eyes, only.

4.3.3 Formation of protein carbonyls

The protein carbonyl concentrations in oleogels during the incubation period are shown in Figure 4.3. Because the protein was extracted as a precipitate prior to the determination of the carbonyl concentration, the values represent the carbonyl groups bound to protein side chains (Headlam & Davies, 2004), which are included with precipitated protein, whereas protein carbonyls from

protein scission are partly soluble and likely to be extracted during the precipitation process before. The carbonyl contents of high-water systems (2.8%–8.4% water addition) strongly increased throughout the entire experiment, whereas in oleogels with low (0.23%) and without (0%) water addition the carbonyl content remained at lower levels throughout the entire storage period. These findings align with the findings for the formation of fluorescent products (Fig. 2). However, these findings are in contrast with the formation of hexanal, a carbonyl that represents a major volatile secondary lipid oxidation product, which was found at similar concentrations in both low- and high-water systems (Meissner et al., 2019). These contradictory findings may be explained by the acid catalysis mechanism of water for the Schiff base reaction of lipid oxidation products, such as between aldehydes and proteins (e.g., imines and further derivatives) (Vollhardt & Schore, 2010). In this reaction, the aldehyde becomes activated by the protonation of the carbonyl group, which leads to the generation of an oxocarbenium ion. This ion has the resonance structure of a carbocation and becomes the site for the nucleophilic addition of the amino-nitrogen. In addition, water may also lead to base-catalyzed aldol reactions. These water-facilitated reactions may also contribute to the increased formation of fluorescent compounds (Fig. 2).

However, at low levels, water can have different effects. Comparing oleogel without water addition with oleogels with 0.23% water addition, we found the degradation of protein carbonyls only in oleogels without water addition during the early stages, whereas the protein carbonyl content was low in 0.23% water samples, starting at the beginning of the storage experiment. Water can catalyze protein carbonyl formation and decomposition reactions, such as the Schiff base carbonyl-amino reaction (Feeney, Blankenhorn, & Dixon, 1975). In contrast with the 0.23% oleogel, the remaining water in the “0%” oleogel after freeze-drying (approximately 7% of dry protein aggregates) is likely strongly bound via hydrogen bonds (because it did not evaporate during lyophilization) and is, therefore, less available for other reactions, resulting in a slower degradation reaction rate for the 0% samples compared with the 0.23% samples. The equilibrium for this condensation reaction may be shifted toward the product side by proteins as generated water is complexed.

The value for protein carbonylation at the beginning of the incubation was slightly above the various values previously reported for whey protein isolate (<2–9.2 nmol/mg) (Cui, Xiong, Kong, Zhao, & Liu, 2012; Keppler, Heyn, Meissner, Schrader, & Schwarz, 2019). This may be due to a difference in the protein absorption factor for denatured protein, as well as the heating and freeze-drying steps performed prior to oleogel preparation (Gatellier, Kondjoyan, Portanguen, & Santé-Lhoutellier, 2010; Keppler et al., 2019), which may induce protein

oxidation. In addition, protein dispersion in the hydrophobic phase results in further protein unfolding, which can reveal buried protein carbonyls that are already present. Furthermore, in this study, the starting value for the protein was obtained after the extraction of the protein from the oleogel. Thus, we hypothesized that the synchronous degradation of protein carbonyls in low-water systems inhibits their accumulation and resulting in their measured concentrations existing in a steady state. During these degradation reactions, primary amines may play roles as nucleophilic reacting agents that degrade protein carbonyls (see Section 4.3.4).

In systems containing more than 2% water addition, carbonyl contents increased in a kinetic manner, similar to peroxide values, and reached 79 ± 27 , 110 ± 8 and 171 ± 12 nmol/mg protein carbonyls after 70 d of incubation, for the addition of 2.8%, 5.6%, and 8.3% water, respectively. On the one hand, these carbonyl values are approximately 4–9-fold higher than the levels measured when whey protein oxidation was triggered by a Fenton reaction system (0.1 mM ascorbic acid, 0.1 mM FeCl₃, 15 mM H₂O₂ incubated 10 h at 20 °C) (Cui et al., 2012). On the other hand, the proteins in this study were incubated 169 times longer, with a radical generating system consisting of approximately 1,000 mmol hydroperoxides/kg oil, after 50 days at 40°C (see Section 4.3.1). Therefore, the protein carbonyl contents may be relatively low in the studied oleogels. In the Fenton system mainly highly reactive hydroxyl radicals are formed rapidly, whereas in the oleogel system, lipid hydroperoxides form more slowly, and less reactive alkoxy (RO*) and alkyl radicals (R*) are present, in addition to hydroxyl radicals. Hydroxyl radicals have been reported to yield the highest amounts of protein (bound and non-bound) carbonyls among various oxidants (Headlam & Davies, 2004). However, lipid hydroperoxide-derived radicals are also formed in the lipid phase, whereas the protein will be partly in the hydrophilic phase of an organogelled emulsion.

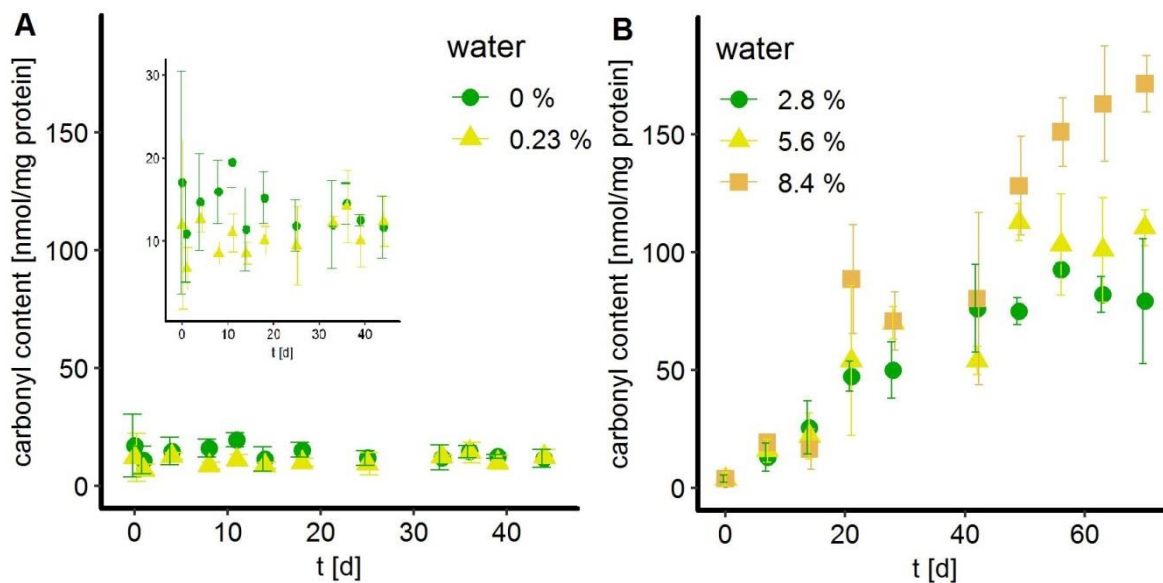


Figure 4.3: Formation of protein carbonyls in protein extracts of oleogels incubated for 6–10 weeks at 40°C. A: Oleogels with low (0.23%) and without (0%) water addition, and B: oleogels with high water addition (2.8%–8.4%). A zoomed in view of the concentrations from 0–30 nmol carbonyls/mg protein is included.

Hydroperoxide-derived radicals can fragment the protein back-bone, which also induces the formation of free amines in high-water systems (see Section 4.3.4, Figure 4.4) (Davies, 1987; Liu, Xiong, & Butterfield, 2000; Srinivasan & Hultin, 1997). Together with the initially present amines (e.g. lysine residues) and the N-terminus newly formed free amines may counteract the accumulation of carbonyls in both gel systems. In general, these residues have suggested to mask the formation of carbonyls derived from either by protein or lipid oxidation.

4.3.4 Formation of primary amines

To investigate the relationship between carbonyl degradation and the formation of free amines the contents of free amines were assessed using the OPA assay, as shown in Figure 4.4.

During the first two weeks, the amounts of free amines significantly increased in all model systems (0% and 0.23% from day 0 to 8, $p = 0.09$ and 0.03 , respectively; 2.8%, 5.6%, and 8.4% to day 28, $p = 0.004$, 0.002 , and 0.009 , respectively), but interestingly, the higher-water-containing systems ($>2\%$) continuously increased up to $37 \mu\text{mol/mg}$ (8.4% added water, day 28), whereas in the low-water containing systems (0% and 0.23%), free amines stagnated at approximately $7.7 \mu\text{mol/mg}$ and slightly decreased. With the increasing content of free amines, the degradation rate of carbonyls in gels becomes enhanced, resulting in a lower steady-state concentration (Fig. 4.3). The amount of free amines in high-water containing systems ($> 2\%$) strongly decreased

after 28 days, which may be due to secondary lipid oxidation products such as aldehydes, which are able to react with free amines (Feeney et al., 1975).

Initially, systems containing less water showed lower free amine contents as shown by the comparison between 0% and 0.23% water addition at day 0 ($5.2 \pm 1.0 \mu\text{mol}/\text{mg}$ *vs.* $6.4 \pm 0.6 \mu\text{mol}/\text{mg}$, Student's t-test $p = 0.071$) and by comparisons between low-water systems and high-water systems at day 0 ($5.8 \pm 0.6 \mu\text{mol}/\text{mg}$ *vs.* $8.0 \pm 0.7 \mu\text{mol}/\text{mg}$, Student's t-test $p = 0.002$). As free amines are in excess relative to carbonyls, a lower concentration of free amines is considered to be negligible for differences in the N-mediated decomposition of carbonyls (as discussed in Section 4.3). Moreover, free amines in the aqueous phase are easier to dissolve and to measure in the assay used in this study. All protein aggregates exhibited a slightly increased concentration of free amines ($5\text{--}9 \mu\text{mol}/\text{mg}$) compared with fresh whey protein isolate, which is in line with the thermal treatment of the protein required to obtain aggregates. The concentration of $1.11 \pm 0.06 \mu\text{mol}/\text{mg}$ observed for fresh whey protein is quite close to the theoretical value for native β -lactoglobulin, which contains 16 free amino groups per molecule (approximately $0.87 \mu\text{mol}/\text{mg}$) (Brownlow et al., 1997; Keppler et al., 2014). This small difference could be due to other whey proteins in the isolate and the drying process used to obtain a powdered whey protein isolate.

Free amine formation was also measured in a model study for myofibrils, by Liu *et al.* (Liu et al., 2000), who tested protein oxidation with a FeCl_3 , H_2O_2 , ascorbate Fenton system. In contrast, their native whey protein isolate did not form significant amounts of free amines after 24 h of incubation (approximately $0.4 \mu\text{mol}/\text{mg}$), and contained a similar amount of protein carbonyls ($\sim 6.4 \text{ nmol}/\text{mg}$ protein) (Liu et al., 2000). The most obvious explanation for this contrast is that the whey protein used in the present study was widely denatured and may have been partly fragmented during storage. Further, the system in the present study is a gel, which displays overall slower diffusion properties; thus, bimolecular reactions, such as the decomposition of carbonyls via reactions with free amines, are rather slow.

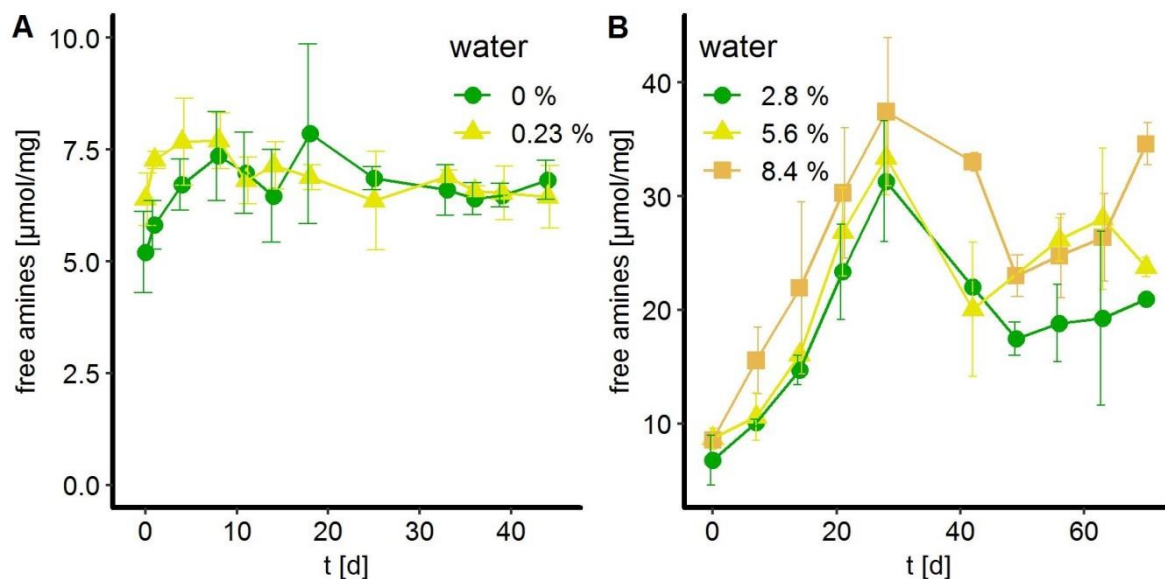


Figure 4.4: Free amines in the extracted proteins of oleogels, after 6-10 weeks of incubation at 40°C. A: low-water addition (no and 0.23% water added) and B: high-water addition 2.8%-8.4% water added). Lines are added for to guide the eyes, only.

4.3.5 Degradation of aldehydes

To investigate the degradation of aldehydes, in comparison with other volatile, typical, lipid oxidation products a mixture of propanol, 3-methylbutanal, butanol, valeric acid, hexanol, hexanal, heptanal, and octanal was used. These compounds represent three different oxidation statuses found in typical lipid oxidation products (alcohols, carbonyls, and carboxylic acids). The decomposition was examined in the presence and absence of protein in MCT-oil (MCT-oil vs. MCT-oleogel), which was used to avoid the additional formation of lipid oxidation products. A high level of aldehyde degradation was observed compared with alcohol and acid during the first 2 weeks (Figure 4.5A), which was expected because aldehydes are generally more reactive than alcohols and acids toward nucleophilic compounds, i.e., N-terminal amino groups of proteins or the amino groups of lysine residues (Vollhardt & Schore, 2010).

Aldehydes can be decomposed by either a Schiff base reaction or an Aldol reaction. Because no degradation was observed in the MCT-oil sample, the degradation of aldehydes by aldol reactions in the oil phase can be neglected (Fig. 5B). In addition, MCT-oil is not vulnerable to lipid oxidation; therefore, degradation reactions cannot to be attributed to reactions with other lipid oxidation products. In contrast, hexanal concentrations decreased in the MCT-oleogel. Consequently, degradation reactions are likely to be impacted by the protein in oleogels as aldol reactions between aldehydes should also be absent. Proteins contain reactive amino groups (e.g.,

lysine side chains) and, thus, can react through the Schiff base reaction with aldehydes, which may be the case for hexanal reacting with proteins, as reactions with proteins are also indicated by the protein carbonyl formation that occurs in oxidized gels (Figure 4.3). Therefore, protein-lipid oxidation interactions contribute considerably to the degradation of aldehydes in protein oleogels.

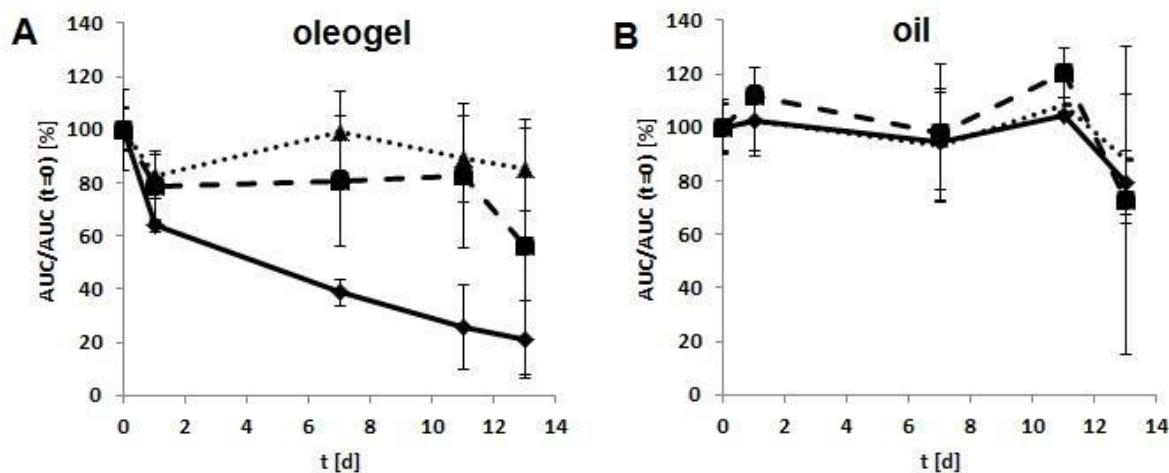


Figure 4.5: Relative concentrations of three representative compounds (hexanal, solid line; valeric acid, dashed line, hexanol, dotted line) over time measured by headspace GC for oleogel samples with 0% water addition (A) and MCT-oil control samples (B).

To further investigate the degradation of aldehydes, the kinetic of each aldehyde in both systems was examined. After 1 week of incubation, the relationships between the aldehydes remained constant, indicating that the degradation follows a similar mechanism (see Figure 4.6). The reaction rate, r , between the alkanal, I, (A), and amino groups (B) can be expressed as a bimolecular reaction equation, with the given reaction rate constant k (I), for products like adducts or polymers, with no backward reaction (concentration indicated by “[]”).

$$\text{Equation I} \quad r_i = k_i \cdot [A_i] \cdot [B]$$

The ratio of two alkanals (i , k), for their degradation rates, is given in equation II. Because the carbonyl groups in hexanal, heptanal and octanal are chemically very similar, the same reaction is likely involved, in addition to similar reaction rates. Thus, the ratio in Equation II should be close to 1.

$$\text{Equation II} \quad \frac{r_i}{r_k} = \frac{k_i}{k_k} \cdot \frac{[A]_i}{[A]_k} \approx 1$$

By contrast, the ratio of r_i/r_k for hexanal *vs.* heptanal was 2.6 ± 0.2 and for hexanal *vs.* octanal was 7.3 ± 0.6 . According to Equation II, the ratio between the reaction rates is the product of the ratios of the reaction constants and concentrations. Thus, any differences in reaction ratios is

either due to either differences in the reaction rate constants for the aldehydes or due to variations in concentrations.

The reaction constants for hexanal, heptanal, and octanal are governed by the electrophilicity of the carbonyl group, which is vulnerable to nucleophilic attacks. Although the lengths of alkyl groups are correlated with positive inductive effects, which would reduce the electrophilicity of the carbonyl C-atom, these increases in the inductive effect decrease with more than three bonds. Therefore, these changes would not explain differences in the ratio (r_i/r_k) for C6–C8. The differences in the reaction rates for aldehydes are more likely explained by different concentration ratios. This explanation appears to be contradictory, as aldehydes added at higher concentrations to achieve similar headspace signals would result in higher reaction rates. But, the measured concentrations within the entire system do not reflect the effective concentrations at the reaction site, i.e. the protein-water phase. Oleogels can be regarded as dispersed systems, in which hydrated proteins form a three-dimensional network displaying a water-protein interface towards the oil phase. Even in gel systems with low-water addition no evidence of the formation of droplets was observed suggesting a hydrated protein phase (Meissner et al., 2019). Therefore, the distribution of each compound between the oil and the hydrated protein phase is considered to be crucial. This partition behavior and the site-specific reactivity have been previously demonstrated for dispersed lipid systems, where emulsifiers govern the interfacial reactivity during lipid oxidation (Oehlke, Heins, Stöckmann, & Schwarz, 2010). An estimation of the distribution between the oil and protein phase is given by the octanol/water partition coefficient [$P_{OW} = c(o)/c(w)$]. Including the P_{OW} coefficient as a correction factor in Equation II leads to Equation II' and III, exhibiting a strong correlation ($R^2 = 0.998$, $[A]_i/[A]_k = 0.12 P_{OW,i}/P_{OW,k} + 0.84$) in oleogels for all aldehydes except for octanal, for 0% and 0.5 % water addition. Octanal was added at a concentration of 0.6 mg/g, which is a higher concentration than soluble in water (approximately 0.21 mg/g); therefore, the partition coefficient is not applicable, and octanal was excluded. Furthermore, the ratio of k (0.12) is lower than initially estimated ($k = 1.0$), which may be due to differences in the real partition between the oil/protein phase.

$$\text{Equation II'} \quad \frac{r_i}{r_k} = \frac{k_i \cdot [A]_i \cdot P_{OW,k}}{k_k \cdot [A]_k \cdot P_{OW,i}} \approx 1$$

$$\text{Equation III} \quad \frac{[A]_i}{[A]_k} \propto \frac{k_i}{k_k} \cdot \frac{P_{OW,i}}{P_{OW,k}}$$

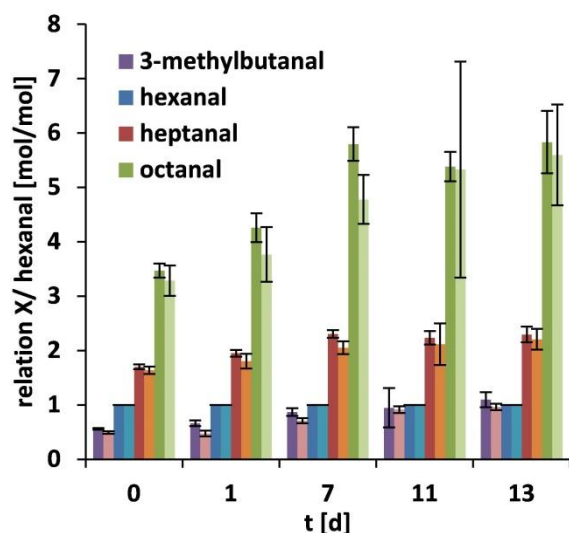


Figure 4.6: Relative concentrations of 3-methylbutanal, hexanal, heptanal, and octanal compared with that of hexanal in MCT-oil gels made from corresponding samples with 0%, and 0.5% water addition. Left darkly colored: 0% water MCT-oil gel samples, right brightly colored: 0.5% water MCT-oil gel samples.

4.4 Conclusion

Water plays a crucial role during lipid protein co-oxidation in oleogels and especially during the interaction between lipid-oxidation-derived compounds and proteins. Reactions are mediated by water or take place in the hydrated protein phase of oleogels. The overall fluorescence formation in all samples showed protein modifications even in samples with low lipid oxidation, whereas protein carbonyls do not accumulate in these samples. The degradation of aldehydes in oleogels consisting of non-oxidizing MCT oil supports the hypothesis of this study that proteins promote the decomposition of lipid oxidation products in oleogels, which are similar to protein carbonyls. Because proteins and hydrolysates are considered to be antioxidative active compounds, further investigation will be necessary to explore the interactions between lipids and proteins during oxidation. Of particular relevance are the findings that markers for lipid oxidation, such as aldehydes, are degraded in the presence of proteins and protein carbonyls, which did not increase in slow oxidizing systems.

Acknowledgments

The authors thank Eilina Jalas and Lisa Andresen for their skilful support and related discussions.

Abbreviations Used

DNPH	2,4-Dinitrophenylhydrazine
MCT	middle chain triglyceride
PV	hydro peroxide value [mmol/g]
TEAA	Triethylammoniumacetate

Conflict of interests

Declarations of interest: none

4.5 References

- Aragao, G. M. F., Corradini, M. G., & Peleg, M. (2008). A Phenomenological Model of the Peroxide Value's Rise and Fall During Lipid Oxidation. *Journal of the American Oil Chemists' Society*, 85(12), 1143. <https://doi.org/10.1007/s11746-008-1305-z>
- Belitz, H.-D., Grosch, W., & Schieberle, P. (2009). *Food Chemistry* (4., rev. and extended ed.). Berlin, Heidelberg: Springer Berlin Heidelberg.
- Berlett, B. S., & Stadtman, E. R. (1997). Protein Oxidation in Aging, Disease, and Oxidative Stress. *Journal of Biological Chemistry*, 272(33), 20313–20316. <https://doi.org/10.1074/jbc.272.33.20313>
- Brownlow, S., Cabral, J. H. M., Cooper, R., Flower, D. R., Yewdall, S. J., Polikarpov, I., . . . Sawyer, L. (1997). Bovine β -lactoglobulin at 1.8 Å resolution — still an enigmatic lipocalin. *Structure*, 5(4), 481–495. [https://doi.org/10.1016/S0969-2126\(97\)00205-0](https://doi.org/10.1016/S0969-2126(97)00205-0)
- Chen, X.-W., Fu, S.-Y., Hou, J.-J., Guo, J., Wang, J.-M., & Yang, X.-Q. (2016). Zein based oil-in-glycerol emulgels enriched with β -carotene as margarine alternatives. *Food Chemistry*, 211, 836–844. <https://doi.org/10.1016/j.foodchem.2016.05.133>
- Crapiste, G. H., Bredvan, M. I. V., & Carelli, A. A. (1999). Oxidation of sunflower oil during storage. *Journal of the American Oil Chemists' Society*, 76(12), 1437. <https://doi.org/10.1007/s11746-999-0181-5>
- Cui, X., Xiong, Y. L., Kong, B., Zhao, X., & Liu, N. (2012). Hydroxyl Radical-Stressed Whey Protein Isolate: Chemical and Structural Properties. *Food and Bioprocess Technology*, 5(6), 2454–2461. <https://doi.org/10.1007/s11947-011-0515-9>

- Davies, K. J. (1987). Protein damage and degradation by oxygen radicals. I. general aspects. *Journal of Biological Chemistry*, 262(20), 9895–9901.
- Feeney, R. E., Blankenhorn, G., & Dixon, H. B.F. (1975). Carbonyl-Amine Reactions in Protein Chemistry. In C.B. Anfinsen, J. T. Edsall, & F. M. Richards (Eds.), *Advances in Protein Chemistry* (pp. 135–203). Academic Press. [https://doi.org/10.1016/S0065-3233\(08\)60412-X](https://doi.org/10.1016/S0065-3233(08)60412-X)
- Frankel, E. N. (1993). Formation of headspace volatiles by thermal decomposition of oxidized fish oils vs. oxidized vegetable oils. *Journal of the American Oil Chemists' Society*, 70(8), 767–772. <https://doi.org/10.1007/BF02542598>
- Friedman, M., & Cuq, J. L. (1988). Chemistry, analysis, nutritional value, and toxicology of tryptophan in food. A review. *Journal of Agricultural and Food Chemistry*, 36(5), 1079–1093. <https://doi.org/10.1021/jf00083a042>
- Fruebis, J., Parthasarathy, S., & Steinberg, D. (1992). Evidence for a concerted reaction between lipid hydroperoxides and polypeptides. *Proceedings of the National Academy of Sciences*, 89(22), 10588. <https://doi.org/10.1073/pnas.89.22.10588>
- Garrison, W. M. (1987). Reaction mechanisms in the radiolysis of peptides, polypeptides, and proteins. *Chemical Reviews*, 87(2), 381–398.
- Gatellier, P., Kondjoyan, A., Portanguen, S., & Santé-Lhoutellier, V. (2010). Effect of cooking on protein oxidation in n-3 polyunsaturated fatty acids enriched beef. Implication on nutritional quality. *Meat Science*, 85(4), 645–650. <https://doi.org/10.1016/j.meatsci.2010.03.018>
- Headlam, H. A., & Davies, M. J. (2004). Markers of protein oxidation: Different oxidants give rise to variable yields of bound and released carbonyl products. *Free Radical Biology and Medicine*, 36(9), 1175–1184. <https://doi.org/10.1016/j.freeradbiomed.2004.02.017>
- Jimenez-Colmenero, F., Salcedo-Sandoval, L., Bou, R., Cofrades, S., Herrero, A. M., & Ruiz-Capillas, C. (2015). Novel applications of oil-structuring methods as a strategy to improve the fat content of meat products. *Trends in Food Science & Technology*, 44(2), 177–188. <https://doi.org/10.1016/j.tifs.2015.04.011>
- Johnson, G. D. (1953). Correlation of color and constitution. I. 2, 4-Dinitrophenylhydrazones. *Journal of the American Chemical Society*, 75(11), 2720–2723.
- Keppler, J. K., Heyn, T. R., Meissner, P. M., Schrader, K., & Schwarz, K. (2019). Protein oxidation during temperature-induced amyloid aggregation of beta-lactoglobulin. *Food Chemistry*, 289, 223–231. <https://doi.org/10.1016/j.foodchem.2019.02.114>
- Keppler, J. K., Koudelka, T., Palani, K., Stuhldreier, M. C., Temps, F., Tholey, A., & Schwarz, K. (2014). Characterization of the covalent binding of allyl isothiocyanate to β -lactoglobulin by fluorescence quenching, equilibrium measurement, and mass spectrometry. *Journal of*

- Biomolecular Structure & Dynamics*, 32(7), 1103–1117.
<https://doi.org/10.1080/07391102.2013.809605>
- Keyse, S. M. (2000). *Stress response: Methods and protocols* (Vol. 99): Springer Science & Business Media.
- Kikugawa, K., Kato, T., & Hayasaka, A. (1991). Formation of dityrosine and other fluorescent amino acids by reaction of amino acids with lipid hydroperoxides. *Lipids*, 26(11), 922.
<https://doi.org/10.1007/BF02535978>
- Lampi, A.-M., & Kamal-Eldin, A. (1998). Effect of α - and γ -tocopherols on thermal polymerization of purified high-oleic sunflower triacylglycerols. *Journal of the American Oil Chemists' Society*, 75(12), 1699–1703. <https://doi.org/10.1007/s11746-998-0319-x>
- Liu, G., Xiong, Y. L., & Butterfield, D. A. (2000). Chemical, Physical, and Gel-forming Properties of Oxidized Myofibrils and Whey- and Soy-protein Isolates. *Journal of Food Science*, 65(5), 811–818. <https://doi.org/10.1111/j.1365-2621.2000.tb13592.x>
- Liu, Z., & Sayre, L. M. (2003). Model Studies on the Modification of Proteins by Lipoxidation-Derived 2-Hydroxyaldehydes. *Chemical Research in Toxicology*, 16(2), 232–241.
<https://doi.org/10.1021/tx020095d>
- Lund, M. N., Heinonen, M., Baron, C. P., & Estévez, M. (2011). Protein oxidation in muscle foods: A review. *Molecular Nutrition & Food Research*, 55(1), 83–95.
<https://doi.org/10.1002/mnfr.201000453>
- Meissner, P. M., Keppler, J. K., Stöckmann, H., Schrader, K., & Schwarz, K. (2019). Influence of Water Addition on Lipid Oxidation in Protein Oleogels. *European Journal of Lipid Science and Technology*, 121(9), 1800479. <https://doi.org/10.1002/ejlt.201800479>
- Min, D., & Jung Kim, H. (2008). Chemistry of Lipid Oxidation. In *Food Science and Technology. Food Lipids*. CRC Press. <https://doi.org/10.1201/9781420046649.pt3>
- Mozaffarian, D., Katan, M. B., Ascherio, A., Stampfer, M. J., & Willett, W. C. (2006). Trans Fatty Acids and Cardiovascular Disease. *New England Journal of Medicine*, 354(15), 1601–1613.
<https://doi.org/10.1056/NEJMra054035>
- Oehlke, K., Heins, A., Stöckmann, H., & Schwarz, K. (2010). Impact of emulsifier microenvironments on acid–base equilibrium and activity of antioxidants. *Food Chemistry*, 118(1), 48–55. <https://doi.org/10.1016/j.foodchem.2009.04.078>
- Oliver, C. N., Ahn, B. W., Moerman, E. J., Goldstein, S., & Stadtman, E. R. (1987). Age-related changes in oxidized proteins. *Journal of Biological Chemistry*, 262(12), 5488–5491.
- Papuc, C., Goran, G. V., Predescu, C. N., & Nicorescu, V. (2017). Mechanisms of Oxidative Processes in Meat and Toxicity Induced by Postprandial Degradation Products: A Review.

- Comprehensive Reviews in Food Science and Food Safety*, 16(1), 96–123.
<https://doi.org/10.1111/1541-4337.12241>
- Prütz, W. A., Butler, J., & Land, E. J. (1983). Phenol Coupling Initiated by One-electron Oxidation of Tyrosine Units in Peptides and Histone. *International Journal of Radiation Biology and Related Studies in Physics, Chemistry and Medicine*, 44(2), 183–196.
<https://doi.org/10.1080/09553008314550981>
- Rade-Kukic, K., Schmitt, C., & Rawel, H. M. (2011). Formation of conjugates between β -lactoglobulin and allyl isothiocyanate: Effect on protein heat aggregation, foaming and emulsifying properties. *Food Hydrocolloids*, 25(4), 694–706.
<https://doi.org/10.1016/j.foodhyd.2010.08.018>
- Sakanaka, S., Tachibana, Y., Ishihara, N., & Raj Juneja, L. (2004). Antioxidant activity of egg-yolk protein hydrolysates in a linoleic acid oxidation system. *Food Chemistry*, 86(1), 99–103.
<https://doi.org/10.1016/j.foodchem.2003.08.014>
- Schaafsma, G. (2000). The protein digestibility-corrected amino acid score. *The Journal of Nutrition*, 130(7), 1865S–7S. <https://doi.org/10.1093/jn/130.7.1865S>
- Smith, B. K., Robinson, L. E., Nam, R., & Ma, D. W. L. (2009). Trans-fatty acids and cancer: a mini-review. *The British Journal of Nutrition*, 102(9), 1254–1266.
<https://doi.org/10.1017/S0007114509991437>
- Srinivasan, S., & Hultin, H. O. (1997). Chemical, Physical, and Functional Properties of Cod Proteins Modified by a Nonenzymic Free-Radical-Generating System. *Journal of Agricultural and Food Chemistry*, 45(2), 310–320. <https://doi.org/10.1021/jf960367g>
- Thiyam, U., Stöckmann, H., & Schwarz, K. (2006). Antioxidant activity of rapeseed phenolics and their interactions with tocopherols during lipid oxidation. *Journal of the American Oil Chemists' Society*, 83(6), 523–528. <https://doi.org/10.1007/s11746-006-1235-6>
- Vollhardt, K.P.C., & Schore, N. E. (2010). *Organic Chemistry*. W. H. Freeman.
- Vries, A. de, Lopez Gomez, Y., Jansen, B., van der Linden, E., & Scholten, E. (2017). Controlling Agglomeration of Protein Aggregates for Structure Formation in Liquid Oil: A Sticky Business. *ACS Applied Materials & Interfaces*, 9(11), 10136–10147.
<https://doi.org/10.1021/acsami.7b00443>

Figure captions

Figure 4.1: Changes in the peroxide value (PV) of oil extracts in gel samples during 7 weeks of incubation at 40°C. A: With no and 0.23% water added. B: with higher water amounts added (2.8-8.4%). Lines were added to guide the eyes, only.107

Figure 4.2: Estimation of dityrosine formation, assessed by fluorescence (excitation 325 nm, emission 410 nm) of protein extracts during a 7 weeks incubation at 40°C. A: low-oxidation systems (no and 0.23% water added) and B: high-oxidation systems (2.8-8.4% water added). Lines were added to guide the eyes, only.108

Figure 4.3: Formation of protein carbonyls in protein extracts of oleogels incubated for 6–10 weeks at 40°C. A: Oleogels with low (0.23%) and without (0%) water addition, and B: oleogels with high water addition (2.8%–8.4%). A zoomed in view of the concentrations from 0–30 nmol carbonyls/mg protein is included.111

Figure 4.4: Free amines in the extracted proteins of oleogels, after 6-10 weeks of incubation at 40°C. A: low-water addition (no and 0.23% water added) and B: high-water addition 2.8%-8.4% water added). Lines are added for to guide the eyes, only.....113

Figure 4.5: Relative concentrations of three representative compounds (hexanal, solid line; valeric acid, dashed line, hexanol, dotted line) over time measured by headspace GC for oleogel samples with 0% water addition (A) and MCT-oil control samples (B).114

Figure 4.6: Relative concentrations of 3-methylbutanal, hexanal, heptanal, and octanal compared with that of hexanal in MCT-oil gels made from corresponding samples with 0%, and 0.5% water addition. Left darkly colored: 0% water MCT-oil gel samples, right brightly colored: 0.5% water MCT-oil gel samples.116

Chapter 5

Changes in Protein Fluorescence in a Lipid-Protein Co-oxidizing Oleogel

Abstract

High and low levels of lipid-induced protein oxidation (tuned by the addition of 0%–8.4% water) were investigated in oleogels, using excitation-emission matrix (EEM) fluorescence spectroscopy, coupled with a partial least squares (PLS) regression and lipid hydroperoxide data. In high-level oxidation models, the intrinsic tryptophan fluorescence decreased and the emission maxima increased from 352.5 nm to 356.0 nm indicating the presence of protein modifications, which was further supported by size-exclusion chromatography. PLS recognized 3 latent components, with several excitation-emission points of interest. These apparent compounds include a region associated with radical mediated protein modifications (approximately 325 nm and 410 nm), lipid oxidation product adducts (approximately 350 nm and 420–425 nm) and malondialdehyde adducts (approximately 375 nm and 425 nm). The separate evaluation of these apparent compounds, at a 420-nm emission, indicated that lipid oxidation promotes protein lipid adduct fluorescence at high water levels, rather than radical mediated protein fluorescence.

Keywords: lipid oxidation, protein oxidation, excitation-emission matrix fluorescence spectroscopy, partial least squares regression

5.1 Introduction

Oleogels represent a relatively new class of lipid-rich foods, in which oleogelators bind liquid oil, providing plasticity and enhancing the viscosity of liquid oils. Oleogelation is an alternative to using fats containing high degrees of saturation and hydrogenation, which are associated with *trans* fatty acids.¹ Therefore, oleogels can be a healthy nutritional option.

Oleogelators consisting of whey proteins have been proposed² because whey proteins have high nutritional value.³ Therefore, the protein oxidation of whey proteins used for oleogelation should be investigated, as oxidation is highly likely to occur in oleogels. Lipid oxidation affects proteins and is a primary factor for the limited shelf life of oleogels and lipid-based foods.⁴ In particular, unsaturated fatty acids, which are found in the oils used for oleogels, are vulnerable to radical chain autocatalyzed reactions with oxygen, resulting in highly reactive products and intermediates.⁵ In contrast with lipid oxidation, protein oxidation has been less discussed with respect to food deterioration, despite most dairy foods containing both proteins and lipids. Further, lipid oxidation products are well-known to deactivate enzymes and modify proteins. Some of these modifications result in fluorescent products, which are often used to assess protein conformations or oxidation states [i.e., modifications of tryptophan (Trp) or tyrosine (Tyr)].⁴ Reactive lipid oxidation species, including oxyl radicals, hydroperoxides, epoxides, and carbonyl products, can damage sensitive amino acids, such as Trp and lysine.⁴ However, little is known regarding the importance of interactions between unsaturated lipids and proteins during oxidation. We therefore assume that all classes of reactive species present in oleogels form different classes of fluorescent protein products. On this basis we hypothesize, that some of the fluorophores can be detected using excitation-emission matrix (EEM) fluorescence spectroscopy and classified by partial least squares (PLS) regression analysis. PLS analyses of EEM fluorescence data have been shown to distinguish between compounds in mixtures;^{6,7} thus, the fluorescent compounds in lipid-protein co-oxidation models can be likely distinguished. In addition, PLS may provide information regarding the relevance of each fluorescent species, by comparing them against general oxidation data. Because each fluorescent species is associated with different formation mechanisms, single EEM combined with PLS may provide information regarding the importance of reactive lipid oxidation species, for the modification of proteins and lipid-protein co-oxidation, in general. Protein oleogels were chosen as test systems for protein-lipid oxidation because these gels are physically stable during storage and the gel strength⁸ and oxidation rate can be tuned by increasing the water concentration.⁹ As an independent approach, protein modification was studied by SEC of peptides after tryptic digestion. The objective of this

study was to explore whether it is possible to relate complex fluorescence data (EEM) via chemometrics (PLS) with results from lipid oxidation and to propose marker compounds that are indicative for underlying mechanisms of lipid-protein co-oxidation.

5.2 Materials & methods

5.2.1 Materials

Oleic-acid-rich safflower oil was purchased from a local supermarket. Whey protein isolate (BiPro) was obtained from Agropur Inc. (Appleton, USA), containing 97.7% protein and 75% beta-lactoglobulin, in dry matter.¹⁰ Al₂O₃, BaCl₂, FeSO₄, guanidine hydrochloride, hydrochloric acid, trichloroacetic acid, and trypsin (5000 USP-U/mg) were obtained from Carl Roth (Karlsruhe, Germany), and 2,4-dinitrophenylhydrazine and triethyl ammonium acetate (TEAA) buffer were obtained from Sigma Aldrich (Steinheim, Germany). All solvents were obtained from VWR (Fontenay-sous-Bois, France). All chemicals were at least high-purity. Water (> 18.2 MΩ) was purified by an Elga Veolia system (Celle, Germany) and was used for all experiments.

5.2.2 Purification of oil

The oil was purified of natural antioxidants by preparative column chromatography, as described by Lampi and Kamal-Eldin,¹¹ with slight modifications. The oil was tested for residual tocopherols (< 0.5 ppm, high-performance liquid chromatography (HPLC)-based standard method from the German Society for Fat Science (DGF) F-II 4a).¹²

5.2.3 Sample preparation

Oleogel samples containing added water were manufactured in 2 batches (A: 0%–0.23% added water, and B: 2.8%–5.6% added water), as described previously,⁹ based on whey protein aggregates.¹³ In brief, whey protein (4% w/w) was dissolved in water, stirred for 2 h, and stored at 4°C, overnight, to fully hydrate the protein. The protein solution was then adjusted to pH 5.7 with 1 M HCl and heated for 20 min, at 85°C. After cooling in an ice bath, a weak gel of protein aggregates was obtained, which was shaken by hand and homogenized with an Ultra Turrax (13,000 rpm, IKA, Staufen, Germany). The protein aggregates were then separated from non-aggregated proteins and peptides by centrifugation (Allegra X-30R, Beckmann Coulter, Krefeld, Germany), for 20 min at 4,000 × *g*, followed by decanting the upper phase, which was discarded. After redispersion of the pellet with water, these centrifugation steps were repeated twice. The achieved protein pellet was finally dispersed into a 1% (w/w) solution, relative to the initial

protein mass, frozen in liquid nitrogen, and lyophilized. Dry protein aggregates were then added to purified oil (6.8% protein) and stirred for 10 min, with a magnetic stir bar. For gels with added water, water was added after 5 min of stirring. Superfluous oil was removed by decanting the gel for 10 min, after centrifugation for 20 min at $4,000 \times g$.

Oleogels were aliquoted into 200-mg samples and stored in sterile, closed, 15-mL centrifuge tubes, which were sealed with parafilm and incubated at 40°C , in a drying cabinet, in the dark, for a specific time until analysis.

5.2.4 Extraction of proteins and determination of primary lipid oxidation products

Oleogel samples were extracted, as described previously,⁹ and used to measure protein fluorescence and lipid peroxides. In brief, gel samples (200 mg) were defatted and washed 3 times with 3 mL cyclohexane, washed 2 times with 5 mL isopropanol, and washed 2 times with 5 mL mass spectrometry (MS)-grade water. Washes were performed by rigorously shaking, followed by centrifugation at $4000 \times g$ for 5 min, (Allegra X-30R, Beckmann Coulter, Krefeld, Germany) and decanting. The combined cyclohexane phase was flushed with nitrogen to dryness, for 20 min at 20°C . Then, the reweighted, extracted fat was dissolved in 5 mL isopropanol and diluted, if necessary. Lipid hydroperoxides were determined using the ferric thiocyanate method, as described by Stöckmann *et al.* and Thiyam *et al.*^{14,15} All measurements were performed in triplicate unless otherwise noted.

5.2.5 Spectroscopic measurements

The fluorescence signal was recorded using a Cary Eclipse (Varian Agilent, Palo Alto, USA) spectrometer. The protein pellet was dispersed in 3 mL MS-grade water, and 1 mL of the dispersion was diluted and incubated in 0.05 M TEAA, containing approximately 1/20 (w/w) trypsin (160 $\mu\text{g}/\text{mL}$), at 37°C for 22 h, with brief agitating after 20 h. A 1-mL sample was taken from the upper, clear phase, diluted with MS-grade water (1/1, v/v) and used for fluorescence measurement. Fluorescence was recorded as a series of emission (λ_{EM}) spectra, from 400–600 nm (600 nm/min, 5-nm slit, a data interval of 1 nm), with an excitation wavelength (λ_{EX}) ranging from 290–395 nm, at 5-nm increments (5-nm slit), using a detector voltage of 600 V. These ranges were chosen to include typical protein oxidation compounds and to avoid high Trp signals and the measurement of direct excitation light scattering. Tyr, phenylalanine (Phe), and Trp fluorescence were recorded using a similar method (λ_{EM} : 260–375 nm, λ_{EX} : 260–285 nm), with a detector voltage of 500 V. Protein concentration was measured at 278 nm (Helios γ

Spectrophotometer, Thermo Electron Corporation, Waltham, USA) and calculated based on the molar absorption coefficient of β -lactoglobulin ($17,600 \text{ M}^{-1} \text{ cm}^{-1}$), with a molar mass of $18,300 \text{ g/mol}$.^{5,16} All measurements were compared against a blank, containing buffer and trypsin.

5.2.6 Size-exclusion chromatography (SEC)

Frozen fluorescence samples in cuvettes were thawed for 20 min, in a water bath at room temperature (RT), and centrifuged for 20 min at $4,000 \times g$, to remove any insoluble material. A 1-mL sample was removed from the upper phase, and a 150- μL aliquot was removed from this sample for SEC. A 50- μL volume was injected into an Agilent 111 HPLC, with Tris(hydroxymethyl)aminomethan (TRIS)-HCl buffer (0.15 M), pH 8 as the eluent (0.3 mL/min), on a Superdex™ 200 increase 10/300 GL column, as previously described.¹⁷ A chromatogram was recorded for 100 min, with a diode array detector (λ_{EX} : 278 nm, λ_{EM} : 325 nm). Calibration was conducted with the “Gel Filtration Calibration Kit LMW”, from GE Healthcare (6.5–75 kDa, including aprotinin, ribonuclease A, carbonic anhydrase, ovalbumin, and conalbumin). Chromatograms were transferred into CSV files, using ChemStation, Agilent. Peaks were deconvoluted, as described in the statistical analysis section, for compounds (retention times: 27.9, 29, 35, 48.8, 56.5, 60.13, 63.08, 66.76, 70.63, 74.65, and 80.25 ± 0.5 min; standard derivation, σ , values were limited from 10% to 150% of 0.75, 5, 1.5, 5, 0.75, 0.75, 0.75, 0.75, 0.75, and 0.75 min, respectively) after baseline subtraction (line fitting between means of 0–20 min and 83–85 min). Area values were normalized using the summed protein absorption at 278 nm, with 0.1 arbitrary units (a.u.) as the threshold.

5.2.7 Statistical analysis

All results were statistically analyzed with Excel and R, with the image package ggplot2, the pls package, and minpack.lm for non-linear regression.^{18–22}

5.1.7.1 Absorption maxima of Tyr and Trp

The Trp absorption maxima were determined by Gaussian curve fitting²³ (see equation I), with the R package minpack.lm²² of the λ_{EM} spectrum, using wavelengths, λ , ranging from 285–375 nm, and λ_{EX} at 275 nm, using the borders 285–310 nm, for Tyr, and 300–400 nm, for Trp.

$$\text{Intensity} = \sum_{i=1}^n k_i \cdot e^{-\frac{1}{2} \left(\frac{\lambda - \bar{\lambda}_i}{\sigma_i} \right)^2} \quad \text{I}$$

5.1.7.2 Partial least squares regression of excitation-emission matrix fluorescence

Partial least squares (PLS) regression was computed using the PLS package in R.^{20,21} EEM fluorescence data (156 samples, λ_{EX} : 290–395 nm, λ_{EM} : 400–600 nm and λ_{EX} : 275, λ_{EM} : 260–375 nm, as a matrix, with λ_{EX} wavelengths as rows and λ_{EM} wavelengths as columns, filled with intensities) was read in R and combined with the hydroperoxide values of the samples. This combined data was reshaped into a matrix of fluorescence intensities, with the columns ‘excitation-emission combination x y’ (X) and the column hydroperoxide content. The hydroperoxide column (Y) was then correlated with the EEM (X), via PLS, using “leave one out” cross-validation [in R: `pls(Y~X, validation = “LOO”)`]. In brief, the original data matrix X can be described as a product of a loading and a scoring matrix, similar to principal component analysis. The basic concept of both PLS and principal component analysis is to find linear combinations (e.g. $b_1a_1 + \dots + b_n a_n$) of the original n variables that can be substituted with fewer new variables, known as the principal components. These linear combinations are weighted with the b values, which are called loadings and are carefully chosen to identify new independent variables, or orthogonal linear combinations vectors, which are mathematically realized by identifying the eigenvectors of the covariance matrix of the data. The loadings represent the weight of each original variable and the scores for the original data, in a rotated coordinate system. The PLS algorithm attempts to maximize the covariation of the X scores, in addition to performing principal component analysis for the Y scores; therefore, PLS can filter relevant X and Y variables, which are causative for correlation. The loading of the ‘excitation-emission combination x y’ variables are finally reshaped to the triple data points ‘excitation’, ‘emission’ and ‘loading value’, for interpretation.

5.1.7.3 Curve fitting of related compounds in the fluorescence spectra

Apparent compounds with expected λ_{EX} maxima of 325, 350, and 370 nm were determined by Gaussian curve fitting²³ (see equation I), with the R package `minpack.lm`²² of the λ_{EX} spectrum (λ_{EX} : >320 nm, λ_{EM} : 420 nm). Standard derivation, σ , was set to 20 nm, and the pre-exponential factor, k , was bordered from 0.1 to 500 a.u., which was also used for plotting.

5.3 Results & Discussion

5.3.1 Intrinsic fluorescence of tryptophan

Intrinsic fluorescence variation was analyzed by curve fitting the fluorescence spectra, with an λ_{EX} at 275 nm. In oleogels with less than 0.25% added water, no change in Trp intensity was observed, whereas in samples with 2.8% to 8.4% added water, Trp decreased significantly after 14 d of incubation in comparison to day 0 ($p = 0.07 \mid 0.004 \mid 0.005$, see Figure 5.1), which is in accordance with the formation of lipid oxidation produced hydroperoxides and conjugated dienes.⁹ After 14 d of incubation, only oleogels with $> 2.8\%$ added water showed evidence of lipid oxidation.⁹

Decreased Trp fluorescence could be caused by protein modifications and the oxidative degradation of Trp.^{4,24} Protein modifications could result in changed protein solubility and decreased trypsin digestibility, which lowers the peptide concentration and, thereby, lowers the overall Trp presence in the measured sample, which was removed from the clear, upper phase after trypsin digestion.

Beta-lactoglobulin contains only two Trp residues: Trp 19, in the hydrophobic pocket, and Trp 61, near the surface of the protein;²⁵ thus, Trp availability is intrinsically limited. Furthermore, decreased Trp fluorescence following protein modification could be due to fluorescence quenching, by ketone-like modifications caused by secondary lipid oxidation products, as the structurally similar acetone and methyl vinyl ketone are known to quench Trp fluorescence,²⁶ which can reflect increased carbonyl contents.^{4,27}

However, decreased Trp fluorescence intensity is also highly likely to be caused by amino acid degradation. The Trp pyrrole moiety was found to be prone to oxidation, and oxidation products, such as oxindolylalanine (Oia), 3 α -hydroxy-1,2,3,3 α ,8,8 α -hexahydropyrrolo[2,3-b]indole-2-carboxylic acid (PIC), *N*-formylkynurenine (NFK), dioxindolylalanine (DiOia), kynurenine (Kyn), and 5-hydroxytryptophan (5-HTP), have been identified in proteins and peptides.²⁴ A strong decrease in Trp fluorescence intensity, associated with increased protein oxidation, has previously been reported in studies examining amyloid-like aggregates of whey protein (i.e., no protein extraction losses due to reduced digestibility).¹⁷ In these studies lipids were absent and the formation of protein carbonyl level was also low (i.e., no quenching by lipid oxidation products).¹⁷

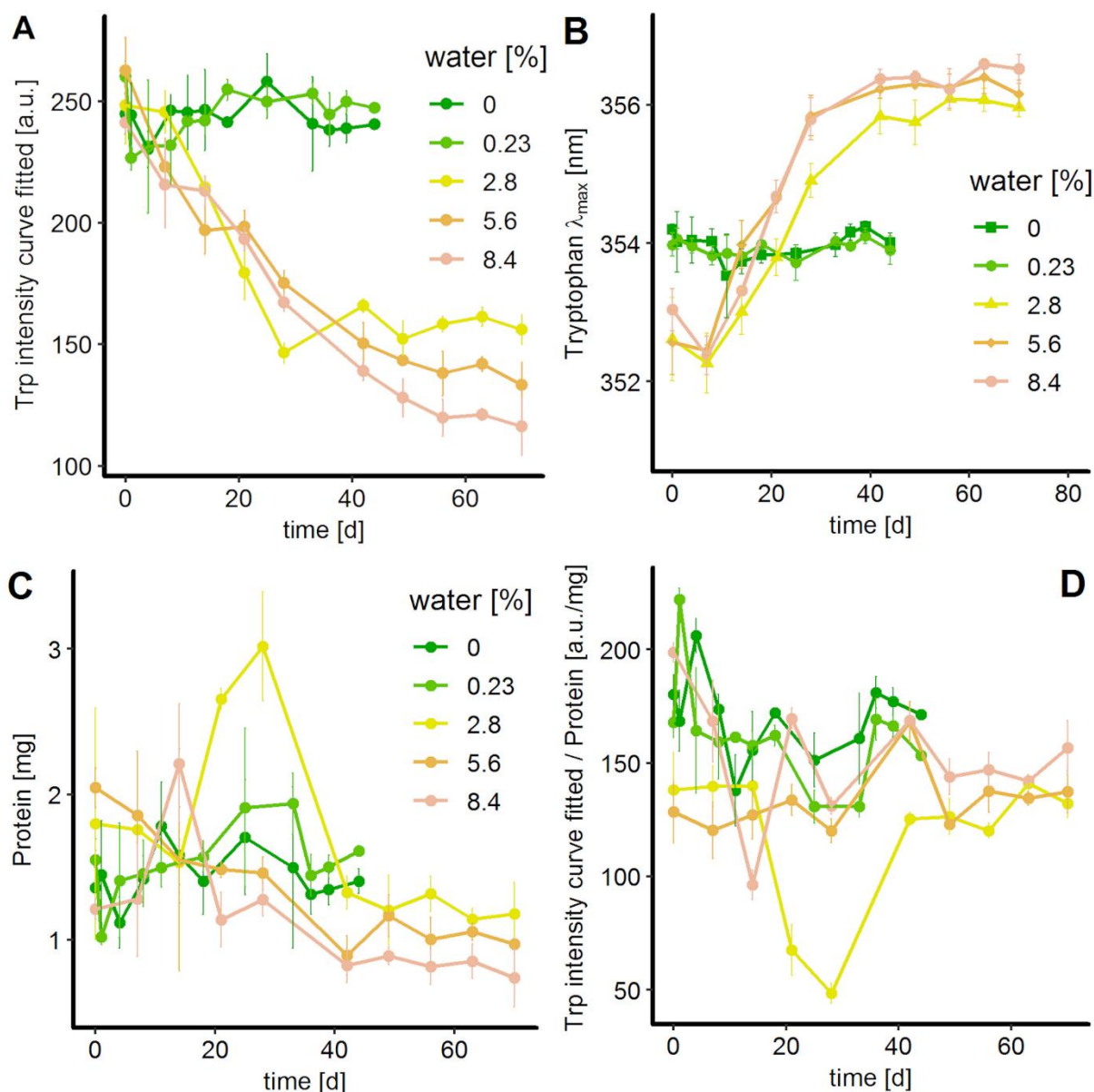


Figure 5.1: Intrinsic fluorescence of tryptophan (Trp) and protein concentrations. A: Intensity of Trp over time, B: Emission maximum of Trp over time, C: Protein contents in the hydrolysate of protein extracts, measured by absorption at 278 nm, D: Relationship between Trp fluorescence and protein contents. Trp fluorescence parameters were calculated by using a Gaussian curve fit.

At day 0, an approximately 1 nm difference can be observed in the Trp emission maxima between low and high oxidation rates, which may be due to slight rearrangements of the protein secondary structures during preparation, as high-oxidation models contain water droplets, whereas low-oxidation models do not.⁹ In samples with high lipid oxidation rates (> 2% added water), the Trp emission maximum for digested proteins isolated from the oleogel increased, from approximately 352.5 nm to approximately 356 nm (see Figure 5.1), after 14 d of incubation. The emission maximum of Trp is sensitive to microenvironmental changes, and an emission maximum of 355 nm represents Trp that is fully dissolved in water,²⁸ with a more polar

environment. A shift in Trp emission during oxidation has been reported previously,²⁹ and Trp residuals found on oil surfaces in lipophilic environments, which have lower emission maxima, are thought to be degraded first, increasing the proportion of Trp in the polar environments, which would increase the emission maximum. This Trp red shift can also be interpreted as the increased exposure of Trp to the surrounding environment through unfolding or peptide scission by lipid oxidation products. Trp exposure to the surrounding environment would also increase the contacts with other amino acid residues in the solution, including Trp-quenching groups, such as free amino groups, carboxyl groups, and amide groups,³⁰ which can also result in decreases Trp intensity. However, this level of contact in a protein hydrolysate would likely be high from the beginning. Therefore, the oxidative deterioration of aromatic amino acids is likely to play an important role in the decreased fluorescence observed at 278 nm. For both reasons, the protein amount determined by absorption at 278 nm must also be considered with caution.¹⁷

5.3.2 Size-exclusion chromatography (SEC)

The peptide composition of the tryptic digest was evaluated using SEC (see Figure 5.2). Trypsin specifically cleaves peptide bonds on the C-terminal side of lysine and arginine residues.³¹ According to the sequence of beta-lactoglobulin (162 amino acids),³² 19 cleavage sites were expected, including 5 tryptic peptides, containing aromatic amino acids, including Trp and Tyr, which strongly absorb at 278 nm. In contrast, Phe absorbance is most likely too low to be detected. However, 4–5 main peaks were observed in the low-kDa region (> 60 min), which is similar to the findings of Jost and Monti, who performed a tryptic digest of whey protein, which was heated for 1 h at 95°C prior to the addition of digestion enzymes.³³ Compared with the native form, 5% (w/v) whey protein that was pretreated in deionized water, at 80°C for 15 min, showed no effects on the peptide size after 24 h of tryptic digestion (native main peak 12.2–19.9 kDa, heat-pretreated 11.8–21.2 kDa),³⁴ which may allow the ideal digestion conditions of native proteins to be determined. These sizes are larger than the theoretically expected sizes of peptides following tryptic digestion, which were expected to be smaller than 10 kDa.

Ideal digestion predicts 2 Trp peptides (approximately 2.7 kDa and 1.1 kDa in size), with the first peptide also containing an expected Tyr residue. Therefore, the major peptide (approximately 2.7 kDa) is likely represented by peak **6**, at 60.13 min, whereas the smaller peptide likely corresponds to peak **10**, at 74.65 min because Trp has a higher absorbance than Tyr.

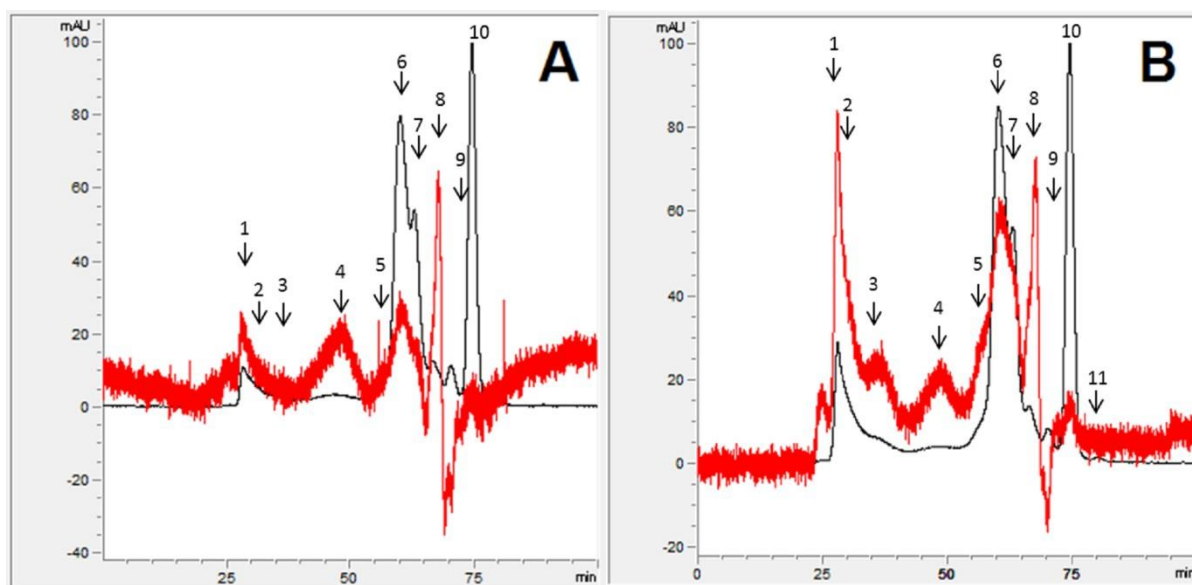


Figure 5.2: Size-exclusion chromatograms (red: 325 nm, black 278 nm, full absorbance range scale) of tryptic digests from protein extracts derived from prepared oleogel with 2.8% added water, for a sample at incubation time 0 d (A) and 7 d (B, included peak assignment).

The 3 peaks between these two peaks (7–9) may be associated with the other 3 Tyr-containing peptides (approximately 2.6 kDa, 1.1 kDa, and 0.9 kDa) and with other peptides from minor proteins in whey protein.³⁵ However, these sizes are only estimates because the clear size determination of peptides < 3 kDa is outside of the calibration limits of the SEC column.

Interestingly, protein aggregates can be disrupted by cystine-reducing agents, which indicates that the larger observed compounds may represent disulfide bridged aggregates.³³ Peak 4 (48.8 min) refers to a size of 24.1 kDa, which is the approximate size of a denatured beta-lactoglobulin monomer, which predominates at pH 9 but can coexist with aggregates under chromatographic conditions (pH 8).³⁶ The increases in the larger peaks (1–3), which were observed after 1 and 2 weeks of incubation with oxidizing oil at 40°C. These larger peaks may represent beta-lactoglobulin oligomers that form from undigested monomers, which are connected by cross-links. As these peaks were accompanied by increased absorbance at 325 nm (see Figure 5.2), they may be associated with radical dimerization products like dityrosine.⁴ Furthermore, the aldehydes formed by lipid oxidation can also cross-link proteins.^{4,37}

Cross-linking increases the particle size, and the binding of lipid oxidation products with proteins is highly associated with Schiff bases and the formation of products with a carbonyl component near the lysine ϵ -amino group.⁴ This lysine modification should prevent the tryptic cleavage of the protein sequence. For example, lysine modifications combined with the most abundant lipid oxidation product, hexanal, can result in protein miscleavages.³⁸ Therefore, longer peptides

should be observed over time with increased oxidation. To investigate this phenomenon, 11 different peptide/protein peaks were separated by deconvolution and normalized against protein concentration (summed absorbance 278 nm, see Figure 5.2). This deconvolution contains a Gaussian fit of the main peaks and the “shoulders” (see supplementary material section 8.2). After incubation 0% added water oleogels containing oxidizing lipids, no changes in beta-lactoglobulin monomers (48.8 min, peak **4**) or tryptic peptides (peaks **6–10**) were observed, after either 8 or 14 d of incubation (peroxide values = 4.4 ± 0.3 mmol O₂/kg oil and 7.1 ± 0.4 mmol O₂/kg oil, respectively, see Figure 5.3), whereas the monomers in oleogels with 2.8% added water increased significantly after 7 (175 ± 12 mmol O₂/kg oil, $p = 0.01$) and 14 d (399 ± 30 mmol O₂/kg oil) of incubation. These results can be interpreted as the decreased digestibility of proteins following lipid-protein co-oxidation. The reduced digestibility, caused by protein oxidation, may be due to binding site modifications or may be caused by changes in protein solubility, hydrophobicity, and conformation,^{39,40} which can reduce the nutritional value of oxidized proteins.⁴¹ However, oligomers also increased (peaks **1–3**), especially peak 3 (35 min, estimated to be approximately 130 kDa), among proteins after 14 d incubation (0% water $p = 0.55$, 2.8 % water $p = 0.0005$). For low-oxidation oleogels, other reactions, such as fatty acid complexation, may play roles in protein oligomerization. In addition, these oligomers may be released from noncovalent aggregates over time. For the tryptic peptides (peaks **6–10**), no clear changes could be observed, which may be the result of random modifications made to lysine residues. However, the compound associated with peak **9** (70.63 min) was significantly decreased after 14 d of incubation, in both systems (0% $p = 0.09$, 2.8% $p = 0.03$). Because this peak belongs to a small-sized tyrosine peptide, this peak may tentatively be assigned to VYVEELK (0.88 kDa), which is less effectively cleaved from subsequent peptides in native protein by trypsin³⁵ and represents a nonattackable core protein-peptide, which is less accessible to protein oxidation. In contrast, peak **5** (56.5 min, 9.5 kDa) may represent miscleaved monomers that were not fully digested. This peak could belong to an extended peptide, as this component is only significantly increased in the 2.8% added water system (7 d: $p = 0.09$, 14 d $p = 0.04$), similar to the monomer. Peptide changes can be attributed to protein oxidation, rather than conformation changes or the complexation of lipids, because lipid oxidation aldehydes⁹ and protein carbonyls²⁷ were only detectable in the 2.8% added water oleogel system after 7 d of incubation.

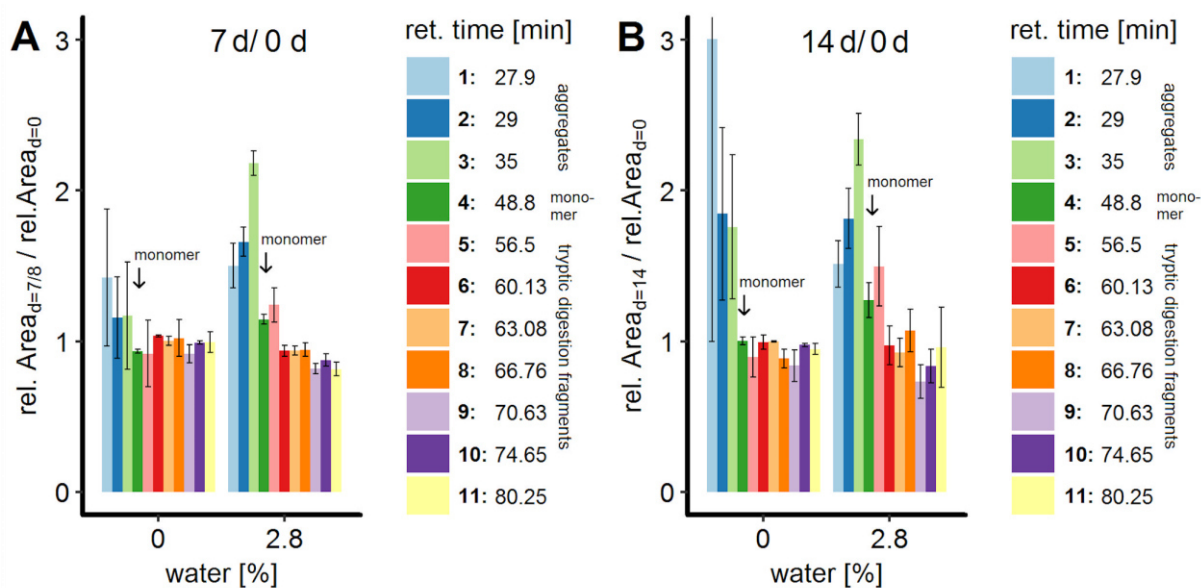


Figure 5.3: Ratio of normalized deconvoluted peak areas of size exclusion chromatograms (recorded absorption signal at 278 nm) for trypsin-digested protein extracts, with low lipid oxidation (0% added water) and high lipid oxidation (2.8% added water) conditions. Deconvoluted areas were related to non-oxidized protein extracts (day 0), for samples after 7 (2.8%), 8 (0%), (A) and 14 d (B) of incubation. All values were measured in triplicate.

5.3.3 Fluorescence signals and PLS

PLS regression was performed on EEM data from tryptic peptide samples derived from oleogels, which differed in their protein-lipid co-oxidation contents, based on hydroperoxide contents,²⁷ which were in accordance to conjugated dienes formation in these gels.⁹ The EEM data for the systems were first modeled using a low-oxidation model and then using a whole-data model (oleogels with 0%, 0.23%, 2.8%, 5.6%, and 8.4% added water). Two models were generated due to the low Trp intensity loss and a lack of significant change observed for Trp emission maximum wavelength, which suggests the low-oxidation status of oleogels with 0% and 0.23% water added.⁹ Also, the addition of different water amounts may alter pathways involved in the formation of fluorescent compounds as water can catalyze reactions due proton donation, acceptor properties or interphase building properties. In addition, early fluorescent compounds associated with the early oxidation phase may be better identified in the low oxidation model. The low-oxidation model was described best with 5 PLS components, which explained 55.8%, 86.2%, 90.1%, 97.3%, and 98.2% of the variance observed for fluorescence data and 22.9%, 46.9%, 82.4%, 83.7%, and 86.9% of the variance observed for hydroperoxide data. These values were similar to the whole-data model, using 5 components, which explained 79.2%, 95.6%, 97.7%, 98.9%, and 99.2% of fluorescence data variance and 85.1%, 90.4%, 91.9%, 92.5%, and

93.3% of hydroperoxide data variance. For both models, the leave-one-out procedure was used to perform cross-validation. In both models, the root mean square errors of prediction (low-oxidation model: 2.9 mmol O₂/kg oil, whole-data model: 147.7 mmol O₂/kg oil) were comparably low for the highest hydroperoxide values (low-oxidation model: 36.5 mmol O₂/kg oil, whole-data model: > 1,400 mmol O₂/kg oil) but were high for the lowest hydroperoxide values. The lack of fluorescence information suggests low-oxidation status, as the fluorophores formed by protein-lipid co-oxidation are not present during the low-oxidation state. However, the slope of the predicted values versus the measured values is very good (1.00 ± 0.05 , 1.00 ± 0.03 , see supplementary material section 8.2), and a t-test indicated proximity to an ideal value of 1 (low-oxidation model: $t = -2.4 \times 10^{-14}$, whole-data model: $t = -1.4 \times 10^{-13}$, in both $p = 1$).

The first 3 PLS components (see Figure 5.4) explained the most variance for hydroperoxide data, and several $\lambda_{\text{EX}} - \lambda_{\text{EM}}$ combinations were notable in the loading contour plots (see Table 5.1). The first region ($\lambda_{\text{EX}} < 300$ nm, $\lambda_{\text{EM}} < 450$ nm) was negative for most PLS components and is likely related to intrinsic Trp absorption and emission. Trp oxidation results in decreased Trp fluorescence and correlates with hydroperoxide formation. In contrast, this region is positive for the first component of the low-oxidation model, which is consistent with a slightly positive trend for such systems during the first 3 weeks (see Figure 5.1). This result may indicate the initially increased solubility of proteins in such systems, due to the release of protein monomers from non-covalent protein aggregates in the lipid oil solvent and the minor oxidation of Trp residues, which is consistent with the SEC findings of slightly increased oligomers after 7 and 14 d.

Table 5.1: Characteristic excitation/emission regions observed and related compounds

λ_{EX} [nm]	λ_{EM} [nm]	PLS component low oxidation	PLS component high oxidation	assigned region(s)	model compounds or systems in this region (λ_{EX} [nm], λ_{EM} [nm])
<300	<450	all	All	-	Tryptophan oxidizing linoleate/ albumin (350, 435) ^{42,43}
335–350	410–435	all	1, 2	①	linoleic acid hydroperoxide, acetaldehyde, hexanal/ polylysine (347, 425) ³⁷
375	425	-	2	④	Raman scattering 1-amino-3-iminopropene derivatives (RNHCH=CHCH=NR') (370, 450)
325	400–500	-	3	②,③	2-hydroxyheptanal/ ribonuclease (325, 409) ⁴⁶ N-formylkynurenine (325, 435) ⁴⁷ dityrosine (325, 420) ⁴⁷

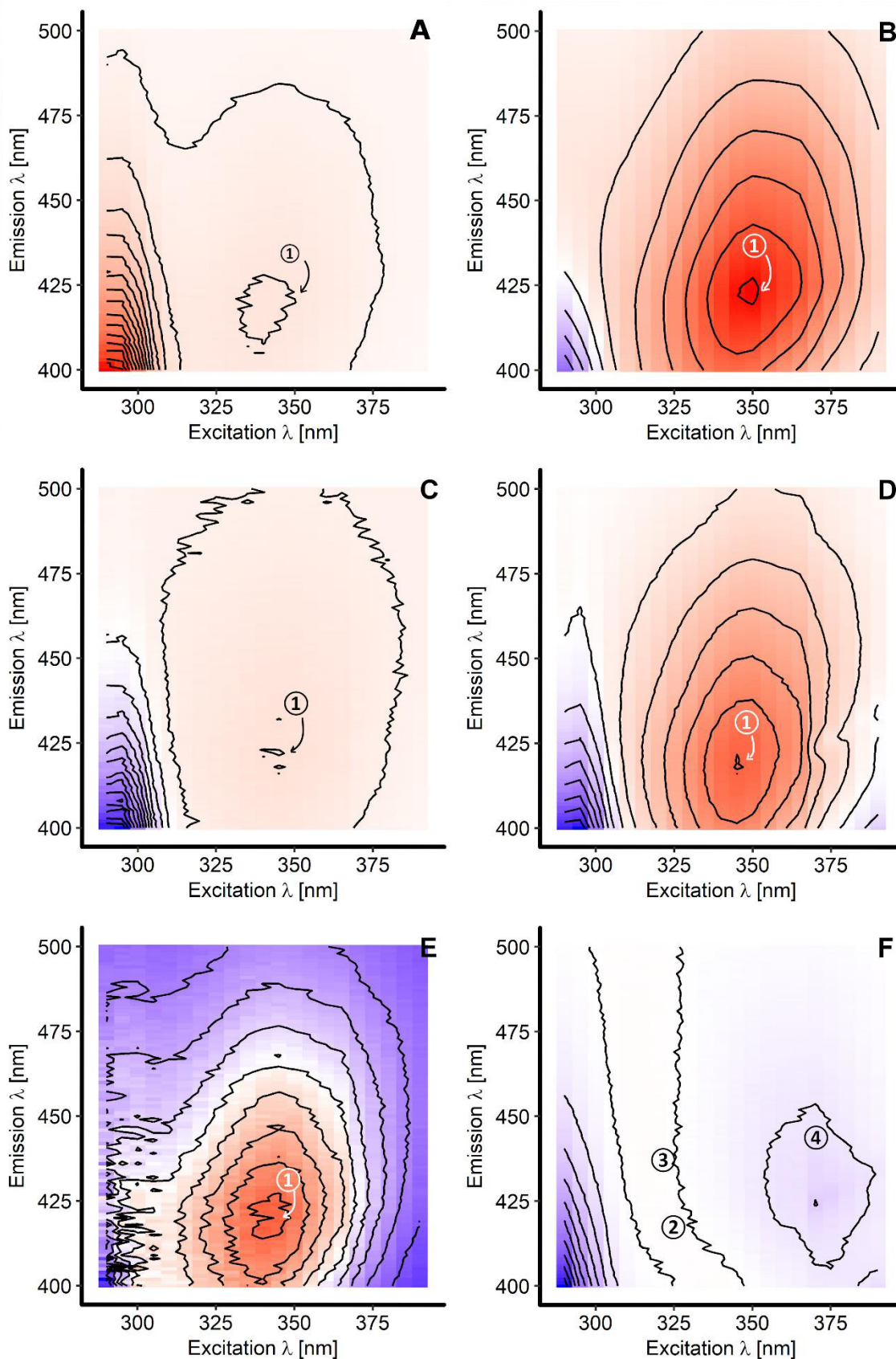


Figure 5.4: PLS loading contour plots for the principal components 1 to 3 for low-oxidation systems (0% and 0.23% added water, A, C, and E) and for all samples (B, D, and F). A positive correlation is indicated by coloring (blue for negative, red for positive) and highlighted by adding 10–15 isolines.

However, a region of λ_{EX} , from 335 to 350 nm, and λ_{EM} , from 410 to 435 nm, was identified for the first 3 components of the low-oxidation systems (Figure 5.4 A), and for components 1 and 2 of the whole-data model, which explain most of the hydroperoxide data variance. Characteristic components in these regions have been previously identified in studies examining protein and lipid oxidation products in model systems. The reaction between oxidizing linoleate and albumin forms cross-links and fluorescent compounds (λ_{EX} : 350 nm, λ_{EM} : 435 nm).^{42,43} Likewise, the reactions between polylysine and linoleic acid hydroperoxide (λ_{EX} : 347 nm, λ_{EM} : 425 nm) and between acetaldehyde and hexanal, which are fragmentation products of hydroperoxides (λ_{EX} : 340–360 nm, λ_{EM} : 410–430 nm) causes fluorescence in this region.³⁷ This result suggested that hexanal formation and degradation occurred in oleogel systems,⁹ due to the decrease in smaller peptides and the increase in larger peptides following the tryptic digestion. In the whole-data model, this region is slightly divided into two fluorescent maxima, for component 1 (λ_{EX} : 350 nm, λ_{EM} : 425 nm, Figure 5.4 B) and component 2 (λ_{EX} : 345 nm, λ_{EM} : 423 nm, Figure 5.4 D). Because principal components are defined as independent, this result indicates that fluorescence is due to a large range of different products in real systems and that lipid oxidation leads to a broad spectrum of aldehydes through the fragmentation of hydroperoxides.

For the second component of the whole-data model (Figure 5.4 D), a line on the bottom of the right corner is visible (λ_{EX} : 375 nm, λ_{EM} : 425 nm), due to first-order Raman scattering, despite blank subtraction. However, the line is negative, as scattering becomes increasingly insignificant as fluorophores increase. However, this region for the third component (Figure 5.4 F) is negatively correlated with hydroperoxides, even above the Raman scattering line, which indicates the presence of a fluorophore. For this region, the Schiff base fluorophores 1-amino-3-iminopropene derivative ($\text{RNHCH}=\text{CHCH}=\text{NR}'$, λ_{EX} : 370 nm, λ_{EM} : 450 nm), formed by glycine, valine, and leucine with malondialdehyde has been known for a long time.⁴⁴ Malondialdehyde and related fluorescence-forming compounds are also primarily formed by linolenic acid, but not by linoleic acid.⁴⁵ Because linolenic acid is oxidized before linoleic acid and other less unsaturated fatty acids, malondialdehyde and related fluorescence products are formed during the very early stages of oxidation. However, linolenic acid ($0.14\% \pm 0.01\%$) is present in relatively low amounts compared with linoleic acid ($14.7\% \pm 0.03\%$).⁹ The correlation with hydroperoxides for component 3 in the PLS regression may be negatively weighted because rapidly formed fluorescent products may also be the first to degrade. Interestingly, a 25-nm broad band around the 325 nm λ_{EX} in component 3 is positively correlated with the concentration of lipid hydroperoxides. In this region, the fluorescent protein adduct between ribonuclease A and 2-hydroxyheptanal (λ_{EX} : 325 nm, λ_{EM} : 409 nm) forms a fluorescent adduct, and 2-hydroxyheptanal

is a degradation product of linoleic acid.⁴⁶ However, this region is also characteristic for the radical decomposition of Trp to *N*-formylkynurenine (λ_{EX} : 325 nm, λ_{EM} : 435 nm) and Tyr to dityrosine (λ_{EX} : 325 nm, λ_{EM} : 420 nm), in milk proteins,⁴⁷ which agrees with the observed Trp degradation.

5.3.4 Curve-fitted compounds

Three fluorescent apparent compounds were derived as latent variables from the PLS regression for further investigation. These apparent compounds were analyzed for their contributions to fluorescence during storage both low- and high-oxidation systems. All apparent compounds showed λ_{EM} values of 420 nm, although the intensity varied and was not always at the maximum. Extracting an excitation spectrum for the emission of 420 nm can provide quantitative information regarding the three latent variables and can be further investigated as 2D data. Further, the fluorescence of all three apparent compounds relies on normal statistical behavior; therefore, the quantities of the compounds can be easily estimated by fitting a sum of Gaussian curves (peak deconvolution). As an approximation, the 3 apparent compounds were fitted with λ_{EX} wavelengths at 325 nm, 350 nm, and 370 nm with a standard derivation of 20 nm (Figure 5.5). In low-oxidation models (oleogel samples with 0% and 0.23% added water, Figure 5.5 A and B) the apparent compound at 370 nm is very low and is most evident during the first 14 d. This finding can be attributed to the formation of malondialdehyde as related Schiff base fluorophores are characteristic for this region. Malondialdehyde in turn fragments from the most labile fatty acid, linolenic acid (content approximately 0.14 %). A similar process should occur in high-oxidation systems (Figure 5.5 C and D); however, saturation occurs, indicating an equilibrium for the formation and degradation of Schiff bases, which are formed as intermediate products. In addition, malondialdehyde may be a degradation product, due to the fragmentation of linoleic acid, and only be present in small amounts,⁴⁸ which could explain the increased occurrence of the apparent compound at 370 nm λ_{EX} in high-oxidation systems. The most striking difference between high- and low-oxidation systems is the increase in the ratio of the apparent compounds with an λ_{EX} at 350 nm to apparent compounds with other λ_{EX} wavelengths. The region with an λ_{EX} at 350 nm is characteristic for Schiff base-derived products, whereas the region with an λ_{EX} at 325 nm is characteristic for radical-driven protein oxidation components like dimerization products.

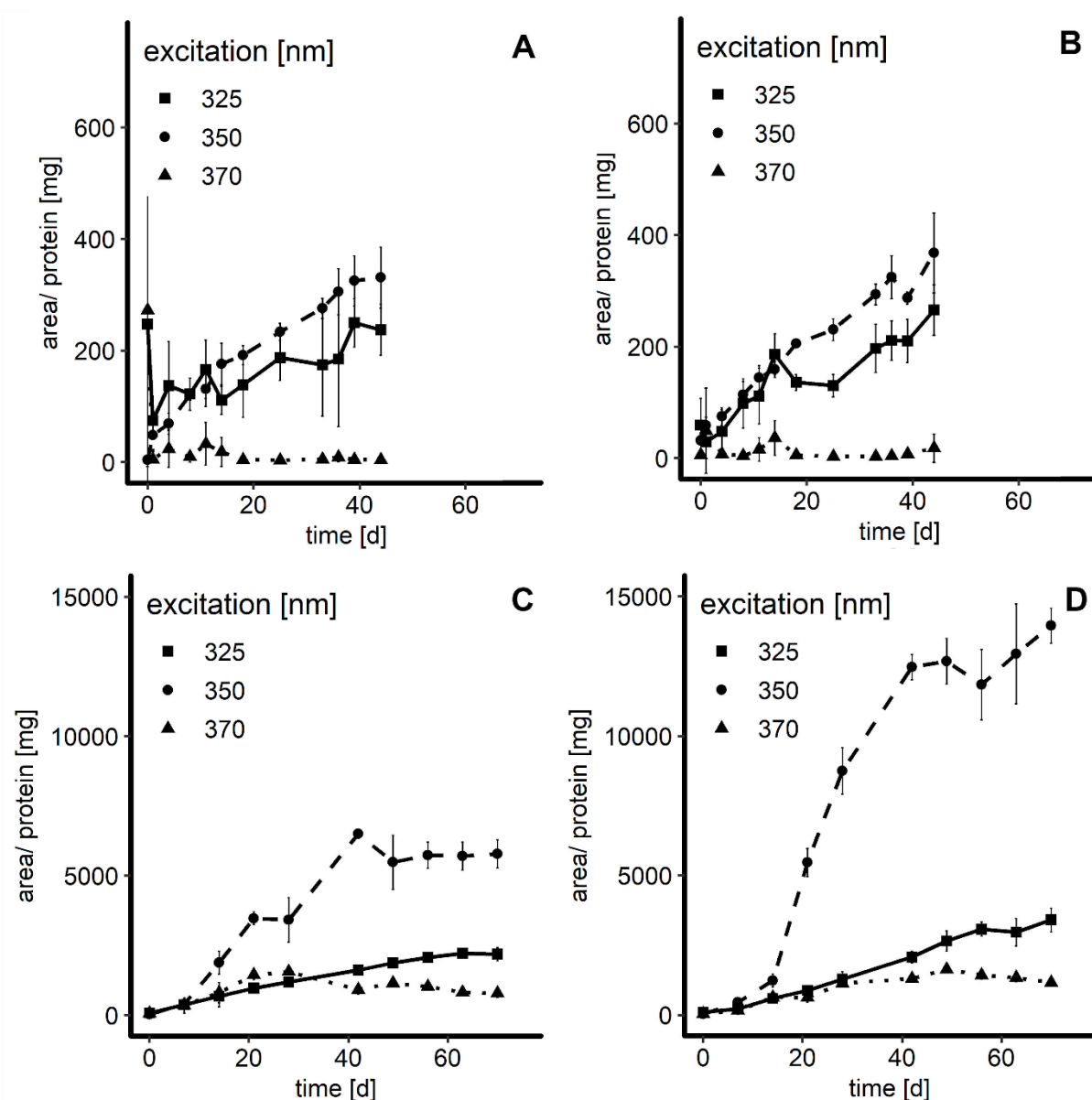


Figure 5.5: Formation of 3 fluorophores, by λ_{EX} at 325, 350, and 370 nm (solid, dashed, and dotted lines, respectively) and emission of 420 nm in oleogel samples with 0%, 0.23% (A and B), 2.8% and 8.4% added water (C and D). Each signal was achieved by deconvolution of the related excitation spectra, at 420 nm emission.

Therefore, the region characteristic for Schiff base fluorophores in these systems contribute more to fluorescence quantum yield than the region characteristic for radical-derived protein modification products. However, because high-oxidation in oleogel systems is provoked by high water contents, acid-base catalyzed reactions become more prominent, which may alter Schiff base fluorophores or simply favor their formation. In addition, water could be an effective barrier against the lipid radicals in the oil phase, inhibiting radical attacks on the protein and thus the formation of the apparent compound at 325 nm excitation. However, an increased Schiff base formation agrees with the lysine residue modifications indicated by SEC results.

In conclusion, intrinsic Trp fluorescence is red-shifted, due to unfolding and denaturing processes that affect the protein and protein aggregates, which also decreases Trp presence over time, in correlation with time and protein modifications, as indicated by the SEC results for tryptic peptides. These effects were also detected in the PLS regression of EEM data. Furthermore, three apparent compounds in the present oleogel protein-lipid co-oxidation system were derived from the PLS regression as latent variables (λ_{EX} 325, 350, and 370 nm), which correlated with lipid oxidation. The first apparent compound (λ_{EX} : 325 nm) is among others characteristic for *N*-formylkynurenine, a product of tryptophan oxidation, which correlates to Trp depletion and the formation of lipid oxidation products. However, it cannot be unequivocally distinguished from dityrosine fluorescence. These three apparent compounds can be also related to different oxidation mechanisms and protein modifications. These mechanisms presumably represent radical mediated modifications of proteins (λ_{EX} : 325 nm) and protein modifications by hexanal, acetaldehyde, or linoleic acid hydroperoxide fragmentation products (λ_{EX} : 350 nm) or malondialdehyde-associated Schiff bases (λ_{EX} : 370 nm). Finally, the deconvolution of the apparent compounds showed that modifications of alkanols and products derived from linoleic acid hydroperoxides may represent the dominant formation mechanisms for fluorescent compounds in oleogel protein-lipid co-oxidation systems, by increasing the water contents and, thus, the oxidation rate. However, in systems with low water contents and, thus, low oxidation rates, radical mediated modifications of proteins expressed by the apparent compound at 325 nm excitation and Trp decomposition may be comparable to aldehyde addition. In combination with the SEC findings, these results suggest that the maldigestibility of proteins is primarily caused by modifications by linoleic acid hydroperoxide fragmentation products, rather than radical mediated protein modifications, in this oleogel-like system.

Abbreviations Used

EEM	excitation-emission matrix
λ_{EM}	emission wavelength
λ_{EX}	excitation wavelength
SEC	size exclusion chromatography
Trp	Tryptophan
Tyr	Tyrosine
PLS	partial least squares

Acknowledgment

The authors thank Eilina Jalas for skillful support and related discussions.

Conflict of interests

The authors declare no competing financial interest.

References

- (1) Patel, A. R.; Dewettinck, K. Edible oil structuring. An overview and recent updates, *Food & Function*. **2016**, *7*, pp. 20–29.
- (2) Vries, A. de; Wesseling, A.; van der Linden, E.; Scholten, E. Protein oleogels from heat-set whey protein aggregates, *Journal of Colloid and Interface Science*. **2017**, *486*, pp. 75–83.
- (3) Hambraeus, L. Importance of milk proteins in human nutrition. Physiological aspects, *Milk proteins*. **1985**, *84*, pp. 63–79.
- (4) Schaich, K. M. Co-oxidation of proteins by oxidizing lipids. In *Lipid oxidation pathways*; Kamal-Eldin, A.; Min, D. B., Eds.; AOCS Press: Urbana, Ill., 2008.
- (5) Belitz, H. D.; Grosch, W.; Schieberle, P. *Lehrbuch der Lebensmittelchemie*; Springer: Garching, 2007.
- (6) Beltrán, J. L.; Ferrer, R.; Guiteras, J. Multivariate calibration of polycyclic aromatic hydrocarbon mixtures from excitation–emission fluorescence spectra, *Analytica Chimica Acta*. **1998**, *373*, pp. 311–319.
- (7) Díez, R.; Sarabia, L.; Ortiz, M. C. Rapid determination of sulfonamides in milk samples using fluorescence spectroscopy and class modeling with n-way partial least squares, *Analytica Chimica Acta*. **2007**, *585*, pp. 350–360.
- (8) Vries, A. de; Jansen, D.; van der Linden, E.; Scholten, E. Tuning the rheological properties of protein-based oleogels by water addition and heat treatment, *Food Hydrocolloids*. **2018**, *79*, pp. 100–109.
- (9) Meissner, P. M.; Keppler, J. K.; Stöckmann, H.; Schrader, K.; Schwarz, K. Influence of Water Addition on Lipid Oxidation in Protein Oleogels, *Eur. J. Lipid Sci. Technol.* **2019**, *121*, p. 1800479.
- (10) Wilde, S. C.; Keppler, J. K.; Palani, K.; Schwarz, K. β -Lactoglobulin as nanotransporter for allicin. Sensory properties and applicability in food, *Food Chem.* **2016**, *199*, pp. 667–674.
- (11) Lampi, A.-M.; Kamal-Eldin, A. Effect of α - and γ -tocopherols on thermal polymerization of purified high-oleic sunflower triacylglycerols, *J Amer Oil Chem Soc.* **1998**, *75*, pp. 1699–1703.

- (12) Yalcin, S.; Schreiner, M. Stabilities of tocopherols and phenolic compounds in virgin olive oil during thermal oxidation, *Journal of Food Science and Technology*. **2018**, *55*, pp. 244–251.
- (13) Vries, A. de; Lopez Gomez, Y.; Jansen, B.; van der Linden, E.; Scholten, E. Controlling Agglomeration of Protein Aggregates for Structure Formation in Liquid Oil. A Sticky Business, *ACS Applied Materials & Interfaces*. **2017**, *9*, pp. 10136–10147.
- (14) Stöckmann, H.; Schwarz, K.; Huynh-Ba, T. The influence of various emulsifiers on the partitioning and antioxidant activity of hydroxybenzoic acids and their derivatives in oil-in-water emulsions, *J Amer Oil Chem Soc*. **2000**, *77*, pp. 535–542.
- (15) Thiyam, U.; Stöckmann, H.; Schwarz, K. Antioxidant activity of rapeseed phenolics and their interactions with tocopherols during lipid oxidation, *J Amer Oil Chem Soc*. **2006**, *83*, pp. 523–528.
- (16) Keppler, J. K.; Koudelka, T.; Palani, K.; Stuhldreier, M. C.; Temps, F.; Tholey, A.; Schwarz, K. Characterization of the covalent binding of allyl isothiocyanate to β -lactoglobulin by fluorescence quenching, equilibrium measurement, and mass spectrometry, *Journal of biomolecular structure & dynamics*. **2014**, *32*, pp. 1103–1117.
- (17) Keppler, J. K.; Heyn, T. R.; Meissner, P. M.; Schrader, K.; Schwarz, K. Protein oxidation during temperature-induced amyloid aggregation of beta-lactoglobulin, *Food Chem*. **2019**, *289*, pp. 223–231.
- (18) R Core Team (2015) R. A Language and Environment for Statistical Computing: Vienna, Austria.
- (19) Wickham, H. *ggplot2. Elegant Graphics for Data Analysis*; Springer-Verlag New York, 2009.
- (20) Mevik, B.-H.; Wehrens, R. The pls Package. Principal Component and Partial Least Squares Regression in R, *Journal of Statistical Software; Vol 1, Issue 2 (2007)*. **2007**.
- (21) Mevik, B.-H.; Wehrens, R.; Liland, K. H. (2018) pls. Partial Least Squares and Principal Component Regression.
- (22) Elzhov, T. V.; Mullen, K. M.; Spiess, A.-N.; Bolker, B. minpack.lm. R Interface to the Levenberg-Marquardt Nonlinear Least-Squares Algorithm Found in MINPACK, Plus Support for Bounds. **2015**.
- (23) Lloyd, J. B. F.; Evett, I. W. Prediction of peak wavelengths and intensities in synchronously excited fluorescence emission spectra, *Analytical Chemistry*. **1977**, *49*, pp. 1710–1715.
- (24) Simat, T. J.; Steinhart, H. Oxidation of Free Tryptophan and Tryptophan Residues in Peptides and Proteins, *Journal of Agricultural and Food Chemistry*. **1998**, *46*, pp. 490–498.
- (25) Albani, J. R.; Vogelaer, J.; Bretesche, L.; Kmiecik, D. Tryptophan 19 residue is the origin of bovine β -lactoglobulin fluorescence, *Journal of Pharmaceutical and Biomedical Analysis*. **2014**, *91*, pp. 144–150.

- (26) Calhoun, D. B.; Vanderkooi, J. M.; Holtom, G. R.; Englander, S. W. Protein fluorescence quenching by small molecules. Protein penetration versus solvent exposure, *Proteins*. **1986**, *1*, pp. 109–115.
- (27) Meissner, P. M.; Keppler, J. K.; Stöckmann, H.; Schwarz, K. Cooxidation of proteins and lipids in whey protein oleogels with different water amounts, *Food Chemistry*. **2020**, *328*, p. 127123.
- (28) Eftink, M. R. *Fluorescence Techniques for Studying Protein Structure*, 1991.
- (29) Estévez, M.; Kylli, P.; Puolanne, E.; Kivikari, R.; Heinonen, M. Fluorescence spectroscopy as a novel approach for the assessment of myofibrillar protein oxidation in oil-in-water emulsions, *Meat Science*. **2008**, *80*, pp. 1290–1296.
- (30) Chen, Y.; Barkley, M. D. Toward understanding tryptophan fluorescence in proteins, *Biochemistry*. **1998**, *37*, pp. 9976–9982.
- (31) Rawlings, N. D.; Barrett, A. J.; Thomas, P. D.; Huang, X.; Bateman, A.; Finn, R. D. The MEROPS database of proteolytic enzymes, their substrates and inhibitors in 2017 and a comparison with peptidases in the PANTHER database, *Nucleic Acids Research*. **2017**, *46*, D624-D632.
- (32) The UniProt consortium UniProt. A worldwide hub of protein knowledge, *Nucleic Acids Research*. **2018**, *47*, D506-D515.
- (33) Jost, R.; Monti, J. C. Partial Enzymatic Hydrolysis of Whey Protein by Trypsin, *Journal of Dairy Science*. **1977**, *60*, pp. 1387–1393.
- (34) Adjonu, R.; Doran, G.; Torley, P.; Agboola, S. Screening of whey protein isolate hydrolysates for their dual functionality. Influence of heat pre-treatment and enzyme specificity, *Food Chem*. **2013**, *136*, pp. 1435–1443.
- (35) Chatterjee, A.; Kanawjia, S. K.; Khetra, Y.; Saini, P. Discordance between in silico & in vitro analyses of ACE inhibitory & antioxidative peptides from mixed milk tryptic whey protein hydrolysate, *Journal of Food Science and Technology*. **2015**, *52*, pp. 5621–5630.
- (36) Majhi, P. R.; Ganta, R. R.; Vanam, R. P.; Seyrek, E.; Giger, K.; Dubin, P. L. Electrostatically Driven Protein Aggregation. B-Lactoglobulin at Low Ionic Strength, *Langmuir*. **2006**, *22*, pp. 9150–9159.
- (37) Kikugawa, K.; TAKAYANAGI, K.; WATANABE, S. Polylysines modified with malonaldehyde, hydroperoxylinoleic acid and monofunctional aldehydes, *Chem. Pharm. Bull*. **1985**, *33*, pp. 5437–5444.
- (38) Fenaille, F.; Tabet, J.-C.; Guy, P. A. Study of peptides containing modified lysine residues by tandem mass spectrometry. Precursor ion scanning of hexanal-modified peptides, *Rapid Commun. Mass Spectrom*. **2004**, *18*, pp. 67–76.

- (39) Wolff, S. P.; Dean, R. T. Fragmentation of proteins by free radicals and its effect on their susceptibility to enzymic hydrolysis, *The Biochemical journal*. **1986**, *234*, pp. 399–403.
- (40) Davies, K. J.; Lin, S. W.; Pacifici, R. E. Protein damage and degradation by oxygen radicals. IV. Degradation of denatured protein, *The Journal of biological chemistry*. **1987**, *262*, pp. 9914–9920.
- (41) Morzel, M.; Gatellier, P.; Sayd, T.; Renerre, M.; Laville, E. Chemical oxidation decreases proteolytic susceptibility of skeletal muscle myofibrillar proteins, *Meat Science*. **2006**, *73*, pp. 536–543.
- (42) Fletcher, B. L.; Tappel, A. L. Fluorescent modification of serum albumin by lipid peroxidation, *Lipids*. **1971**, *6*, pp. 172–175.
- (43) Shimasaki, H.; Ueta, N.; Privett, O. S. Covalent binding of peroxidized linoleic acid to protein and amino acids as models for lipofuscin formation, *Lipids*. **1982**, *17*, pp. 878–883.
- (44) Chio, K.; Tappel, A. L. Synthesis and characterization of the fluorescent products derived from malonaldehyde and amino acids, *Biochemistry*. **1969**, *8*, pp. 2821–2827.
- (45) Bidlack, W. R.; Tappel, A. L. Fluorescent products of phospholipids during lipid peroxidation, *Lipids*. **1973**, *8*, pp. 203–207.
- (46) Liu, Z.; Sayre, L. M. Model Studies on the Modification of Proteins by Lipoxidation-Derived 2-Hydroxyaldehydes, *Chemical Research in Toxicology*. **2003**, *16*, pp. 232–241.
- (47) Scheidegger, D.; Pecora, R. P.; Radici, P. M.; Kivatinitz, S. C. Protein oxidative changes in whole and skim milk after ultraviolet or fluorescent light exposure, *Journal of Dairy Science*. **2010**, *93*, pp. 5101–5109.
- (48) Frankel, E. N. *Lipid oxidation*; Elsevier, 2014.

Chapter 6

Lipid oxidation induced Protein Scission measured by high resolution mass spectrometry and evaluated by partial least squares regression

Abstract

Lipid oxidation induced protein scission was investigated using beta-lactoglobulin rich whey protein oleogels. Extracted cleaved peptides were measured using high resolution mass spectrometry (FT-ICR-MS), which was provided by an automatically generated annotation list approach to identify relevant masses and sum formula using the isotopic pattern. The identified oxidized peptides were then further evaluated using partial least squares regression to relevant lipid hydroperoxide formation data, which provide the significance and importance of the peptides toward lipid induced scission. Thereby, the most important peptides are located on the surface of the protein in random coil segments and especially on the ends of the protein sequence. The most important amino acids were cysteine and aliphatic amino acids, which undergo scission mostly by the α amidation pathway. These findings in the modification of amino acids by oxidizing lipids were finally compared to the oxidation by lipid hydroperoxides, secondary oxidation products, Fenton systems and γ radiation.

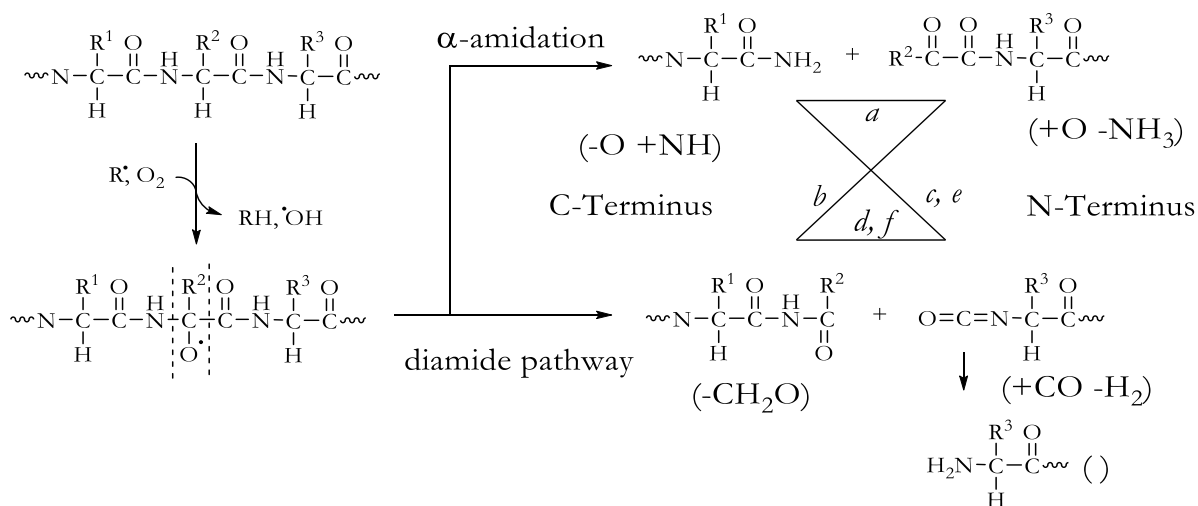
keywords: protein oxidation, lipid oxidation, scission, α -amidation, diamide pathway

Highlights:

- Lipid induced scission peptides are located on the surface of the protein in random coil segments
- Scission is especially present at the N- and C-terminus of beta lactoglobulin
- Cysteine and aliphatic amino acids were most important cleavage sites
- The α -amidation pathway was the predominant mechanism in this study
- The comparison of various oxidants of proteins are compared to their ability of protein scission and modification

6.1 Introduction

Lipid oxidation is known to be one of the most likely reasons for the deterioration of foods and cosmetics, but the scission of proteins by lipid oxidation radicals is less investigated. They are amino acid specific (proline [1], asparagine and glutamine [2]) and unspecific cleavage of proteins, which both contribute to the formation of to the common protein carbonyls measured by standard assays. By the unspecific scission, which is the dominant process, proteins are initially radicalized on the α -C atom of amino acids, which leads to the formation of protein hydroperoxides, which in turn break to protein alkoxyl radicals and following either the α -amidation (AA) or the diamide (DA) pathway [2, 3] (see Scheme 6.1). Thereby new N- and C-termini are introduced with the modifications of the underlying regular oligopeptides. As the decomposition of the protein hydroperoxides leads to hydroxyl radicals, we hypothesize that this would lead to a second scission in the near environmental protein sequence in proteins, by which small peptide fragments are formed. These oxidized peptides will minimally have two amino acids (AAc) or 3-4 in case of alpha helices, which have about 3.6 AAc in a turn [4]. In contrast, this value might be greater in beta-sheets. However, when a protein is cleaved at two sides four combinations of AA and DA are possible, which may be *a* AA, AA, *b* AA, DA, *c* DA, AA and *d* DA, DA. As the DA leads to water instable isocyanates, which react further to new N-termini, *e* and *f* were introduced as modification of the C-terminus by AA and DA.



Scheme 6.1: Scission of the protein chain following either the α -amidation or diamide pathway according to [2, 3] with the change of the sum formula in comparison to a hydrolyzed amid bond in brackets. The modifications *a-f* were indicated using the relation matrix with the new C- and N-terminus.

We recently established a protein lipid cooxidation system using oleogels [5, 6]. In these systems proteins are denatured and aggregated [7]. This design will be well suited for the investigation of

oxidized peptides, as they could be easily extracted as the protein aggregates are centrifugable and less soluble. We therefore hypothesize, further to their limited size caused by local radical mechanism, that such oxidized peptides will be formed by the lipid radicals, too. Thus, mostly hydrophobic amino acids on the protein lipid interface get oxidized. The objective of this study is therefore to characterize peptides from oxidative protein scission by using a list of all possible peptide candidates of a protein with know sequence, from which peptides are identified using high resolution mass spectrometry and the chemometric approach partial least squares regression to evaluate their relation to lipid oxidation this system.

6.2 Materials & Methods

6.2.1 Materials

Oleic acid rich safflower oil was purchased from a local supermarket (C16:0= 4.65 ± 0.02 %, C18:0= 2.38 ± 0.02 %, C18:1= 76.7 ± 0.2 %, 18:2= 14.7 ± 0.03 %, 18:3= 0.14 ± 0.01 % [5]). Whey protein isolate (BiPro) was obtained from Agropur Inc.(Appleton, USA) with 97.7% protein dry matter according to [8]. Al_2O_3 , BaCl_2 , FeSO_4 and hydrochloric acid were from Carl Roth (Karlsruhe, Germany). Phosphatidylcholines (PC 5:0, 11:0 and 19:0; 1,2-divaleryl-sn-glycero-3-phosphocholine, 1,2-diundecanoyls-sn-glycero-3-phosphocholine, 1,2-dinonadecanoyl-sn-glycero-3-phosphocholine) in chloroform were purchased from Avanti (Alabaster, USA). All solvents were from VWR (Fontenay-sous-Bois, France). All chemicals were used as received without further purification unless indicated otherwise. Water (>18.2 M Ω) was purified by an Elga Veolia system (Celle, Germany) and was used unless otherwise noted.

6.2.2 Purification of Safflower Oil

The purification of safflower oil from natural antioxidants and trace metals was based on the method described by Lampi & Kamal-Eldin [9] with slight modifications [5]. The oil was tested of residual tocopherols (HPLC, < 0.5 ppm, method DGF F-II 4a).

6.2.3 Sample Preparation

Whey protein aggregates were produced by the method described by de Vries *et al*, by lyophilizing frozen protein aggregates, which were dropped into liquid nitrogen beforehand [10]. Dry whey protein aggregates (6.8%) were then mixed with stripped oil and stirred for 10 min. In the water containing model, the water (0.23%) was added slowly after 5 min [6]. After centrifugation for 20 min by 4000g (Allegra X-30R, Beckmann Coulter, Krefeld, Germany), superfluous oil was removed by decanting the gel for 10 min and the received gel was reweighted.

200 mg gel samples were then stored at 40 °C and extracted for measurements as described before. In brief, the lipid phase was extracted 3 times with 3 mL cyclohexane and centrifugation at 4000g for 5 min each time. Combined extracts were used for measuring lipid hydroperoxides. The defatted protein was then washed 2 times with 5 mL isopropanol and finally extracted 2 times with 5 mL MS-grade water by decanting after centrifugation. All water extracts were stored at -80 °C until further analysis.

6.2.4 Measurement of Protein Conformation with Fourier Transformation Attenuated Total Reflection Infrared Spectroscopy

The protein conformation was investigated by FT-ATR-FTIR measurements using a Confocheck™ Bruker Tensor 2 System (Bruker Optik GmbH, Ettlingen, Germany) optimized for protein analysis in liquids with a thermally controlled BioATR II unit (25 °C). The spectra were acquired against MS-grade water as background and averaged over 120 scans at a resolution of 0.7 cm⁻¹. The spectra (1600–1700 cm⁻¹) were then normalized. The second derivative was then calculated as calculation of the slope from point to point twice (Excel, Microsoft). Protein samples or freeze dried protein aggregates were suspended in MS-grade water (10 mg/mL), stirred for 2 h at moderate speed (300 rpm), and hydrated overnight at 4 °C. Result of protein aggregates were given as mean from 3 individual batches by measurement in two concentrations (3.3 mg/mL, 10 mg/L). For comparison, 2 oleogels with adding 2.8 % and 5.6 % water (no oxidation [5]) were also measured directly against safflower oil twice, which result was then averaged.

6.2.5 Determination of Lipid Hydroperoxides

The lipid phase of the extraction with cyclohexane was flushed with nitrogen to dryness. Then, the reweighted extracted fat was dissolved in 5 mL isopropyl alcohol and diluted if necessary. Lipid hydroperoxides were determined by ferric thiocyanate method as described by Stöckmann *et al.*, Thiyam *et al.* and as reported before [11, 12].

6.2.6 Measurement of Peptides with Fourier Transformation Ion Cyclotron Resonance Mass Spectroscopy

840 µL of the combined water extract was added to 140 µL isopropanol containing phosphatidylcholines (PC 5:0, 11:0 and 19:0 each 50 mg/L) as internal mass standard. Compounds were measured using a 7 Tesla FT-ICR-MS (SolariXR, Bruker, Bremen, Germany) in the flow-injection mode. Thereby, an liquid chromatography system (1260 Infinity from Agilent, Waldbronn, Germany) was used as autosampler with water/methanol (50/50, v/v) with 0.1% acetic acid as eluent in a random order. For ionization, positive electrospray was conducted

(65 - 950 Da, average resolution at 400 m/z 600,000). The main instrument parameters were dry gas temperature (nitrogen) of 200 °C at 4 L/min; nebulizer 1 bar, a quadrupole mass 150 m/z with an RF frequency 2 MHz and detector sweep excitation power of 18%. The average resolution at 400 m/z was 600,000. Data evaluation was conducted with MetaboScape 4.0 from Bruker (Bremen, Germany).

6.2.7 Preparation of the Annotation List

The annotation list was prepared using the free statistical software R (version 3.4.2) [13]. Therefore the protein sequence from bovine beta-lactoglobulin (amino acid 17-178), the most abundant protein from whey protein isolate (~75% beta-lactoglobulin in dry matter [8]), was loaded from the UniProt protein database (entry P02754) [14]. As radical attacks lead to scission of the amide bond, all possible oligopeptides ranged from 2 to 10 amino acids (AAc) were created as a list in R. This range was chosen, because the initial alkoxy radical originate in the decomposition of a hydroperoxide radical, whereby the highly reactive formed hydroxyl radical should harm AAc in the near environment.

For all oligopeptides and oxidized peptides the sum formula was given, whereby for the oxidized peptides the sum formula was adjusted according to their modification *a-f* (*a*: -H₂, *b*: -CNH₅, *c*: +CN -H, *d*: -H₄, *e*: +NH -O, *f*: -COH₂, see scheme 1). As *c* and *d* decomposed in water, an annotation list was created using all unique sum formulas for the oligopeptides and their modifications *a*, *b*, *e*, and *f* (5739 entries).

6.2.8 Data Evaluation

Annotation was done using the peptide list, which was implemented in MetaboScape (Bruker, Germany), whereby Na and K adducts are allowed besides H adducts and the exact masses of the peaks were recalibrated using a list of ubiquitous polyethylenglycol (PEG), the PC, amino acids and beta-lactoglobulin. Sum formulas were checked based on the mass error (below 2 ppm) and based on the isotopic pattern and fine structure (mSigma < 50), which is an additional identification information to the mass. This was done to reduce false-positive results according to the 7 golden rules of Kind and Fiehn [15]. To further reduce false-positive results, partial least squares regression was conducted with the annotated peptides to lipid hydroperoxide data [6] using MetaboScape (Bruker, Germany). Thereby, Pareto scaling or level scaling as normalization was conducted to ensure a comparability of all peptides measured with varying abundancies and reducing asymmetric variable distribution [16].

6.2.9 Statistical Analysis

From the partial least squares statistics, the importance of each peptide for the model was extracted as final value, which was further statistically analyzed and summed up for the amino acids by R [13]. Thereby, from repeating peptides (compounds, which were not seen as the same compound between samples by Metaboscape) only the one with the highest importance were considered and the importance was either given to the first and the last amino acid in the oligopeptide, or, for in sequence assignable oligopeptides, to the relevant mechanism amino acid R^2 (see Scheme 6.1). Based on these factors the relevant mechanism and the target amino acid were determined. This means that in case *a* this importance was given to the first amino acid in the peptide and the following, by *b* to the first and last amino acid, by *c* and *e* to the amino acid before and after, by *d* and *f* to the amino acid before and the last amino acid of the peptide. In case of regular peptides, start and end amino acid were taken. If the peptide was on the start or end of the sequence no importance was added to the sum statistics. In the mechanistic case and in the only first/last AAC model, the value of each amino acid was adjusted to the theoretical value, which is given for the annotation list, where all peptides have an importance of 1. If the peptide was found repeatedly, only the one with the highest importance was considered. For a further look on the attributes of the measured oxidized peptides, the underlying oligo peptides were characterized using the R package ‘peptides’ [17], which includes the instability index [18], the hydrophobicity [19], and the theoretical position in the protein [20, 21].

6.3 Results & Discussion

6.3.1 Identification of oxidized peptides

According to the oxidized peptide list, 37 peptides were identified, which are in the 2 ppm mass accuracy. From these 37 peptides 12 had a mSigma value below 50 and 9 were unique (See table 6.1). From the peptides, which were not unique, doublets occur. These doublets belong to the same compound, but were wrongly ordered not to the same bucket of one compound in the statistical model of MetaboScape (compounds, which were not seen as the same compound between samples). To overcome this, only the one with the highest relevance in term of partial least squares importance were further used (see below). mSigma values are between 0 and 1000 and indicate the correctness of the isotopic pattern of isotopes (M+1, M +2, M+3 peaks according to the probability of the combination of isotopes like D, ^{13}C , ^{15}N , ^{18}O and $^{34}, ^{35}\text{S}$). Thereby an error of 5% reflects the 50 mSigma mark [22]. For a mSigma value below 50 and a Δmass of 5 ppm 6 sum formulas can be addressed [22]. However, these calculations include the possibility of phosphorous compounds, which are not present in the lipid protein mixtures. In

addition, a certain C/H/N/O ratio can be assumed as the compounds have to be of protein nature, as lipophilic compounds, like lipid oxidation products are extracted before and lactose adducts in the protein may occur in a low concentration. To further check the identified oxidized peptides for authenticity their instability index was calculated. Thereby the peptides are checked for the occurrence of certain dipeptides, which are significantly prevalent in unstable proteins. In this study, a protein was regarded to be unstable *in vivo* when it had an instability index above 40, but there was an exception of a stable protein over 40. All peptides, except AQSAP, comply with this condition. Therefore, only AQSAP is a questionable sum compound, which had in addition a relatively high mSigma value of 47.6 in comparison to the other peptides (<30 mSigma).

Table 6.1: Identified oxidized peptides of the FT-ICR-MS measurement with mSigma (mSigma) <50 and $\Delta m < 2$ ppm. The relevant AAc R², which is the initial radical site, was highlighted. In case of regular peptide first and last AAc were taken for statistics and from repeating peptides only the one with the highest importance were considered. Importance for PLS models are given for Pareto and level scaling. For comparisons the instability index and charge was added.

AAc before	Peptide	AAc after	Formula	mSigma	Importance Pareto scaling	Importance Level scaling	Instability index [18]
-	e_LI	V	C ₁₂ H ₂₅ N ₃ O ₂	4.6	1.90	1.79	0
-	(e_LI)	V	C ₁₂ H ₂₅ N ₃ O ₂	3.8	1.86	1.70	-
A	CQCL	V	C ₁₇ H ₃₁ N ₅ O ₆ S ₂	24.2	1.53	0.84	18
A	(CQCL)	V	C ₁₇ H ₃₁ N ₅ O ₆ S ₂	25.4	0.89	0.34	-
V	LDT	D	C ₁₄ H ₂₅ N ₃ O ₇	32.5	0.77	0.48	-43
-	e_LIV	T	C ₁₇ H ₃₄ N ₄ O ₃	10.3	0.69	1.15	-22
-	e_LIVT	Q	C ₂₁ H ₄₁ N ₅ O ₅	27.5	0.55	1.31	-35
D	AQSAP	L	C ₁₉ H ₃₂ N ₆ O ₈	47.6	0.48	0.78	134
W	a_ENGE	C	C ₁₆ H ₂₃ N ₅ O ₁₀	17.1	0.29	0.48	-49
-	(e_LIV)	T	C ₁₇ H ₃₄ N ₄ O ₃	15.1	0.29	0.73	-
K	f_PTPEG	D	C ₂₀ H ₃₁ N ₅ O ₈	23.4	0.15	0.58	43
W	(a_ENGE)	C	C ₁₆ H ₂₃ N ₅ O ₁₀	20.8	0.13	0.27	-

Besides AQSAP, CQCL is questionable, too, as two cysteine residues are present in this peptide, which were expected to bond in disulfide bridges. However, as the mSigma value is low, it can be concluded that the sum formula is correct. Therefore, the presence of two S indicates also two cysteines as methionine is rare in beta-lactoglobulin and can be excluded by their mass difference. Thus, the two cysteines may form an intramolecular disulfide bridge, which prevents the compound from adding to other cysteines on the protein. The free S-bridged CQCL may then be reduced in the environment. In addition, the radical cleavage at the sulfuric AAc may be different, resulting in a cleavage of the disulfide bridges. Free regular peptides in whey protein isolate based oleogels may also form from proteases initially present in whey protein, but this possibility seems to be unlikely as the protein was denaturated to aggregates and separated from

smaller proteins like free proteases and free peptides by centrifugation washing steps. Therefore, the proteases present in protein aggregates have to be inactivated as they are bound and immobilized.

However, there was also a noticeable group of ϵ peptides (LI, LIV, LIVT) with a similar AAc sequence. This sequence is at the beginning of the sequence of beta-lactoglobulin (LIVTQTMK ...) [14] and therefore the frequency of these peptides can be explained by the fact that for their occurrence only one radical attack is needed with following AA. In addition, this sequence end of the denatured protein may be rather on the outside of the protein and therefore more prone to oxidation. However, it has to be also seen as another modification as ϵ , because the amino N-terminus does not undergo oxidization.

6.3.2 Correlation of peptides with lipid oxidation

It was hypothesized, that the oxidized peptides are derived from the initial attack of lipid radicals, which are formed from lipid hydroperoxides on the lipid protein interface. Therefore, those AAc on the surface of the protein will be more prone to the radical attack and become oxidized more often, which ideally results in an increased correlating concentration of peptides ending or starting with a specific AAc. To compare lipid oxidation with oxidized peptides, lipid hydroperoxide data was therefore correlated to the oxidized peptide data using partial least squares regression (PLS). Thereby, the identified peptides correlate well with lipid oxidation hydroperoxide data using the Pareto or level scaling (goodness of prediction $Q^2 = 0.81/0.81$ using 6 or 9 principal components) and the relation of each peptide to lipid hydroperoxides can be read in the relevance for the model. This relevance of each compound can be first seen in the loading weights of each compound in the principal components of the PLS model. To generate a single weight value of each compound, the idea is to sum up the weights of each compound in each principal component weighted by their sum of squares in component [23] (the more the less). This weighted value is called variable importance in the projection (VIP) and will be for the sake of convenience further called importance of the compound. Interestingly, the LIVT sequence peptides are ranked highly either in the Pareto and level scaled models. This further indicates a high relevance of the protein scission at the N-terminus of beta-lactoglobulin in the oleogels protein lipid cooxidation systems. Thereby ϵ LI is well correlated to time (0% water $R^2 = 0.993$, 0.23% water $R^2 = 0.98$) and slightly less to lipid hydroperoxides ($R^2 = 0.96 / 0.93$) (see Figure 6.1). However, ϵ LI is first present after 4 days of incubation at 40 °C, which may be explained by the initial diffusion time of lipid hydroperoxides to the protein lipid interface. Furthermore, above 15 mmol/ kg oil lipid hydroperoxides the intensity of ϵ LI is decreased. This

in turn may indicate a saturation point of e LI on the interface, which will be further influenced by competing secondary lipid oxidation products.

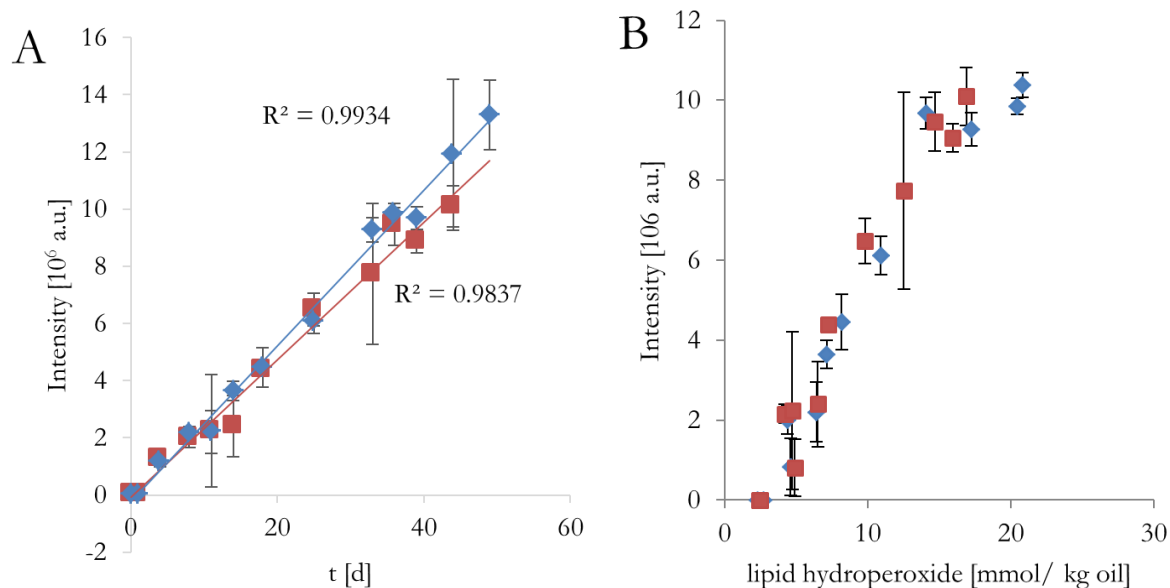


Figure 6.1: Measured Intensity e LI versus time (A) and versus lipid hydroperoxides (B), red squares: no water addition, blue diamond: 0.23% water addition.

The hydrophobicity of a peptide can be estimated by taking a hydrophobicity index of each single AAc residue in consideration [19]. For this purpose, it can be further estimated that the oxidized peptides are very similar to their regular analogues. Thereby, the PLS importance correlates well for Pareto and level scaled models to the calculated hydrophobicity index (see Figure 6.2). This indicates that hydrophobic AAc are more present at the protein lipid interface due to hydrophobic forces, where radicals are formed from lipid hydroperoxides. However, this in turn also requires that the specific AAc are on the surface of the protein. Despite proteins are denatured to aggregates, it is likely that the proteins partly renature during incubation, whereby former secondary structures can even be rebuilt. To investigate the protein conformation in the oleogels, ATR-IR spectra of the amid I band (see Figure 6.2 C, F) have been recorded. In the second derivative of the spectra characteristic secondary protein structures can be seen as negative peaks [24]. In the spectra the aggregation is visible as decrease of intramolecular β -sheets (1632 cm^{-1}) and increase of intramolecular β -sheets (1617 cm^{-1} , 1622 cm^{-1}) and random coils (1640 cm^{-1}). However, intramolecular β -sheets (1632 cm^{-1}) dominates over α -helices (1663 cm^{-1}), and turns (1679 cm^{-1} and in part 1691 cm^{-1}) in protein aggregates, β -lactoglobulin and whey protein isolate. In addition, no change is observed α -helices (1663 cm^{-1}), thus it can be concluded that prepared whey protein aggregates have a similar secondary structure in comparison with the native protein. The spectra of oleogels is less detailed, but α -helices (1666 cm^{-1}) and intramolecular β -sheets (1630 cm^{-1}) are detected, despite slightly shifted and of lower signal

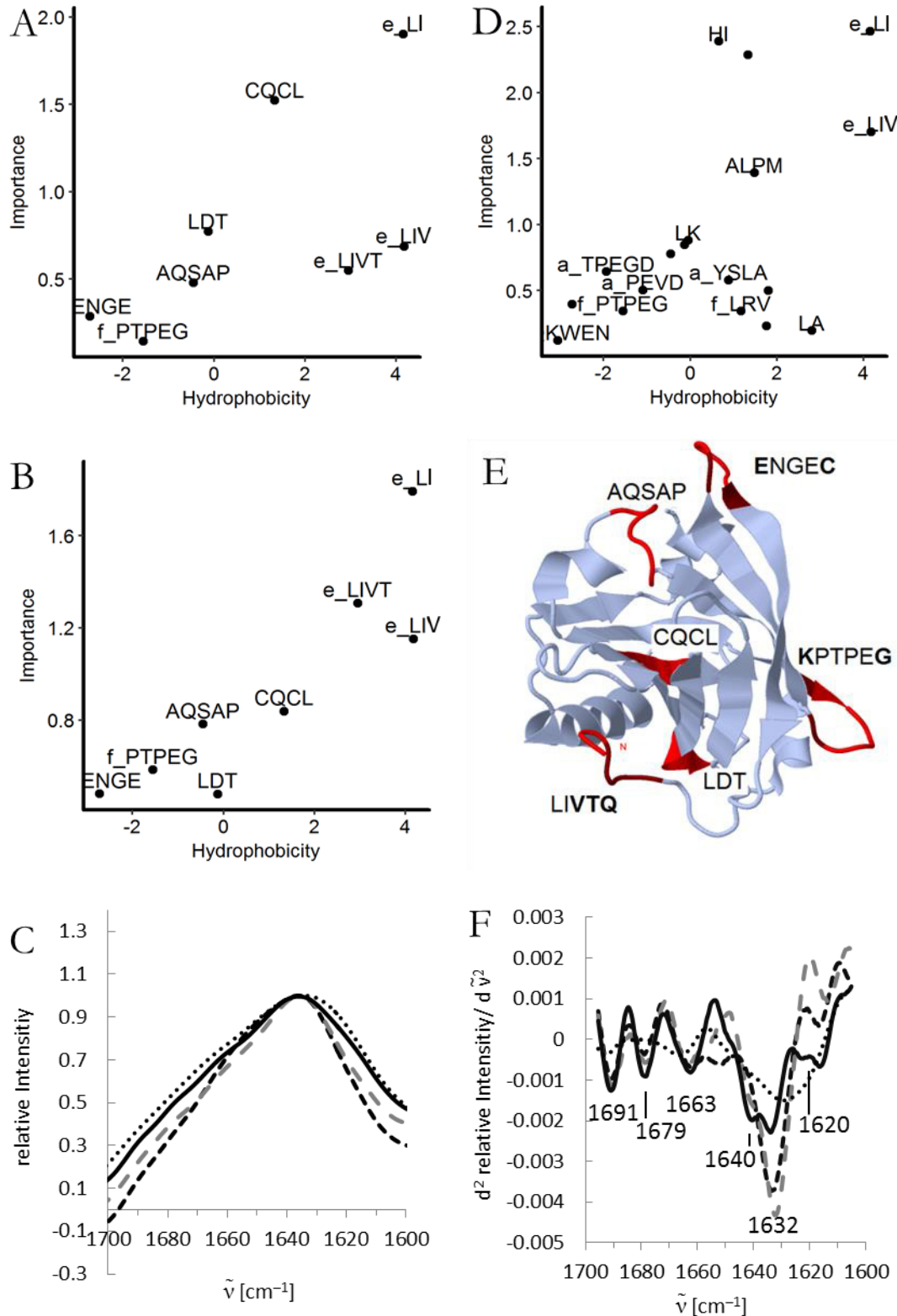


Figure 6.2: PLS importance of oxidized peptides versus their calculated hydrophobicity neglecting modifications using Pareto scaling (A), level scaling (B) or Pareto scaling of all peptides ($\Delta m < 2$ ppm, (D), with labeling of some) and (E) the position of the parent peptides (red) in unliganded native beta-lactoglobulin (drawn with JSmol Jena3D) [25], where the radical receiving AAc R² are highlighted in dark red. FT-ATR-IR spectra of the protein amid I band (C) and second derivative (F) of whey protein isolate (black dashed), beta lactoglobulin (grey dashed), whey protein protein aggregates in water (black line) and whey protein protein aggregates in oil (black dotted)

intensity. This may be due the changed background of liquid oil, which may be overlay in parts the spectra of the protein structure. However, the secondary structure-similar aggregates have been used for oleogel preparation, that in turn it can concluded that native beta-lactoglobulin can be an estimate for such a protein aggregates in oleogels. In the colored model structure of beta-lactoglobulin (see Figure 6.2 E) it can be seen, that the parent chain parts of the oxidized peptides are mostly on the surface on the protein and in random coil structure, which in turn remain random coil after denaturation and renaturation and therefore be present at surfaces. In addition, Cys121 in CQCL is known to be exposed to the surface by heat exposure [26]. As water soluble proteins mostly display hydrophilic AAC on the surface, it can be concluded that these regions have an amphiphilic character. This attribute is also highly characteristic for protein sequences of surface proteins, which are located between the hydrophilic cell interior and the lipophilic cell membrane [20, 21]. As structure data of these proteins is often lacking due problems in preparation, theoretical calculations have been proposed, which are based on the repetition of hydrophilic and hydrophobic AAC in amphiphilic α -helices [20, 21]. Even though these calculations are based are based on “windows” of 11 AAC, it is remarkable that either in level scaled PLS systems predicted surface peptides are significantly more important than the predicted globular peptides (student t test, $p = 0.02$, Pareto scaling $p = 0.23$). However, embedding these oxidized peptides, whose position is clear, in larger snippets of the sequence lead to the prediction of globular sequences, which can be expected since beta-lactoglobulin is a globular protein. Interestingly, hydrophobicity and surface correlation can also be seen in oxidized peptides, which have a mSigma value above 50 or no mSigma value as the isotopic pattern could not be determined (see Figure 6.2 C). Most of the additional peptides are associated to the position or directly beside of the ones with a clear mSigma value (e.g. for *e* LIVT: *f* VVT, for AQSAP: *f* LRV, for *a* ENGE: *a* QKWENG and for *f* PTPEG: *a* TPEGD). Therefore many oxidized peptides with higher or no mSigma value may too low concentrated, which leads to lacking of isotopic patterns for the calculation of mSigma value. However, as they show good correlations in PLS, they may can be accepted.

Apart from the relation of peptides being on the surface, it was shown that generated radicals migrate from anywhere along the protein backbone to glycine residues in radiation experiments [27]. This was explained by hyperconjugation of the π -orbitals of planar peptid groups and the α -C atoms. When the configuration of AAC is orthogonal in case of glycine, the migration stops. In the latter this was taken as explanation for all aliphatic AAC [28]. However, as the identified oxidized peptides mostly belong to random coil regions, it can be assumed that this planar migration stops at these sites, as the configuration gets more orthogonal.

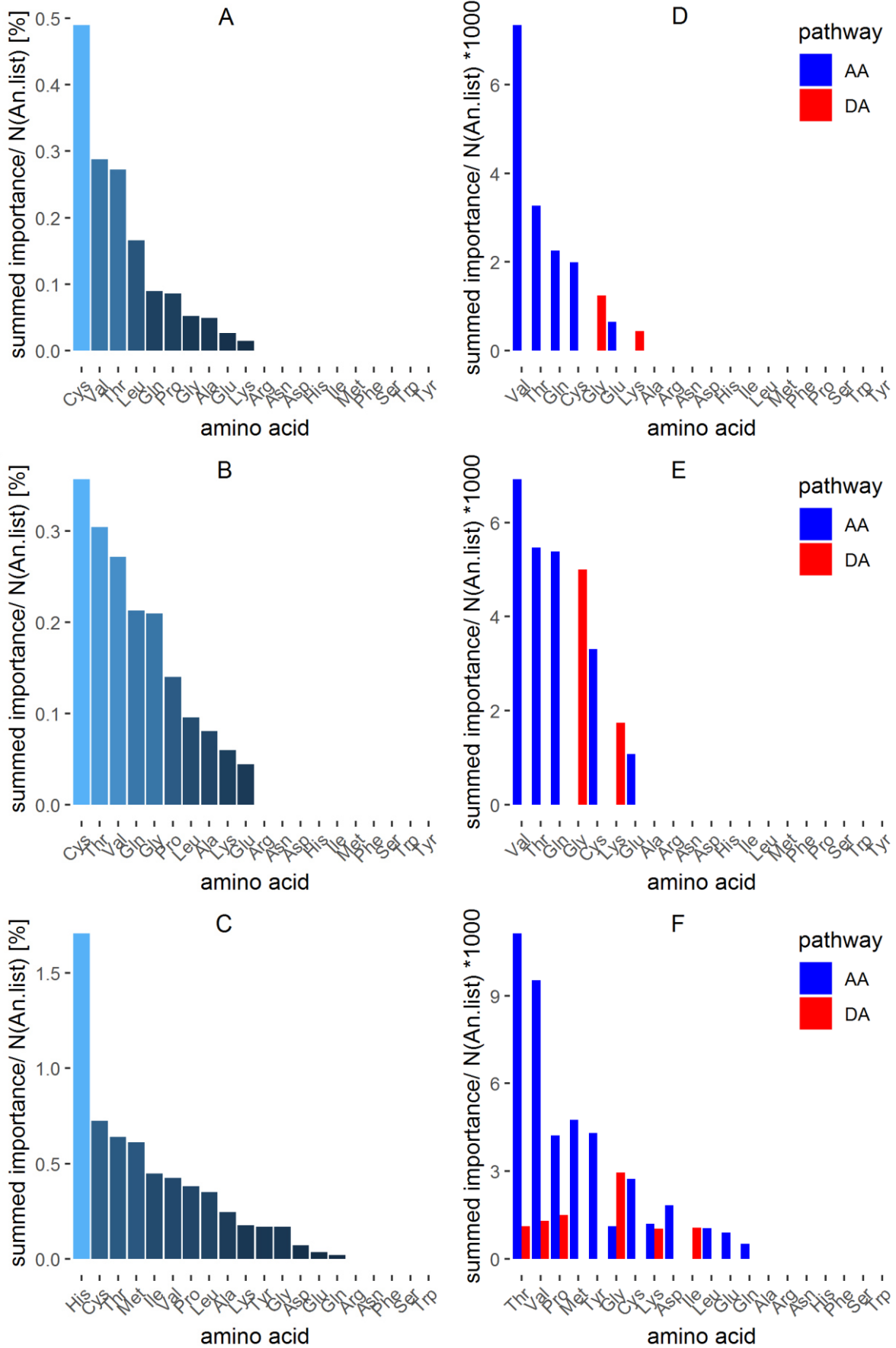


Figure 6.3: To the occurrence relative PLS importance of individual AA and the statistical pathways involved (regular peptides excluded) for Pareto scaling (A, D), level scaling (B, E) and Pareto scaling of all peptides ($\Delta m < 2$ ppm, C, F).

6.3.3 Amino Acid Scission Sites

If one connects the importance of the oxidized peptides with their relevant oxidation AAc (R^2) relative to their occurrence in beta-lactoglobulin (in the annotation list, see Figure 6.3), the important cleavage sites in this study can be compared to other studies where depletion of AAc is measured after treatment with various oxidants. It can be seen that beside glycine the aliphatic AAc threonine, valine, proline, leucine and alanine are important cleavage sites in this study, too. This can be attributed to radical migration, too, which is also present in other protein oxidation studies including those of treatment with lipid oxidation products (see Table 6.2). The highest difference to these studies may be the lower depletion of lysine, methionine, tryptophan and tyrosine. Lysine has the free ϵ -amino group, which is prone to modifications by secondary lipid oxidation products like aldehydes by aldol and Michael reaction pathways [28]. In these model systems a decrease of lipid aldehydes and amino groups was measured before [6] and amino group modification was detected by fluorescence spectroscopy (see chapter 5). Therefore, it can be concluded that these oxidized peptides may not have been detected as lysine adducts are fairly variable and were not included in the annotation list, which is based on the backbone scission theory. This is also true for tryptophan and tyrosine, which form the fluorescent compounds *N*-formylkynurenine and dityrosine through radical attack [29–31] and methionine, which is oxidized to methionine sulfone, sulfoxide or methional [32, 33]. From the regular AAc found cysteine has achieved the highest importance in all mSigma filtered models, which is in accordance with the high depletion of cysteine residues in proteins treated with oxidizing lipids [34]. Electron paramagnetic resonance (EPR) experiments indicate that oxidizing methyl linoleate primarily induce carbon-centered radicals, but sulfur centered radicals are especially relevant in cysteine containing proteins [35]. However, other radical sites from high importance may not be detectable by EPR, as radicals have to be long living. An explanation for the affinity of cysteines is that the thiol groups complex Fe(III) ions, which are generated by lipid hydroperoxides with Fe(II) ions in Fenton reactions. These complexes undergo an intramolecular electron shift from sulfur to iron, which leads to a thiyl radical [36, 37], which may also be able to abstract the hydrogen atom from the neighboring AAc α -C atom. This complexation model suites well to CQCL, which even contains two cysteine residues. However, histidine is the most important AAc in the mSigma unfiltered data, which is in accordance to all other studies, where histidine has a decent relevance. However, this importance is from the regular peptide HI, which has two positions in beta-lactoglobulin. The most likely position will be at the end of the sequence of beta-lactoglobulin (...QCHI), which has a similar pattern to CQCL and also contains a cysteine. Therefore, HI may also be seen as *f* modification, where the radical attack is at cysteine.

Lipid oxidation induced Protein Scission

Table 6.2: Importance of each amino acid divided by their occurrence in the annotation list in the partial least squares regression models with correlation of lipid hydroperoxide data to oxidized peptide data which is generated via scission in comparison to studies of amino acid loss or electron paramagnetic resonance signal gain (G value) of various proteins after treatment with various oxidants (oxidizing lipids: linoleic acid (LA) as dominating oxidation fatty acid in safflower oil, ethyl arachidonate [34], hydroxyl radical generating [38], LAHPO: LA hydroperoxide, SPLA:

oxidant	oxidizing lipids										Y- radiation		mLA		
Ref	this study (1, 2, 3)			[34]	Cu/H2O2 [38]		Fe/H2O2 [39]		SPLA	LAHPO	SP	LAHPO	SP	[41]	[42]
AAC	BLG par. [Imp.]	BLG level [Imp.]	BLG par. All [Imp]	BSA [%]	Y- Globulin [%]	Collagen [%]	Collagen [%]	Lysozyme [%]	Lysozyme [%]	RNase [%]	RNase [%]	Trypsin [%]	Trypsin [%]	amino acid [G value]	Gelatin [%]
Cys	0.49	0.36	0.73	64.00	32.80	-	-	0.00	-	40.00	s	s	0.00	50.00	0.00
Val	0.29	0.27	0.43	47.70	21.00	-	-	6.00	17.00	0.00	0.00	0.00	12.00	12.00	6.64
Thr	0.27	0.30	0.64	46.20	14.80	-	-	5.00	9.00	s	0.00	14.00	17.00	0.43	8.07
Leu	0.17	0.10	0.35	34.40	22.20	-	-	0.00	5.00	22.00	12.00	0.00	s	0.41	11.34
Gln	0.09	0.21	0.02	-	-	-	-	-	-	-	-	-	-	-	-
Pro	0.09	0.14	0.38	s	16.00	25.60	7.50	-	0.00	s	0.00	0.00	s	0.67	22.31
Gly	0.05	0.21	0.17	82.50	21.20	-	-	0.00	0.00	s	0.00	s	16.00	0.28	6.60
Ala	0.05	0.08	0.24	50.00	18.80	-	-	0.00	0.00	0.00	0.00	0.00	0.00	0.53	-3.52
Glu	0.03	0.04	0.04	41.00	24.10	-17.90	5.70	4.00	17.00	10.00	0.00	0.00	14.00	0.53	-4.48
Lys	0.01	0.06	0.18	40.80	58.80	53.7	38.80	17.00	73.00	51.00	50.00	0.00	s	0.34	25.18
Arg	-	-	-	11.50	26.50	20.70	18.00	9.00	14.00	s	s	0.00	0.00	0.79	13.88
Asn	-	-	-	-	-	-	-	-	-	-	-	-	-	-	-
Asp	-	-	0.07	39.80	11.30	-57.00	6.90	0.00	0.00	0.00	0.00	0.00	0.00	0.15	-16.67
His	-	-	1.71	54.10	51.80	67.7	32.30	42.00	67.00	54.00	49.00	12.00	42.00	0.03	31.43
Ile	-	-	0.45	42.80	20.00	-	-	0.00	8.00	s	17.00	0.00	s	-	16.96
Met	-	-	0.61	47.50	38.30	50.80	38.10	14.00	84.00	99.00	80.00	83.00	89.00	0.03	38.81
Phe	-	-	-	44.10	32.00	53.30	18.60	0.00	6.00	0.00	0.00	s	19.00	0.48	23.28
Ser	-	-	-	43.20	24.40	-	-	0.00	4.00	0.00	0.00	0.00	0.00	0.26	7.90
Trp	-	-	-	-	-	-	-	56.00	95.00	-	-	-	-	0.22	-
Tyr	-	-	0.17	45.20	50.70	100.00	100.00	0.00	19.00	62.00	17.00	0.00	20.00	0.21	28.57

secondary lipid oxidation products (SIP) of LA) and γ -radiation; s: slight loss.

6.3.4 Radical Scission Pathways

For the comparison of AAc scission sites it was assumed that AAc depletion correlates with AAc site scission. However, this study reveals some information of the involved pathways, too. As shown in Figure 6.3 D-F, the α -amidation (AA) pathway is the most common pathway in peptide formation. This may be explained by the kinetic nature of the reaction, as the AA pathway can even start by the abstraction of a hydroperoxyl radical from the protein peroxy radical and the DA pathway is dependent on oxygen and a former isomerization of the following peptide bond [28]. In addition, the alkoxy radical may abstract a hydrogen atom off from the amino acid residue. This leads to an alcohol, which is a good leaving group. Thus, rearrangement of the amino group with the alcohol leads to the formation of water and an imine, which in turn is hydrolyzed to the end products of the AA pathway. As thereby the AAc residue of the N-terminus is modified, the predicted AA N-terminus modification cannot be detected, which is supported by the lower importance for *a* oxidized peptides and the absence of *b* oxidized peptides. Furthermore, this residue enabled hydrogen transfer is supported by the fact that the primarily aliphatic valine is most important for AA, while glycine shows only the DA pathway. This hydrogen abstraction is not possible in glycine due to the lacking residue and in valine the abstraction of the hydrogen atom forms a hyperconjugation stabilized C radical. However, in mSigma filtered models, the most AA pathway relevant AAc gain their importance by the amide C-terminus. This amide C-terminus can also be formed by the alkaline hydrolysis of diamide (RCONHCOR, 1 M NaOH or 15 min), though these conditions were not met in the conducted experiment [43]. In addition, it is also possible that the identified regular peptides belong at least from the N-terminus to the DA pathway due to the hydrolysis of the isocyanate to a regular peptide amino group. A hydrolysis conversion of the amides can lead further to the carboxyl C-terminus. However, iron hydroperoxide complex catalyzed hydrolysis of the peptide bond is also known [44].

6.3.5 Comparison of oxidants

For the classification of calculated importance of AAc in this study, the studies referred in Table 6.26.2 of oxidants were used to calculate a principal component analysis (PCA) with normalized data (sum of AAc loss or importance was adjusted to 1), where missing values in one study are replaced by the mean of the others (see Figure 6.4). After calculation, the points of this study (1-3) were projected using the loadings. Thereby the first three principal components declare 55 %, 17 % and 14 % of variance in the model (in sum 86 %). In general, in the PCA plots a separation to about 3 directions is visible. These directions include linoleic acid hydroperoxides (principal component 1 and 3), Fenton oxidation systems and γ -radiation (γ -radiation) (principal

component 2). This can be explained by slight differences of the oxidants. All oxidants have in common that they form hydroxyl radicals, but the formation is more slowly in case of the decomposition of lipid hydroperoxides. In addition, this decomposition leads to the formation of lipid alkoxyl radicals, which are another kind of oxidant. Other oxidants are also present in the other directions. In gamma radiation free electrons e_{aq}^- , hydrogen radicals H^* , superoxide radicals O_2^- and hydrogen peroxide (radical) are present [2], whereas in Fenton systems only the latter three are present and additionally the metal ions, which can facilitate electron shifts and redox reactions like the decomposition of protein hydro peroxides. These different side oxidants may lead to a different modification pattern in proteins. Oxidizing lipids, including this study and secondary lipid oxidation products of linoleic acid (SPLA) are in the center of these directions. This may rely on the elongated incubation time of these oxidants, which in turn lead to the formation of a lot of the named oxidants due to decomposition of lipid and protein hydroperoxides. The loadings of the AAc reveal that there are mainly two groups of AAc. The largest group contains mainly aliphatic groups pointing towards oxidizing lipids and γ -radiation, which indicates that lipid induced scission and depletion of AAc by these oxidants is unspecific as the radical interaction with γ -radiation with these AAc is unspecific [28]. In contrast, lysine, histidine, tryptophan, tyrosine (outside of scope) and cysteine point towards Fenton systems. These amino acids contain either sulfur residues, nitrogen atoms in long residues or electron π -configuration systems, which provide lone electron pairs and therefore the possibility to complex metals used in Fenton systems. The high affinity of sulfur towards iron has already been mentioned above. As these complexes form localized hydroxyl radicals, AAc modification is localized, too, which makes in turn Fenton system oxidation more specific than lipid induced modifications. By using metal chelating enzyme receptors or site specific agents, this attribute is even used as artificial protease as catalytic drug [45]. However, in the third component the nitrogen AAc lysine, tryptophan and histidine are orthogonal and therefore not relevant for Fenton systems. Instead, they are in correlation with SPLA, which can be explained by the modification of the amino groups by secondary lipid oxidation carbonyls by Schiff base formation and Micheal reaction adducts [6, 28].

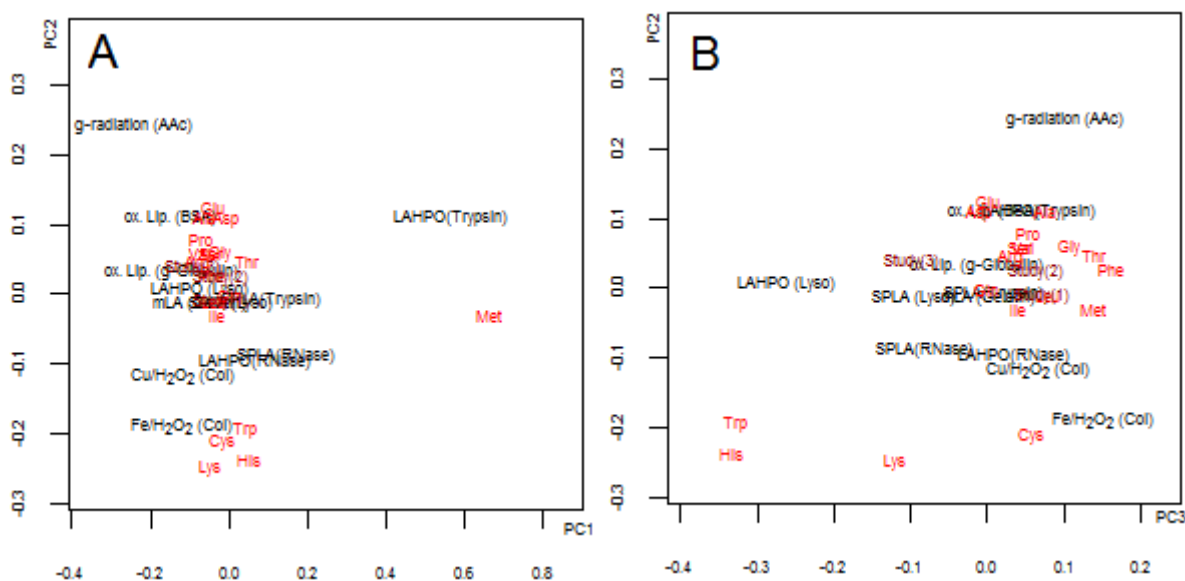


Figure 6.4: principal component analysis of oxidants (black) in table 6.3 with the principal components (PC) plotted against each other, NA values were replaced with the mean after the sum of values of each experimental data was set to 1 for a better comparison, data of this study was projected (dark red) using the loadings of AAc (red), A: PC1 vs PC2, B: PC3 vs PC2.

6.4 Conclusion

Peptides have been found using a full list of possible peptides, which can be products by scission from the protein sequence. Thereby, lipid oxidation mediated protein backbone scission is located on the surface of proteins, which was supported by a high correlation of cysteine and lipophilic AAc to scission on the surface of beta-lactoglobulin. These AAc should interact with the lipophilic oil phase and there was evidence, that these AAc were located in amphiphilic sequences. In addition, the scission was located especially at random coil sequences in beta-lactoglobulin, which was explained by stopping radical migration in secondary structure turns. This is also an explanation for the correlation of scission with proline residues in bovine serum albumin [3, 46], which is located especially in β -turns [4]. However, N- (LIVT) and C-termini (HI) are notably highly abundant cleavage sites, as only one radical attack is needed for cleavage. In this study the radical cleavage mechanisms rely mostly on the α -amidation pathway, but the diamide pathway may be underestimated. Further investigation of other proteins and the inclusion of AAc specific cleavage sites will be necessary for a wider understanding of lipid induced scission. General lipid induced protein scission may better be declared by γ -radiation experiments than by Fenton oxidation systems as metal complexation alters the oxidation pattern. But to conclude, secondary lipid oxidation products alter the pattern of protein modifications and therefore lipid protein cooxidation models will be necessary to fully understand the alteration of proteins in oxidizing food and cosmetic matrices.

Abbreviations Used

Acknowledgment

The authors thank Dr. Tobias Demetrowitsch and Julia Jensen-Kroll for their helpful advices in mass spectrometry and related discussions.

Supporting Information description

Figure captions

Figure 6.1: Measured Intensity e_LI versus time (A) and versus lipid hydroperoxides (B), red squares: no water addition, blue diamond: 0.23% water addition.....156

Figure 6.2: PLS importance of oxidized peptides versus their calculated hydrophobicity neglecting modifications using Pareto scaling (A), level scaling (B) or Pareto scaling of all peptides ($\Delta m < 2$ ppm, (D), with labeling of some) and (E) the position of the parent peptides (red) in unliganded native beta-lactoglobulin (drawn with JSmol Jena3D) [25], where the radical receiving AAc R² are highlighted in dark red. FT-ATR-IR spectra of the protein amid I band (C) and second derivate (F) of whey protein isolate (black dashed), beta lactoglobulin (grey dashed), whey protein protein aggregates in water (black line) and whey protein protein aggregates in oil (black dotted).....157

Figure 6.3: To the occurrence relative PLS importance of individual AAc and the statistical pathways involved (regular peptides excluded) for Pareto scaling (A, D), level scaling (B, E) and Pareto scaling of all peptides ($\Delta m < 2$ ppm, C, F).....159

Figure 6.4: principal component analysis of oxidants (black) in table 6.3 with the principal components (PC) plotted against each other, NA values were replaced with the mean after the sum of values of each experimental data was set to 1 for a better comparison, data of this study was projected (dark red) using the loadings of AAc (red), A: PC1 vs PC2, B: PC3 vs PC2.164

Tables

Table 6.1: Identified oxidized peptides of the FT-ICR-MS measurement with mSigma (mSigma) <50 and $\Delta m < 2$ ppm. The relevant AAc R^2 , which is the initial radical site, was highlighted. In case of regular peptide first and last AAc were taken for statistics and from repeating peptides only the one with the highest importance were considered. Importance for PLS models are given for Pareto and level scaling. For comparisons the instability index and charge was added.154

Table 6.2: Importance of each amino acid divided by their occurrence in the annotation list in the partial least squares regression models with correlation of lipid hydroperoxide data to oxidized peptide data which is generated via scission in comparison to studies of amino acid loss or electron paramagnetic resonance signal gain (G value) of various proteins after treatment with various oxidants (oxidizing lipids: linoleic acid (LA) as dominating oxidation fatty acid in safflower oil, ethyl arachidonate [34], hydroxyl radical generating [38], LAHPO: LA hydroperoxide, SPLA: secondary lipid oxidation products (SP) of LA) and γ -radiation; s: slight loss.161

Conflict of interests

The authors declare no conflicts of interests.

6.5 References

- [1] Kato, Y., Uchida, K., Kawakishi, S., Oxidative fragmentation of collagen and prolyl peptide by Cu(II)/H₂O₂. Conversion of proline residue to 2-pyrrolidone. *Journal of Biological Chemistry* 1992, 267, 23646–23651.
- [2] Garrison, W. M., Reaction mechanisms in the radiolysis of peptides, polypeptides, and proteins. *Chemical Reviews* 1987, 87, 381–398.
- [3] Berlett, B. S., Stadtman, E. R., Protein Oxidation in Aging, Disease, and Oxidative Stress. *Journal of Biological Chemistry* 1997, 272, 20313–20316.
- [4] Berg, J. M., Tymoczko, J. L., Stryer, L., *Biochemistry, Fifth Edition*, W.H. Freeman 2002.

- [5] Meissner, P. M., Keppler, J. K., Stöckmann, H., Schrader, K., Schwarz, K., Influence of Water Addition on Lipid Oxidation in Protein Oleogels. *Eur. J. Lipid Sci. Technol.* 2019, 0, 1800479.
- [6] Meissner, P. M., Keppler, J. K., Stöckmann, H., Schwarz, K., Oxidation of Proteins in Whey Protein Oleogels with different water amounts 2019.
- [7] Vries, A. de, Wesseling, A., van der Linden, E., Scholten, E., Protein oleogels from heat-set whey protein aggregates. *Journal of Colloid and Interface Science* 2017, 486, 75–83.
- [8] Wilde, S. C., Keppler, J. K., Palani, K., Schwarz, K., β -Lactoglobulin as nanotransporter for allicin: Sensory properties and applicability in food. *Food Chem.* 2016, 199, 667–674.
- [9] Lampi, A.-M., Kamal-Eldin, A., Effect of α - and γ -tocopherols on thermal polymerization of purified high-oleic sunflower triacylglycerols. *J. Amer. Oil Chem. Soc.* 1998, 75, 1699–1703.
- [10] Vries, A. de, Lopez Gomez, Y., Jansen, B., van der Linden, E., Scholten, E., Controlling Agglomeration of Protein Aggregates for Structure Formation in Liquid Oil: A Sticky Business. *ACS Appl. Mater. Interfaces* 2017, 9, 10136–10147.
- [11] Thiyam, U., Stöckmann, H., Schwarz, K., Antioxidant activity of rapeseed phenolics and their interactions with tocopherols during lipid oxidation. *J. Amer. Oil Chem. Soc.* 2006, 83, 523–528.
- [12] Stöckmann, H., Schwarz, K., Huynh-Ba, T., The influence of various emulsifiers on the partitioning and antioxidant activity of hydroxybenzoic acids and their derivatives in oil-in-water emulsions. *J. Amer. Oil Chem. Soc.* 2000, 77, 535–542.
- [13] Team, R. C., R: A Language and Environment for Statistical Computing 2015, Vienna, Austria, <https://www.R-project.org/>.
- [14] Consortium, T. U., UniProt: A worldwide hub of protein knowledge. *nar* 2018, 47, D506–D515.
- [15] Kind, T., Fiehn, O., Seven Golden Rules for heuristic filtering of molecular formulas obtained by accurate mass spectrometry. *BMC Bioinformatics* 2007, 8, 105.
- [16] Eriksson, L., Antti, H., Gottfries, J., Holmes, E., Johansson, E., Lindgren, F., Long, I., Lundstedt, T., Trygg, J., Wold, S., Using chemometrics for navigating in the large data sets of genomics, proteomics, and metabonomics (gpm). *Analytical and Bioanalytical Chemistry* 2004, 380, 419–429.

- [17] Osorio, D., Rondon-Villarreal, P., Torres, R., Peptides: A Package for Data Mining of Antimicrobial Peptides. *The R Journal* 2015, 7, 4–14.
- [18] Guruprasad, K., Reddy, B.V.B., Pandit, M. W., Correlation between stability of a protein and its dipeptide composition: A novel approach for predicting in vivo stability of a protein from its primary sequence. *peds* 1990, 4, 155–161.
- [19] Kyte, J., Doolittle, R. F., A simple method for displaying the hydropathic character of a protein. *Journal of Molecular Biology* 1982, 157, 105–132.
- [20] Eisenberg, D., Weiss, R. M., Terwilliger, T. C., The helical hydrophobic moment: A measure of the amphiphilicity of a helix. *Nature* 1982, 299, 371.
- [21] Eisenberg, D., Three-dimensional structure of membrane and surface proteins. *Annual review of biochemistry* 1984, 53, 595–623.
- [22] Kind, T., Fiehn, O., Metabolomic database annotations via query of elemental compositions: Mass accuracy is insufficient even at less than 1 ppm. *BMC Bioinformatics* 2006, 7, 234.
- [23] Wold, S., Sjöström, M., Eriksson, L., *Partial Least Squares Projections to Latent Structures (PLS) in Chemistry* 1998.
- [24] Shivu, B., Seshadri, S., Li, J., Oberg, K. A., Uversky, V. N., Fink, A. L., Distinct β -Sheet Structure in Protein Aggregates Determined by ATR–FTIR Spectroscopy. *Biochemistry* 2013, 52, 5176–5183.
- [25] Loch, J., Polit, A., Górecki, A., Bonarek, P., Kurpiewska, K., Dziedzicka-Wasylewska, M., Lewiński, K., Two modes of fatty acid binding to bovine β -lactoglobulin--crystallographic and spectroscopic studies. *Journal of molecular recognition : JMR* 2011, 24, 341–349.
- [26] Surroca, Y., Haverkamp, J., Heck, A.J.R., Towards the understanding of molecular mechanisms in the early stages of heat-induced aggregation of β -lactoglobulin AB. *Journal of Chromatography A* 2002, 970, 275–285.
- [27] Patten, F., Gordy, W., TEMPERATURE EFFECTS ON FREE RADICAL FORMATION AND ELECTRON MIGRATION IN IRRADIATED PROTEINS. *Proc Natl Acad Sci U S A* 1960, 46, 1137–1144.
- [28] Schaich, K. M., in: Kamal-Eldin, A., Min, D. B. (Eds.), *Lipid oxidation pathways*, AOCS Press, Urbana, Ill. 2008.

- [29] Simat, T. J., Steinhart, H., Oxidation of Free Tryptophan and Tryptophan Residues in Peptides and Proteins. *Journal of Agricultural and Food Chemistry* 1998, 46, 490–498.
- [30] Andersen, S. O., Characterization of a new type of cross-linkage in resilin, a rubber-like protein. *Biochimica et Biophysica Acta* 1963, 69, 249–262.
- [31] Andersen, S. O., The cross-links in resilin identified as dityrosine and trityrosine. *Biochimica et biophysica acta (BBA)-general subjects* 1964, 93, 213–215.
- [32] Garner, B., Waldeck, A. R., Witting, P. K., Rye, K.-A., Stocker, R., Oxidation of High Density Lipoproteins. *Journal of Biological Chemistry* 1998, 273, 6088–6095.
- [33] Wainwright, T., McMahon, J. F., McDowell, J., Formation of methional and methanethiol from methionine. *J. Sci. Food Agric.* 1972, 23, 911–914.
- [34] Roubal, W. T., Tappel, A. L., Damage to proteins, enzymes, and amino acids by peroxidizing lipids. *Archives of Biochemistry and Biophysics* 1966, 113, 5–8.
- [35] Schaich, K. M., Karel, M., Free radical reactions of peroxidizing lipids with amino acids and proteins: An ESR study. *Lipids* 1976, 11, 392–400.
- [36] Friedman, M., Chemistry and biochemistry of the sulfhydryl group in amino acids, peptides and proteins 1973.
- [37] Gardner, H. W., Weisleder, D., Kleiman, R., Addition of N-acetylcysteine to linoleic acid hydroperoxide. *Lipids* 1976, 11, 127–134.
- [38] XIONG, Y. L., DECKER, E. A., ALTERATIONS OF MUSCLE PROTEIN FUNCTIONALITY BY OXIDATIVE AND ANTIOXIDATIVE PROCESSES¹. *Journal of Muscle Foods* 1995, 6, 139–160.
- [39] 金沢, 和., 団野, 源., 名武, 昌., LYSOZYME DAMAGE CAUSED BY SECONDARY DEGRADATION PRODUCTS DURING THE AUT-OXIDATION PROCESS OF LINOLEIC ACID. *Journal of Nutritional Science and Vitaminology* 1975, 21, 373–382.
- [40] Gamage, P. T., Matsushita, S., Interactions of the Autoxidized Products of Linoleic Acid with Enzyme Proteins. *Agricultural and Biological Chemistry* 1973, 37, 1–8.
- [41] AMBE, K. S., Tappel, A. L., Oxidative Damage to Amino acids, peptides, and proteins by Radiation. *J. Food Sci.* 1961, 26, 448–451.

- [42] Matoba, T., Kurita, O., Yonezawa, D., Changes in Molecular Size and Chemical Properties of Gelatin Caused by the Reaction with Oxidizing Methyl Linoleate. *Agricultural and Biological Chemistry* 1984, 48, 2633–2638.
- [43] Garrison, W. M., Kland-English, M. J., Sokol, H. A., Jayko, M. E., Radiolytic degradation of the peptide main chain in dilute aqueous solution containing oxygen. *The Journal of physical chemistry* 1970, 74, 4506–4509.
- [44] Rana, T. M., Meares, C. F., Transfer of oxygen from an artificial protease to peptide carbon during proteolysis. *Proceedings of the National Academy of Sciences* 1991, 88, 10578.
- [45] Suh, J., Chei, W. S., Metal complexes as artificial proteases: Toward catalytic drugs. *Current Opinion in Chemical Biology* 2008, 12, 207–213.
- [46] Schuessler, H., Schilling, K., Oxygen Effect in the Radiolysis of Proteins. *International Journal of Radiation Biology and Related Studies in Physics, Chemistry and Medicine* 1984, 45, 267–281.

Chapter 7

General Discussion

7 General Discussion

The main objective was to characterize protein lipid cooxidation because the deterioration of protein rich lipid matrices, where typical lipid oxidation markers are lacking, is of interest. The interaction of the compounds is complex and knowledge about their individual contribution is limited. Therefore, three working hypotheses were investigated:

1. The water content of complex systems (oleogels and suspensions) influences the colloidal and structural properties of the system and thereby the reaction of lipid protein cooxidation.
2. Lipid oxidation derived aldehydes and other oxygen containing products react with proteins and amino acids to aldol-, addition- and other condensation products, which are followed by the formation of protein modifications. This reactivity of lipid oxidation markers causes rather the reduction of lipid oxidation compounds than the inhibition of lipid oxidation.
3. Lipid and protein oxidation are complex processes, which partly gear into each other. These complex processes are rather characterized and classified using non-target analysis and multivariate statistics than by single compound evaluation. Thereby the correlation to known, leading oxidation compounds will reveal unnoticed compounds and hidden aspects of interest.

The oxidation was investigated in low moisture suspensions and in so called oleogels, which can represent low moisture suspensions and can be seen as organogelled emulsions, when water is added. The cooxidation of the lipid and protein phase in oleogels was analyzed and evaluated for the first time in protein-based gels. Thereby, the lipid oxidation markers such as volatiles and lipid hydroperoxides were compared to protein modifications such as carbonyls, free amines and fluorescence formation. Further insights of the protein deterioration were gained by using multivariate statistics and kinetics, which include fluorescence formation and protein backbone scission pattern in oleogels and low moisture suspensions.

7.1 Reaction of Radicals with Proteins

Prior to the formation of secondary lipid oxidation aldehydes (**Hypothesis 2**) primary lipid oxidation compounds are formed [1]. Thereby the formation rate of lipid hydroperoxides is initially monomolecular and then bimolecular in low moisture suspensions except starch-based suspensions and oleogels prepared by solvent-exchange method. The time point of change between the mono- and bimolecular reaction kinetic strongly varies, so the point in CaCl_2 suspension is probably after the first day, in methylcellulose suspensions after 7 days, in solvent exchange manufactured gels ($\sim 0.8\%$ water [2]) after 21 days, **Manuscript I**), and in oleogels from freeze-dried material after >44 days (0% water addition), after 33 days (0.23% water addition, and after 1-7 days ($>2\%$ water addition) (**Paper II, III**). Therefore, this time point can be seen as water dependent. However, this is not favored in theory as a complex of two hydroperoxide molecules in the bimolecular decomposition reaction is stabilized by hydrogen bonds [3, 4]. Water will destabilize this complex by its hydrogen donating ability and will therefore increase the reaction activation energy for this reaction pathway, which was also observed in the decreased bimolecular decomposition constant k_2 of the lipid hydroperoxide in oleogels with 0% , 0.23% , 2.8% , 5.6% , and 8.4% water addition (0.026 ± 0.013 (mmol/kg d) $^{-1}$, 0.020 ± 0.022 (mmol/kg d) $^{-1}$, 0.0029 ± 0.0002 (mmol/kg d) $^{-1}$, 0.0101 ± 0.0006 (mmol/kg d) $^{-1}$, 0.009 ± 0.005 (mmol/kg d) $^{-1}$, see **Figure 3.3, Paper II**). In addition, the absence of the bimolecular oxidation in starch-based suspension cannot be explained.

Water, lipid hydroperoxides, and amphiphilic secondary lipid oxidation products will lead to the formation of additional interphases and therefore for an increased bimolecular reaction as the local concentration of hydroperoxides is increased at the interphases (**Hypothesis 1, Paper II**, see 7.4). Thus, the increase of water in oleogels and the ability of starch to complex lipid fragmentation products [5], lead to a shift of the time point, when critical micelle formation concentration is reached and new interphases are generated.

The reaction of lipid hydroperoxides and alkoxyl radicals with protein may inhibit the typical fragmentation causing aldehydes. Protein modifications by radicals are mostly described for the reaction with hydroxyl radicals which are formed by the decomposition of lipid hydroperoxides. Common products are dityrosine and *N*-formylkynurenine [6, 7], which were measured by fluorescence formation even at the beginning of incubation (**Paper III, Manuscript IV**) or at the initiation of the autocatalyzed bimolecular phase (**Manuscript I**). In the latter, the absence of fluorescence signal can be attributed to a lower sensitivity of the method, as the protein was not digested. However, despite hydroxyl radicals are formed by lipid autoxidation it is not clear

whether radical attacks are based on radicals formed by the decomposition of lipid hydroperoxides or protein hydroperoxides, as proteins are able to undergo a similar peroxidation mechanism like lipids [8, 9]. Therefore, oxidation of lipids and proteins in the models is called cooxidation. Protein fragments formed by known radical scission mechanism build a good partial linear least squared correlation model to lipid hydroperoxides (**Hypothesis 3**). Thereby, radical scission of the protein backbone occurs mainly on the surface of the protein in amphilic random coil regions and therefore at the protein lipid interface (**Manuscript V**), which indicates in sum that involved radicals in protein modifications originate from the decomposition of lipid hydroperoxides. For these findings, the oxidation of the protein may be better described by the term lipid oxidation induced protein modification in the investigated oleogels. This can be explained by the same kinetic mechanism as by lipid hydroperoxides, which is related to colloidal interfaces (**Hypothesis 1, Paper II**, see 7.4) in oleogels as organogelled emulsions. In this process, the formation and decomposition of lipid hydroperoxides is explained by the increased bimolecular autocatalyzation by the local increased concentration on interfaces or nanomicelles [10, 11]. However, protein hydroperoxides will be not able to accumulate as they are not able to migrate due the structured nature of a protein. Thereby, the proposed decomposition complex of two hydroperoxides [3, 4] cannot be formed, which in turn inhibit a bimolecular autocatalyzed decomposition of proteins (**Hypothesis 1**). Therefore, the texture will have influence on the kinetics of lipid hydroperoxides, which will be influenced by water, as water form droplets in the oleogels and alter the lipid interfaces in suspensions.

7.2 Reaction of Secondary Lipid Oxidation Products with Protein

Secondary lipid oxidation products are oxygen radical mediated fragmentation products of lipids and have been measured in low moisture suspension (**Manuscript I**) and oleogels (**Manuscript I, Paper II, III**). Thereby, an increased concentration was detected after a specific time of incubation, whereby the total amount was decreased in comparison with the bulk oil in case of hexanal, propanal, and other volatiles. Hexanal was especially chosen for comparison as it is the most abundant degradation product of linoleic acid [12], which was the most abundant unsaturated fatty acid in the used safflower oil (~15 %). This decreasing was even so intensive that propanal was not detectable the first 14 days in low water oleogels (<0.5 % water addition), where in bulk oil propanal was detectable after 3 days of incubation (**Paper II**). This effect was even stronger in a solvent exchange oleogel where no propanal or hexanal formation was evident in the first 24 days of incubation after the formation of 34 ± 4 mmol O₂/ kg oil lipid hydroperoxides (**Manuscript I**). However, in the latter oleogel samples there was a

contamination of hexanal and single samples were irregularly increased (**Figure 2.14**). The ability of protein to decrease aldehydes was then checked in nonoxidizing MCT-oil oleogels, where ~80% of 0.15 mg hexanal/mg oil (~350 AUC) was decreased during 11 days of incubation (**Hypothesis 2, Paper III**), whereas in bulk oil no depletion was found. However, the complete reaction of aldehydes with the protein in enriched samples can be doubted, as aldehydes are decreased after prolonged incubation also in the bulk oil system and was especially in aldehyde enriched safflower bulk oil samples stronger than in enriched safflower oleogels (not shown), which might be attributed to the decomposition by other reactions (**Hypothesis 3**). These reactions may include the aldol reaction between two aldehyde molecules and may be therefore increased in oxidizing systems. However, this reaction pathway cannot explain a full depletion of all aldehydes like observed as a certain level of reaction partners is needed in this bimolecular reaction.

Like these aldehydes, lipid oxidation fragmentation compounds contain oxygen groups like epoxides that are reactive towards nucleophils like amino groups in proteins. It has long been known, that the rancid flavor is caused by lipid oxidation aldehydes and that these can be depleted by proteins and free amino acids [13] (**Manuscript I, Paper II, III**). However, even when protein modifications products are tasteless and odorless, they can have a toxic potential [14–18] and it can be estimated that these depletion takes place in protein lipid containing systems, too. Water has a strong impact on the lipid aldehydes on decomposition reaction rates with the protein (see next section, **Hypothesis 1, 2**). Like these compounds, other secondary lipid oxidation compounds may be lowered, too. Further decomposition of compounds like carboxylic acids and alcohols may thereby be involved in decomposition reaction of aldehydes and epoxides, or their formation is inhibited as aldehydes and epoxides are precursor compounds of these. However, lipid aldehydes are the most abundant fragmentation products of lipid hydroperoxides [19]. Secondary lipid oxidation product induced protein modifications have been detected using fluorescence spectroscopy (**Manuscript I, Paper III, Manuscript IV**), carbonyl staining with 2,4-dinitrophenylhydrazine (DNPH) (**Manuscript I, Paper III**), by size exclusion chromatography of tryptic digest (**Manuscript IV**), and by the reaction of amino groups with *ortho*-phtalaldehyde (OPA) (**Paper III**). Modifications of cysteine residues could not be investigated as the structured protein is based on disulfide bridges. However, all of these measurements underestimate or give a misleading picture of the real modification of proteins as protein modifications are manifold and cannot be covered by one specific method. There are several protein modifications which are reactive towards DNPH. For example, modifications derived from Micheal additions provide the addition of a carbonyl group to the protein, but these groups can react with further groups of the protein (crosslinks), Schiff base formation of lipid

aldehydes do not maintain the carbonyl group, and cyclization of adducts leads also to the depletion of protein carbonyl groups, which was shown for lysine adducts [20–22]. Further, despite there will be a distinct ratio between fluorescent compounds and nonfluorescent compounds, the nonfluorescent adducts cannot be measured by fluorescence spectroscopy. However, there are some complementary characteristics, for example these compounds formed by cyclization reaction, which depleted the DNPH sensitivity, are often of aromatic nature and therefore fluorescent. In addition, size exclusion chromatography of tryptic digest can detect miscleavages induced from nonfluorescent and noncarbonylic lysine adducts.

Some measurements have to be taken with caution. The measurement of free amines and protein or lipid carbonyls may be the most misleading, as protein backbone scission induce amino group and carbonyl formation [8], whereas the reaction of amino groups with the carbonyls leads to their depletion [9] (**Paper II, III**). So no formation of protein carbonyl could be observed in oleogels with low lipid oxidation (<1 % water, ~20 mmol O₂/kg oil lipid hydroperoxides, **Manuscript I, Paper III**). In addition, the concentration of free amines initially increased in all oleogels, but then decreased or stagnate, which can be attributed to their decomposition reaction with secondary lipid oxidation compounds (**Hypothesis 2, Paper III**). These findings in sum indicate that **hypothesis 2** can be accepted. In addition, as protein amines and lipid, protein carbonyls compete in formation, which is followed by concerted decomposing, the first statement of complexity in **hypothesis 3** cannot be rejected. Further, non-targeted approaches (fluorescence and mass spectrometry) help to get a view of the whole cooxidation process. Thereby, the correlation of fluorescence signals to lipid hydroperoxides highlight fluorescence signals, which are related to radical and additive protein modifications (**Hypothesis 3**). Most of the detected fluorescence and therefore likely most of the protein modifications was related to apparent compounds, which are related to secondary lipid oxidation fragmentation products in high water containing oleogels (**Manuscript IV**).

7.3 Influence of Water on Lipid Protein Cooxidation

The influence of water on lipid protein cooxidation was investigated in two model systems (**Manuscript I, Paper II, III**), which included low moisture suspensions and oleogels. In the first one, changing water amounts are typically attributed to changing water activity as the base materials, which are needed to prepare a solid-fluid suspension, have the ability to absorb and adsorb water molecules in their structure, where in oleogels different amounts of water were added. Thus, the water activity from methylcellulose suspension (0.52–0.77), CaCl₂ suspension

(0.033) (**Manuscript I**) and oleogels (0.52–0.94) vary significantly (**Paper II**). This changed water activity was shown to have a moderate influence on the formation of lipid hydroperoxide fragmentation products (**Manuscript I, Paper II, Hypothesis 1**), where water forms an additional interface to the lipid, which accelerate lipid autoxidation [10, 11] (see next section). In terms of surfaces, a monolayer of water should slightly inhibit oxygen transfer to the lipid. In addition, water also disturbs the hydrogen bond between two lipid hydroperoxides and therefore the bimolecular radical initiation reaction [3, 4]. Contrary, the monomolecular decomposition reaction rate is increased by the mobilization of trace metals, as metals complex lipid hydroperoxides and provide electron transfer reactions. The water activity has a decent influence on the decomposition of amino acids, too. Therefore, the formation of isovaleraldehyde as a decomposition product of leucine was investigated in suspensions with varying water activity (CaCl₂ 0.033, methylcellulose 0.52, and sea sand with an estimated high water activity, **Figure 2.3**, and in early stages of methylcellulose 0.52–0.77, **Figure 2.9** day 14). The concentration of isovaleraldehyde is increased by water availability, which could be explained with the water depended reaction of the amino group of leucine with secondary lipid oxidation products under formation of aldol-, Schiff base and Micheal adduct like intermediates (**Hypothesis 1, 2**). The reactions are known to be water facilitated by acid base catalysis and there are adducts on the amino groups of amino acids that are identified, e.g. adducts on lysine residue like formyl dehydropiperidino lysine, ethylmethylpyridinium lysine or 2-pentyl pyrrol lysine [20–22]. Principal component analysis has been proven to be a useful tool to handle large amounts of data for the identification of underlying latent variables [23, 24]. Thus, the influence of the water activity on the lipid oxidation and decomposition of leucine was further evaluated in a principal component analysis of all lipid oxidation volatiles (**Hypothesis 3**). Thereby, the decomposition product of leucine isovaleraldehyde has a loading vector in the direction of increasing water activity, which means that the decomposition of leucine and the formation of isovaleraldehyde highly correlate with water content of the system (**Hypothesis 1**).

To focus on the protein lipid interface and to investigate a more realistic amino acid composition representing foods, oleogels with different amounts of water were investigated. Water increased the macroscopic gel strength of those gels made with freeze dried protein material up to a saturation level (76 ± 18 kPa, 98 mg/g added water, **Paper II**). This was in accordance with a similar behavior of solvent exchange manufactured whey protein oleogels using refined sunflower oil [2]. This can be explained by the formation of capillary forces between protein aggregates up to a certain level. Once water droplets occur in the gel (>2% water), capillary forces are weaker [25]. Water droplets formation is crucial in the lipid and protein oxidation in these systems (**Paper II, Hypothesis 1**), as in oleogels with increased water addition ($\geq 2\%$, e.g., for

2 % ~36 mmol/kg oil conjugated dienes after 14 days of incubation at 40 °C) lipid hydroperoxides were significantly higher than in gels with lower water addition (≤ 1 %, e.g. for 1 % ~2.2 mmol/kg oil conjugated dienes for the same conditions). These differences result from a different catalyzing system, where lipid hydroperoxides are probably accumulated at the lipid water interphases (see next section 7.4). In contrast, lipid aldehydes were in general decomposed by water depended reactions (**Manuscript I, Paper II, III**). I. e., water droplets that are not bound to the protein phase are available for water dependent reactions. The decomposition of aldehydes was higher with increasing water amounts (**Paper II**), which can be explained by a better solvation and thus increased acid base catalytic process (**Hypothesis 1**) involving the reaction with protein amino groups (**Hypothesis 2**). This is in accordance with a higher protein modification rate with water resulting from secondary oxidation products, which was monitored by protein carbonyls and fluorescence formation (**Paper III**) by which the adduct formation of specific secondary lipid oxidation products [26–28] was evidenced (**Manuscript IV**) by the chemometric approach using partial least squares regression statistic [29, 30] of excitation emission matrix fluorescence data which corresponds to a non-target approach (**Hypothesis 3**). The importance of the water for protein lipid cooxidation was further highlighted by the increased decomposition of aldehydes according to their partition behavior (**Paper II**), as the involved reaction rates will be strongly increased in the water phase in comparison with the lipid phase. In conclusion, the results indicate that **hypotheses 1** has to be accepted in terms that water has a moderate influence on the decomposition of compounds as water facilitate reactions probably by solvation, hydrogen bonds and acid base catalysis. In addition, increased water concentration impacts the physical texture of oleogels, where new interphases were introduced, which have new consequences.

7.4 Influence of Texture and Lipid Protein Ratio

The formation of isovaleraldehyde follows a similar kinetic as the lipid hydroxide fragmentation volatiles, which can be related to the formation and decomposition of lipid hydroperoxides (**Manuscript I**). This kinetic of volatiles was attributed to lipid hydroperoxides, which accumulated at different interphases. It can be estimated, that lipid derived hydroxyl radicals at interphases influence the oxidation of leucine. This can be explained by a similar amphiphilic character of leucine and lipid hydroperoxides. Lipid oxidation as decomposition of lipid hydroperoxides can be followed by the measurement of their fragmentation products like the most abundant lipid oxidation compound hexanal [9]. Thereby volatiles were measured as sum of fragmentations of lipid hydroperoxides located at the different lipid interfaces to the air, water

and to the base material (**Manuscript I, Figure 2.10**). Influenced different proposed interfaces are thereby the continuation of the idea of the accumulation of amphiphilic lipid hydroperoxides and hydrophilic antioxidants on the lipid air interface or lipid water interface in bulk oils (**Hypothesis 1**). This idea is based on the observation that the lipid autoxidation process of bulk oils can be described as water-in-oil nanoemulsions as a pseudo continuous phase [10, 11] and that lipid peroxidation is altered by emulsifiers in emulsions [31]. Thereby, the increased concentration of lipid hydroperoxides results in a highly increased bimolecular decomposition rate, which leads in turn to an increased radical formation. Similar to the low moisture suspensions, water interfaces occurred in oleogels as water droplets, which turn them effectively into organogelled emulsions, and which have a strong influence on the lipid oxidation (**Paper II**). However, this is also in accordance with lipid oxidation nanoemulsion model [10, 11] in oleogels with no water droplets. In oleogels the initially added water will decrease the level of lipid oxidation products, which are needed to form second phases, as critical concentration of lipid hydroperoxides will be a function of lipid hydroperoxides, lipid oxidation compounds, and water.

The relevant lipid-protein ratio, which is found in lipid oxidation marker systems, may be partly translated to the ratio of the oxidation product formation site and absorption or decomposition site. Therefore, the ratio of importance in **hypothesis II** is the ratio between secondary lipid oxidation products and protein. This was evidenced by oleogels with low lipid hydroperoxide formation rate (4.5 ± 2 mmol/kg oil conjugated dienes after 44 days of incubation at 40 °C, **Paper II, Paper III**), where lipid oxidation aldehydes are lacking in the first 14 days of oxidation and aldehydes are decomposed by the protein. These observations were supported by the formation of apparent fluorescent protein modifications like dityrosine (7.7 ± 1.2 a.u./mg, **Paper III**) or Schiff Bases and lipid aldehyde adducts (excitation 350 nm, emission 420 nm, **Manuscript IV**), which are known lipid protein cooxidation products [6, 26–28] and the formation of peptides (**Manuscript V**), which are formed by radical scission of the protein backbone [8]. Both, cleaved peptides and fluorescent products are thereby evident even before lipid aldehydes occur in static headspace measurements. Furthermore, these results are in accordance with the lipid protein interface model as most of the formed peptides are on the protein surface region in random coil regions with an amphiphilic character, which are likely lipid protein interface active (**Manuscript V**). This was further highlighted as the radical cleaved N-terminus (as e-LI, e-LIV, e-LIVT fragments) was identified, which is likely the most versatile part of the protein towards the lipid interphase. These findings were based on the importance of identified cleaved peptides in a partial linear least squares regression model with lipid hydroperoxide data. Therefore, the identification and observation of N-terminus fragments as well as the identification of apparent fluorescence compounds were revealed using the correlation

to the leading oxidation compounds lipid hydroperoxides with chemometric approaches, why **hypothesis 3** can be accepted. Although correlation is not necessarily a causal relationship and the focus of the created observations highly relies on the comparable behavior to the leading compound, this disadvantage may be acceptable as only increasing compounds are of interest in case of interest to prove oxidation.

There was a comparable protein modification by primary and secondary lipid oxidation compounds in oleogels system with no water droplets, which changed towards the secondary lipid oxidation related modifications (**Manuscript IV**). Though, this correlation related results have to take with caution as the apparent radical based product dityrosine has the same exciting emission characteristics as other fluorescent compounds, like the adduct of 2-hydroxyheptanal with ribonuclease A [32]. However, this adduct is not likely to be present as the fluorescence of this adducts was not in correlation with the increase of a fluorescence region (excitation 350 nm, emission 410–430 nm) related to hexanal in oleogels in with higher water addition [28]. In addition, this region is also related to the hydroxyl radical products *N*-formylkynurenine and polytyrosine [6, 33]. Thus, despite this was measured as fluorescence, where protein modifications are not mandatory fluorescent, this change can only be explained by either a lowered radical modification or a higher modification by lipid aldehydes. This differentiation is scarcely made in the literature, but, the latter point can be explained easily by water facilitated reactions (Schiff base formation, Michael reaction or aldol reaction, **Hypothesis 2**). However, the lower radical modification can also be explained by water droplet formation (**Hypothesis 1**). It was shown, that the protein backbone is mostly cleaved by radicals on the surface of the protein (**Manuscript V**). Therefore, it could be estimated that the radical oxidation of tyrosine and tryptophan may also be favored at the protein lipid interface as in addition, which was also indicated by the red shift of the tryptophan maximum (**Manuscript IV**). This red shift is likely caused by the favored oxidation of hydrophobic tryptophan peptides. The remaining tryptophan molecules will thereby be shifted more into a polar environment, which leads to a higher interaction with the solvent, and in turn to a lowered emission energy. To conclude, nonlipid protein or simply new interfaces were introduced by the occurrence of water droplets, where lipid hydroperoxides accumulate, degenerate, and form radicals and aldehydes (in accordance with **Manuscript I**). However, as the formed radicals are highly reactive, they do not migrate into the interior of the protein. This migration can only be conducted by the less reactive lipid oxidation aldehydes. Furthermore, this migration kinetic has also be measured to be faster for smaller aldehydes in the protein phase as those aldehydes have a higher water/octanol distribution ratio (**Paper II**). In conclusion, **hypothesis 1** can be accepted as water impact the colloidal and structural properties of the oleogels, whereby the formed new interphases have a high impact on

the oxidation of lipid hydroperoxides. Lipid hydroperoxides get a locally increased concentration at the interphases, which strongly accelerate their bimolecular decomposition and thereby other related oxidations.

7.5 Closing remarks and outlook

In this study, the gained knowledge about interface phenomena, relation of protein modification from primary and secondary lipid oxidation products, and aspects of protein backbone scission will benefit future studies on lipid protein cooxidation by showing complexity of the reactions and new approaches. Further, this study demonstrates the usefulness of the physical stable lipid protein cooxidation model system oleogel and will provide helpful information for related foods and cosmetic products. The work that follows this thesis will build on the obtained lipid protein cooxidation characteristics. Following the fluorescent measurement in this study, multivariate statistic of tryptic digest of oxidized proteins analyzed with LC-MS-MS experiments will lead to a broader spectrum of interesting modifications of protein modifications. This approach would greatly benefit from already gained knowledge from the proteomics or metabolomics field and related multivariate statistics. Thereby, the fragmentation pattern of peptides is determined by specific rules, which can be used to define and identify peptides of model proteins. However, the modification mass will be seen in the mother ion spectra as difference to the original peptide, whereby the location of the modification can be seen at the pattern and pattern gap of daughter ions. Intelligent algorithms assisted by artificial intelligence such as neural networks will thereby help and easily suggest the modification site. This lipid oxidation driven protein modifications in foods can be seen in family with post translational modifications (PTM), which is an upcoming research field in proteomics, medicine and especially epigenetic as PTM are involve in cell regulations [34]. PTM are seen products from oxidative stress compounds like unsaturated aldehydes, which can accumulate to high levels in cells [34]. Thereby developed software will help also in the investigation of already known and new food related protein modifications on high accuracy mass spectrometry data like in the FT-ICR-MS measurements. However, MSⁿ and NMR approaches will thereby be needed to fully receive the adduct constitution, molecular configuration, and the conformation of the involved protein. In addition, isotopic labeling will help to understand the fate of single protein or lipid compounds in lipid protein oxidation systems. Further, especially in lipid based oleogels the hydrogen deuterium exchange reaction can reveal the conformation of the protein in MS (HDX-MS) and NMR methods (decrease of signal), as the protein surface prone to water is marked. However, the structure of radical cleaved peptides can be formed and simulated *in silico*, thus characteristic cleaved peptides were already

characterized in parts using multivariate statistics in combination with a metabolomics measurement approach in this study. Thereby, identified characteristic peptides may be quantified by more sensitive and selective approaches like LC-MS-MS (multi-)methods in oleogels and other matrices, and used as oxidation marker in future. However, the results of this thesis are promising and can be seen in a row with markers identified by metal induced oxidation of tryptic protein digest [35, 36] or those obtained by single amino acid experiments [20, 21, 37].

In a wider context of thesis, the fate of lipid induced aldehyde formation and protein related decomposition and formation of peptides is touched upon in this thesis. Aldehydes and peptides are known flavor compounds in aroma research, by which the aldehydes can yield very high flavor dilution factors and odor activity values [12, 38, 39]. The identified lipid induced protein peptides may have a bitter taste, as the peptides were proposed to have an amphiphilic character with a hydrophobic tendency, which includes hydrophilic binding and stimulating sites to a receptor [40, 41]. However, bitterness is evolutionary known to indicate altered food. Currently, protein oxidation getting more and more interest, which is no longer limited to milk and meat products [42] and recently, the international agency for research on cancer (IARC), which is part of the world health organization (WHO) stated that red and processed meat to probably carcinogenic to humans [43]. Thereby, the relevant compounds and the involved mechanism remained unclear, but the presence of known carcinogenic compounds N-nitroso compounds, polyaromatic hydrocarbons, and heterocyclic aromatic amines have been named, whereby lipid peroxidation and DNA damage is caused [44]. The color red can be associated to hem iron complexes in the meat. Therefore, red meat containing oxidation promoting iron has a high risk of lipid oxidation. Thus, lipid-induced protein modifications, which are prior accumulated in absence of in cell repair mechanisms, may have also taken into consideration. Further research on the metabolism and toxicological potential of protein modifications will be therefore necessary in case of milk proteins, but also of all other possible proteins in foods. In addition, relevant compounds should be quantified in order to provide important information for the evaluation of food security and harmlessness. However, lipid protein modifications are rather in low concentrations and our metabolism, which is affected by oxygen metabolism and related lipid peroxidation since eons, is able to provide protection mechanisms. Together with improved food quality and security, our nutrition is getting more and more satisfying for a healthy and happy life.

7.6 References

- [1] Headlam, H. A., Davies, M. J., Markers of protein oxidation: Different oxidants give rise to variable yields of bound and released carbonyl products. *Free Radical Biology and Medicine* 2004, *36*, 1175–1184.
- [2] Vries, A. de, Wesseling, A., van der Linden, E., Scholten, E., Protein oleogels from heat-set whey protein aggregates. *Journal of Colloid and Interface Science* 2017, *486*, 75–83.
- [3] Semenov, N. N., *Some problems in chemical kinetics and reactivity, Volume II* 1959, Chapter XII, p. 262.
- [4] Labuza, T. P., Dugan, L. R., Kinetics of lipid oxidation in foods. *CRC Critical Reviews in Food Technology* 1971, *2*, 355–405.
- [5] Putseys, J. A., Lamberts, L., Delcour, J. A., Amylose-inclusion complexes: Formation, identity and physico-chemical properties. *Journal of Cereal Science* 2010, *51*, 238–247.
- [6] Scheidegger, D., Pecora, R. P., Radici, P. M., Kivatinitz, S. C., Protein oxidative changes in whole and skim milk after ultraviolet or fluorescent light exposure. *Journal of Dairy Science* 2010, *93*, 5101–5109.
- [7] Simat, T. J., Steinhart, H., Oxidation of Free Tryptophan and Tryptophan Residues in Peptides and Proteins. *Journal of Agricultural and Food Chemistry* 1998, *46*, 490–498.
- [8] Garrison, W. M., Reaction mechanisms in the radiolysis of peptides, polypeptides, and proteins. *Chemical Reviews* 1987, *87*, 381–398.
- [9] Schaich, K. M., in: Kamal-Eldin, A., Min, D. B. (Eds.), *Lipid oxidation pathways*, AOCS Press, Urbana, Ill. 2008.
- [10] Frankel, E. N., Huang, S.-W., Kanner, J., German, J. B., Interfacial Phenomena in the Evaluation of Antioxidants: Bulk Oils vs Emulsions. *Journal of Agricultural and Food Chemistry* 1994, *42*, 1054–1059.
- [11] Chaiyasit, W., Elias, R. J., McClements, D. J., Decker, E. A., Role of Physical Structures in Bulk Oils on Lipid Oxidation. *Critical Reviews in Food Science and Nutrition* 2007, *47*, 299–317.
- [12] Belitz, H. D., Grosch, W., Schieberle, P., *Lehrbuch der Lebensmittelchemie*, Springer, Garching 2007.
- [13] Pokorný, J., Janíček, G., Wechselwirkung zwischen Proteinen und oxydierten Lipiden. *Molecular Nutrition & Food Research* 1975, *19*, 911–920.
- [14] Gardner, H. W., Lipid hydroperoxide reactivity with proteins and amino acids: A review. *J. Agric. Food. Chem.* 1979, *27*, 220–229.

- [15] Davies, M. J., The oxidative environment and protein damage. *Biochimica et biophysica acta* 2005, *1703*, 93–109.
- [16] Jackson, L. S., Chemical food safety issues in the United States: Past, present, and future. *Journal of Agricultural and Food Chemistry* 2009, *57*, 8161–8170.
- [17] MacGregor, J. T., Wilson, R. E., Neff, W. E., Frankel, E. N., Mutagenicity tests of lipid oxidation products in *Salmonella typhimurium*: Monohydroperoxides and secondary oxidation products of methyl linoleate and methyl linolenate. *Food and Chemical Toxicology* 1985, *23*, 1041–1047.
- [18] Hidalgo, F. J., Zamora, R., Amino acid degradations produced by lipid oxidation products. *Critical Reviews in Food Science and Nutrition* 2016, *56*, 1242–1252.
- [19] Frankel, E. N., *Lipid oxidation*, Elsevier 2014.
- [20] Uchida, K., Kanematsu, M., Sakai, K., Matsuda, T., Hattori, N., Mizuno, Y., Suzuki, D., Miyata, T., Noguchi, N., Niki, E., Osawa, T., Protein-bound acrolein: Potential markers for oxidative stress. *Proceedings of the National Academy of Sciences of the United States of America* 1998, *95*, 4882–4887.
- [21] Ichihashi, K., Osawa, T., Toyokuni, S., Uchida, K., Endogenous formation of protein adducts with carcinogenic aldehydes: Implications for oxidative stress. *The Journal of biological chemistry* 2001, *276*, 23903–23913.
- [22] Globisch, M., Kaden, D., Henle, T., 4-Hydroxy-2-nonenal (4-HNE) and Its Lipation Product 2-Pentylpyrrole Lysine (2-PPL) in Peanuts. *Journal of Agricultural and Food Chemistry* 2015, *63*, 5273–5281.
- [23] Bro, R., Smilde, A. K., Principal component analysis. *Anal. Methods* 2014, *6*, 2812–2831.
- [24] Barker, M., Rayens, W., Partial least squares for discrimination. *J. Chemometrics* 2003, *17*, 166–173.
- [25] Vries, A. de, Jansen, D., van der Linden, E., Scholten, E., Tuning the rheological properties of protein-based oleogels by water addition and heat treatment. *Food Hydrocolloids* 2018, *79*, 100–109.
- [26] Fletcher, B. L., Tappel, A. L., Fluorescent modification of serum albumin by lipid peroxidation. *Lipids* 1971, *6*, 172–175.
- [27] Shimasaki, H., Ueta, N., Privett, O. S., Covalent binding of peroxidized linoleic acid to protein and amino acids as models for lipofuscin formation. *Lipids* 1982, *17*, 878–883.
- [28] Kikugawa, K., TAKAYANAGI, K., WATANABE, S., Polylysines modified with malonaldehyde, hydroperoxylinoleic acid and monofunctional aldehydes. *Chem. Pharm. Bull.* 1985, *33*, 5437–5444.

- [29] Wold, S., Sjöström, M., Eriksson, L., *Partial Least Squares Projections to Latent Structures (PLS) in Chemistry* 1998.
- [30] Mevik, B.-H., Wehrens, R., Liland, K. H., pls: Partial Least Squares and Principal Component Regression 2018, <https://CRAN.R-project.org/package=pls>.
- [31] Schwarz, K., Huang, S.-W., German, J. B., Tiersch, B., Hartmann, J., Frankel, E. N., Activities of Antioxidants Are Affected by Colloidal Properties of Oil-in-Water and Water-in-Oil Emulsions and Bulk Oils. *J. Agric. Food. Chem.* 2000, 48, 4874–4882.
- [32] Liu, Z., Sayre, L. M., Model Studies on the Modification of Proteins by Lipoxidation-Derived 2-Hydroxyaldehydes. *Chemical Research in Toxicology* 2003, 16, 232–241.
- [33] Briza, P., Ellinger, A., Winkler, G., Breitenbach, M., Characterization of a DL-dityrosine-containing macromolecule from yeast ascospore walls. *Journal of Biological Chemistry* 1990, 265, 15118–15123.
- [34] Grimsrud, P. A., Xie, H., Griffin, T. J., Bernlohr, D. A., Oxidative Stress and Covalent Modification of Protein with Bioactive Aldehydes. *Journal of Biological Chemistry* 2008, 283, 21837–21841.
- [35] Koivumäki, T., Gürbüz, G., Poutanen, M., Heinonen, M., A Novel LC–MS Application To Investigate Oxidation of Peptides Isolated from β -Lactoglobulin. *J. Agric. Food. Chem.* 2012, 60, 6799–6805.
- [36] Koivumäki, T. P., Gürbüz, G., Heinonen, I. M., Tryptophan and Cysteine Oxidation Products Dominate in α -Lactalbumin-Derived Peptides Analyzed with LC–MSn. *Journal of Food Science* 2017, 82, 2062–2069.
- [37] Hellwig, M., Löbmann, K., Orywol, T., Voigt, A., Model Studies on the Oxidation of Benzoyl Methionine in a Carbohydrate Degradation System. *J. Agric. Food. Chem.* 2014, 62, 4425–4433.
- [38] Grosch, W., Detection of potent odorants in foods by aroma extract dilution analysis. *Trends in Food Science & Technology* 1993, 4, 68–73.
- [39] Grosch, W., Evaluation of the Key Odorants of Foods by Dilution Experiments, Aroma Models and Omission. *chemse* 2001, 26, 533–545.
- [40] Ishibashi, N., Kouge, K., Shinoda, I., Kanehisa, H., Okai, H., A Mechanism for Bitter Taste Sensibility in Peptides. *Agricultural and Biological Chemistry* 1988, 52, 819–827.
- [41] Tamura, M., Miyoshi, T., Mori, N., Kinomura, K., Kawaguchi, M., Ishibashi, N., Okai, H., Mechanism for the Bitter Tasting Potency of Peptides Using O-Aminoacyl Sugars as Model Compounds+. *Agricultural and Biological Chemistry* 1990, 54, 1401–1409.
- [42] Hellwig, M., The Chemistry of Protein Oxidation in Food. *Angew. Chem. Int. Ed.* 2019, 0.

- [43] Organization, W. H., IARC monographs evaluate consumption of red meat and processed meat. *International agency for research on cancer* 2015.
- [44] Domingo, J. L., Nadal, M., Carcinogenicity of consumption of red meat and processed meat: A review of scientific news since the IARC decision. *Food and Chemical Toxicology* 2017, *105*, 256–261.

Chapter 8

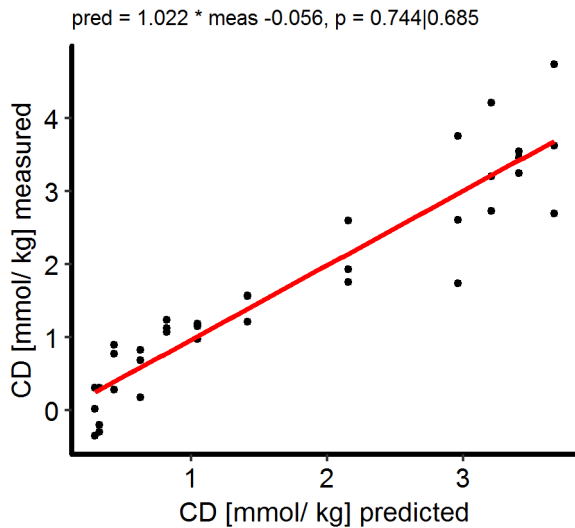
Appendix

8.1 Supporting information for chapter 3

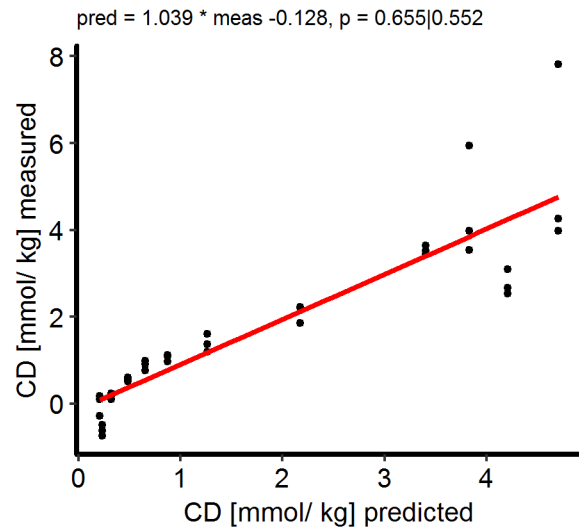
The final performances of regression are here further checked by proving if there are significant differences of the slope of predicted versus measured values to one and for the intercept to zero.

Due to no significant differences in all models ($p > 0.05$), all models could not rejected.

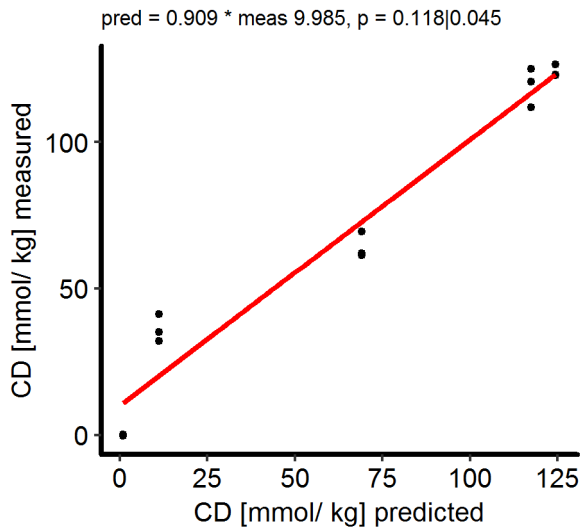
0% added water oleogel



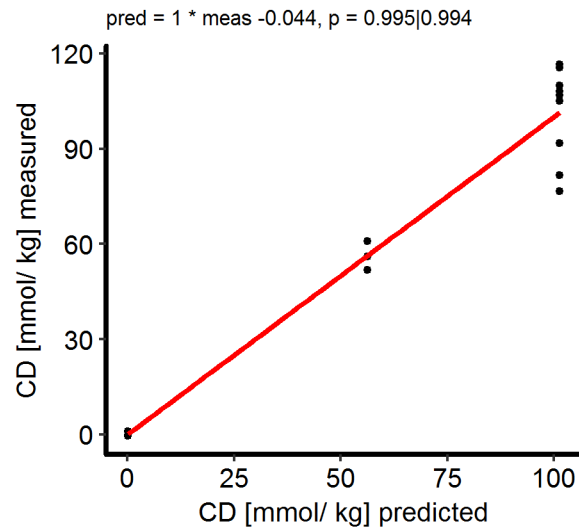
0.23% added water oleogel



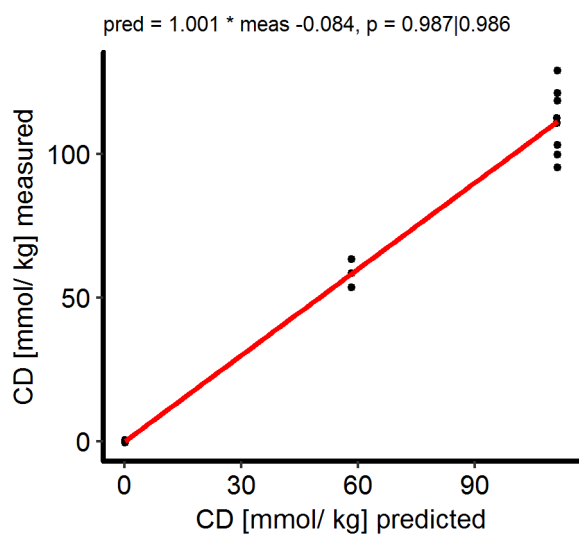
2.8% added water oleogel



5.6% added water oleogel



8.4% added water oleogel



8.2 Supporting information for chapter 5

The size exclusion chromatograms were deconvoluted using Gaussian fitting (retention times: 27.9, 29, 35, 48.8, 56.5, 60.13, 63.08, 66.76, 70.63, 74.65, 80.25 \pm 0.5 min, standard derivation σ was limited from 10 to 150% of 0.75, 5, 1.5, 5, 0.75, 0.75, 0.75, 0.75, 0.75, 0.75 and 0.75 min) after baseline subtraction (line fitting between mean of 0–20 min and 83–85 min). The Area was normalized using the summed protein absorption at 278 nm, with 0.1 a.u. as threshold (see figure 1).

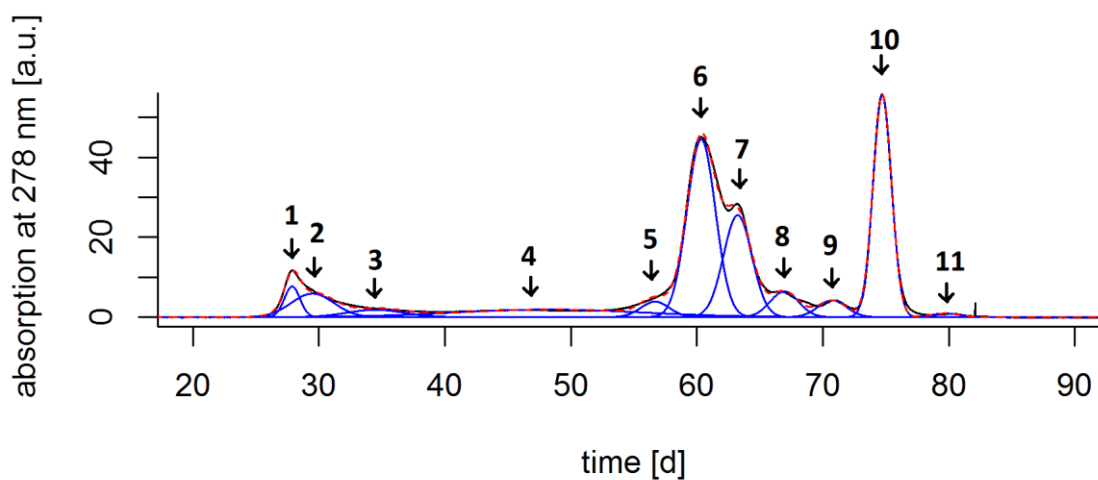


Figure 1: Typical size exclusion chromatogram recorded at 278 nm with highlighted deconvoluted peaks (1–11, blue and sum red dashed)

The low oxidation model was described best with 5 PLS components, whereas the PLS components from 1 to 5 explain 55.8%, 86.2%, 90.1%, 97.3% and 98.2% of variance in fluorescence data and 22.9%, 46.9%, 82.4%, 83.7% and 86.9% of variance in hydroperoxide data. This was similar to the whole data model, where also 5 components are used, which explained 79.2%, 95.6%, 97.7%, 98.9% and 99.2% of variance in fluorescence data and 85.1%, 90.4%, 91.9%, 92.5% and 93.3% in hydroperoxide data. For both models, the leave-one-out procedure was used for cross validation. In both models the root mean square errors of prediction (low oxidation model: 2.9 mmol O₂/kg oil, whole data model: 147.7 mmol O₂/kg oil) were comparably low for the highest hydroperoxide values (low oxidation model: 36.5 mmol O₂/kg oil, whole data model: > 1400 mmol O₂/kg oil), but high for the lowest hydroperoxide values

The slope from predicted versus measured values is very good (1.00 ± 0.05 low oxidation, see figure 2, 1.00 ± 0.03 high oxidation, see figure 3) and the t-test indicates the proximity to the ideal value of 1 (low oxidation model: $t = -2.4 \cdot 10^{-14}$, whole data model: $t = -1.4 \cdot 10^{-13}$, in both

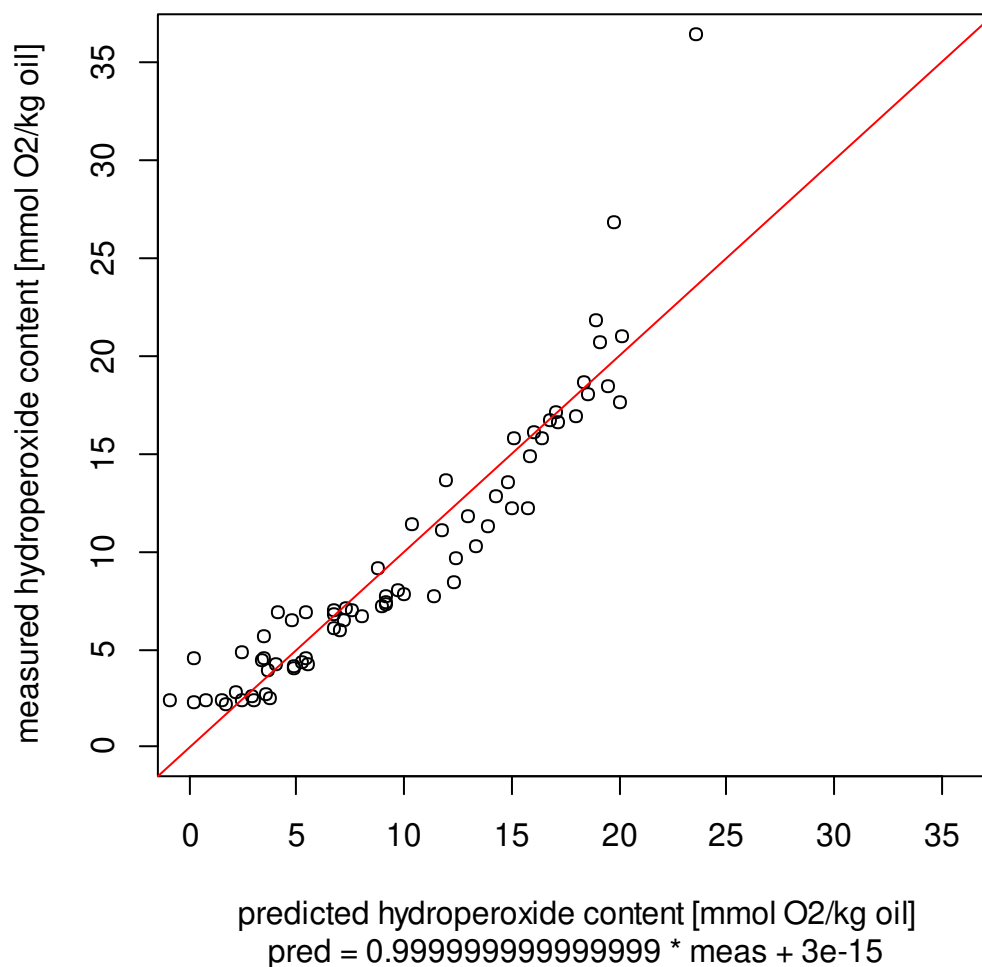
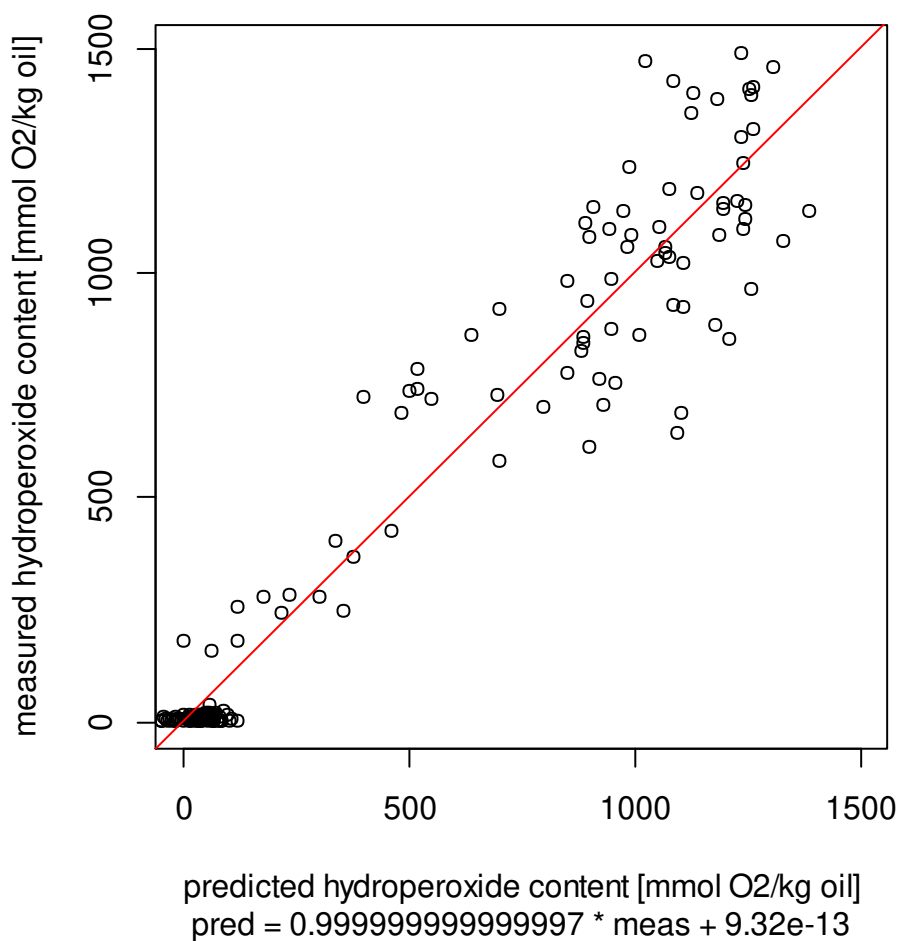


Figure 2: partial least squares regression predicted hydroperoxide content versus measured hydroperoxide content of the low oxidation model.



$p \approx 1$).

Figure 3: partial least squares regression predicted hydroperoxide content versus measured hydroperoxide content of the whole oxidation model.

8.3 Scripts used with R

The scripts written in R used throughout the whole thesis would fill several hundreds of pages. Therefore, only some excerpts can be given here. This will include self-created functions as well as important R code lines.

8.3.1 R-scripts related to chapter 2

Reading a chromatogram of a given file *f* in a given set *s*:

```
name.chrom <- paste(Directory,"\\", Number,".D\\REPORT01.CSV", sep = "")
print(name.chrom)

chromatogram <- read.csv(name.chrom, sep = ",",comment.char = "#",header =
FALSE, fileEncoding = "UCS-2LE")
chromatogram
for(c in 1:N.Compounds)
```

```

{
  master[s,f,c] <- 0
  for(p in 1:length(chromatogram[,1]))
  {
    if (is.null(chromatogram[p,2]) != TRUE) {
      if (Compounds[c,1]-Error <= chromatogram[p,2]) {
        if (Compounds[c,1]+Error >= chromatogram[p,2]) {
          master[s,f,c] <- master[s,f,c] + chromatogram[p,5]*g
        }
      }
    }
  }
}

```

Doing a kinetic fit A->B->C:

```

library("minpack.lm")
parStart <- list(k1=0.165,k2=0.1648, A0=max(master[,f,c]),t0 = 1
  , k12 = 0.018, k22 = 0.015, A02=max(master[,f,c]) ,t02=15
  , k13 = 0.09, k23 = 0.075, t03 = 80,A03=max(master[,f,c])*0.5 )

getPred <- function(parS, xx){

  if (modes == 0){
    parS$t0 <- parS$t0 # one t0 modell
    parS$t03 <- parS$t0 # one t0 modell
  }

  parS$k22 <- parS$k2 # one degradation modell
  parS$k23 <- parS$k2

  abc1 <- parS$k1*parS$A0/(parS$k2-parS$k1)*(exp(parS$k1*(parS$t0-xx))-
exp(parS$k2*(parS$t0-xx)))
  abc2 <- parS$k12*parS$A02/(parS$k22-parS$k12)*(exp(parS$k12*(parS$t02-xx))-
exp(parS$k22*(parS$t02-xx)))
  abc3 <- parS$k13*parS$A03/(parS$k23-parS$k13)*(exp(parS$k13*(parS$t03-xx))-
exp(parS$k23*(parS$t03-xx)))
  abc4 <-0

  abc1[xx<parS$t0] <- 0
  abc2[xx<parS$t02] <- 0
  abc3[xx<parS$t03] <- 0
  abc4 <- abc1 + abc2 + abc3*1
  return(abc4)
}

## residual function
residFun <- function(p, observed, xx) observed - getPred(p,xx)

```



```

simDNoisy <- cbind(master_sc[,f,c][-(1:step)],master_sc[,f+1,c][-(1:step)])
#master_scaled

nls.out <- nls.lm(par=parStart, fn = residFun, observed = simDNoisy, lower =
c(0,0.01,max(master[,f,c])/100,0,0,0,0,0,0,0,0), upper =
c(0.3,0.3,max(master[,f,c])*5,t0_up,0.3,0.3,max(master[,f,c])*5,t0_up1,0.3,0.3,max(m
aster[,f,c])*5,t0_up2), xx = x, control = nls.lm.control(nprint=0, maxiter = 1024, maxfev
= 10^5))

integrand <- function(x,parS) {getPred(parS,x)}
integ <- integrate(integrand, lower = 0, upper = Inf,as.list(coef(nls.out)))

```

8.3.2 R-scripts related to chapter 3

Doing a differential fit according to the formula:

$$\text{(Formula 3.1): } \frac{dCD}{dt} = k_1CD - k_2CD^2$$

```

require(deSolve) # library for solving differential equations
require(minpack.lm) # library for least squares fit using levenberg-marquart algorithm

pv <- read.csv("Diene.csv", as.is = T)

pv1 <- cbind(pv1, rbind(as.matrix(pv[,i*3-1]), as.matrix(pv[,3*i]), as.matrix(pv[,3*i+1])))

t=c(seq(0,105,1),pv$Tage)
t=sort(unique(t))

pvrate=function(t,c,parms){
  #print(c)
  # rate constant passed through a list called parms

  k1=as.numeric(parms$k01)#*exp(-
1*as.numeric(parms$dE1)/(8.3144598*(40+273.15)))
  k2=as.numeric(parms$k02)#*exp(-
1*as.numeric(parms$dE2)/(8.3144598*(40+273.15)))

  # c is the concentration of species

  # derivatives dc/dt are computed below
  r=rep(0,length(c))
  r[1]=k1*c["A"]-k2*(c["A"])^2 #dcA/dt

  # the computed derivatives are returned as a list
  # order of derivatives needs to be the same as the order of species in c
  return(list(r))
}

```

```
ssq2=function(parms2){  
  
  # initial concentration  
  cinit = (c(A=as.numeric(parms2[3])))  
  
  # Tage points for which conc is reported  
  # include the points where data is available  
  t=c(seq(0,105,1),pv$Tage)  
  t=sort(unique(t))  
  
  # parameters from the parameter estimation routine  
  k01=as.numeric(parms2[1])  
  k02=as.numeric(parms2[2])  
  A0=as.numeric(parms2[3])  
  
  # solve ODE for a given set of parameters  
  out=ode(y=cinit,times=t,func=pvrate,parms=list(k01=k01,k02=k02))  
  
  # Filter data that contains Tage points where data is available  
  outdf=data.frame(out)  
  outdf=outdf[outdf$time %in% pv$Tage,]  
  
  expdf= pv #melt(df2,id.var="Tage",variable.name="species",value.name="conc")  
  ##  
  if (t0_question == F) {  
    A0 <- 0  
  }  
  
  # print(  
  #cor((c(outdf$A,outdf$A,outdf$A)-A0), pv$conc, method = "spearman"))  
  
  ssqres= c(c(outdf$A,outdf$A,outdf$A) - pv$conc -A0) #preddf$conc-expdf$conc  
  #ssqres[preddf$species != "B" ] <- 0  
  #ssqres=preddf[preddf$species=="A",]$conc - -expdf[expdf$species=="ca",]$conc  
  #preddf$conc-expdf$conc  
  print(sum(ssqres^2))  
  # return predicted vs experimental residual  
  return(ssqres)  
  
}  
  
# for validation including the Jack knife Procedure  
ssq_JK=function(parms2){  
  
  # initial concentration  
  cinit = (c(A=as.numeric(parms2[3])))  
  
  # Tage points for which conc is reported  
  # include the points where data is available
```

```

t=c(seq(0,105,1),pv$Tage)
t=sort(unique(t))

# parameters from the parameter estimation routine
k01=as.numeric(parms2[1])
k02=as.numeric(parms2[2])
A0=as.numeric(parms2[3])

# solve ODE for a given set of parameters
out=ode(y=cinit,times=t,func=pvrate,parms=list(k01=k01,k02=k02))

# Filter data that contains Tage points where data is available
outdf=data.frame(out)
outdf=outdf[outdf$time %in% pv$Tage,]

expdf= pv #melt(df2,id.var="Tage",variable.name="species",value.name="conc")
##
if (t0_question == F) {
  A0 <- 0
}

ssqres= c(c(outdf$A,outdf$A,outdf$A)[-k] - pv$conc -A0) #preddf$conc-expdf$conc
#ssqres[preddf$species != "B" ] <- 0
#ssqres=preddf[preddf$species=="A",]$conc - -expdf[expdf$species=="ca",]$conc
#preddf$conc-expdf$conc
print(sum(ssqres^2))
# return predicted vs experimental residual
return(ssqres)

}

# doing the fit:

parms2= list(k01= 0.5, k02 =0.05, A0 =0.3)
fitval <- nls.lm(par=parms2,fn=ssq2, lower = c(0,0.001,bottemborder), upper =
c(100,1,topborder))
parms2=as.list(as.list(coef(fitval)))

kk <- rbind(parms0,parms0.23,pars2.8_40,
           pars5.6_40,
           pars8.4_40)
kkg <- kk

print(
  sum_d %>%
  ggplot(aes(x = ykurve2, y = AUC, group= water)) +
  scale_y_continuous(limits = c(0,150) ) +
  aes(shape = water, color = water, line = water)+
  geom_point(size = 2.75)+
  # geom_line()+

```

```

theme(
  panel.background = element_rect(fill = "white"),
  legend.key = element_rect(fill = "white"),
  legend.key.height = unit(0.55,"cm"),
  legend.background = element_rect(fill = "transparent"),
  legend.justification=c(0.01,1), legend.position=c(0.01,1),

  axis.line.x = element_line(colour = "black", size = 1),
  axis.line.y = element_line(colour = "black", size = 1),#,
  legend.text = element_text(size = 10),
  legend.title = element_text(size = 12),
  axis.text = element_text(size = 10, colour = "black"),
  axis.title = element_text(size = 10)
  #legend.position = "bottom"
)+

geom_line(data=as.data.frame(ode(y=c(A=as.numeric(kkg[3,3]))
  ,times=seq(0,35, by = 0.1),func=pvrate,parms=kkg[3,]))
  ,aes(x=time,y=A-A01), inherit.aes = F, show.legend = F,
  color = cbPalette[1])+
geom_line(data=as.data.frame(ode(y=c(A=as.numeric(kkg[4,3]))
  ,times=seq(0,35, by = 0.1),func=pvrate,parms=kkg[4,]))
  ,aes(x=time,y=A-A02), inherit.aes = F, show.legend = F,
  color = cbPalette[2])+
geom_line(data=as.data.frame(ode(y=c(A=as.numeric(kkg[5,3]))
  ,times=seq(0,35, by = 0.1),func=pvrate,parms=kkg[5,]))
  ,aes(x=time,y=A-A03), inherit.aes = F, show.legend = F,
  color = cbPalette[3])+

  geom_errorbar(aes(ymin = AUC - Error, ymax = AUC + Error),size = 0.3, na.rm =
T, width = pd, position = position_dodge(0.9))+
  labs(y = "CD [mmol/ kg]",x= "t [d]")+

  #scale_linetype(labels = names)
  #scale_fill_manual(values=c("#CC6666", "#9999CC",
"#66CC99", "#66CC98", "#66CC49")+
  scale_shape(labels = names[3:5])+
  scale_colour_manual(values=cbPalette, labels = names[3:5])#+
  #scale_color_discrete(labels= names)
)

# Jack knife Procedure:
pv <- pv1[-k,]

fitval <- nls.lm(par=parms2,fn=ssq_JK, lower = c(0,0.001,bottemborder), upper =
c(100,1,topborder))
  parms2=as.list(as.list(coef(fitval)))

JK[[j]] <- rbind(JK[[j]], c(k,parms2, pv_meas = as.numeric(y_meas[2]),pv_pred =
as.numeric(y_pred)))

```

```

kk_JK <- cbind(kk,rbind(
  apply(matrix(as.numeric((JK[[1]])), ncol= 6),2, sd)[2:4]*35/sqrt(36),
  apply(matrix(as.numeric((JK[[2]])), ncol= 6),2, sd)[2:4]*35/sqrt(36),
  apply(matrix(as.numeric((JK[[3]])), ncol= 6),2, sd)[2:4]*14/sqrt(15),
  apply(matrix(as.numeric((JK[[4]])), ncol= 6),2, sd)[2:4]*14/sqrt(15),
  apply(matrix(as.numeric((JK[[5]])), ncol= 6),2, sd)[2:4]*14/sqrt(15)
))

```

8.3.3 R-Scripts related to chapter 5

For evaluation of SEC Data

```

## function for reading chromatogramm
### for this you must make a csvfile of the chromatogram
### 1) load the macro makecsv.MAC with the following command in
### the chemstation console:
### macro makecsv.MAC
### 2) convert chromatogramm to csv by the command:
### csvfile

read_Chrom <- function(Name){
  Chromatogram <- read.csv(Name, header = F, sep = ",",
    ,fileEncoding = "UTF16", as.is = T)
  names <- Chromatogram[1,]
  Chrom <- Chromatogram[-1,]
  colnames(Chrom) <- names
  Chrom

  ### data rerangement, as all 5 wavelengths are under each other
  ### first column is the time, the other the wavelengths
  Chrom2 <- cbind(as.numeric(Chrom[1:(nrow(Chrom)/5),1]),
    as.numeric(Chrom[1:(nrow(Chrom)/5),2]),
    as.numeric(Chrom[((nrow(Chrom)/5)+1):(2*(nrow(Chrom)/5)),2]),
    as.numeric(Chrom[(2*(nrow(Chrom)/5)+1):(3*(nrow(Chrom)/5)),2]),
    as.numeric(Chrom[(3*(nrow(Chrom)/5)+1):(4*(nrow(Chrom)/5)),2]),
    as.numeric(Chrom[(4*(nrow(Chrom)/5)+1):(5*(nrow(Chrom)/5)),2]))

  # rename matrix
  colnames(Chrom2) <- c("time", "214nm", "278nm", "325nm", "340nm", "370nm")
  return(Chrom2)
}

require(minpack.lm)

### ffn is a function, which calculate a gaussian curve
ffn = function(parms, prefac){
  m = as.numeric(parms[1])
  sd = as.numeric(parms[2])

```

```
k = as.numeric(parms[3])

rhat <- k * exp(-0.5 * ((x - m)/sd)^2)*prefac

# k4 * exp(-0.5 * ((x - m4)/sd4)^2)
return (rhat)
}

ffn_sum <- function(parms){
  L <- length(times)
  peak <- x*0
  i <- 4
  for (i in 1:L){
    parms2 <- c(parms[i+2*L],parms[i], parms[i+L])#c(times[i],parms[i], parms[i+L])
    peak <- peak + ffn(parms2,prefact[i])
  }
  #plot(x, peak, type = "l", xlim = c(50,80))
  sq <- (Chrom2[,2] - peak)
  print(sum(sq^2))
  return(sq)
}

fitval <- nls.lm(par=parms,fn=ffn_sum,
                lower = c(broadest*0.1,ks*0, times -tdif),#,
                #370,1,0.1),

                upper = c(broadest*1.5, ks*10, times +tdif))#,
                #370,35,500))

# with A0 fitting
#fitval <- nls.lm(par=parms4,fn=ssq2_t0, lower =
c(104000,13900,0.1,38350,48470,0), upper = c(104000,13900,90,
38350,48470,100))

# shapiro.test(nAread0_0w) # nur 2 proben
shapiro.test(nAread8_0w) # p = 0.25 > 0.05 => NV!
shapiro.test(nAread0_2.8w) # p = 0.7 > 0.05 => NV!
shapiro.test(nAread7_2.8w) # p = 0.8 > 0.05 => NV!
shapiro.test(nAread14_0w) # p = 0.27 > 0.05 => NV!
shapiro.test(nAread14_2.8w) # p = 0.21 > 0.05 => NV!

t.test(nAread8_0w,nAread0_0w, "greater")
# p = 0.12 => nicht sign größer

t.test(nAread7_2.8w,nAread0_2.8w, "greater")
# p = 0.07 => nicht so sign größer

t.test(nAread14_0w,nAread0_0w, "greater")
# p = 0.11 => nicht sign größer
```

```
t.test(nAread14_2.8w,nAread0_2.8w, "greater")
# p = 0.07 => nicht sign größer
```

For fluorescence measurements:

```
PK278 <- rbind(
  PK278,
  read.csv(paste("Daten\\278nm\\",i,".csv", sep = ""), dec = ".", sep = ";",
    as.is = T)
)

FluorBiblang <- as.list(1:nrow(PK278))

Spektrum <- read.csv(paste("Daten\\Proteinverdau_",i,".csv",sep = ""), header = T)
Spektrum <- (Spektrum[-1,-(ncol(Spektrum))])

for (j in 1:ncol(Spektrum)){
  Spektrum[,j] <- as.numeric(as.character(Spektrum[,j]))
}

cSpektrum <- Spektrum[,c(1,1:22*2)]
colnames(cSpektrum) <- c("Emwave",seq(290,395,by = 5))
cSpektrum
ccSpektrum <- melt(cSpektrum[,],id.vars =c("Emwave"),
  variable.name = "Exwave",
  value.name = "Intensity")
ccSpektrum$Intensity <- ccSpektrum$Intensity - Reference$Intensity
FluorBiblang[[i]] <- ccSpektrum

fnTrp = function(parms){
  m = as.numeric(parms[1])
  sd = as.numeric(parms[2])
  k = as.numeric(parms[3])

  m2 = as.numeric( parms[4])
  sd2 = as.numeric(parms[5])
  k2 = as.numeric(parms[6])

  #m3 = as.numeric( parms[7])
  #sd3 = as.numeric(parms[8])
  #k3 = as.numeric(parms[9])

  rhat <- k * exp(-0.5 * ((x - m)/sd)^2) #+
  #k2 * exp(-0.5 * ((x - m2)/sd2)^2)# +
  #k3 * exp(-0.5 * ((x - m3)/sd3)^2)
  #ssq = sum((Spektrum$Intensity - rhat)^2)
  return (rhat)
}
```

```
fitval <- nls.lm(par=parms,fn=ffn22,
  lower = c(325,1,0.1,
            350,1,0.1,
            370,1,0.1),#,
            #370,1,0.1),

  upper = c(325,35,500,
            350,35,500,
            370,35,500))#,

Results <- cbind(Results, P410 = Results$F.Ex325.Em410/Results$Protein) # m =
M*A/e*V[mg]

#PLS:
pca_data <- NULL

for ( Probe in Results$Probe[Results$Wassergehalt < 20]){ #[Results$Wassergehalt
< 2]

  #Probe <- Results$Probe[6]
  pre_Spektrum <- FluorBibkurz[[Probe]]
  Spektrum_AS <- pre_Spektrum[pre_Spektrum$Exwave == 275,][,c(1,3)]

  pre_Spektrum <- FluorBiblang[[Probe]]
  pca_data <- rbind(pca_data,
    c(Probe, Results$Wassergehalt[Results$Probe==Probe],
      Results$Tag[Results$Probe==Probe],
      Results$CO[Results$Probe==Probe],
      Results$LOOH[Results$Probe==Probe],
      Spektrum_AS$Intensity,pre_Spektrum$Intensity)
  )
}

colnames(pca_data) <- c("Probe","water","day","CO","LOOH",
  Spektrum_AS$Emwave,
paste("em",pre_Spektrum$Emwave[], "_ex", pre_Spektrum$Exwave[], sep = ""))
)

require(pls)
Mgas <- pls(pca_data[,4] ~ pca_data[,-(1:5)] , ncomp = 5, validation= "LOO")
```

8.3.4 R-Scripts related to chapter 6

Prepare oxidized Peptides in silico:

```
SF.name <- function(CHNOS){
  name <- ""
  if (CHNOS[1] > 0){
    name <- paste(name, "C", CHNOS[1], sep = "")
  }
}
```



```

}
if (CHNOS[2] > 0){
  name <- paste(name, "H", CHNOS[2], sep = "")
}
if (CHNOS[3] > 0){
  name <- paste(name, "N", CHNOS[3], sep = "")
}
if (CHNOS[4] > 0){
  name <- paste(name, "O", CHNOS[4], sep = "")
}
if (CHNOS[5] > 0){
  name <- paste(name, "S", CHNOS[5], sep = "")
}

return(name)
}

#alpha
Compound <- c(SF.name(SF -c(0,2,0,1,0)),paste("a_", Peptide, sep =
""),"alpha",Peptide)
test <- rbind(test,Compound)
Line <- Line +1

#beta
Compound <- c(SF.name(SF-c(1,5,1,1,0)),paste("b_", Peptide, sep =
""),"beta",Peptide)
test <- rbind(test,Compound)
Line <- Line +1

#epsilon
Compound <- c(SF.name(SF-c(0,-1,-1,1,0)),paste("e_", Peptide, sep =
""),"epsilon",Peptide)
test <- rbind(test,Compound)
Line <- Line +1

#zeta
Compound <- c(SF.name(SF-c(1,2,0,1,0)),paste("f_", Peptide, sep =
""),"zeta",Peptide)
test <- rbind(test,Compound)
Line <- Line +1

Template <- cbind(Mass,RT,Formula,Name)
head(Template)
write.csv2(Template, "oxBLGsingle_af-cd_template.csv", row.names = F)

For unique Sum formulas:

Sum <- read.csv(reades[syst]) #Sum <- Sum[order(Sum$m.z),]
Sum <- cbind(Sum, Diff =Sum$m.z,
            pH =Sum$m.z,

```

```

pINa = Sum$m.z + 22.989221 -1.007276,
pIKa = Sum$m.z + 38.963158 -1.007276, uni = T)

```

```

if (Sum$formula[i-1]==Sum$formula[i]){

```

```

  Sum$uni[i]<- FALSE
}

```

Statistik:

```

Pep <- read.csv(paste("Importances\\csv\\", Übersicht$method[model]
, "\\", comp, ".csv", sep = ""), sep = ",", as.is = T)

```

```

Pepideal <- read.csv("SF_unique_ox_βLG_af-cd_Template.csv")

```

```

Statistic <- cbind(ASL[,c(2,1,5,6,7,8,9)],ASL[,c(5,6,7,8,9)],ASL[,c(5,6,7,8)])
colnames(Statistic) <-
c("AS","Kürzel","Pep_N","a_N","b_N","c_N","d_N","e_N","f_N","Pep_C","a_C","b_C",
c_C","d_C","e_C","f_C")

```

```

##first AS or before
# relevant amino acid

```

```

if (Modification == 1 | Modification == 2| Modification == 0){
  Start_AA <- strsplit(ac_Pep, "")[[1]][1+sign(Modification)*2]
} else {
  Start_AA <- findAA(ac_Pep,"Start") # is "X" when no is found or at beginning of
sequence
}
if (Start_AA != "X"){
  for (AS in 1:20){
    if (Statistic$AS[AS] == Start_AA){
      Statistic[AS,3+Modification] <- Statistic[AS,3+Modification] +
as.numeric(Un_Pep[c,2])#+1/ as importance used
      break
    }
  }
}

```

```

# last AS or following
if (Modification == 2 | Modification == 4 | Modification == 6| Modification == 0){
  End_AA <- strsplit(ac_Pep, "")[[1]][length(strsplit(ac_Pep, "")[[1]])]
} else {
  End_AA <- findAA(ac_Pep,"End") # is "X" when no is found or at end of sequence
}
if(End_AA != "X"){
  for (AS in 1:20){
    if (Statistic$AS[AS] == End_AA){
      Statistic[AS,10+Modification] <- Statistic[AS,10+Modification]
+as.numeric(Un_Pep[c,2])#+1

```

```

    break
  }
}
}

Statistic_end <- cbind(Statistic_end, Sum_AA =
sapply(as.data.frame(t(Statistic[,c(4,5,11,13,15)])),sum))
Statistic_end <- cbind(Statistic_end, Sum_DA =
sapply(as.data.frame(t(Statistic[,c(6:9, 12,14,16)])),sum))

if (Peps ==1){
  Statistic_end_ideal <- Statistic_end
}

Statistic_end_real <- Statistic_end

Sum_T <-
as.data.frame(cbind(as.character(Statistic_end[,2]),Statistic_end[,19]/Statistic_end_id
eal$Sum))
colnames(Sum_T) <- c("Kürzel","Sum")

Sum_T <- (subset(Statistic_end, select = c(2,19)))
Sum_T[,2] <- Statistic_end[,19]/Statistic_end_ideal$Sum*100 # 100 mögliche
Peptide als Basis
#Sum_T[,2] <- Statistic_end[,19]/Statistic_end[,20] # 100 mögliche Peptide als Basis

Ubersicht_all_v[[3]][model,4:23] <- Sum_T[,2]

write.csv(Ubersicht_all_v[[3]],
"Statistik_VIP_Mech\\resul_values\\result_Sum_Annotationlist.csv")

pca_pre <- Ubersicht_all_v[[3]]
pca1 <- pca_pre[c(1:8),c(4:23)]
rownames(pca1) <- c("af_L","af_P","af_L_s","af_P_s",
"af-cd_L","af-cd_P","af-cd_L_s","af-cd_P_s")#pca_pre[,c(24)]

require(pls)
Model <-cbind(Model = c(1,1,1,1,-1,-1,-1,-1),pca1)
Model <- as.matrix(Model)

Mgas <- plsrf(Model[,1] ~ Model[,-1] , ncomp = 10, validation= "LOO")

findAA<- function(ac_Pep, mode){
# ac_Pep <- "CQCL"
sPep <- strsplit(wMod(ac_Pep), "")[[1]]
gefunden <- 0
AA <- 1
position <- 0

for (i in 1:length(P)){

```

```
if (P[i] == sPep[AA]){
  AA <- AA +1
  if (AA > length(sPep)){
    AA <- 1
    gefunden <- gefunden +1
    position <- i
  }
} else {
  AA <- 1
}
}
if (gefunden != 1){
  AA <- "X"
} else {
  if (mode == "Start") {
    if (position - length(sPep) < 1){
      AA <- "X"
    } else {
      AA <- P[position - length(sPep)]
    }
  }
  if (mode == "End") {
    if (position +1 > length(P)){
      AA <- "X"
    } else {
      AA <- P[position +1]
    }
  }
}
}

return(AA)
}
```

PLS für Fluoreszenzspektroskopie

...

Lists of Figures and Tables

Appendix

List of Figures

Figure 1.1: A typical triacylglyceride – an ester of glyceryl with stearic acid (no double bonds), linolenic acid (two double bonds) and linoleic acid (one double bond).	6
Figure 1.2: β -scission of monohydroperoxides, example of linoleic acid [42].	11
Figure 1.3: Oxidation of tyrosine and tryptophan, which produces the fluorescent products dityrosine and N-formylkynurenine according to [44, 45].	13
Figure 1.4: Scission of the protein backbone and introducing of amino acids and carbonyls according to [34, 46].	14
Figure 1.5: Aldol reaction of an aldehyde (alkanal) to 3-hydroxyalkanal and aldolcondensation to the 2-alkenal.	15
Figure 1.6: Formation of cyclic products by addition on lysine residues by 2-alkenals, e.g. the formation of formyl dehydropiperidino lysine (FDP-Lys) via 1,4 addition Michael addition pathway and the fluorescent ethylmethylpyridinium lysine (EMP-Lys) via the 1,2 addition Schiff base pathway [12, 32, 33].	15
Figure 1.7: Scheme of the colloidal network of fat crystals in fat.	16
Figure 1.8: Scheme of the colloidal network of fat crystals in fat and oleogelators in liquid oil.	17
Figure 1.9: Vitamin E – a class of different methylated tocopherols.	18
Figure 1.10: Mechanism of fatty acid methyl ester formation with TMSH.	26
Figure 1.11: Reaction of DNPH with carbonyl to hydrazone derivatives.	28
Figure 1.12: Reaction of OPA with primary amine and thiols to thio-isoindole derivatives according to [90].	29
Figure 1.13: ICR cell, ions trapped in a cube of 3 pairs of electric plates, with specific functions.	34
Figure 1.14: first principal axis/ component in a 2D coordinate system.	37
Figure 2.1: Formation of lipid hydroperoxides in open low moisture models of mixtures (10 % oil, 5 %, (0.25 % Leucine or Lysine)) during the first 3 weeks of incubation at 40 °C. Each point was a single measurement.	53
Figure 2.2: Volatile compounds of two oxidized safflower oils with 6.8 % whey protein identified with dynamic headspace gas chromatography mass spectrometry. Hexanal was eluted twice due high concentration and limited cryo focusing.	54
Figure 2.3: Formation of volatiles (Hexanal, propanal and isovaleraldehyde) in open low moisture models (Starch, Methylcellulose (MC), CaCl ₂ , silica gel (KG) and sea sand)of mixtures (10 % oil, 5 % water, (0/0.25 % Leucine or Lysine)) incubated at 40 °C. Left the first 3 weeks, right : formation until week 14. . Each point was a single measurement.	56
Figure 2.4: Formation of volatiles (Hexanal, propanal and pentanal) in open low moisture methylcellulose, leucine models (MC + Leu, 10 % oil, 5 % water, (0/0.25 % Leucine or Lysine)) incubated at 40 °C as difference to the MC system and scaled to compare the different compounds.	57
Figure 2.5: Formation of volatiles in see first 6 weeks of incubation at 40 °C; left MC + Leu; right: CaCl ₂ + Leu. Peaks volatiles are colored according to their retention time. Each measurement was conducted twice.	58

- Figure 2.6: Principal component analysis of the models with the volatiles formed after 3 weeks of incubation at 40 °C. The first principal component most influencing compounds are printed and highlighted in red and isovaleraldehyde (3MB) in dark red. 59
- Figure 2.7: Lipid hydroperoxide value (PV) vs. time; formation of lipid hydroperoxides in methylcellulose (left) and CaCl₂ (right) Systems at 40 °C. Each measurement was conducted twice. 60
- Figure 2.8: Peroxid value vs. time; formation of lipid hydroperoxides in petroleum ether extracted fat (“free fat” FF), remaining fat (“inner fat” IF) and a whole fat sample (GF) in the 71 methylcellulose model; left: data uncorrected, right: corrected to oil mass gain after 20 min of drying at 105 °C and slightly increased PV. 61
- Figure 2.9: Formation of propanal, isovaleraldehyde and hexanal / g oil vs. time at 40 °C incubation in each sample model. Each measurement was conducted twice. 62
- Figure 2.10: Formation of propanal at 40 °C and fitted curve of underlying regions in methylcellulose material with decreasing water activity (MC 45, 80, 85) and CaCl₂. The sum of the regions is marked in red. 64
- Figure 2.11: Integrated areas (A1-3) of compounds at the certain regions as well as the base amounts of starting material (A1_0 to A3_0) in models using the same t₀. Integrals are from t₀ to infinity or to the last day of the experiment. The logarithmic scale was used to make the 3 compounds comparable. 65
- Figure 2.12: Formation of lipid hydroperoxides (PV) in solvent exchange mct oil and safflower gel (mct-gel, s-gel) and a whey protein isolate suspension in safflower oil (s-suspension) during incubation at 40 °C. A logarithmic scale was chosen to demonstrate the huge differences between the models. 68
- Figure 2.13: Aldol condensation of acetone to 4-methylpent-3-en-2-on (1). 69
- Figure 2.14: Formation of hexanal in solvent exchange mct oil and safflower gel (mct-gel, s-gel) and a whey protein isolate suspension in safflower oil (s-suspension) during incubation at 40 °C. Two scales are given to show the large differences. Left: zoom to the mct-oil and low concentration gel samples. Right: concentration of hexanal in suspension to comparison with the gel, where one points equals one measurement. All measurements were conducted as duplicate. 69
- Figure 2.15: Concentration of protein carbonyls in solvent exchange mct oil and safflower gel (mct-gel, s-gel) and a whey protein isolate suspension in safflower oil (s-suspension) during incubation at 40 °C. Linear fitting curves were added to indicate the overall trend. 70
- Figure 2.16: Formation of protein fluoresce of protein extracts from solvent exchange mct oil and safflower gel (mct-gel, s-gel) and a whey protein isolate suspension in safflower oil (s-suspension) model during incubation at 40 °C. The fluorescence at 410 nm (325 excitation) is characteristic for dityrosine and 435 nm (325 excitation) for NFK. 71
- Figure 3.1: Changes of conjugated dienes (CD, 234 nm) in extracted oil of stored gel samples by 40 °C, added 0 to 3 % water, after 3 (blue), 9 (red) 14 (green) days of incubation by 40 °C in comparison to the oxidation of bulk oil stored under same conditions for 14 days (red dashed). All values are listed as mean and standard deviation of three independent replicates. 83
- Figure 3.2: Changes of conjugated dienes (CD, 234 nm) in extracted oil of stored gel samples by 40 °C, left: 0 % and 0.23 % water added, right: 2.8 – 8.4 % water added. Fitting lines are according to formula 3.1 using a nonlinear least square regression to the raw data, not to means (standard error of estimates from 0 to 8.4 % water: 0.47, 0.83, 11.9, 10.8 and 8.05 mmol/kg). All values are listed as mean and standard deviation of three independent replicates. 84

Figure 3.3: left: constant k_1 and right: k_2 in gel samples from 0 % to 8.4 % water addition for fitting curves in figure 3.2. Standard deviation was estimated using the Jack knife delete one procedure [22].	85
Figure 3.4: Left: Formation of hexanal and right: propanal in gel samples from 0 % to 8.4 % water addition and in bulk oil, lines are added to guide the eyes only.	86
Figure 3.5: Appearances of oleogels with 0 % (A), 2.8 % (B), 5.6 % (C) and 8.4 % (D) water added during preparation.	88
Figure 3.6: Color formation in oleogels with 2.8 to 8.4 % water addition during incubation at 40 °C.	89
Figure 3.7: Left: water content in gel measured gravimetrically after drying for 4 h over water added in premix, linear fit for first nine values (water added < 10 mg/g, dotted) and second order polynomial (line). Right: relation of gel yield after centrifugation over water added in premix.	90
Figure 3.8: Left: frequency sweep plot from gels with no water addition (filled symbols) and water addition about 100 mg/g (open symbols). ○: G' ; □: G'' ; right: storage modulus G' as a function of water addition in premix.	91
Figure 4.1: Changes in the peroxide value (PV) of oil extracts in gel samples during 7 weeks of incubation at 40°C. A: With no and 0.23% water added. B: with higher water amounts added (2.8-8.4%). Lines were added to guide the eyes, only.	107
Figure 4.2: Estimation of dityrosine formation, assessed by fluorescence (excitation 325 nm, emission 410 nm) of protein extracts during a 7 weeks incubation at 40°C. A: low-oxidation systems (no and 0.23% water added) and B: high-oxidation systems (2.8-8.4% water added). Lines were added to guide the eyes, only.	108
Figure 4.3: Formation of protein carbonyls in protein extracts of oleogels incubated for 6–10 weeks at 40°C. A: Oleogels with low (0.23%) and without (0%) water addition, and B: oleogels with high water addition (2.8%–8.4%). A zoomed in view of the concentrations from 0–30 nmol carbonyls/mg protein is included.	111
Figure 4.4: Free amines in the extracted proteins of oleogels, after 6-10 weeks of incubation at 40°C. A: low-water addition (no and 0.23% water added) and B: high-water addition 2.8%-8.4% water added). Lines are added for to guide the eyes, only.	113
Figure 4.5: Relative concentrations of three representative compounds (hexanal, solid line; valeric acid, dashed line, hexanol, dotted line) over time measured by headspace GC for oleogel samples with 0% water addition (A) and MCT-oil control samples (B).	114
Figure 4.6: Relative concentrations of 3-methylbutanal, hexanal, heptanal, and octanal compared with that of hexanal in MCT-oil gels made from corresponding samples with 0%, and 0.5% water addition. Left darkly colored: 0% water MCT-oil gel samples, right brightly colored: 0.5% water MCT-oil gel samples.	116
Figure 5.1: Intrinsic fluorescence of tryptophan (Trp) and protein concentrations. A: Intensity of Trp over time, B: Emission maximum of Trp over time, C: Protein contents in the hydrolysate of protein extracts, measured by absorption at 278 nm, D: Relationship between Trp fluorescence and protein contents. Trp fluorescence parameters were calculated by using a Gaussian curve fit.	131
Figure 5.2: Size-exclusion chromatograms (red: 325 nm, black 278 nm, full absorbance range scale) of tryptic digests from protein extracts derived from prepared oleogel with 2.8% added water, for a sample at incubation time 0 d (A) and 7 d (B, included peak assignment).	133
Figure 5.3: Ratio of normalized deconvoluted peak areas of size exclusion chromatograms (recorded absorption signal at 278 nm) for trypsin-digested protein extracts, with low lipid oxidation (0% added water) and high lipid oxidation (2.8% added water) conditions. Deconvoluted areas were related to non-oxidized protein extracts (day 0), for samples after 7 (2.8%), 8 (0%), (A) and 14 d (B) of incubation. All values were	137

measured in triplicate.

Figure 5.4: PLS loading contour plots for the principal components 1 to 3 for low-oxidation systems (0% and 0.23% added water, A, C, and E) and for all samples (B, D, and F). A positive correlation is indicated by coloring (blue for negative, red for positive) and highlighted by adding 10–15 isolines. 137

Figure 5.5: Formation of 3 fluorophores, by λ EX at 325, 350, and 370 nm (solid, dashed, and dotted lines, respectively) and emission of 420 nm in oleogel samples with 0%, 0.23% (A and B), 2.8% and 8.4% added water (C and D). Each signal was achieved by deconvolution of the related excitation spectra, at 420 nm emission. 140

Scheme 6.1: Scission of the protein chain following either the α -amidation or diamide pathway according to [2, 3] with the change of the sum formula in comparison to a hydrolyzed amid bond in brackets. The modifications *a-f* were indicated using the relation matrix with the new C- and N-terminus. 149

Figure 6.1: Measured Intensity e_LI versus time (A) and versus lipid hydroperoxides (B), red squares: no water addition, blue diamond: 0.23% water addition. 156

Figure 6.2: PLS importance of oxidized peptides versus their calculated hydrophobicity neglecting modifications using Pareto scaling (A), level scaling (B) or Pareto scaling of all peptides ($\Delta m < 2$ ppm, (D), with labeling of some) and (E) the position of the parent peptides (red) in unliganded native beta-lactoglobulin (drawn with JSmol Jena3D) [25], where the radical receiving AAc R2 are highlighted in dark red. FT-ATR-IR spectra of the protein amid I band (C) and second derivate (F) of whey protein isolate (black dashed), beta lactoglobulin (grey dashed), whey protein protein aggregates in water (black line) and whey protein protein aggregates in oil (black. dotted) 157

Figure 6.3: To the occurrence relative PLS importance of individual AAc and the statistical pathways involved (regular peptides excluded) for Pareto scaling (A, D), level scaling (B, E) and Pareto scaling of all peptides ($\Delta m < 2$ ppm, C, F). 159

Figure 6.4: principal component analysis of oxidants (black) in table 6.3 with the principal components (PC) plotted against each other, NA values were replaced with the mean after the sum of values of each experimental data was set to 1 for a better comparison, data of this study was projected (dark red) using the loadings of AAc (red), A: PC1 vs PC2, B: PC3 vs PC2. 164

List of Tables

Table 2.1: Composition of low moisture model systems with changing water activity	50
Table 5.1: Characteristic excitation/emission regions observed and related compounds	136
Table 6.1: Identified oxidized peptides of the FT-ICR-MS measurement with mSigma (mSigma) <50 and $\Delta m < 2$ ppm. The relevant AAc R2, which is the initial radical site, was highlighted. In case of regular peptide first and last AAc were taken for statistics and from repeating peptides only the one with the highest importance were considered. Importance for PLS models are given for Pareto and level scaling. For comparisons the instability index and charge was added.	154
Table 6.2: Importance of each amino acid divided by their occurrence in the annotation list in the partial least squares regression models with correlation of lipid hydroperoxide data to oxidized peptide data which	162

is generated via scission in comparison to studies of amino acid loss or electron paramagnetic resonance signal gain (G value) of various proteins after treatment with various oxidants (oxidizing lipids: linoleic acid (LA) as dominating oxidation fatty acid in safflower oil, ethyl arachidonate [34], hydroxyl radical generating [38], LAHPO: LA hydroperoxide, SPLA:

Curriculum Vitae

Personal Data

Name	Philipp Matthias Meissner
Date of birth	June 14th 1989
Place of birth	Potsdam, Germany
Nationality	Germany

Education

11/2019 – 10/2020	Student at Behörde für Gesundheit und Verbraucherschutz, Institut für Umwelt und Hygiene (State examination in Food Chemistry)
11/2015 – 09/2020	PhD student, Institute of Human Nutrition and Food Science - Division of Food Technology, Kiel University, Germany
10/2011 – 07/2015	Student at the Institute of Food Technology and Food Chemistry (Diploma in Food Chemistry) Technical University of Berlin, Germany
08/2002 – 07/2009	Student at the Wolkenberg-Gymnasium Michendorf, Germany <i>Abitur</i> (Certificate of maturity)

Experience

since 11/2020	Research Scientist Vitamin Analytics, AGROLAB Lufa GmbH, Kiel
11/2019 – 02/2020	Division of Research and Development, GALAB Laboratories GmbH, Hamburg
11/2015 – 10/2019	Research associate at Food Science and Nutrition, Department of Food Technology
01/2016 – 03/2016	Three courses of Statistics with R, Graduate Center, University of Kiel
07/2013 – 07/2015	Student representative of semester and institute
07/2009 – 09/2011	Operations management, national Service, Kurmark-Kaserne Storkow

Eidesstattliche Erklärung

Hiermit erkläre ich, dass die von mir vorgelegte Dissertation - abgesehen von der Beratung durch meine Betreuer – selbstständig und ohne Zuhilfenahme unerlaubter Hilfsmittel angefertigt habe. Alle benutzten Quellen und Hilfsmittel habe ich vollständig angegeben und die Zusammenarbeit mit Dritten habe ich kenntlich gemacht. Ich versichere, dass diese Arbeit unter Einhaltung der Regeln guter wissenschaftlicher Praxis der Deutschen Forschungsgemeinschaft verfasst wurde, und dass sie nach Form und Inhalt meine eigene Arbeit ist. Weder diese noch eine ähnliche Arbeit wurden an einer anderen Abteilung oder Hochschule im Rahmen eines Prüfungsverfahrens vorgelegt, veröffentlicht oder zur Veröffentlichung vorgelegt. Ein akademischer Grad wurde nicht entzogen.

Kiel, den

Philipp Matthias Meissner

